NOAA Atlas NESDIS 28

WORLD OCEAN ATLAS 1998
VOLUME 2: Temperature of the Pacific Ocean

John I. Antonov
Sydney Levitus
Timothy P. Boyer
Margarita E. Conkright
Todd D. O'Brien
Cathy Stephens

National Oceanographic Data Center
Ocean Climate Laboratory

Silver Spring, MD
December 1998

U.S. DEPARTMENT OF COMMERCE
William M. Daley, Secretary

National Oceanic and Atmospheric Administration
D. James Baker, Under Secretary

National Environmental Satellite, Data, and Information Service
Robert Winokur, Assistant Administrator

1998 International Year of the Ocean

National Oceanographic Data Center
USER SERVICES

Additional copies of this publication, as well as information about NODC data holdings, products, and services, are available on request directly from the NODC. NODC information and data are also available over the Internet through the NODC World Wide Web and Gopher sites.

National Oceanographic Data Center
User Services Branch
NOAA/NESDIS E/OC1
SSMC3, 4th Floor
1315 East-West Highway
Silver Spring, MD 20910-3282

Telephone: (301) 713-3277

Fax: (301) 713-3302

E-mail: services@nodc.noaa.gov

NODC World Wide Web site: http://www.nodc.noaa.gov/

NODC Gopher site: gopher.nodc.noaa.gov

Contents

Preface viii

Acknowledgments ix

Abstract 1

1. Introduction 1

2. Data and data distribution 1
   - 2.1 Data source 2
   - 2.2 Data quality control 2
     - 2.2a Duplicate elimination 2
     - 2.2b Range checks and gradient checks 2
     - 2.2c Statistical checks 2
     - 2.2d Static stability check 3
     - 2.2e Subjective flagging of data 3
     - 2.2f Representativeness of the data 4
     - 2.2g XBT drop-rate error correction 4

3. Data processing procedures 4
   - 3.1 Vertical interpolation to standard levels 4
   - 3.2 Methods of analysis 5
     - 3.2a Overview 5
     - 3.2b Derivation of Barnes' (1964) weight function 6
     - 3.2c Derivation of Barnes' (1964) response function 7
     - 3.2d Choice of response function 7
     - 3.2e First-guess field determination 8
   - 3.3 Choice of objective analysis procedures 8
   - 3.4 Choice of spatial grid 8

4. Results 9
   - 4.1 Computation of annual and seasonal fields 9
   - 4.2 Explanation of standard level figures 9
   - 4.3 Standard level analyses 9
   - 4.4 Contents of the *World Ocean Atlas 1998* CD-ROM 9

5. Summary 10

6. Future work 10

7. References 11

8. Appendix A: Annual distribution by one-degree squares of the number of temperature observations and the mean at selected standard levels for the climatological annual compositing period.

9. Appendix B: Seasonal distribution of temperature observations, seasonal mean, and seasonal minus annual means at selected standard levels.

10. Appendix C: Monthly distribution of temperature observations, mean, and seasonal minus annual means at selected standard levels.

List of Tables

Table 1 Acceptable distances (m) for defining interior and exterior values used in the Reiniger-Ross scheme for interpolating observed level data to standard levels.

Table 2 Response function of the objective analysis scheme as a function of wavelength for WOA98 and earlier analyses.

Table 3 Basins defined for objective analysis and the shallowest depth level for which each basin is defined.

List of Figures

Fig. 1a Annual temperature standard deviation (°C) at 500 meters depth by one-degree squares.

Fig. 1b Annual temperature standard error of the mean (°C) at 500 meters depth by one-degree squares.

Fig. 2 Response function of the WOA98, WOA94, and Levitus (1982) objective analysis schemes.

Fig. 3 Scheme used in computing annual, seasonal, and monthly objectively analyzed means for a variable.

Fig. 4 Annual observed one-degree square temperature mean value minus objectively analyzed annual mean temperature values (°C) at 500 meters depth.

APPENDIX A

Fig. A1 Annual temperature observations at the surface.

Fig. A2 Annual temperature observations at 50 m depth.

Fig. A3 Annual temperature observations at 75 m depth.

Fig. A4 Annual temperature observations at 100 m depth.

Fig. A5 Annual temperature observations at 150 m depth.

Fig. A6 Annual temperature observations at 200 m depth.

Fig. A7 Annual temperature observations at 250 m depth.

Fig. A8 Annual temperature observations at 400 m depth.

Fig. A9 Annual temperature observations at 500 m depth.

Fig. A10 Annual temperature observations at 700 m depth.

Fig. A11 Annual temperature observations at 1000 m depth.

Fig. A12 Annual temperature observations at 1500 m depth.

Fig. A13 Annual temperature observations at 2000 m depth.

Fig. A14 Annual temperature observations at 2500 m depth.

Fig. A15 Annual temperature observations at 3000 m depth.

Fig. A16 Annual temperature observations at 4000 m depth.

Fig. A17 Annual mean temperature (°C) at the surface.

Fig. A18 Annual mean temperature (°C) at 50 m depth.

Fig. A19 Annual mean temperature (°C) at 75 m depth.

Fig. A20 Annual mean temperature (°C) at 100 m depth.

Fig. A21 Annual mean temperature (°C) at 150 m depth.

Fig. A22 Annual mean temperature (°C) at 200 m depth.

Fig. A23 Annual mean temperature (°C) at 250 m depth.

Fig. A24 Annual mean temperature (°C) at 400 m depth.

Fig. A25 Annual mean temperature (°C) at 500 m depth.

Fig. A26 Annual mean temperature (°C) at 700 m depth.

Fig. A27 Annual mean temperature (°C) at 1000 m depth.

Fig. A28 Annual mean temperature (°C) at 1500 m depth.

Fig. A29 Annual mean temperature (°C) at 2000 m depth.

Fig. A30 Annual mean temperature (°C) at 2500 m depth.

Fig. A31 Annual mean temperature (°C) at 3000 m depth.

Fig. A32 Annual mean temperature (°C) at 4000 m depth.

APPENDIX B

Fig. B1 Winter (Jan.-Mar.) temperature observations at the surface.

Fig. B2 Winter (Jan.-Mar.) temperature observations at 50 m depth.
Fig. B3 Winter (Jan.-Mar.) temperature observations at 75 m depth.
Fig. B4 Winter (Jan.-Mar.) temperature observations at 100 m depth.
Fig. B5 Winter (Jan.-Mar.) temperature observations at 150 m depth.
Fig. B6 Winter (Jan.-Mar.) temperature observations at 250 m depth.

Fig. B7 Spring (Apr.-Jun.) temperature observations at the surface.
Fig. B8 Spring (Apr.-Jun.) temperature observations at 50 m depth.
Fig. B9 Spring (Apr.-Jun.) temperature observations at 75 m depth.
Fig. B10 Spring (Apr.-Jun.) temperature observations at 100 m depth.
Fig. B11 Spring (Apr.-Jun.) temperature observations at 150 m depth.
Fig. B12 Spring (Apr.-Jun.) temperature observations at 250 m depth.

Fig. B13 Summer (Jul.-Sep.) temperature observations at the surface.
Fig. B14 Summer (Jul.-Sep.) temperature observations at 50 m depth.
Fig. B15 Summer (Jul.-Sep.) temperature observations at 75 m depth.
Fig. B16 Summer (Jul.-Sep.) temperature observations at 100 m depth.
Fig. B17 Summer (Jul.-Sep.) temperature observations at 150 m depth.
Fig. B18 Summer (Jul.-Sep.) temperature observations at 250 m depth.

Fig. B19 Fall (Oct.-Dec.) temperature observations at the surface.
Fig. B20 Fall (Oct.-Dec.) temperature observations at 50 m depth.
Fig. B21 Fall (Oct.-Dec.) temperature observations at 75 m depth.
Fig. B22 Fall (Oct.-Dec.) temperature observations at 100 m depth.
Fig. B23 Fall (Oct.-Dec.) temperature observations at 150 m depth.
Fig. B24 Fall (Oct.-Dec.) temperature observations at 250 m depth.

Fig. B25 Winter (Jan.-Mar.) mean temperature (°C) at the surface.
Fig. B26 Winter (Jan.-Mar.) minus annual temperature (°C) at the surface.
Fig. B27 Winter (Jan.-Mar.) mean temperature (°C) at 50 m depth.
Fig. B28 Winter (Jan.-Mar.) minus annual temperature (°C) at 50 m depth.
Fig. B29 Winter (Jan.-Mar.) mean temperature (°C) at 75 m depth.
Fig. B30 Winter (Jan.-Mar.) minus annual temperature (°C) at 75 m depth.
Fig. B31 Winter (Jan.-Mar.) mean temperature (°C) at 100 m depth.
Fig. B32 Winter (Jan.-Mar.) minus annual temperature (°C) at 100 m depth.
Fig. B33 Winter (Jan.-Mar.) mean temperature (°C) at 150 m depth.
Fig. B34 Winter (Jan.-Mar.) minus annual temperature (°C) at 150 m depth.
Fig. B35 Winter (Jan.-Mar.) mean temperature (°C) at 250 m depth.
Fig. B36 Winter (Jan.-Mar.) minus annual temperature (°C) at 250 m depth.

Fig. B37 Spring (Apr.-Jun.) mean temperature (°C) at the surface.
Fig. B38 Spring (Apr.-Jun.) minus annual temperature (°C) at the surface.
Fig. B39 Spring (Apr.-Jun.) mean temperature (°C) at 50 m depth.
Fig. B40 Spring (Apr.-Jun.) minus annual temperature (°C) at 50 m depth.
Fig. B41 Spring (Apr.-Jun.) mean temperature (°C) at 75 m depth.
Fig. B42 Spring (Apr.-Jun.) minus annual temperature (°C) at 75 m depth.
Fig. B43 Spring (Apr.-Jun.) mean temperature (°C) at 100 m depth.
Fig. B44 Spring (Apr.-Jun.) minus annual temperature (°C) at 100 m depth.
Fig. B45 Spring (Apr.-Jun.) mean temperature (°C) at 150 m depth.
Fig. B46 Spring (Apr.-Jun.) minus annual temperature (°C) at 150 m depth.
Fig. B47 Spring (Apr.-Jun.) mean temperature (°C) at 250 m depth.
Fig. B48 Spring (Apr.-Jun.) minus annual temperature (°C) at 250 m depth.

Fig. B49 Summer (Jul.-Sep.) mean temperature (°C) at the surface.
Fig. B50 Summer (Jul.-Sep.)minus annual temperature (°C) at the surface.
Fig. B51 Summer (Jul.-Sep.) mean temperature (°C) at 50 m depth.
Fig. B52 Summer (Jul.-Sep.) minus annual temperature (°C) at 50 m depth.
Fig. B53 Summer (Jul.-Sep.) mean temperature (°C) at 75 m depth.

Fig. B54 Summer (Jul.-Sep.) minus annual temperature (°C) at 75 m depth.
Fig. B55 Summer (Jul.-Sep.) mean temperature (°C) at 100 m depth.
Fig. B56 Summer (Jul.-Sep.) minus annual temperature (°C) at 100 m depth.
Fig. B57 Summer (Jul.-Sep.) mean temperature (°C) at 150 m depth.
Fig. B58 Summer (Jul.-Sep.) minus annual temperature (°C) at 150 m depth.
Fig. B59 Summer (Jul.-Sep.) mean temperature (°C) at 250 m depth.
Fig. B60 Summer (Jul.-Sep.) minus annual temperature (°C) at 250 m depth.

Fig. B61 Fall (Oct.-Dec.) mean temperature (°C) at the surface.
Fig. B62 Fall (Oct.-Dec.) minus annual temperature (°C) at the surface.
Fig. B63 Fall (Oct.-Dec.) mean temperature (°C) at 50 m depth.
Fig. B64 Fall (Oct.-Dec.) minus annual temperature (°C) at 50 m depth.
Fig. B65 Fall (Oct.-Dec.) mean temperature (°C) at 75 m depth.
Fig. B66 Fall (Oct.-Dec.) minus annual temperature (°C) at 75 m depth.
Fig. B67 Fall (Oct.-Dec.) mean temperature (°C) at 100 m depth.
Fig. B68 Fall (Oct.-Dec.) minus annual temperature (°C) at 100 m depth.
Fig. B69 Fall (Oct.-Dec.) mean temperature (°C) at 150 m depth.
Fig. B70 Fall (Oct.-Dec.) minus annual temperature (°C) at 150 m depth.
Fig. B71 Fall (Oct.-Dec.) mean temperature (°C) at 250 m depth.
Fig. B72 Fall (Oct.-Dec.) minus annual temperature (°C) at 250 m depth.

APPENDIX C

Fig. C1 January temperature observations at the surface.
Fig. C2 January temperature observations at 75 m depth.
Fig. C3 February temperature observations at the surface.
Fig. C4 February temperature observations at 75 m depth.
Fig. C5 March temperature observations at the surface.
Fig. C6 March temperature observations at 75 m depth.
Fig. C7 April temperature observations at the surface.
Fig. C8 April temperature observations at 75 m depth.
Fig. C9 May temperature observations at the surface.
Fig. C10 May temperature observations at 75 m depth.
Fig. C11 June temperature observations at the surface.
Fig. C12 June temperature observations at 75 m depth.
Fig. C13 July temperature observations at the surface.
Fig. C14 July temperature observations at 75 m depth.
Fig. C15 August temperature observations at the surface.
Fig. C16 August temperature observations at 75 m depth.
Fig. C17 September temperature observations at the surface.
Fig. C18 September temperature observations at 75 m depth.
Fig. C19 October temperature observations at the surface.
Fig. C20 October temperature observations at 75 m depth.
Fig. C21 November temperature observations at the surface.
Fig. C22 November temperature observations at 75 m depth.
Fig. C23 December temperature observations at the surface.
Fig. C24 December temperature observations at 75 m depth.

Fig. C25 January mean temperature (°C) at the surface.
Fig. C26 January minus annual temperature (°C) at the surface.
Fig. C27 January mean temperature (°C) at 75 m depth.
Fig. C28 January minus annual temperature (°C) at 75 m depth.
Fig. C29 February mean temperature (°C) at the surface.
Fig. C30 February minus annual temperature (°C) at the surface.
Fig. C31 February mean temperature (°C) at 75 m depth.
Fig. C32 February minus annual temperature (°C) at 75 m depth.
Fig. C33 March mean temperature (°C) at the surface.

Fig. C34 March minus annual temperature (°C) at the surface.
Fig. C35 March mean temperature (°C) at 75 m depth.
Fig. C36 March minus annual temperature (°C) at 75 m depth.
Fig. C37 April mean temperature (°C) at the surface.
Fig. C38 April minus annual temperature (°C) at the surface.
Fig. C39 April mean temperature (°C) at 75 m depth.
Fig. C40 April minus annual temperature (°C) at 75 m depth.
Fig. C41 May mean temperature (°C) at the surface.
Fig. C42 May minus annual temperature (°C) at the surface.
Fig. C43 May mean temperature (°C) at 75 m depth.
Fig. C44 May minus annual temperature (°C) at 75 m depth.
Fig. C45 June mean temperature (°C) at the surface.
Fig. C46 June minus annual temperature (°C) at the surface.
Fig. C47 June mean temperature (°C) at 75 m depth.
Fig. C48 June minus annual temperature (°C) at 75 m depth.
Fig. C49 July mean temperature (°C) at the surface.
Fig. C50 July minus annual temperature (°C) at the surface.
Fig. C51 July mean temperature (°C) at 75 m depth.
Fig. C52 July minus annual temperature (°C) at 75 m depth.
Fig. C53 August mean temperature (°C) at the surface.
Fig. C54 August minus annual temperature (°C) at the surface.
Fig. C55 August mean temperature (°C) at 75 m depth.
Fig. C56 August minus annual temperature (°C) at 75 m depth.
Fig. C57 September mean temperature (°C) at the surface.
Fig. C58 September minus annual temperature (°C) at the surface.
Fig. C59 September mean temperature (°C) at 75 m depth.
Fig. C60 September minus annual temperature (°C) at 75 m depth.
Fig. C61 October mean temperature (°C) at the surface.
Fig. C62 October minus annual temperature (°C) at the surface.
Fig. C63 October mean temperature (°C) at 75 m depth.
Fig. C64 October minus annual temperature (°C) at 75 m depth.
Fig. C65 November mean temperature (°C) at the surface.
Fig. C66 November minus annual temperature (°C) at the surface.
Fig. C67 November mean temperature (°C) at 75 m depth.
Fig. C68 November minus annual temperature (°C) at 75 m depth.
Fig. C69 December mean temperature (°C) at the surface.
Fig. C70 December minus annual temperature (°C) at the surface.
Fig. C71 December mean temperature (°C) at 75 m depth.
Fig. C72 December minus annual temperature (°C) at 75 m depth.

Preface

The oceanographic analyses described by this atlas series expand on earlier works, *e.g.* the *World Ocean Atlas 1994* (WOA94) and *Climatological Atlas of the World Ocean*. Previously published oceanographic objective analyses have proven to be of great utility to the oceanographic, climate research, and operational environmental forecasting communities. Such analyses are used as boundary and/or initial conditions in numerical ocean circulation models and atmosphere-ocean models, for verification of numerical simulations of the ocean, as a form of "sea truth" for satellite measurements such as altimetric observations of sea surface height, for computation of nutrient fluxes by Ekman transport, and for planning oceanographic expeditions.

We have expanded our earlier analyses to include an all-data annual analysis of chlorophyll, monthly analyses of oxygen, and seasonal analyses of nutrients. Additional data for these variables have become available and there is a need for such analyses of these data in order to:

1) study the role of biogeochemical cycles in determining how the earth's climate system works, particularly the vulnerability of ocean ecosystems to climate change (IPCC, 1996);

2) help verify remotely sensed estimates of chlorophyll (SeaWIFS, ADEOS missions) requires knowledge of *in situ* variables such as chlorophyll and plankton;

3) provide the most comprehensive set of oceanographic databases and products based on these data to the international research and forecasting communities.

We continue preparing climatological analyses on a one-degree grid. This is because higher resolution analyses are not justified for all the variables we are working with and we wish to produce a set of analyses for which all variables have been analyzed in the same manner. High-resolution analyses as typified by the work of Boyer and Levitus (1997) will be published as separate atlases.

In the acknowledgment section of this publication we have expressed our view that creation of global ocean profile and plankton databases and analyses are only possible through the cooperation of scientists, data managers, and scientific administrators throughout the international scientific community. I would also like to thank my colleagues and the staff of the Ocean Climate Laboratory of NODC for their dedication to the project leading to publication of this atlas series. Their integrity and thoroughness have made this database possible. It is my belief that the development and management of national and international oceanographic data archives is best performed by scientists who are actively working with the historical data.

Sydney Levitus
National Oceanographic Data Center
Silver Spring, MD
December 1998

Acknowledgments

This work was made possible by a grant from the NOAA Climate and Global Change Program which enabled the establishment of a research group at the National Oceanographic Data Center. The purpose of this group is to prepare research quality oceanographic databases, as well as to compute objective analyses of, and diagnostic studies based on, these databases.

The data on which this atlas is based include the oceanographic data archives maintained by NODC/WDC-A as well as data acquired as a result of the NODC Oceanographic Data Archaeology and Rescue (NODAR) project and the IODE/IOC Global Oceanographic Data Archaeology and Rescue (GODAR) project. At NODC/WDC-A, "data archaeology and rescue" projects are supported with funding from the NOAA Environmental Science Data and Information Management (ESDIM) Program and NOAA Climate and Global Change Program. Support for some of the regional IOC/GODAR meetings was provided by the MAST program of the European Union.

We would like to acknowledge the scientists, technicians, and programmers who have submitted data to national and regional data centers as well as the managers and staff at the various data centers. Their efforts have made this and similar works possible.

We thank Joe Reid, Steve Worley, Gary Lagerloef, Stephan Howden, Clara Deser, and David Adamec for reviewing the manuscript version of this atlas series.

WORLD OCEAN ATLAS 1998, VOLUME : Temperature of the Pacific Ocean

John I. Antonov, Sydney Levitus, Timothy P. Boyer,
Margarita E. Conkright, Todd D. O'Brien, and *Cathy Stephens*
National Oceanographic Data Center
Silver Spring, MD

ABSTRACT

This atlas contains maps of the distribution of temperature at selected standard depth levels of the Pacific Ocean on a one-degree grid. Maps for all-data annual, seasonal, and monthly compositing periods are presented at standard depth levels. Seasonal and monthly difference (from the annual mean) fields are also presented. The fields used to generate these maps were computed by objective analysis of historical data. Data distribution maps are presented for all-data annual, seasonal, and monthly compositing periods at selected standard levels.

1. INTRODUCTION

This atlas is an analysis of all historical temperature profile data available from the National Oceanographic Data Center (NODC) and World Data Center-A (WDC-A) for Oceanography, Silver Spring, MD, plus data gathered as a result of several data management projects including:

a) the Intergovernmental Oceanographic Commission (IOC) Global Oceanographic Data Archaeology and Rescue (GODAR) project;

b) the NODC Oceanographic Data Archaeology and Rescue (NODAR) project;

c) the NODC Global Ocean Database project (GODB);

d) the IOC Global Temperature Salinity Profile Project (GTSPP).

Data used in this atlas have been analyzed in a consistent, objective manner on a one-degree latitude-longitude grid at standard oceanographic levels between the surface and ocean bottom to a maximum depth of 5500m. The procedures used are very similar to, but not identical with those used to produce earlier analyses [Levitus (1982), Levitus and Boyer (1994a,b), Levitus *et al.* (1994a) and Conkright *et al.* (1994)]. Annual, seasonal, and monthly analyses have been computed for temperature.

Objective analyses shown in this atlas are limited by the nature of the data base (data are non-synoptic and scattered in space) and characteristics of the objective analysis techniques, and the grid used. These limitations and characteristics will be discussed below.

Since the publication of WOA94, substantial amounts of additional historical data have become available. However, even with these additional data, we are still hampered in a number of ways by a lack of data. Because of the lack of data, we are forced to examine the annual cycle by compositing all data regardless of the year of observation. In some areas, quality control is made difficult by the limited number of data. Data may exist in an area for only one season, thus precluding any representative annual analysis. In some areas there may be a reasonable spatial distribution of data points on which to base an analysis, but there may be only a few (perhaps only one) data in each one-degree latitude-longitude square.

2. DATA AND DATA DISTRIBUTION

Data sources and quality control procedures are briefly described below. For further information on the data sources used in WOA98 refer to the World Ocean Database 1998 (WOD98) series [Boyer *et al.* (1998a, b,c); Conkright *et al.* 1998a,b); Levitus *et al.* (1998a, b) and O'Brien *et al.* (1998)]. The quality control procedures we have used in preparing these analyses are outlined by Conkright *et al.* (1998c).

2.1 Data sources

Historical Ocean Station Data (OSD), Mechanical Bathythermograph (MBT), Conductivity-Temperature-Depth (CTD), Digital Bathythermograph (DBT), and Expandable Bathythermograph (XBT) temperature profiles used in this project were obtained from the NODC/WDC-A archives and includes all data gathered as a result of the NODAR and GODAR projects.

Appendix A shows the geographic distribution of all historical temperature observations at selected standard depth levels. Appendix B shows the distribution of historical temperature observations at selected standard depth levels for individual seasons. Appendix C shows the distribution of historical temperature observations for individual months. In all data distribution maps that appear in the appendices, a small dot indicates a one-degree square containing one to four observations and a large dot indicates a square containing five or more observations.

We define the terms "standard level data" and "observed level data" here so the reader can understand the various data distribution figures, summary figures, and tables we present in this atlas. We refer to the actual measured value of an oceanographic variable *in situ* (Latin for "in place") as an "observation," and to the depth at which such a measurement was made as the "observed level depth." We may refer to such data as "observed level data." Before the development of oceanographic instrumentation that measure at high frequencies in the vertical, oceanographers often attempted to make measurements at selected "standard levels" in the water column. Sverdrup *et al.* (1942) presented the suggestions of the International Association of Physical Oceanography (IAPSO) as to which depths oceanographic measurements should be made or interpolated to for analysis. Different nations or institutions have a slightly different set of standard levels defined. For many purposes, including preparation of this atlas, observed level data are interpolated to standard observation levels, if such data do not occur exactly at a standard observation levels. We have prepared objective analyses at the NODC standard levels as given in Table 1 and added levels at 3500, 4500, and 5500 m. Section 3.1 discusses the vertical interpolation procedures used in our work.

2.2 Data quality control

Quality control of the data is a major task, the difficulty of which is directly related to lack of data (in some areas) upon which to base statistical checks. Consequently certain empirical criteria were applied, and as part of the last processing step, subjective judgment was used. Individual data, and in some cases entire profiles or cruises, have been flagged because these data produced features that were judged to be non-representative or in error. As part of our work, we have made available *World Ocean Database 1998* (WOD98) which contains both observed level profile data as well as standard level profile data with various quality control flags applied. Our knowledge of the variability of the world ocean now includes a greater appreciation and understanding of the ubiquity of eddies, rings, and lenses in some parts of the world ocean as well as interannual and interdecadal variability of water mass properties associated with modal variability of the atmosphere such as the North Atlantic Oscillation and El Nino/Southern Oscillation. Therefore, we have simply flagged data, not eliminated them. Thus, individual investigators can make their own decision regarding the representativeness or correctness of the data. Investigators studying the distribution of features such as eddies will be interested in those data that we may regard as unrepresentative for the preparation of the analyses shown in this atlas.

2.2a Duplicate elimination

Because data are received from many sources, sometimes the same data set is received at NODC/WDC-A more than once but with slightly different time and/or position and/or data values, and hence are not easily identified as duplicate stations. Therefore, our databases were checked for the presence of exact and "near" exact replicates using eight different criteria. The first checks involve identifying stations with exact position/date/time and data values; the next checks involve offsets in position/date/time. Profiles identified as duplicates in the checks with a large offset were individually verified to ensure they were indeed duplicate profiles.

All but one profile from each set of replicate profiles were eliminated at the first step of our processing.

2.2b Range checks and gradient checks

Range checking (checking whether data is within set minimum and maximum values as a function of depth) was performed on all data as a first error check to flag and eliminate from further use the relatively few data that seemed to be grossly in error. Range checks were prepared for individual regions of the world ocean. Conkright *et al.* (1998c) and Boyer and Levitus (1994) detail the quality control procedures and include tables showing the ranges selected for each basin.

A check as to whether excessive gradients occur in the data were made for each variable in WOD98 both in terms of positive and negative gradients.

2.2c Statistical checks

Statistical checks were performed as follows. All data for each variable (irrespective of season), at each standard level, were averaged by five-degree latitude-longitude

squares to produce a record of the number of observations, mean, and standard deviation in each square. Statistics were computed for the annual, seasonal, and monthly compositing periods. Below 50 m depth, if data were more than three standard deviations from the mean, the data were flagged and eliminated from further use in our objective analyses. Above 50 m depth, a five-standard-deviation criterion was used in five-degree squares that contained any land area. In selected five degrees squares that are close to land areas, a four standard-deviation check was used. In all other squares a three-standard-deviation criterion was used.

The reason for the weaker criterion in coastal and near-coastal regions is the exceptionally large variability in the coastal five-degree square statistics for some variables. Frequency distributions of some variables in some coastal regions are observed to be skewed or bimodal. Thus to avoid eliminating possibly good data in highly variable environments, the standard deviation criteria were weakened.

The total number of temperature measurements in each cast, as well as the total number of observations exceeding the criterion, were recorded. If more than two observations in a cast were found to exceed the standard deviation criterion, then the entire cast was flagged. This check was imposed after tests indicated that surface data from particular casts (which upon inspection appeared to be erroneous) were being flagged but deeper data were not. Other situations were found where erroneous data from the deeper portion of a cast were flagged, while near-surface data from the same cast were not flagged because of larger natural variability in surface layers. One reason for this was the decrease of the number of observations with depth and the resulting change in sample statistics. The standard-deviation check was applied twice to the data set for each compositing period. Individual flags were set for each period.

In summary, first the five-degree square statistics were computed, and the elimination procedure described above was used to provide a preliminary data set. Next, new five-degree-square statistics were computed from this preliminary data set and used with the same statistical check to produce a new, "clean" data set. The reason for applying the statistical check twice was to flag (and eliminate from further use), in the first round, any grossly erroneous or non-representative data from the data set that would artificially increase the variances. The second check is then more effective in eliminating smaller, but still erroneous or non-representative, observations. The standard deviation for temperature observations at 500 meters depth on a one-degree latitude-longitude square are shown in Figure 1a; the standard error of the mean for the same depth is shown in Figure 1b.

2.2d Static stability check

Each OSD and CTD cast was checked for static stability as defined by Hesselberg and Sverdrup (1914). Neumann and Pierson (1966, p. 139) review this definition. The computation is a "local" one in the sense that adiabatic displacements between adjacent temperature-salinity measurements in the vertical are considered rather than displacements to the sea surface. Lynn and Reid (1968) discuss the reasons for use of the local stability computation. The procedure for computation follows that used by Lynn and Reid (1968) and is given by

$$E = \lim_{\partial z \to 0} \frac{1}{\rho_o} \frac{\delta \rho}{\partial z}$$

in which $\rho_o = 1.02$ g cm^{-3}. As noted by Lynn and Reid, the term "is the individual density gradient defined by vertical displacement of a water parcel (as opposed to the geometric density gradient). For discrete samples the density difference ($\delta\rho$) between two samples is taken after one is adiabatically displaced to the depth of the other". For the results at any standard level (k), the computation was performed by displacing parcels at the next deeper standard level (k+l) to level k.

The actual procedure for using stability checks to flag sets of data points was as follows. To a depth of 30m, inversions in excess of 3×10^{-5}g cm^{-3} were flagged, and below this depth down to the 400 m level, inversions in excess of 2×10^{-5}g cm^{-3} were flagged. Below 400 m any inversion was flagged. To eliminate an inversion both temperature and salinity were flagged and eliminated from further use at both standard levels involved in the computation. In the actual processing a count was kept of the number of inversions in each cast. If a cast had two or more unacceptable inversions, as defined above, then the entire cast was eliminated from further use.

2.2e Subjective flagging of data

The data were averaged by one-degree squares for input to the objective analysis program. After initial objective analyses were computed, the input set of one-degree means still contained suspicious data contributing to unrealistic distributions, yielding intense bull's-eyes or gradients. Examination of these features indicated that some of them were due to particular oceanographic cruises. In such cases, data from an entire cruise were eliminated from further use by setting a flag on each profile from the cruise. In other cases, individual profiles or measurements were found to cause these features and were eliminated from use.

2.2f Representativeness of the data

Another quality control issue is data representativeness. The general paucity of data forces the compositing of all historical data to produce "climatological" fields. In a given one-degree square, there may be data from a month or season of one particular year, while in the same or a nearby square there may be data from an entirely different year. If there is large interannual variability in a region where scattered sampling in time has occurred, then one can expect the analysis to reflect this. Because the observations are scattered randomly with respect to time, except for a few limited areas, the results cannot, in a strict sense, be considered a true long-term climatological average.

We present smoothed analyses of historical means, based (in certain areas) on relatively few observations. We believe, however, that useful information about the oceans can be gained through our procedures and that the large-scale features are representative of the real ocean. We believe that, if a hypothetical global synoptic set of ocean data (temperature, salinity, or oxygen) existed, and one were to smooth this data to the same degree as we have smoothed the historical means overall, the large-scale features would be similar to our results. Some differences would certainly occur because of interannual-to-decadal-scale variability.

To clarify discussions of the amount of available data, quality control techniques, and representativeness of the data, the reader should examine in detail the maps showing the distribution of data (Appendices A, B, and C) and the *World Ocean Database 1998* atlas series which shows the distribution of oceanographic stations as a function of year and instrument type. These maps are provided to give the reader a quick, simple way of examining the historical data distributions. Basically, the data diminish in number with increasing depth. In the upper ocean, the all-data annual mean distributions are quite good for defining large-scale features, but for the seasonal periods, the data base is inadequate for some regions. With respect to the deep ocean, in some areas the distribution of observations may be adequate for some diagnostic computations but inadequate for other purposes. If an isolated deep basin or some region of the deep ocean has only one observation, then no horizontal gradient computations are meaningful. However, useful information is provided by the observation in the computation of other quantities (*e.g.*, a volumetric mean over a major ocean basin).

2.2g XBT drop rate error correction

Recently it has been demonstrated that XBT temperature profiles made using T4, T6, and T7 probes exhibit a systematic error with depth that is associated with an inadequate drop rate equation for these instruments (Banes and Sessions, 1984; Hanawa and Yoritaka, 1987; Wright and Szabados, 1989; Singer, 1990; Hallock and Teague, 1992). The error in depth has a magnitude that equals approximately five percent of the actual depth. XBT instruments only measure temperature and time directly. The depth of an instrument is estimated from a manufacturer supplied drop rate equation using the time elapsed after the probe enters the water. T4, T6, and T7 XBT probes in fact, fall faster than the manufacture's specification.

A task team of the International Global Ocean Services System (IGOSS) of the Intergovernmental Oceanographic Commission (IOC) on "Quality Control for Automated Systems" has addressed the problem of how the international community should treat XBT data (IOC, 1992a ; IOC, 1992b). One of their recommendations is that IGOSS continue using the existing drop-rate equations, until international agreement is reached on a solution. It has been recommended that data centers continue to receive and distribute XBT data that are uncorrected for the systematic error. Following this philosophy **we have made no correction to the depths of the observed level XBT profiles**. Thus, investigators, if they desire, can make whatever correction they desire to the observed level profiles we are providing since we have not corrected these profiles for this error. However, in order to merge XBT data with other types of temperature measurements, and in order to produce climatologies and other analyses, by necessity we have corrected the drop-rate error in XBT profiles, as part of the process of interpolating to standard levels (the drop rate correction was applied to the observed level data before interpolation to standard levels). **All T4, T6, T7 XBT profiles that we have used in generating products at standard levels, or made available as part of our standard level profile data sets, have been corrected for the drop-rate error.** T5 XBT profiles were not corrected because depth estimates using the manufacturer's equation for this instrument type were found to be within the limit stated by the manufacturer (Boyd and Linzell, 1992). **If in fact, users wish to use another procedure, but still use the XBT data set we have compiled, they can do so by applying their correction procedure to our observed level XBT profile data set, which has not been corrected for the drop rate error.**

The correction for XBT drop rate (Hanawa *et al.*, 1994) is

$$z_c = 1.0417 z_0 - 75.906(1 - (1 - 2.063 \times 10^{-4} z_0)^{1/2})$$

in which z_0 is originally calculated depth.

3. DATA PROCESSING PROCEDURES

3.1 Vertical interpolation to standard levels

Vertical interpolation of observed level data to standard levels followed procedures in UNESCO (1991). These

procedures are in part based on the work of Reiniger and Ross (1968). Four observed level values surrounding the standard level values were used, two values from above the standard level and two values below the standard level. The pair of values furthest from the standard level are termed "exterior" points and the pair of values closest to the standard level are termed "interior" points. Paired parabolas were generated via Lagrangian interpolation. A reference curve was fitted to the four data points and used to define unacceptable interpolations caused by "overshooting" in the interpolation. When there were too few data points above or below the standard level to apply the Reiniger and Ross technique, we used a three-point Lagrangian interpolation. If three points were not available (either two above and one below or vice-versa), we used linear interpolation. In the event that an observation occurred exactly at the depth of a standard level, then a direct substitution was made. Table 1 provides the range of acceptable distances for which observed level data could be used for interpolation to a standard level.

3.2 Methods of analysis

3.2a Overview

An objective analysis scheme of the type described by Barnes (1964) was used to produce the fields shown in this atlas. This scheme had its origins in the work of Cressman (1959). In WOA94, the Barnes (1973) scheme was used. This required only one "correction" to the first-guess field at each grid point in comparison to the successive correction method of Cressman (1959) and Barnes (1964). This was to minimize computer time used in the processing. Barnes (1994) recommends a return to a multi-pass analysis when computer time is not an issue. Based on our own experience we agree with this assessment. The single pass analysis, used in WOA94, caused an artificial front in the Southeastern Pacific Ocean in a data sparse area (Anne Marie Treguier, personal communication). The analysis scheme used in generating WOA98 analyses uses a three-pass "correction" which eliminates this artificial front.

Inputs to the analysis scheme were one-degree square means of data values at standard levels (for whatever period and variable being analyzed), and a first-guess value for each square. For instance, one-degree square means for our annual analysis were computed using all available data regardless of date of observation. For July, we used all historical July data regardless of year of observation.

Analysis was the same for all standard depth levels. Each one-degree latitude-longitude square value was defined as being representative of its square. The 360x180 gridpoints are located at the intersection of half-degree lines of latitude and longitude. An influence radius was then specified. At those grid points where there was an observed mean value, the difference between the mean and the first-guess field was computed. Next, a correction to the first-guess value at all gridpoints was computed as a distance-weighted mean of all gridpoint difference values that lie within the area around the gridpoint defined by the influence radius. Mathematically, the correction factor derived by Barnes (1964) is given by the expression

$$C_{i,j} = \frac{\sum_{s=1}^{n} W_s Q_s}{\sum_{s=1}^{n} W_s} \qquad (1)$$

in which

(i,j) = coordinates of a gridpoint in the east-west and north-south directions respectively;

$C_{i,j}$ = the correction factor at gridpoint coordinates (i,j);

n = the number of observations that fall within the area around the point i,j defined by the influence radius;

Q_s = the difference between the observed mean and the first-guess at the S^{th} point in the influence area;

W_s = $\exp(-E\, r^2 R^{-2})$ for $r \le R$;

0 for $r > R$;

r = distance of the observation from the gridpoint;

R = influence radius;

E = 4.

The derivation of the weight function, W_s, will be presented in the following section. At each gridpoint we computed an analyzed value $G_{i,j}$ as the sum of the first-guess, $F_{i,j}$, and the correction $C_{i,j}$. The expression for this is

$$G_{i,j} = F_{i,j} + C_{i,j} \qquad (2)$$

If there were no data points within the area defined by the influence radius, then the correction was zero, the first-guess field was left unchanged, and the analyzed value was simply the first-guess value. This correction procedure was applied at all gridpoints to produce an analyzed field. The resulting field was first smoothed with a median filter (Tukey, 1974; Rabiner *et al.,* 1975) and

then smoothed with a five-point smoother of the type described by Shuman (1957). The choice of first-guess fields is important and we discuss our procedures in section 3.2e.

The analysis scheme is based on the work of several researchers analyzing meteorological data. Bergthorsson and Doos (1955) computed corrections to a first-guess field using various techniques: one assumed that the difference between a first-guess value and an analyzed value at a gridpoint was the same as the difference between an observation and a first-guess value at a nearby observing station. All the observed differences in an area surrounding the gridpoint were then averaged and added to the gridpoint first-guess value to produce an analyzed value. Cressman (1959) applied a distance-related weight function to each observation used in the correction in order to give more weight to observations that occur closest to the gridpoint. In addition, Cressman introduced the method of performing several iterations of the analysis scheme using the analysis produced in each iteration as the first-guess field for the next iteration. He also suggested starting the analysis with a relatively large influence radius and decreasing it with successive iterations so as to analyze smaller scale phenomena with each pass.

Sasaki (1960) introduced a weight function that was specifically related to the density of observations, and Barnes (1964, 1973) extended the work of Sasaki. The weight function of Barnes (1964) has been used here. The objective analysis scheme we used is in common use by the mesoscale meteorological community. Several studies of objective analysis techniques have been made. Achtemeier (1987) examined the "concept of varying influence radii for a successive corrections objective analysis scheme." Seaman (1983) compared the "objective analysis accuracies of statistical interpolation and successive correction schemes." Smith and Leslie (1984) performed an "error determination of a successive correction type objective analysis scheme." Smith *et al.* (1986) made "a comparison of errors in objectively analyzed fields for uniform and non-uniform station distribution."

3.2b Derivation of Barnes' (1964) weight function

The principle upon which Barnes' (1964) weight function is derived is that "the two-dimensional distribution of an atmospheric variable can be represented by the summation of an infinite number of independent harmonic waves, that is, by a Fourier integral representation". If f(x,y) is the variable, then in polar coordinates (r,θ), a smoothed or filtered function h(x,y) can be defined:

$$h(x,y)=\frac{1}{2\pi}\int_0^{2\pi}\int_0^{\infty}\eta f(x+r\cos\theta,y+r\sin\theta)\,d(r^2/4K)d\theta \qquad (3)$$

in which r is the radial distance from a gridpoint whose coordinates are (x,y). The weight function is defined as

$$\eta = \exp(-r^2/4K) \qquad (4)$$

which resembles the Gaussian distribution. The shape of the weight function is determined by the value of K, which depends on the distribution of data. The determination of K follows. The weight function has the property that

$$\frac{1}{2\pi}\int_0^{2\pi}\int_0^{\infty}\eta d\left(\frac{r^2}{4K}\right)d\theta = 1. \qquad (5)$$

This property is desirable because in the continuous case (3) the application of the weight function to the distribution f(x,y) will not change the mean of the distribution. However, in the discrete case (1), we only sum the contributions to within the distance R. This introduces an error in the evaluation of the filtered function, because the condition given by (5) does not apply. The error can be pre-determined and set to a reasonably small value in the following manner. If one carries out the integration in (5) with respect to θ, the remaining integral can be rewritten as

$$\int_0^R \eta d\left(\frac{r^2}{4K}\right)+\int_R^{\infty}\eta d\left(\frac{r^2}{4K}\right)=1. \qquad (6)$$

Defining the second integral as ϵ yields

$$\int_0^R \exp\left(-\frac{r^2}{4K}\right)d\left(\frac{r^2}{4K}\right)=1-\varepsilon \qquad (7)$$

in which

$$\varepsilon=\exp(-R^2/4K)$$

Levitus (1982) chose ϵ = 0.02, which implies with respect to (6) the representation of 98 percent of the influence of any data around the gridpoint in the area defined by the influence radius, R. In terms of the weight function used in the evaluation of (1) this choice leads to a value of E=4 since

$$E = R^2/4K = -\ln\varepsilon.$$

Thus,

$$K = R^2/16.$$

The choice of ϵ and the specification of R determine the shape of the weight function.

Barnes (1964) proposed using this scheme in an iterative fashion similar to Cressman (1959). Levitus (1982) used a four iteration scheme with a variable influence radius for each pass. Levitus *et al.* (1994a,b) used a one-iteration scheme. WOA98 uses a three iteration scheme with a variable influence radius. The three influence radii are 888, 666, and 444 km.

3.2c Derivation of Barnes' (1964) response function

It is desirable to know the response of a data set to the interpolation procedure applied to it. Following Barnes (1964) we let

$$f(x) = A\sin(ax) \tag{8}$$

in which $a = 2\pi/\lambda$ with λ being the wavelength of a particular Fourier component, and substitute this function into equation (3) along with the expression for η in equation (4). Then

$$g(x) = D(A\sin(ax)) = Df(x) \tag{9}$$

in which D is the response function for one application of the analysis. The phase of each Fourier component is not changed by the interpolation procedure. The results of an analysis pass are used as the first-guess for the next analysis pass in an iterative fashion. The response function after N iterations as derived by Barnes (1964) is

$$g_n = f(x)D\sum_{n=1}^{N=1}(1-D)^{n-1} \tag{10}$$

Equation (10) differs trivially from that given by Barnes. The difference is due to our first-guess field being defined as a zonal average, annual mean, seasonal mean, or monthly mean, whereas Barnes used the first application of the analysis as a first-guess. Barnes (1964) also showed that applying the analysis scheme in an iterative fashion will result in convergence of the analyzed field to the observed data field. However, it is not desirable to approach the observed data too closely, because at least seven or eight gridpoints are needed to represent a Fourier component.

The response function given in (10) is useful in two ways: it is informative to know what Fourier components make up the analyses, and the computer programs used in generating the analyses can be checked for correctness by comparison with (10).

3.2d Choice of response function

The distribution of observations (see appendices) at different depths and for the different averaging periods, are not regular in space or time. At one extreme, regions exist in which every one-degree square contains data and no interpolation needs to be performed. At the other extreme are regions in which few if any data exist. Thus, with variable data spacing the average separation distance between gridpoints containing data is a function of geographical position and averaging period. However, if we computed and used a different average separation distance for each variable at each depth and each averaging period, we would be generating analyses in which the wavelengths of observed phenomena might differ from one depth level to another and from one season to another. In WOA94, a fixed influence radius of 555 kilometers was used to allow uniformity in the analysis of all variables. For this analyses, a three-pass analysis, based on Barnes (1964), with influence radii of 888, 666 and 444 km was used.

Inspection of (1) shows that the difference between the analyzed field and the first-guess at any gridpoint is proportional to the sum of the weighted-differences between the observed mean and first-guess at all gridpoints containing data within the influence area.

The reason for using the five-point smoother and the median smoother is that our data are not evenly distributed in space. As the analysis moves from regions containing data to regions devoid of data, small-scale discontinuities may develop. The five-point and median smoothers are used to eliminate these discontinuities. The five-point smoother does not affect the phase of the Fourier components that comprise an analyzed field.

The response function for the analyses presented in this atlas is given in Table 2 and Figure 2. For comparison purposes, the response function used by Levitus (1982) and Levitus *et al.* (1994a,b) are also presented. The response function represents the smoothing inherent in the objective analysis described above plus the effects of one application of the five-point smoother and one application of a five-point median smoother. The effect of varying the amount of smoothing in North Atlantic sea surface temperature (SST) fields has been quantified by Levitus (1982) for a particular case. In a region of strong SST gradient such as the Gulf Stream, the effect of smoothing

can easily be responsible for differences between analyses exceeding 1.0 °C.

To avoid the problem of the influence region extending across land or sills to adjacent basins, the objective analysis program uses basin "identifiers" to preclude the use of data from adjacent basins. Table 3 lists these basins and the depth at which no exchange of information between basins is allowed during the objective analysis of data, i.e., "depths of mutual exclusion." Some regions are nearly, but not completely, isolated topographically. Because some of these nearly isolated basins have water mass properties that are different from surrounding basins, we have chosen to treat these as isolated basins as well. Not all such basins have been identified because of the complicated structure of the sea floor. In Table 3, a region marked with a "*" can interact with adjacent basins except for special areas such as the Isthmus of Panama.

3.2e First-guess field determination

For all variables and compositing periods, there are gaps in the data coverage. In some parts of the world ocean, there exist adjacent basins whose water mass properties are individually nearly homogeneous but have distinct basin-to basin differences. Spurious features can be created when an influence area extends over two basins of this nature (basins are listed in Table 3). Our choice of first-guess field attempts to minimize the creation of these features. To provide a first-guess field for the annual analysis at any standard level, we first zonally averaged the observed data in each one-degree latitude belt by individual ocean basins. An annual analysis of a variable was then used as the first-guess for each seasonal analysis and each seasonal analysis was used as a first-guess for the appropriate monthly analysis if computed.

We then reanalyzed the data for each variable using the newly produced analyses as first-guess fields described as follows and as shown in Fig. 3. A new annual mean was computed as the mean of the twelve monthly analyses for the upper 1500 m, and the mean of the four seasons below 1500 m depth. This new annual mean was used as the first-guess field for new seasonal analyses. These new seasonal analyses were used to produce new monthly analyses. This procedure produces slightly smoother means. More importantly we recognize that fairly large data-void regions exist, in some cases to such an extent that a seasonal or monthly analysis in these regions is not meaningful. We are interested in computing integral quantities such as heat storage that are deviations from annual means. Geographic distribution of observations for the all-data annual periods (see appendices) is excellent for upper layers of the ocean. By using an all-data annual mean, first-guess field regions where data exists for only one season or month will show no contribution to the annual cycle. By contrast, if we used a zonal average for each season or month, then, in those latitudes where gaps exist, the first-guess field would be heavily biased by the few data points that exist. If these were anomalous data in some way, an entire basin-wide belt might be affected.

One advantage of producing "global" fields for a particular compositing period (even though some regions are data void) is that such analyses can be modified by investigators for use in modeling studies. For example, England (1992) noted that the temperature distribution produced by Levitus (1982) for the Antarctic is too high (due to a lack of winter data for the Southern Hemisphere) to allow for the formation of Antarctic Intermediate Water in an ocean general circulation model. By decreasing the temperature of the "observed" field the model was able to produce this water mass.

3.3 Choice of objective analysis procedures

Optimum interpolation (Gandin, 1963) has been used by some investigators to objectively analyze oceanographic data. We recognize the power of this technique but have not used it to produce analyzed fields. As described by Gandin (1963), optimum interpolation is used to analyze synoptic data using statistics based on historical data. In particular, second-order statistics such as correlation functions are used to estimate the distribution of first order parameters such as means. We attempt to map most fields in this atlas based on relatively sparse data sets. By necessity we must composite all data regardless of year of observation, to have enough data to produce a global, hemispheric, or regional analysis for a particular month or season. Because of the paucity of data, we prefer not to use an analysis scheme that is based on second order statistics. In addition, as Gandin has noted, there are two limiting cases associated with optimum interpolation. The first is when a data distribution is dense. In this case, the choice of interpolation scheme makes little difference. The second case is when data are sparse. In this case, an analysis scheme based on second order statistics is of questionable value. For additional information on objective analysis procedures see Thiebaux and Pedder (1987) and Daley (1991).

3.4 Choice of spatial grid

The analyses that comprise WOA98 have been computed using a new land-sea topography to define ocean depths at each grid point (ETOPO5, 1988). From the ETOPO5 mask, a quarter-degree mask was created based on ocean bottom depth and land criteria. If four or more 5-minute square values out of a possible nine in a one-quarter-degree box were defined as land, then the quarter-degree gridbox was defined to be land. If no more than two of the 5-minute squares had the same depth value in a quarter-degree box, then the average value of the 5-minute ocean depths in that box was defined to be the depth of the

quarter-degree gridbox. If three or more 5-minute squares out of the nine had a common bottom depth, then the depth of the quarter-degree box was set to the most common depth value. The same method was used to go from a quarter-degree to a one-degree resolution. In the one-degree resolution case, at least four points out of a possible sixteen (in a one-degree square) had to be land in order for the one-degree square to remain land and three out of sixteen had to have the same depth for the ocean depth to be set. These criteria yielded a mask that was then modified by :

a) Connecting the Isthmus of Panama,

b) maintaining an opening in the Straits of Gibraltar and in the English Channel,

c) connecting the Kamchatka Peninsula and the Baja Peninsula to their respective continents.

The quarter-degree mask was created as an intermediate step to ensure consistency between the present work and future high resolution analysis of temperature and salinity.

4. RESULTS

4.1 Computation of annual and seasonal fields

After completion of all of our analyses we define a final annual analysis as the average of our twelve monthly mean fields in the upper 1500 m of the ocean. Below 1500 m depth we define an annual analysis as the mean of the four seasonal analyses. Our final seasonal analyses are defined as the average of monthly analyses in the upper 1500 m of the ocean.

4.2 Explanation of standard level figures

All figures showing standard level analyses in this atlas series use similar symbols for displaying information. Continents are indicated as solid - black areas. Ocean areas shallower than the standard depth level being displayed are gray. Regions with negative temperature are dot stippled. Gridpoints for which there were less than four one-degree-square values available to correct the first-guess are indicated by an X. Dashed lines represent non-standard contours. "H" and "L" indicate locations of the absolute maximum and minimum of the entire field. All figures were computer drafted.

4.3 Standard level analyses

Global distributions of annual mean temperature at standard analysis levels are presented in Appendix A. Seasonal analyses are presented in Appendix B. Seasonal mean minus annual mean difference fields of these variables are also presented in Appendix B. Monthly analyses and monthly minus annual mean difference fields are presented in Appendix C.

4.4 Contents of the *World Ocean Atlas 1998* CD-ROM

This atlas presents data for selected standard levels in the Pacific Ocean. Associated with this atlas, is a CD-ROM containing the following digital fields for the world ocean:

(a) fields containing the number of observations by one-degree squares as a function of depth;

(b) one-degree annual objectively analyzed temperature fields at 33 standard levels;

(c) one-degree seasonal objectively analyzed temperature fields at 33 standard levels;

(d) one-degree monthly objective analyses for 24 standard levels;

(e) one-degree seasonal minus annual temperature analyses at 33 standard levels;

(f) one-degree monthly minus annual analyses for 24 standard levels;

(g) one-degree fields of the annual standard deviation of temperature at 33 standard depth levels;

(h) one-degree fields of the seasonal standard deviation at 33 standard depth levels;

(i) one-degree fields of the monthly standard deviation at 24 standard depth levels;

(j) one-degree fields of the annual standard error of the mean for temperature at 33 standard depth levels;

(k) one-degree fields of the seasonal standard error of the mean at 33 standard depth levels;

(l) one-degree fields of the monthly standard error of the mean at 24 standard depth levels;

(m) one-degree fields of the unanalyzed annual temperature mean field at 33 standard depth levels;

(n) one-degree fields of the unanalyzed seasonal mean field at 33 standard depth levels;

(o) one-degree fields of the unanalyzed monthly mean field at 24 standard depth levels;

(p) one-degree temperature unanalyzed annual mean minus objectively analyzed mean values at 33 standard depth levels. These fields represent the

combined interpolation and smoothing "error" of our analyses An example of these statistics is shown in Fig.4;·

(q) one-degree unanalyzed seasonal mean minus objectively analyzed seasonal mean values at 33 standard levels;

(r) one-degree unanalyzed monthly mean minus objectively analyzed monthly mean values for 24 depth levels;

(s) land-sea file used in the analysis;

(t) definition of ocean basin masks used in the analysis.

The sample standard deviation in a gridbox was computed using:

$$s = \sqrt{\frac{\sum_{n=1}^{N} (x_n - \bar{x})^2}{N-1}} \qquad (11)$$

in which x_n= the n^{th} data value in the gridbox, $\bar{x}$ =mean of all data values in the gridbox, and N= total number of data values in the gridbox. The standard error of the mean was computed by dividing the standard deviation by the square root of the number of observations in each gridbox.

5. SUMMARY

In the preceding sections we have described the results of a project to objectively analyze all historical temperature data archived at NODC/WDC-A, including substantial amounts of data gathered as a result of the NODC and IOC data archaeology and rescue projects. We desire to build a set of climatological analyses that are as similar as possible in all respects for all variables including relatively data sparse variables such as nutrients. This provides investigators with a consistent set of analyses to work with.

One advantage of the analysis techniques used in this atlas is that we know the amount of smoothing by objective analyses as given by the response function in Table 2 and Figure 2. We believe this to be an important function for constructing and describing a climatology of any geophysical parameter. Particularly when computing anomalies from a standard climatology, it is important that the synoptic field be smoothed to the same extent as the climatology, to prevent generation of spurious anomalies simply through differences in smoothing. A second reason is that purely diagnostic computations require a minimum of seven or eight gridpoints to represent any Fourier component with accuracy. Higher order derivatives will require more smoothing.

We have attempted to create objectively analyzed fields and data sets that can be used as a "black box." We emphasize that some quality control procedures used are subjective. For those users who wish to make their own choices, all the data used in our analyses are available both at standard depth levels as well as observed depth levels (*World Ocean Database 1998* CD-ROM set - Conkright *et al.*, 1998c). The results presented in this atlas show some features that are suspect and may be due to nonrepresentative or incorrect data that were not flagged by the quality control techniques used. Although we have attempted to eliminate as many of these features as possible by flagging the data which generate these features some obviously remain. Some may eventually turn out not to be artifacts but rather to represent real features, not yet capable of being described in a meaningful way due to lack of data.

6. FUTURE WORK

Our analyses will be updated when justified by additional observations. As more data are received at NODC/WDC-A, we will also be able to produce higher resolution climatologies for each variable as Boyer and Levitus (1997) have done for temperature and salinity.

References

Achtemeier, G. L., 1987: On the concept of varying influence radii for a successive corrections objective analysis. *Monthly Weather Review,* 11, 1761-1771.

Banes, J., and M.H. Sessions, 1984: A field performance test of the Sippican deep aircraft-deployed expendable bathythermograph. *J. Geophys. Res.*, 89, 3615-3621.

Barnes, S. L., 1964: A technique for maximizing details in numerical weather map analysis. *J. App. Meteor.*, 3, 396-409.

_____ 1973: Mesoscale objective map analysis using weighted time series observations. *NOAA Technical Memorandum ERL* NSSL-62, 60 pp.

_____ 1994: Applications of the Barnes Objective Analysis Scheme, Part III: Tuning for Minimum Error. *J. Atmosph. and Oceanic Tech.* 11:1459-1479.

Bergthorsson, P., and B. Doos, 1955: Numerical Weather map analysis. *Tellus*, 7, 329-340.

Boyd, and Linzell, 1992: The temperature and depth accuracy of Sippican T-5 XBTs. *J. Atmosph. and Oceanic Tech.*, 10, 128-136.

Boyer, T. P., and S. Levitus, 1994: Quality control and processing of historical temperature, salinity and oxygen data. *NOAA Technical Report NESDIS 81*, 65 pp.

Boyer, T.P., and S. Levitus, 1997: *Objective Analyses of temperature and salinity for the world ocean on a 1/4 °grid. NOAA/NESDIS Atlas 11.* U.S. Gov. Printing Office, Wash., D.C., 62 pp.

Boyer, T. P., J. Antonov, Levitus, S., M.E. Conkright, T. O'Brien, C. Stephens, D. Johnson, and R. Gelfeld,1998a: *World Ocean Database 1998 Volume 3: Temporal Distribution of Expendable Bathythermograph Profiles*. NOAA Atlas NESDIS 20, U.S. Government Printing Office, Wash., D.C. 170 pp.

Boyer, T.P., M.E. Conkright, S. Levitus, C. Stephens, T. O'Brien, J. Antonov, D. Johnson, R. Gelfeld, 1998b: *World Ocean Database 1998, Volume 4: Temporal Distribution of Conductivity-Temperature-Depth Profiles. NOAA Atlas NESDIS 21*, U.S. Government Printing Office, Wash., D.C., 163 pp.

Boyer, T.P., M.E. Conkright, S. Levitus, , D. Johnson, T. O'Brien, C. Stephens, R. Gelfeld, 1998c: *World Ocean Database 1998, Volume 5: Temporal Distribution of Ocean Station Data (Bottle) Temperature-Salinity Profiles. NOAA Atlas NESDIS 22*, U.S. Government Printing Office, Wash., D.C., 108 pp.

Conkright, M. E., Levitus, S., and Boyer, T. P., 1994: *World Ocean Atlas 1994, Vol 1: Nutrients*. National Oceanic and Atmospheric Administration, Wash., D.C., 150 pp.

Conkright, M.E. , T.P. Boyer, S. Levitus, D. Johnson, T. O'Brien, C. Stephens, R. Gelfeld, 1998a: *World Ocean Database 1998, Volume 6: Temporal Distribution of Ocean Station Data (Bottle) Nutrient profiles. NOAA Atlas NESDIS 23*, U.S. Government Printing Office, Wash., D.C., 296 pp.

Conkright M.E., L. Stathoplos, T. O'Brien, T.P. Boyer, C. Stephens, D. Johnson, S. Levitus, 1998b: *World Ocean Database 1998, Volume 8: Temporal Distribution of Ocean Station Data (Bottle) Chlorophyll Profiles and Plankton Data. NOAA Atlas NESDIS 25*, U.S. Government Printing Office, Wash., D.C.,

Conkright, M. E., S. Levitus, T. O'Brien, T.P. Boyer, C. Stephens, D. Johnson, L. Stathoplos, O. Baranova, J. Antonov, R. Gelfeld, J. Burney, J. Rochester, and C. Forgy, 1998c: *World Ocean Database 1998 CD-ROM Data Set Documentation.* National Oceanographic Data Center, Silver Spring, MD, 43 pp.

Cressman, G. P., 1959: An operational objective analysis scheme. *Mon. Wea. Rev.*, 87, 329-340.

Daley, R., 1991: *Atmospheric Data Analysis.* Cambridge University Press, Cambridge, 457 pp.

England, M.H., 1992: On the formation of Antarctic Intermediate and Bottom Water in Ocean general circulation models. *J. Phys. Oceanogr., 22, 918- 926.*

ETOPO5, 1988: Data Announcements 88-MGG-02, Digital relief of the Surface of the Earth. NOAA, National Geophysical Data Center, Boulder, CO.

Intergovernmental Panel on Climate Change, 1996: *Climate Change 1995 - The Science of Climate Change, Contribution of Working Group I to thte Second Assessment Report of the Intergovernmental Panel on Climate Change.* Editors J.J. Houghton, L.G. Meiro Filho, B.A. Callander, N. Harris, A. Kattenberg, and K. Maskell. Cambridge University Press, Cambridge, UK, 572 pp.

Gandin, L.S., 1963: *Objective Analysis of Meteorological fields.* Gidrometeorol Izdat, Leningrad (translation by Israel program for Scientific Translations, Jerusalem, 1966); 242 pp.

Hallock, Z. R., and W.J. Teague, 1992: The fall rate of the T-7 XBT. *J. Atmosph. and Oceanic Tech.*, 9, 470-483.

Hanawa, K., and H. Yoritaka, 1987: Detection of systematic errors in XBT data and their correction. *J. Oceanogr. Soc. Japan*, 32, 68-76.

Hanawa, K., P. Rual, R. Bailey, A. Sy, and M. Szabados, 1994: Calculation of new depth equations for expendable bathythermographs using a temperature-error-free method (application to Sippican/TSK T-7, T-6 and T-4 XBTs). *IOC Technical Series* 42, 46 pp.

Hesselberg, T., and H. U. Sverdrup, 1914: Die Stabilitutsverhaltnisse des Seewassers bei Vertitalen Verschiebungen. *Aarb. Bergen Mus.*, No. 14, 17 pp.

IOC, 1992a: Summary report of the IGOSS task team on quality control for automated systems and addendum to the summary report. *IOC/INF-888,* 1992.

IOC, 1992b: Summary report of the IGOSS task team on quality control for automated sytems and addendum to the summary report. *IOC/INF-888-append.,* 1992.

Levitus, S., 1982: *Climatological Atlas of the World Ocean,* NOAA Professional Paper No. 13, U.S. Gov. Printing Office, 173 pp.

Levitus, S., and T. Boyer, 1994a: *World Ocean Atlas 1994, Vol 2: Oxygen.* NOAA Atlas NESDIS 2, Wash., D.C., 186 pp.

Levitus, S. and T. Boyer, 1994b: *World Ocean Atlas 1994, Vol 4: Temperature.* NOAA Atlas NESDIS 4, U.S. Government Printing Office, Wash., D.C., 117 pp.

Levitus, S., R. Burgett and T. Boyer, 1994a: *World Ocean Atlas 1994, Vol 3: Salinity.* NOAA Atlas NESDIS 3, Wash., D.C., 93 pp

Levitus, S., R. Gelfeld, T. Boyer, and D. Johnson, 1994b: *Results of the NODC Oceanographic Data Archaeology and Rescue Projects.* Key to Oceanographic Records Documentation No. 19, NODC, Wash., D.C. , 73 pp.

Levitus, S., T.P. Boyer, M.E. Conkright, T. O'Brien, J. Antonov, C. Stephens, L. Stathoplos, D. Johnson, and R. Gelfeld, 1998a: *World Ocean Database 1998 Volume 1: Introduction.* NOAA Atlas NESDIS 18, U.S. Government Printing Office, Wash., D.C., 346 pp.

Levitus, S., T.P. Boyer, M.E. Conkright, D. Johnson, T. O'Brien, J. Antonov, C. Stephens, and R. Gelfeld, 1998b: *World Ocean Database 1998, Volume 2: Temporal Distribution of Mechanical Bathythermograph Profiles. NOAA Atlas NESDIS 19,* U.S. Government Printing Office, Wash., D.C., 286 pp.

O'Brien, T., M.E. Conkright, T.P. Boyer, S. Levitus, , D. Johnson, C. Stephens, R. Gelfeld, 1998: *World Ocean Database 1998, Volume 7: Temporal Distribution of Station Data (Bottle) Oxygen Profiles. NOAA Atlas NESDIS 24*, U.S. Government Printing Office, Wash., D.C., 235 pp.

Lynn, and J. L. Reid, 1968: Characteristics and circulation of deep and abyssal waters. *Deep Sea Research.*, 15, 577-598.

Neumann, G. and W. J. Pierson, 1966: *Principles of Physical Oceanography*. Prentice Hall Inc., Englewood Cliffs, N.J., 545 pp.

Rabiner, L. R., M. R. Sambur, and C. E. Schmidt, 1975: *Applications of a nonlinear smoothing algorithm to speech processing, IEEE Trans. on Acoustics, Speech and Signal Processing*, Vol. Assp-23, 552-557.

Reiniger, R.F., and C.F. Ross, 1968: A method of interpolation with application to oceanographic data. *Deep-Sea Res.*, 9, 185-193.

Sasaki, Y., 1960: An objective analysis for determining initial conditions for the primitive equations. Ref. 60-1 6T, Atmospheric Research Lab., Univ. of Oklahoma Research Institute, Norman, 23 pp.

Seaman, R. S., 1983. Objective Analysis accuracies of statistical interpolation and successive correction schemes. *Australian Meteor. Mag.*, 31, 225-240.

Shuman, F. G., 1957: Numerical methods in weather prediction: II. Smoothing and filtering. *Mon. Wea. Rev.*, 85, 357-361.

Singer, J. J., 1990: On the error observed in electronically digitized T-7 XBT data. *J. Atmos. Oceanic Technol.*, 7, 603-611.

Smith, D. R., and F. Leslie, 1984: Error determination of a successive correction type objective analysis scheme. *J Atm. and Oceanic Tech.*, 1, 121-130.

Smith, D.R., M.E. Pumphry, and J.T. Snow, 1986: A comparison of errors in objectively analyzed fields for uniform and nonuniform station distribution, *J. Atm. Oceanic Tech.*, 3, 84-97.

Spilhaus, A. F., A. Ehrlich, and A.R. Miller, 1950: Hydrostatic instability in the ocean. *Transactions Amer. Geophys. Union.*, 31(2).

Sverdrup, H.U., M.W. Johnson, and R.H. Fleming, 1942: *The Oceans: Their physics, chemistry, and general biology.* Prentice Hall, 1060 pp.

Thiebaux, H.J., M.A. Pedder, 1987: *Spatial Objective Analysis: with applications in atmospheric science*. Academic Press, 299 pp.

Tukey, J. W., 1974: Nonlinear (nonsuperposable) methods for smoothing data, in *"Cong. Rec."*, 1974 EASCON, 673 pp.

UNESCO, 1991: *Processing of Oceanographic Station Data.* Imprimerie des Presses Unibversitaires de France, Imprimerie des Presses Universitaires de France, Vendome, 138 pp.

Wright, D., and M. Szabados, 1989: Field evaluation of real-time XBT systems. *Oceans 89 Proc.*, 5, 1621-1626.

Table 1. Acceptable distances (m) for defining interior and exterior values used in the Reiniger-Ross scheme for interpolating observed level data to standard levels.

Standard Level number	Standard depths (m)	Acceptable distances (m) for interior values	Acceptable distances (m) for exterior values
1	0	5	200
2	10	50	200
3	20	50	200
4	30	50	200
5	50	50	200
6	75	50	200
7	100	50	200
8	125	50	200
9	150	50	200
10	200	50	200
11	250	100	200
12	300	100	200
13	400	100	200
14	500	100	400
15	600	100	400
16	700	100	400
17	800	100	400
18	900	200	400
19	1000	200	400
20	1100	200	400
21	1200	200	400
22	1300	200	1000
23	1400	200	1000
24	1500	200	1000
25	1750	200	1000
26	2000	1000	1000
27	2500	1000	1000
28	3000	1000	1000
29	3500	1000	1000
30	4000	1000	1000
31	4500	1000	1000
32	5000	1000	1000
33	5500	1000	1000

Table 2. Response function of the objective analysis scheme as a function of wavelength for WOA98 and earlier analyses.

Wavelength*	Levitus (1982)	WOA94	WOA98
360ΔX	1.000	0.999	1.000
180ΔX	1.000	0.997	0.999
120ΔX	1.000	0.994	0.999
90ΔX	1.000	0.989	0.998
72ΔX	1.000	0.983	0.997
60ΔX	1.000	0.976	0.995
45ΔX	1.000	0.957	0.992
40ΔX	0.999	0.946	0.990
36ΔX	0.999	0.934	0.987
30ΔX	0.996	0.907	0.981
24ΔX	0.983	0.857	0.969
20ΔX	0.955	0.801	0.952
18ΔX	0.923	0.759	0.937
15ΔX	0.828	0.671	0.898
12ΔX	0.626	0.532	0.813
10ΔX	0.417	0.397	0.698
9ΔX	0.299	0.315	0.611
8ΔX	0.186	0.226	0.500
6ΔX	3.75×10^{-2}	0.059	0.229
5ΔX	1.34×10^{-2}	0.019	0.105
4ΔX	1.32×10^{-3}	2.23×10^{-3}	2.75×10^{-2}
3ΔX	2.51×10^{-3}	1.90×10^{-4}	5.41×10^{-3}
2ΔX	5.61×10^{-7}	5.30×10^{-7}	1.36×10^{-6}

* For ΔX = 111 km

Table 3. Basins defined for objective analysis and the shallowest standard depth level for which each basin is defined.

BASIN	STANDARD DEPTH LEVEL	BASIN	STANDARD DEPTH
Aleutian Basin	28	Hudson Bay	1
Andaman Basin	25	Indian Ocean	1 *
Arabian Sea	30	Java Sea	6
Arctic Ocean	1 *	Kara Sea	8
Argentine Basin	31	Marianas Basin	30
Atlantic Indian Basin	31	Mascarene Basin	30
Atlantic Ocean	1 *	Mediterranean Sea	1 *
Baffin Bay	14	North Caribbean	26
Baltic Sea	1	North American Basin	31
Banda Sea	23	Pacific Ocean	1 *
Barents Sea	28	Persian Gulf	1
Bay of Bengal	1 *	Philippine Sea	30
Beaufort Sea	28	Red Sea	1
Black Sea	1	Sea of Okhotsk	19
Brazil Basin	30	Sea of Japan	1
Caribbean Sea	23	Somali Basin	30
Caspian Sea	1	South China Sea	28
Celebes Sea	25	Southeast Pacific	29
Central Indian Ocean	29	Southeast Indian	29
Chile Basin	30	Southeast Atlantic	29
Coral Sea	29	Southern Ocean	1 *
Crosat Basin	30	Southwest Atlantic	29
East Indian Ocean	29	Sulu Sea	10
East Mediterranean	16	Sulu Sea II	14
East Caroline Basin	30	Tasman Sea	30
Fiji Basin	29	Venezuela	14
Guatemala Basin	29	West Mediterranean	19
Guinea Basin	30	West European Basin	31
Gulf of Mexico	26		

Basins marked with a "" can interact with adjacent basins

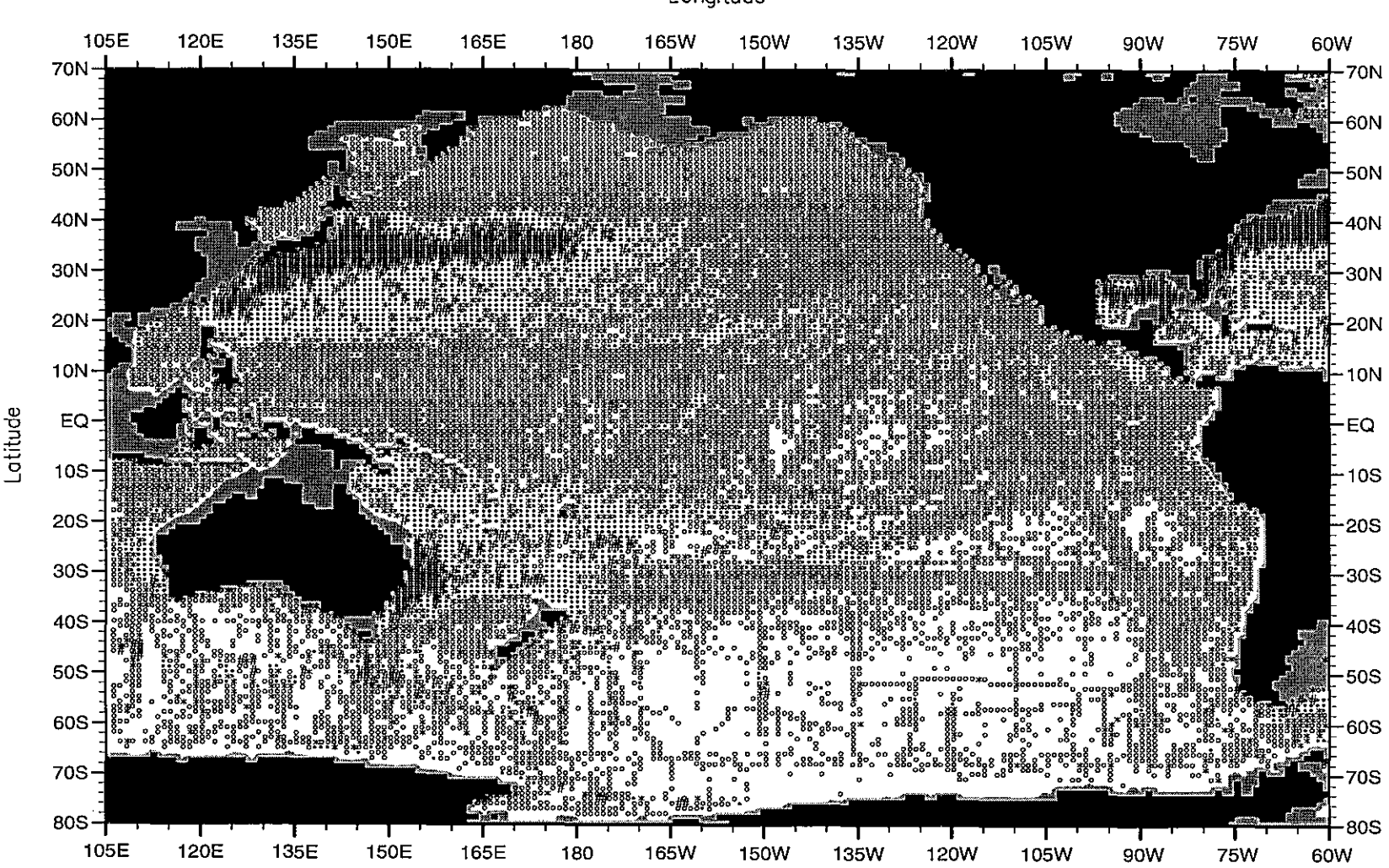


Fig. 1a. Annual temperature standard deviation (°C) at 500 meters depth by one-degree squares.

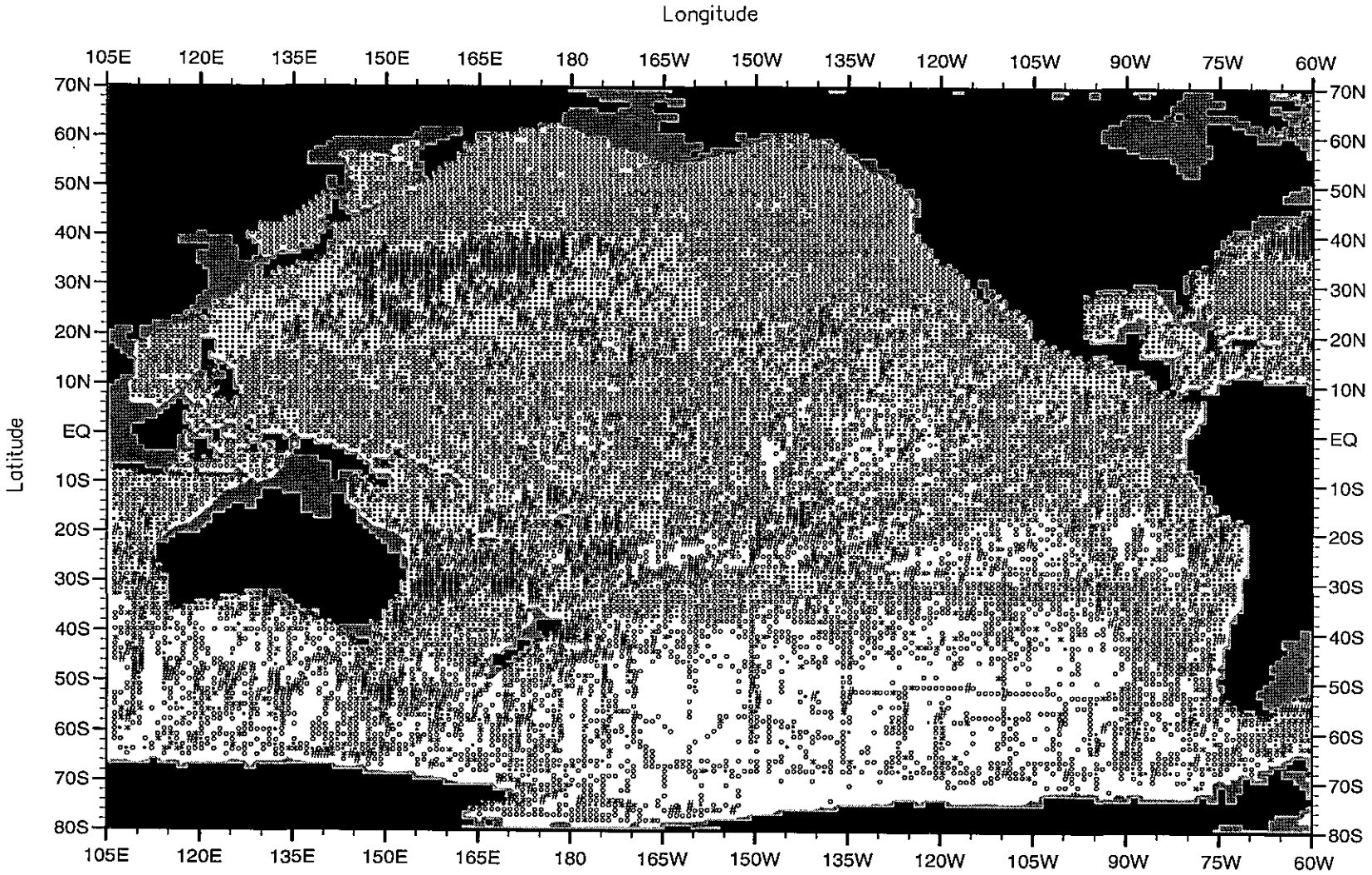


Fig. 1b. Annual temperature standard error of the mean (°C) at 500 meters depth by one-degree squares.

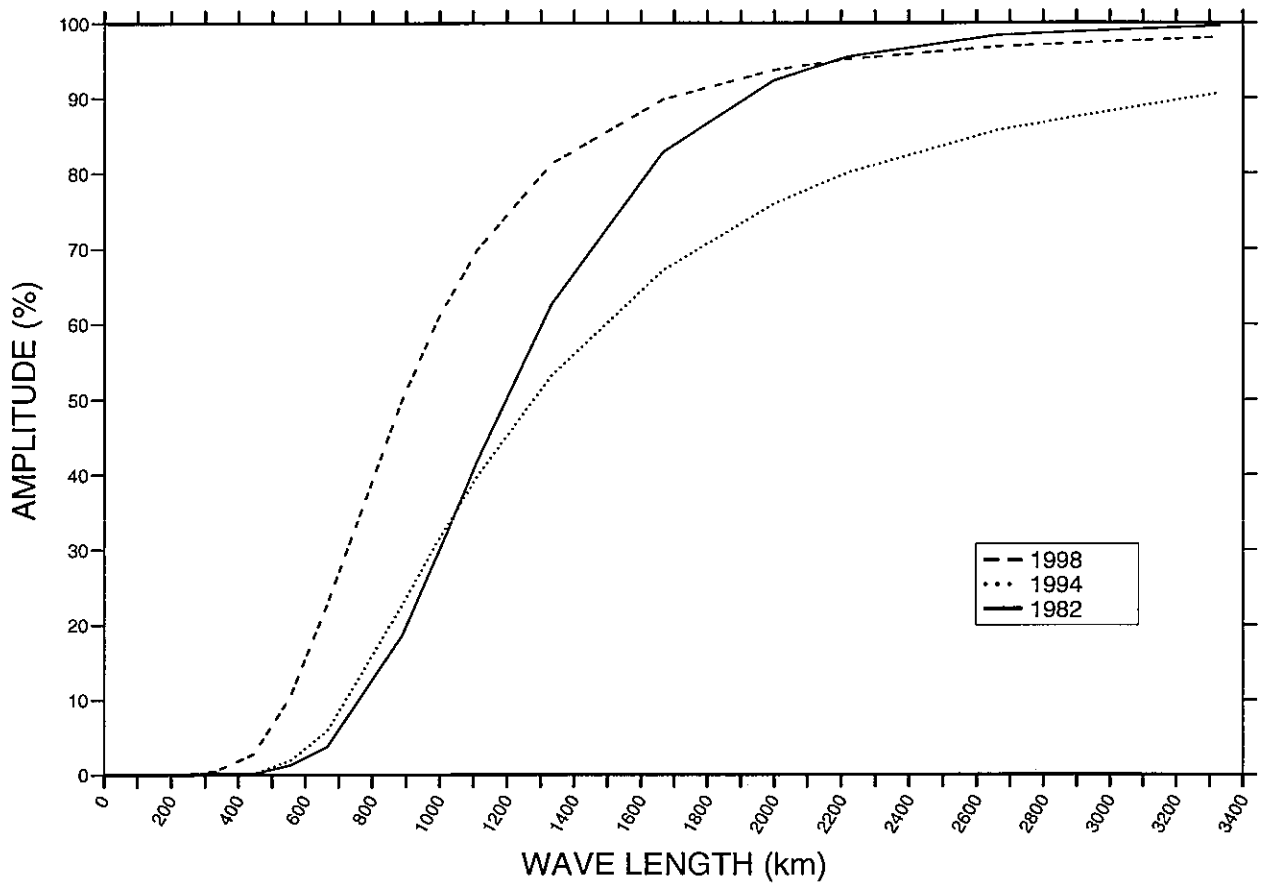


Figure 2. Response function of the WOA98, WOA94, and Levitus (1982) objective analysis schemes.

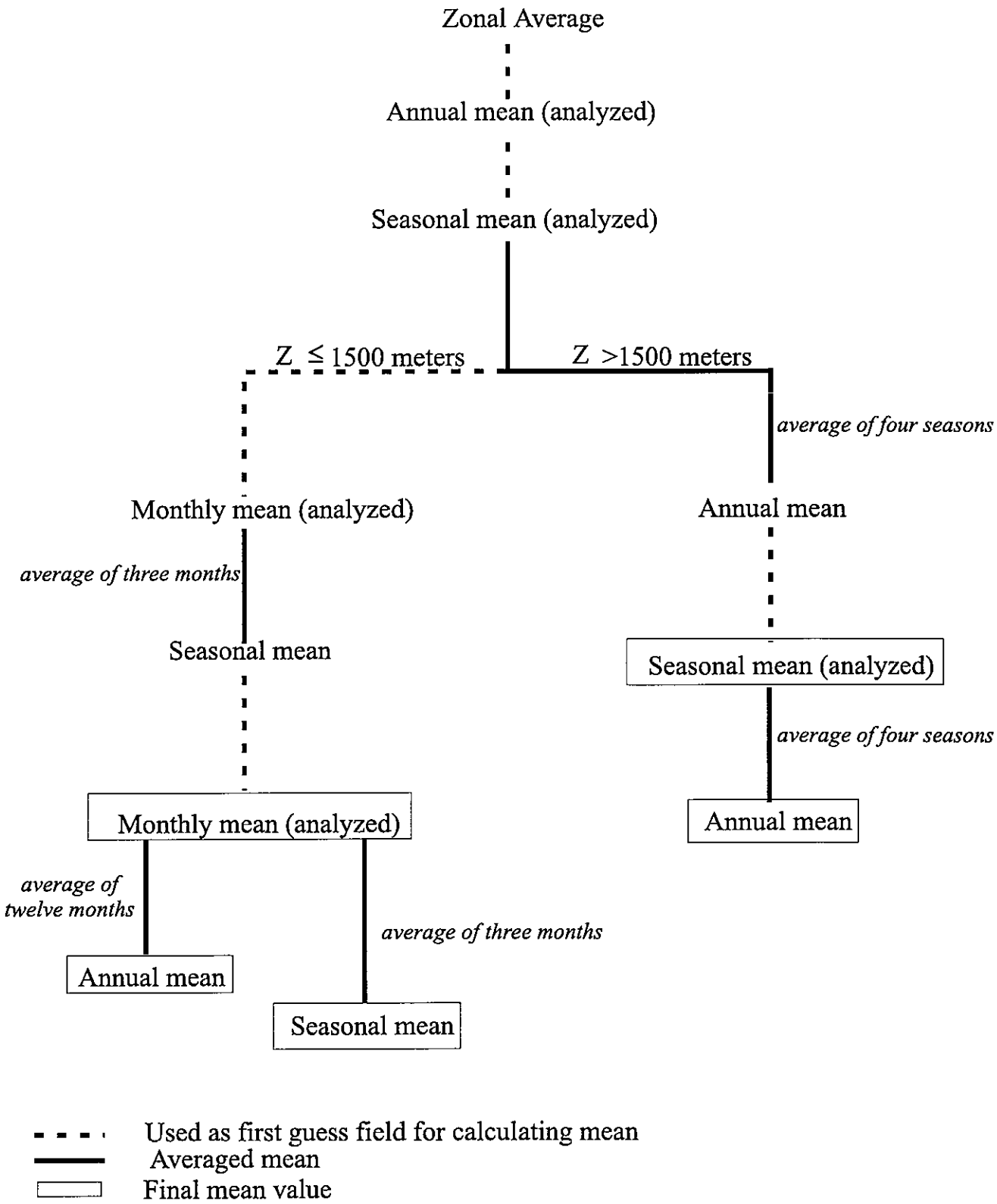


Figure 3. Scheme used in computing annual, seasonal, and monthly objectively analyzed means for a variable.

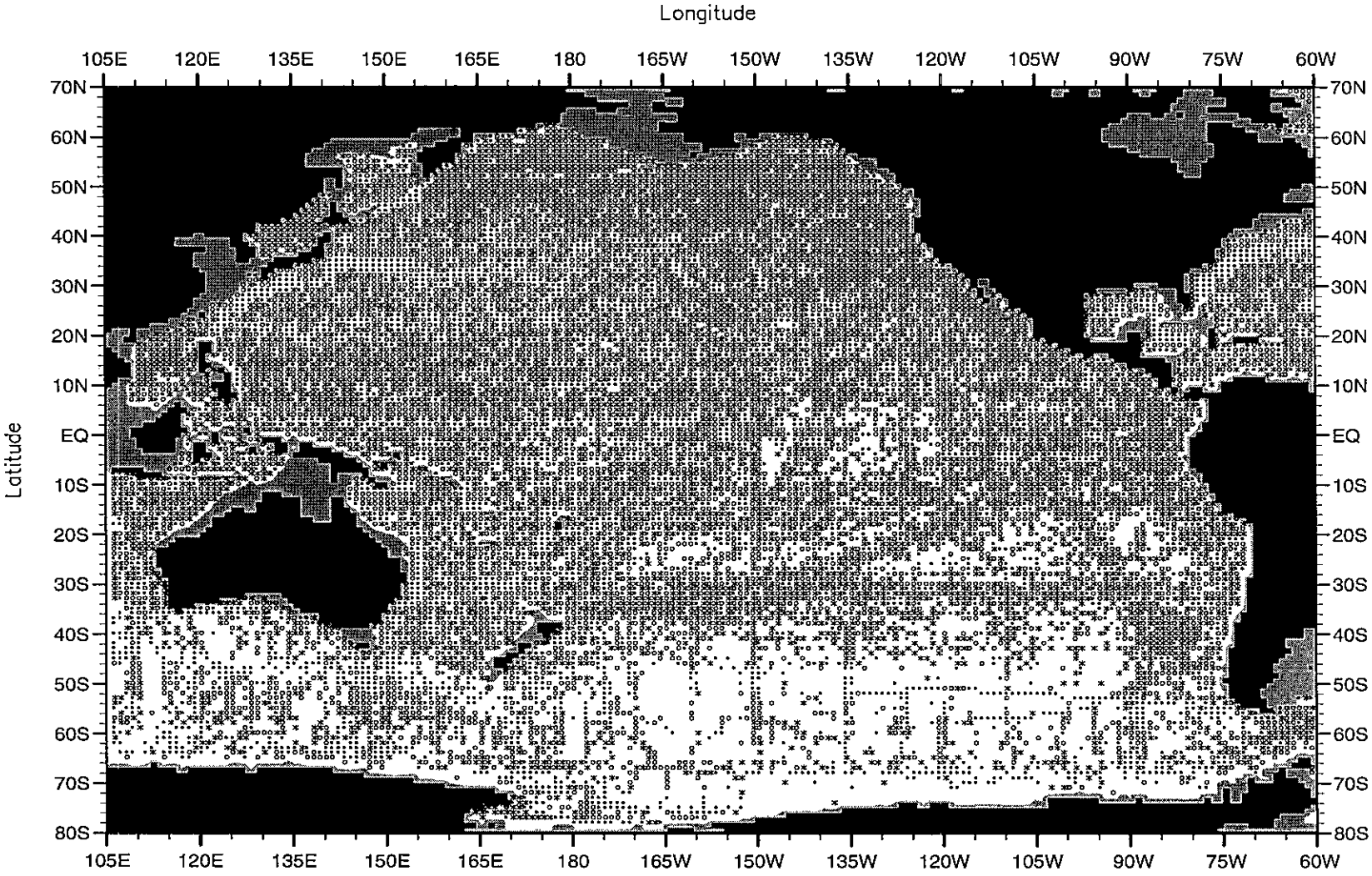


Fig. 4. Annual observed one-degree square temperature mean value minus objectively analyzed annual mean temperature values (°C) at 500 meters depth.

APPENDICES

In each data distribution figure in each appendix, a small dot indicates a one-degree square containing 1-4 observations and a large dot indicates a one-degree square containing five or more observations.

In each figure showing an objectively analyzed mean field or difference between seasonal (monthly) mean and annual mean, gridpoints for which there were less than four one-degree square values available to correct the first-guess are indicated by an "x".

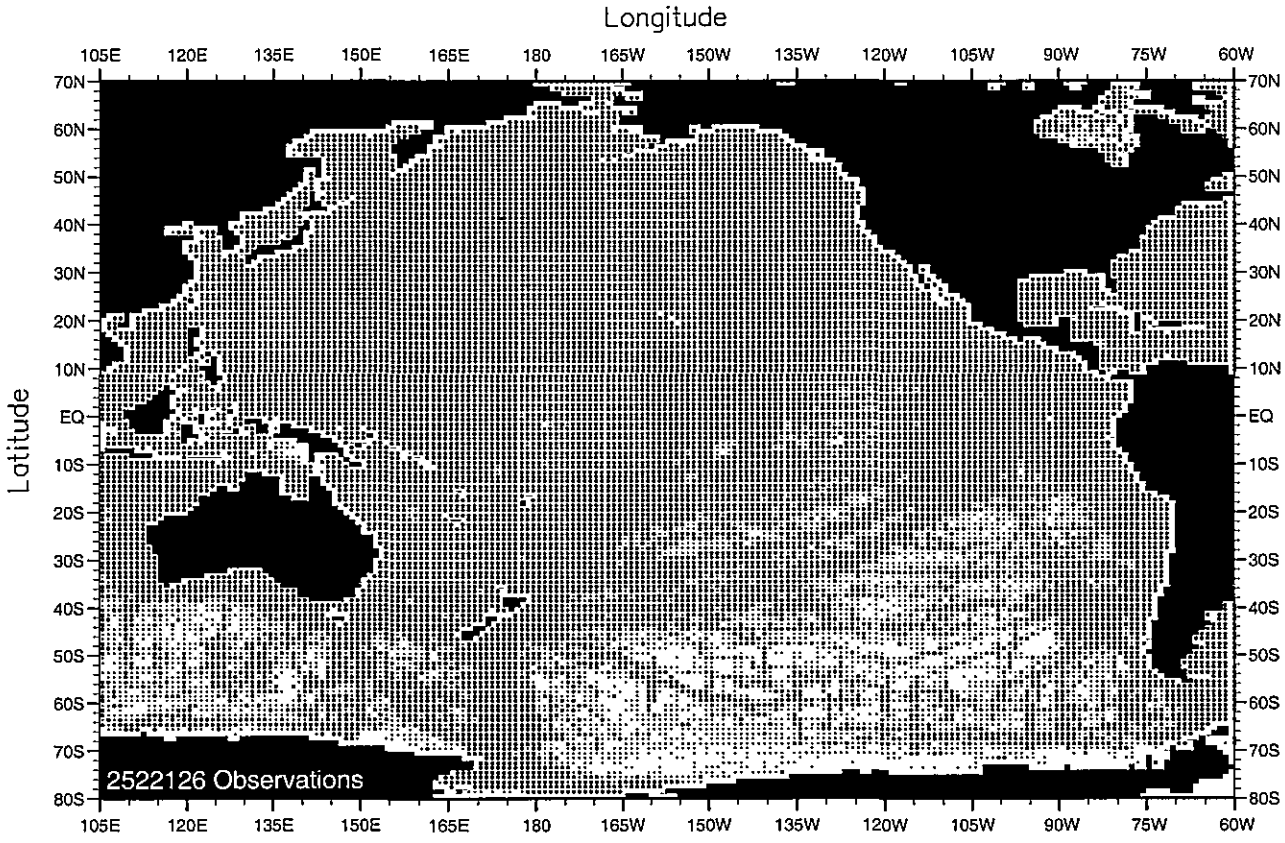


Fig. A1. Annual temperature observations at the surface .

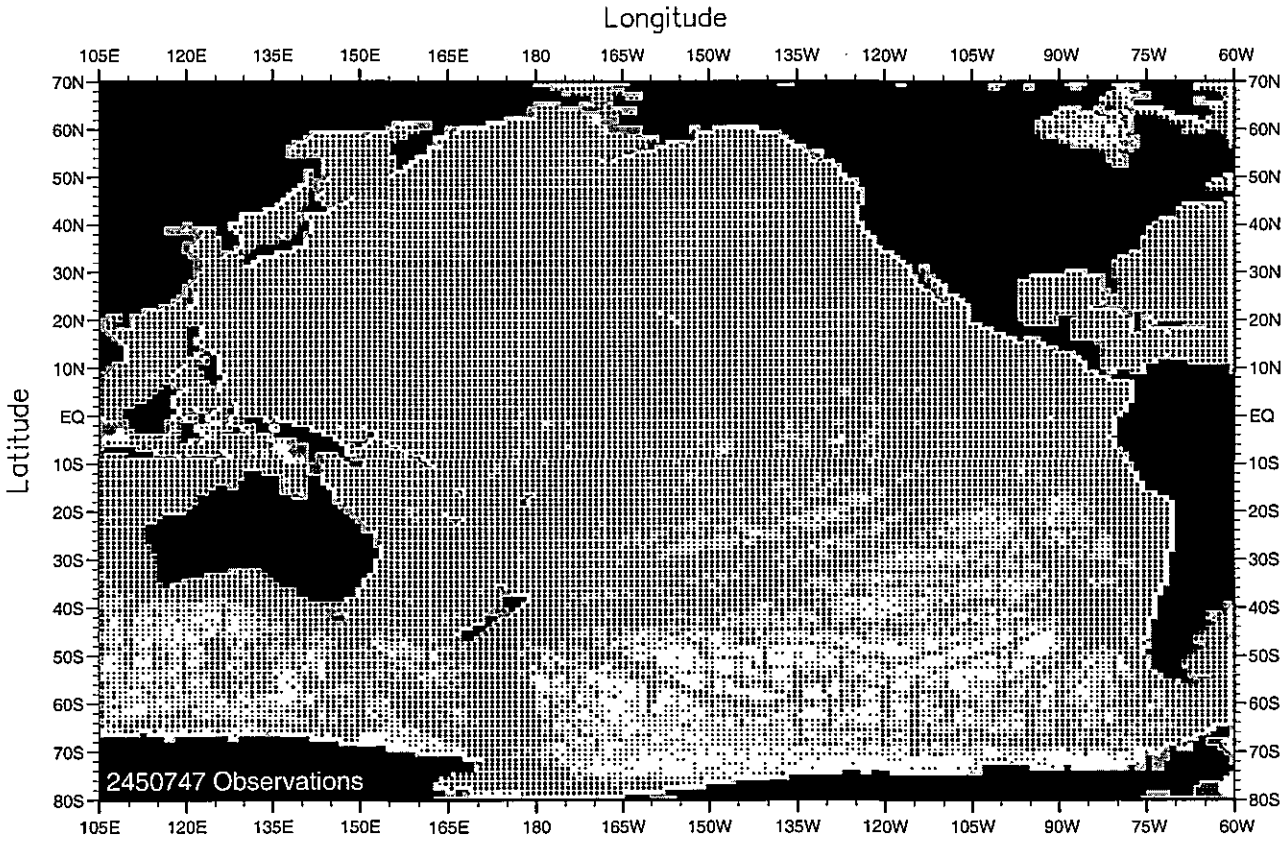


Fig. A2. Annual temperature observations at 50 m. depth .

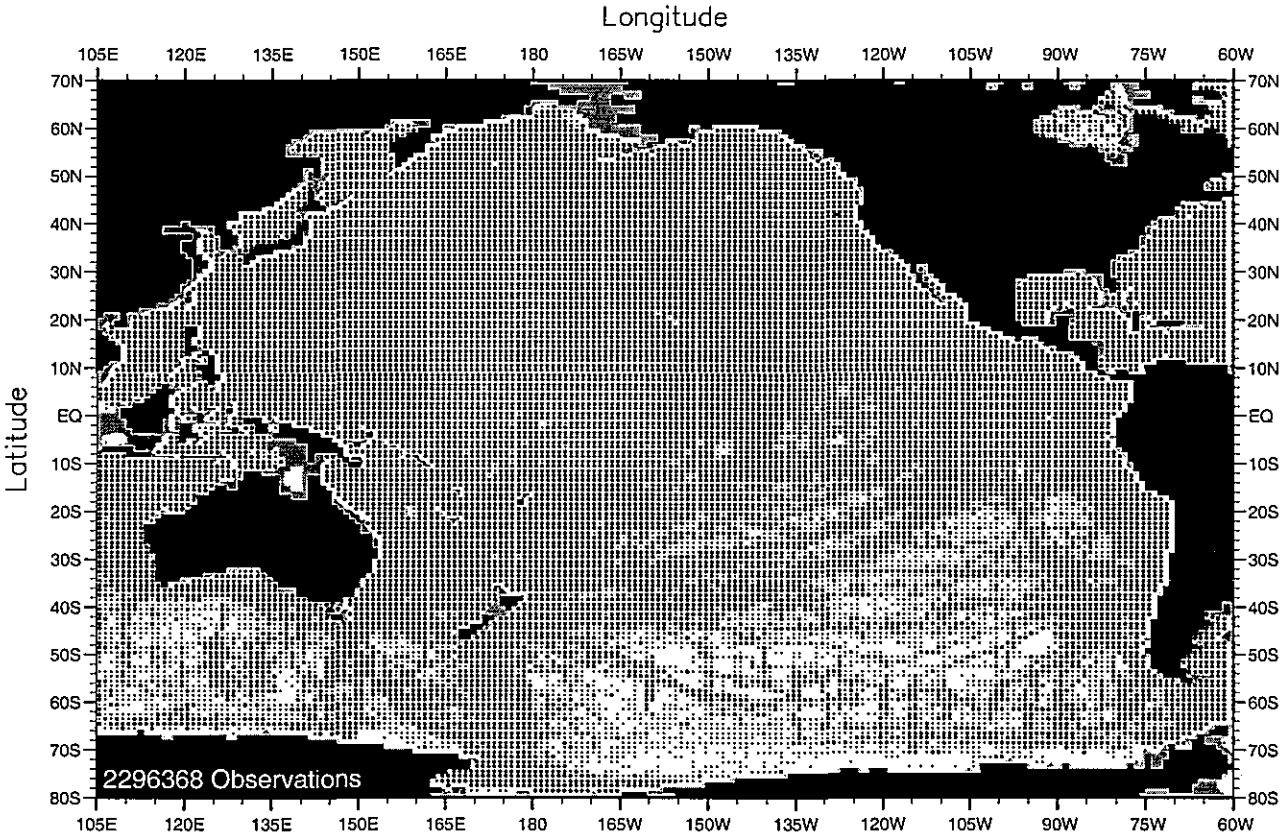


Fig. A3. Annual temperature observations at 75 m. depth .

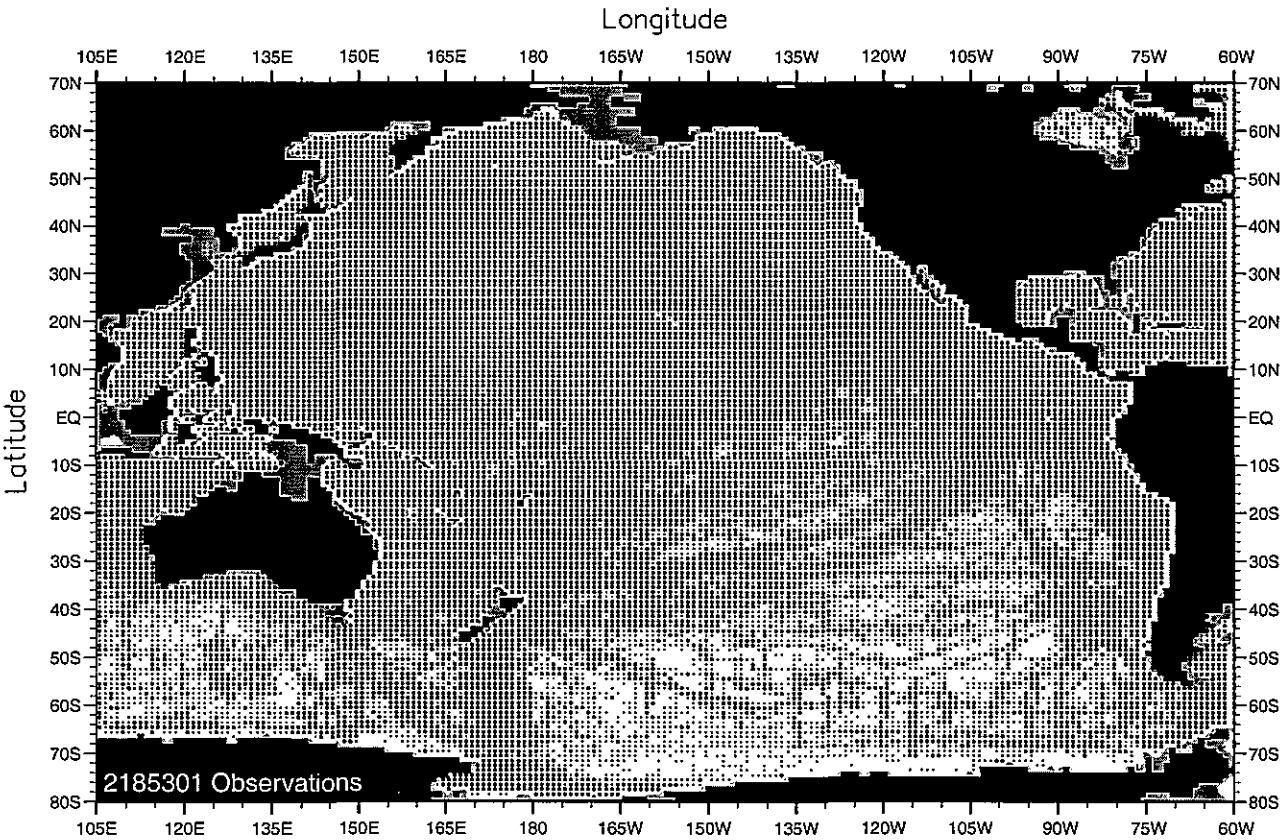


Fig. A4. Annual temperature observations at 100 m. depth .

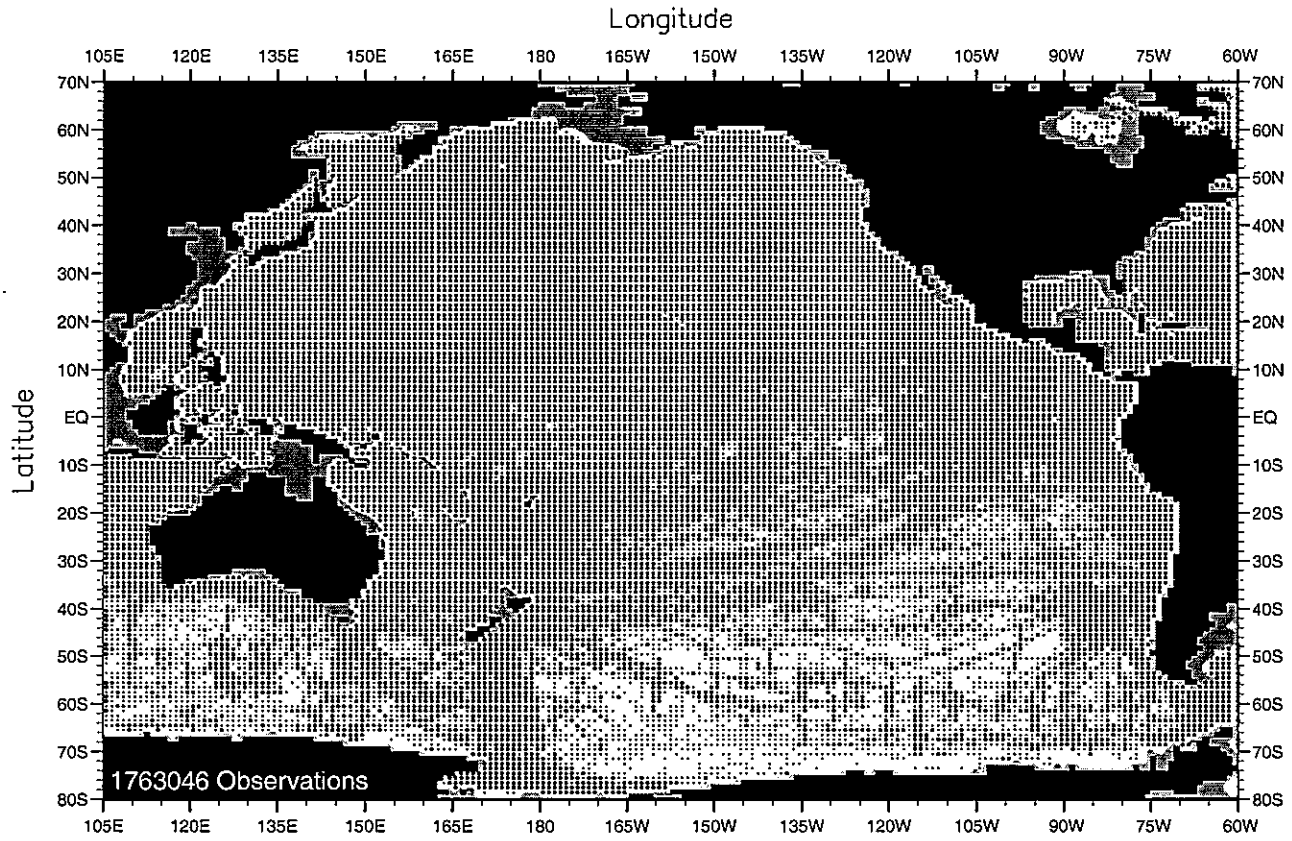


Fig. A5. Annual temperature observations at 150 m. depth .

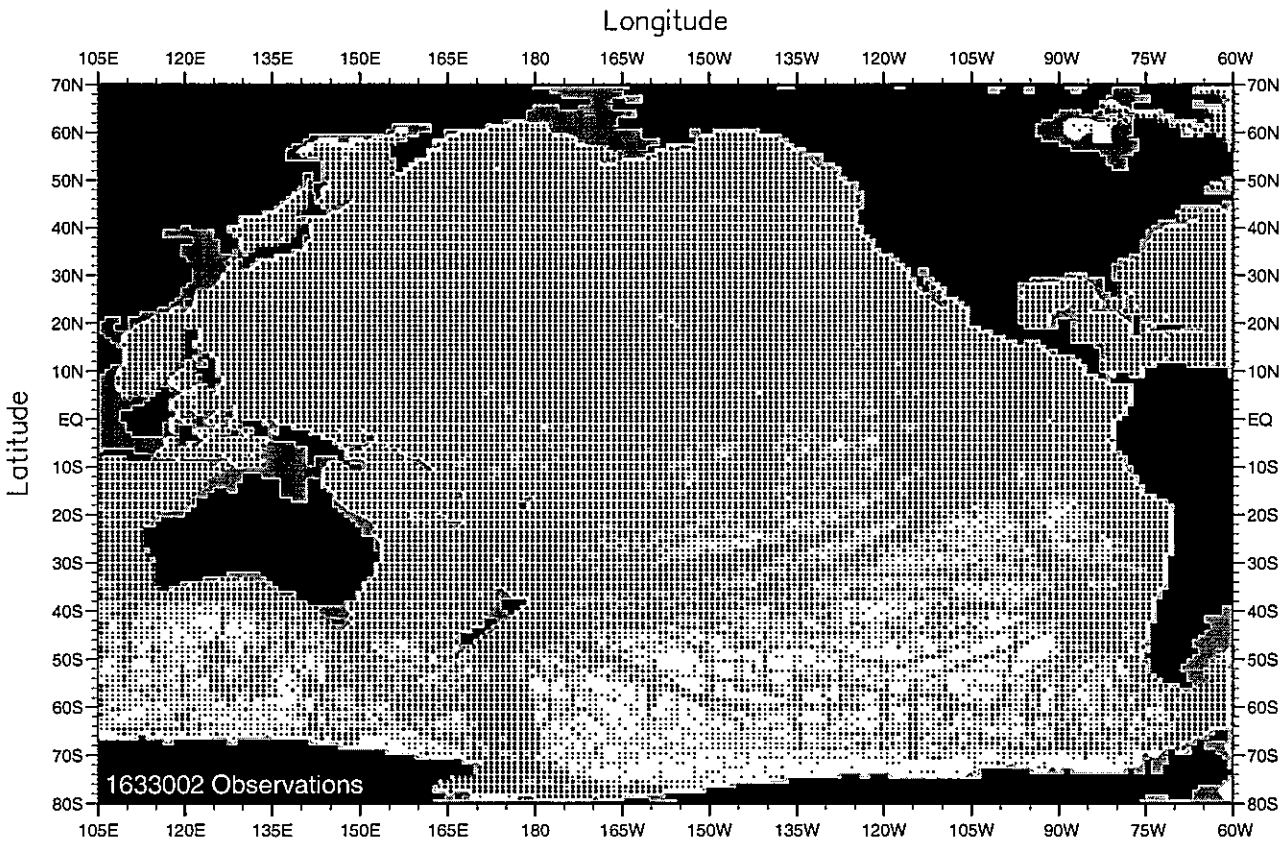


Fig. A6. Annual temperature observations at 200 m. depth .

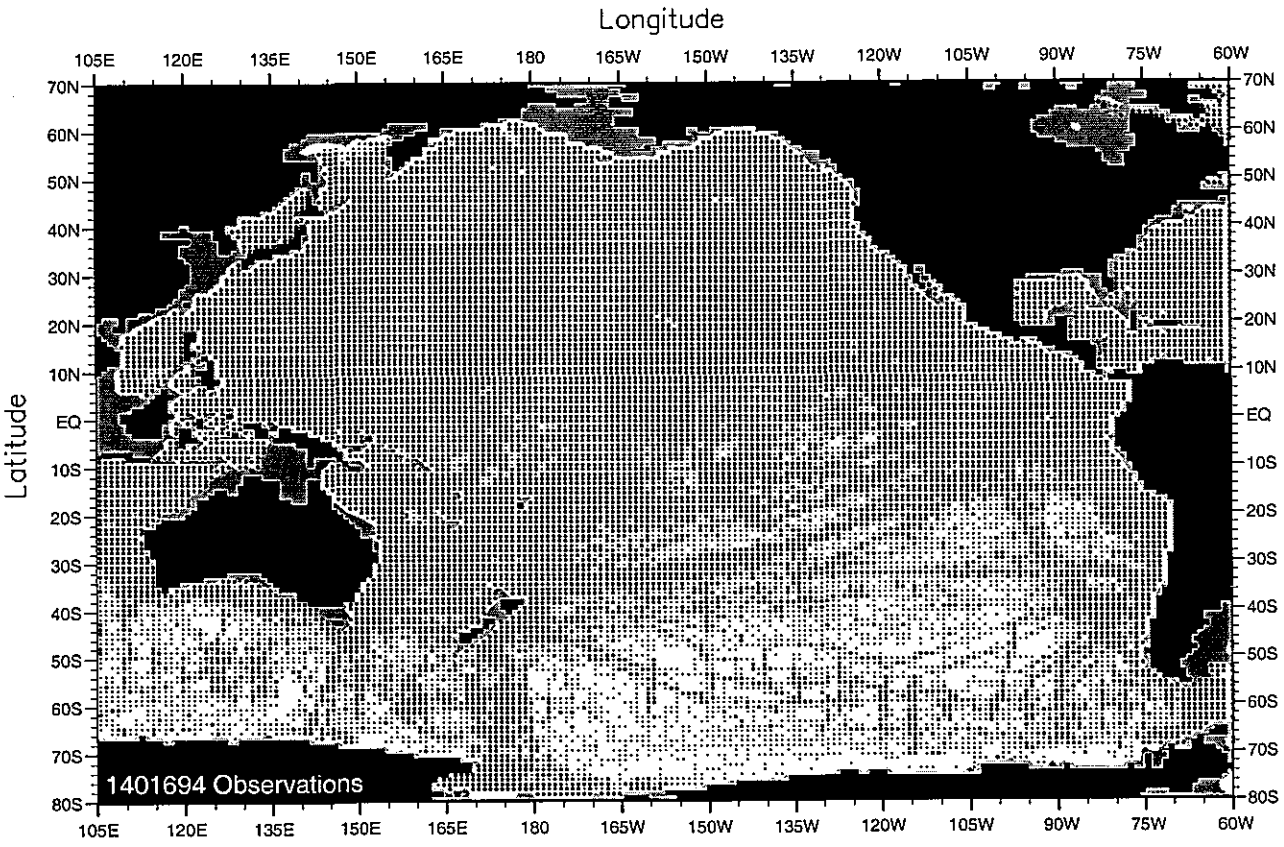


Fig. A7. Annual temperature observations at 250 m. depth .

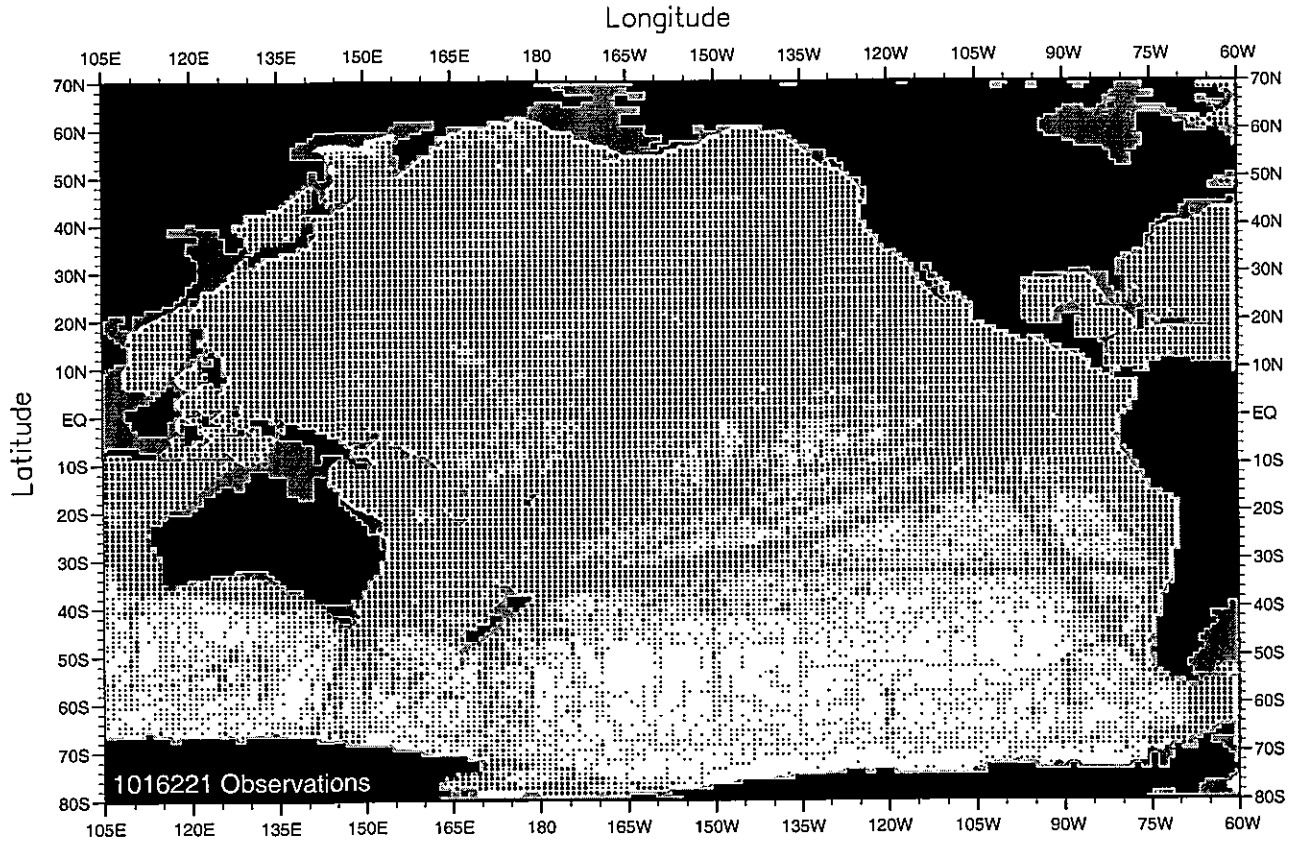


Fig. A8. Annual temperature observations at 400 m. depth .

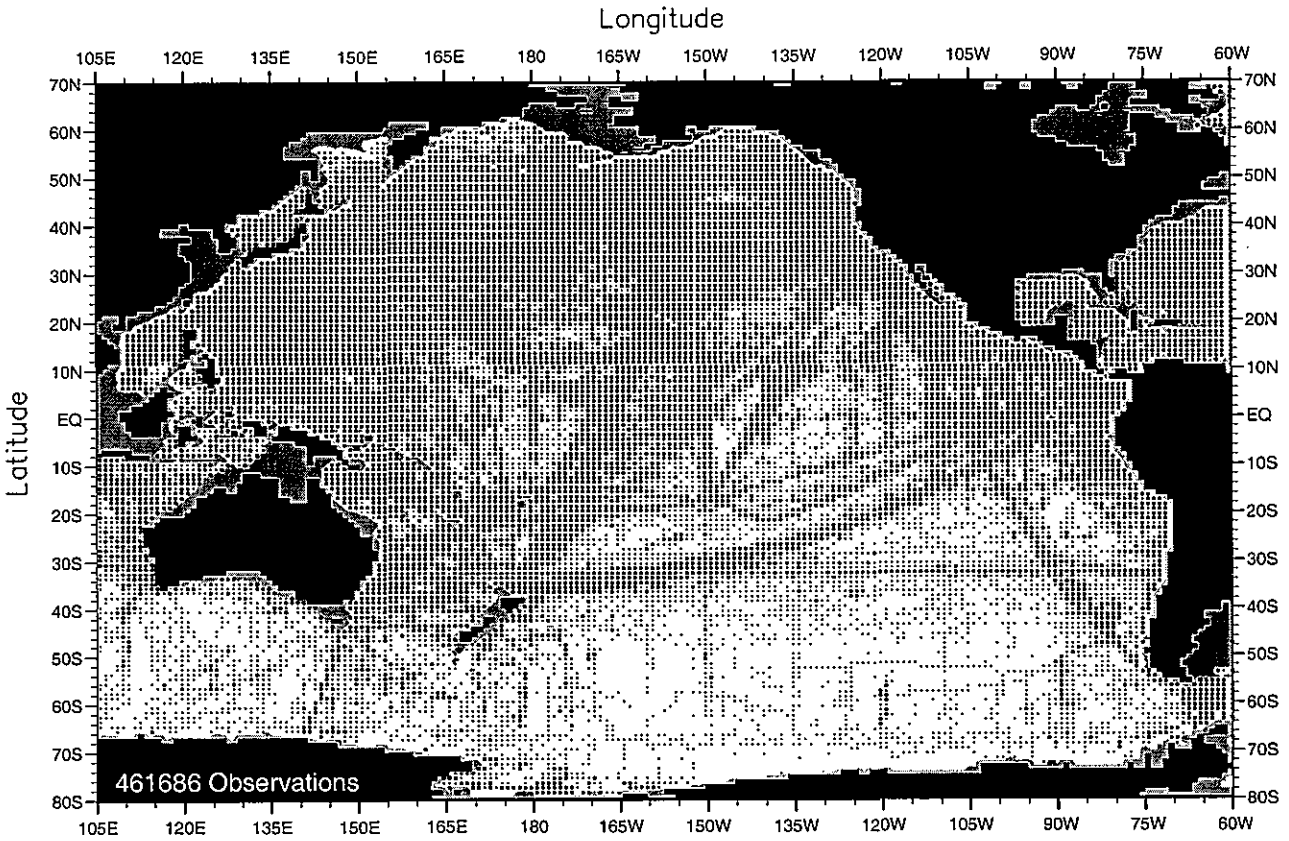


Fig. A9. Annual temperature observations at 500 m. depth .

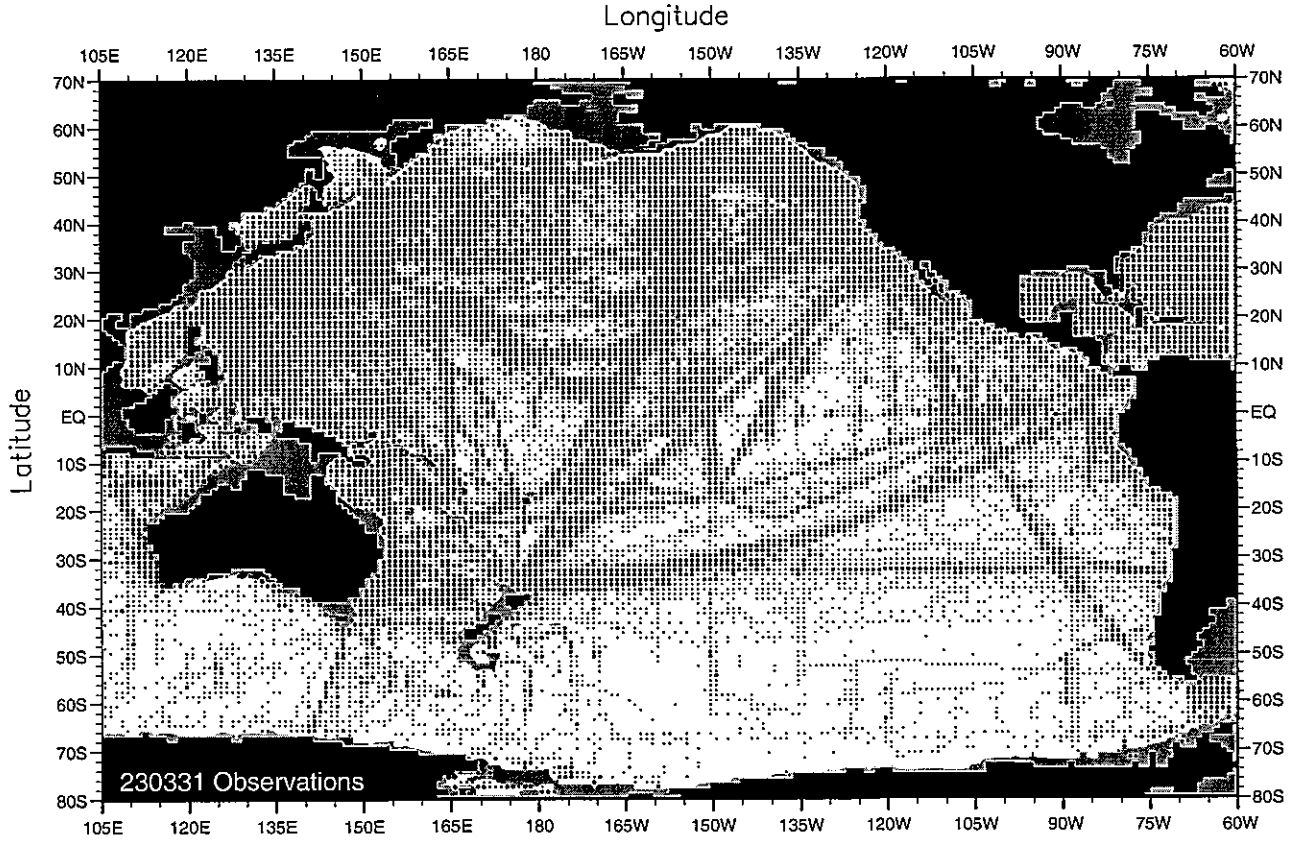


Fig. A10. Annual temperature observations at 700 m. depth .

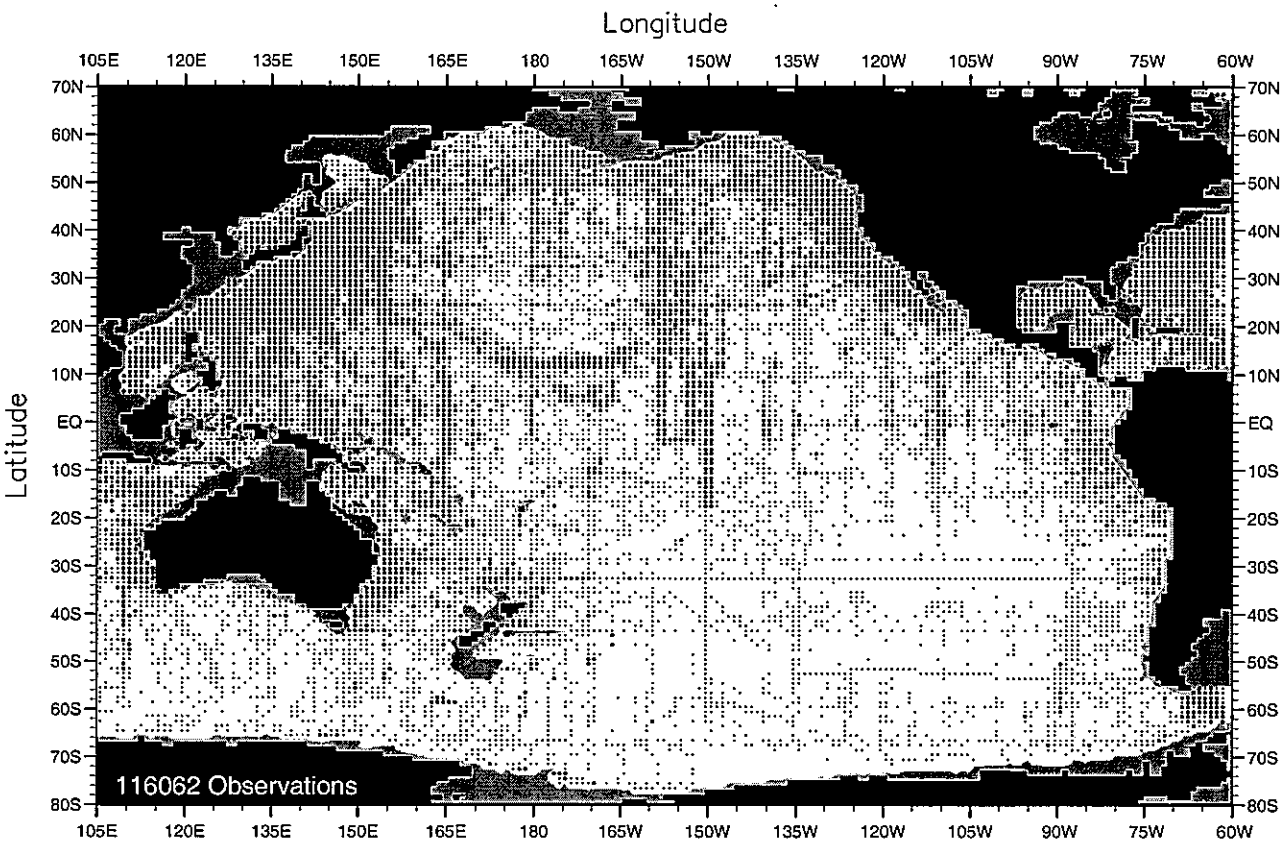


Fig. A11. Annual temperature observations at 1000 m. depth .

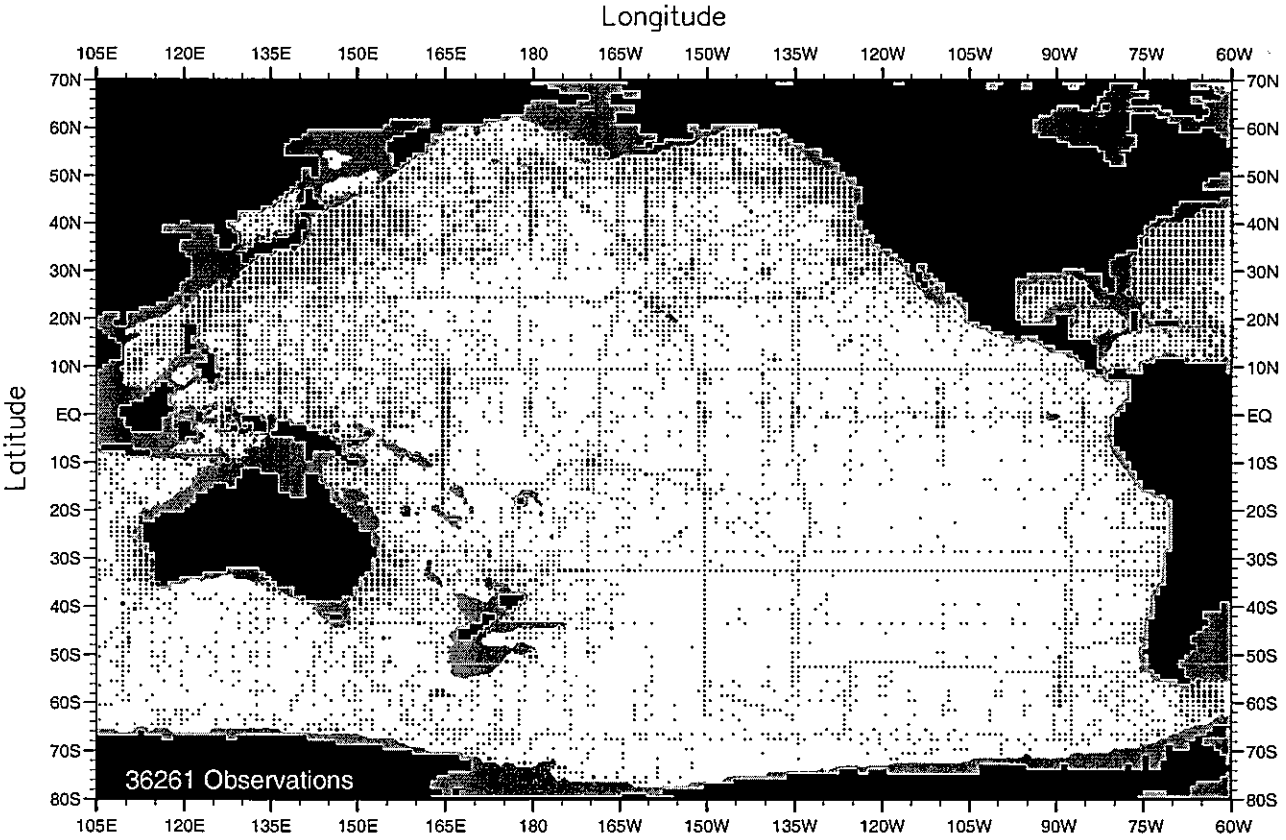


Fig. A12. Annual temperature observations at 1500 m. depth .

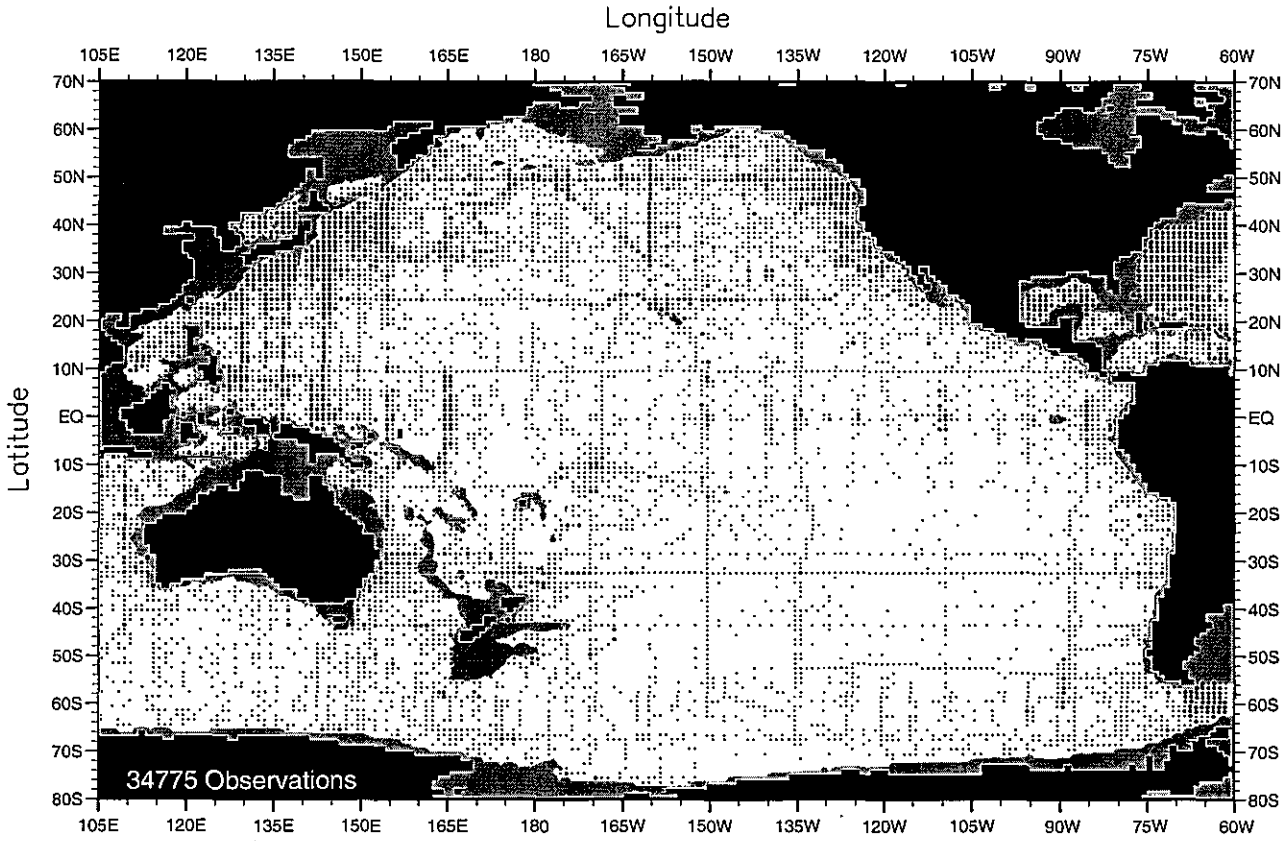


Fig. A13. Annual temperature observations at 2000 m. depth .

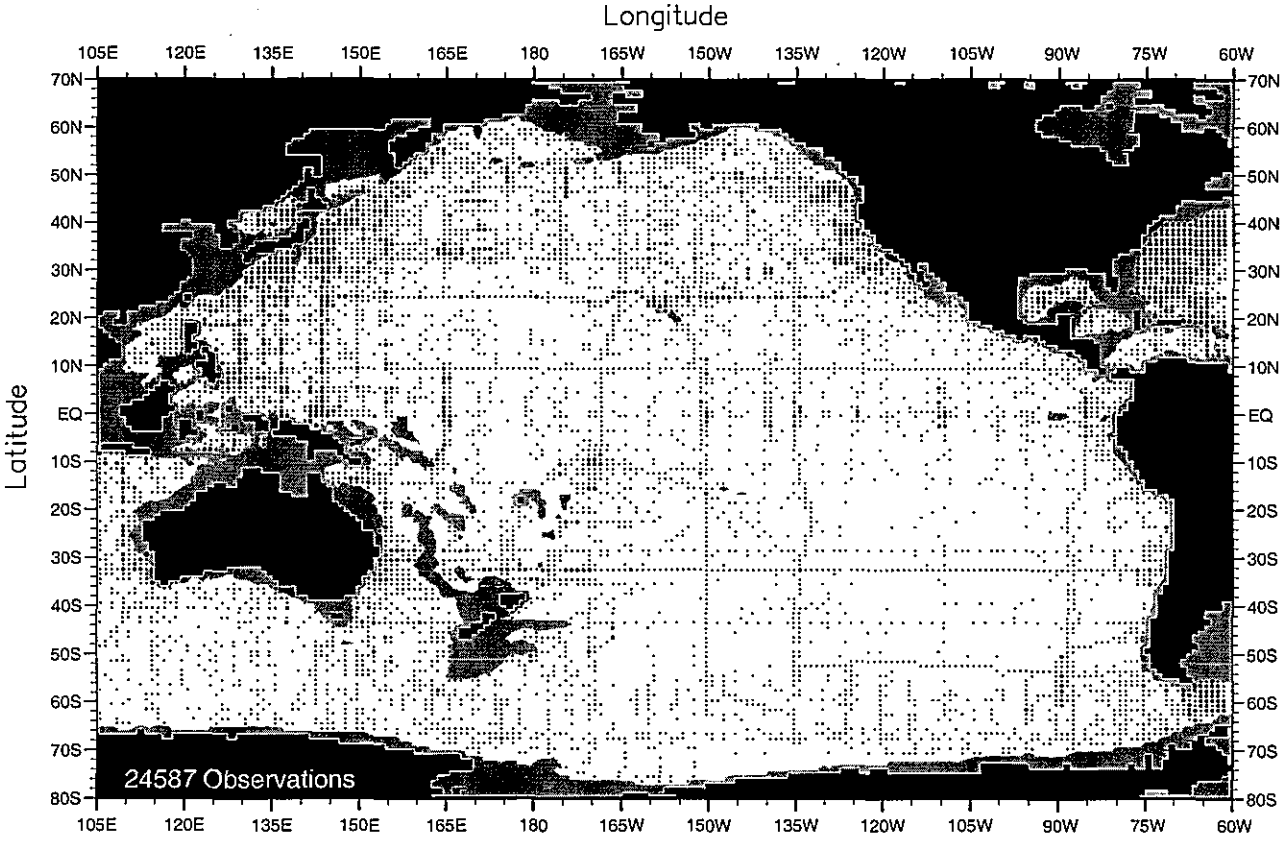


Fig. A14. Annual temperature observations at 2500 m. depth .

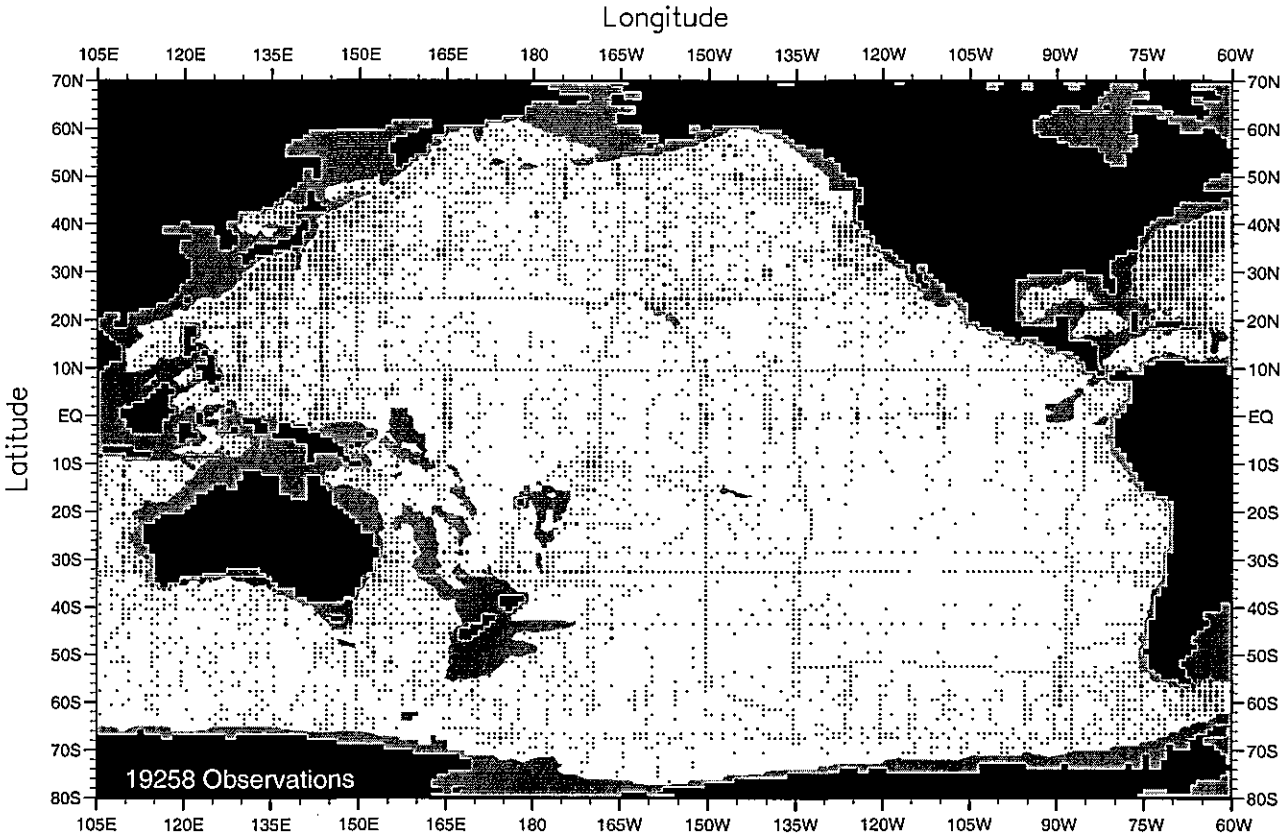


Fig. A15. Annual temperature observations at 3000 m. depth .

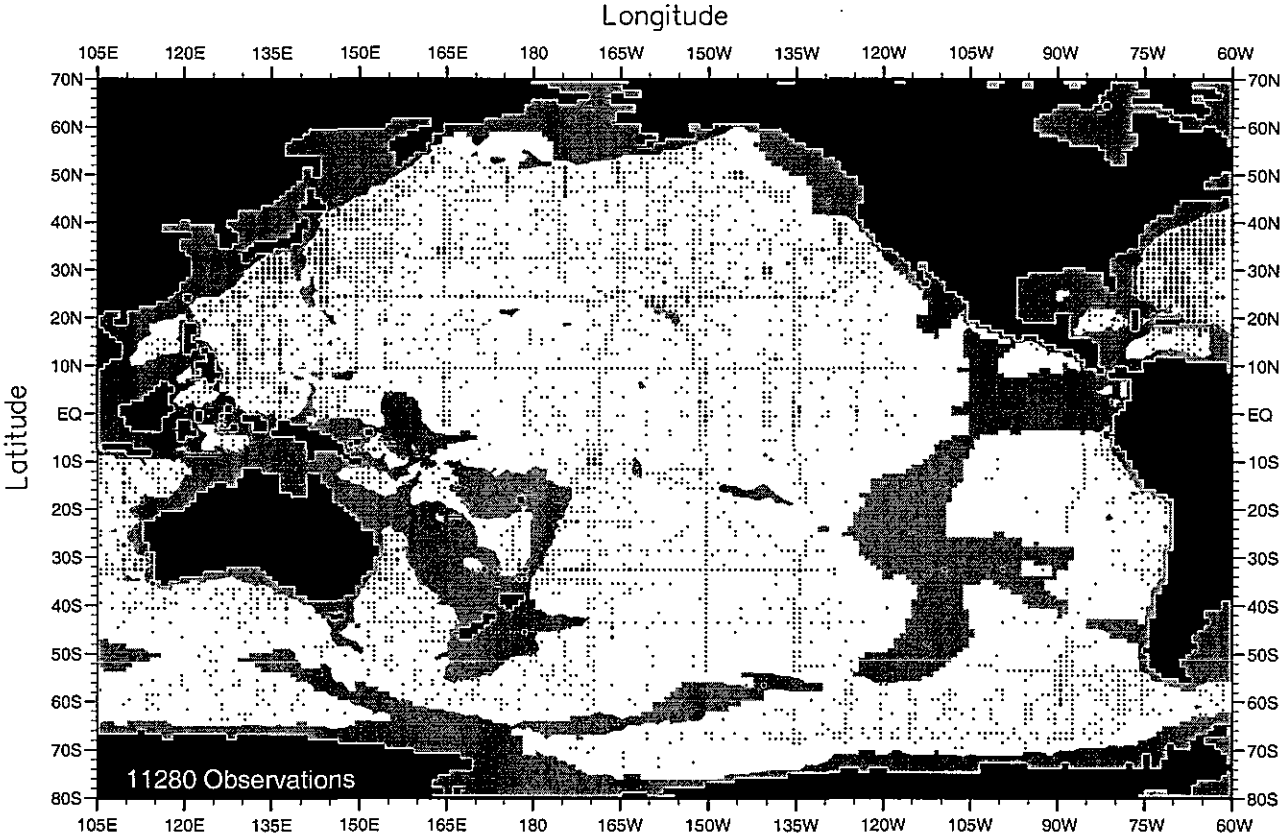


Fig. A16. Annual temperature observations at 4000 m. depth .

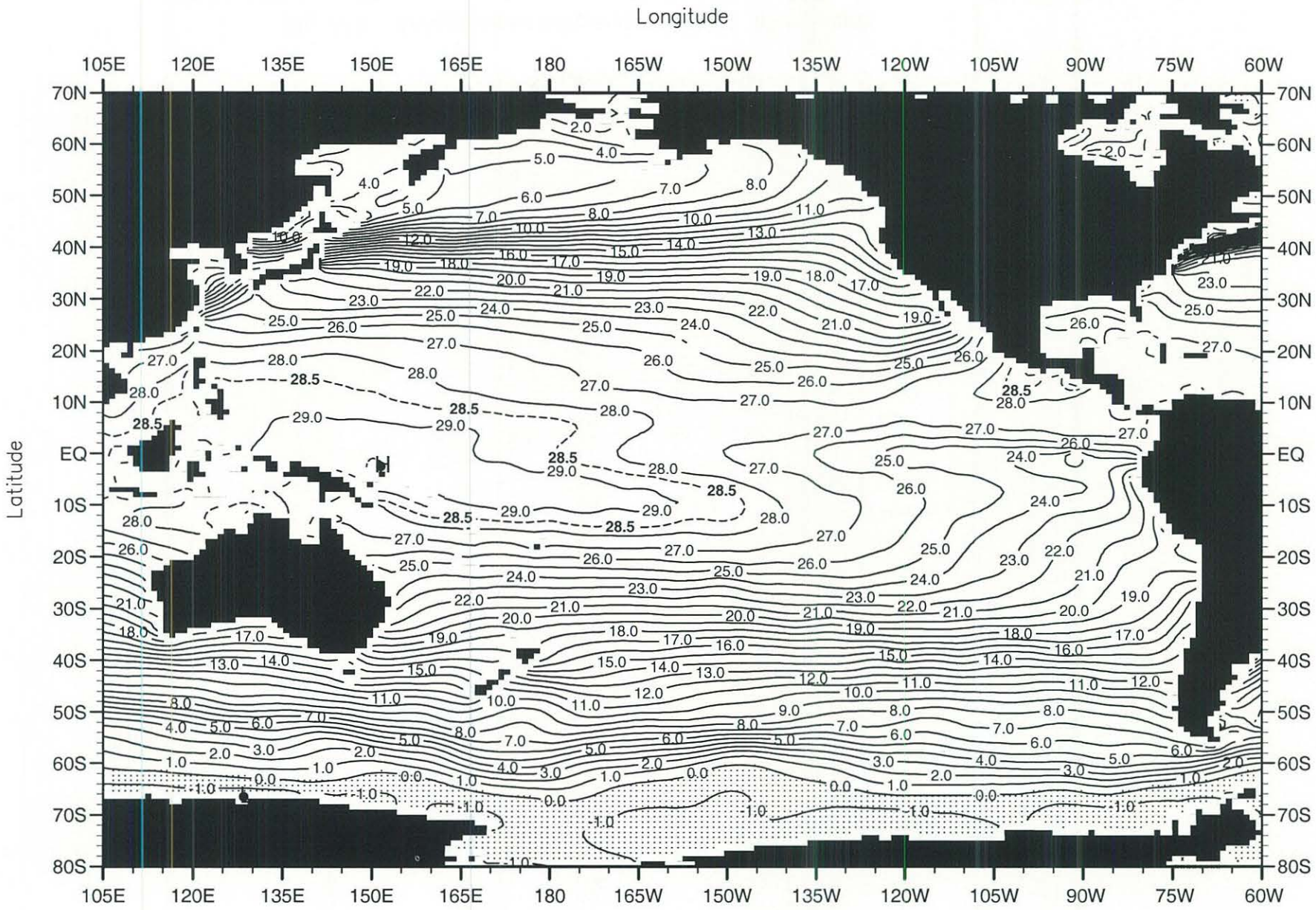


Fig. A17. Annual mean temperature (°C) at the surface .

Minimum Value= -1.93 Maximum Value= 29.60 Contour Interval: 1.00

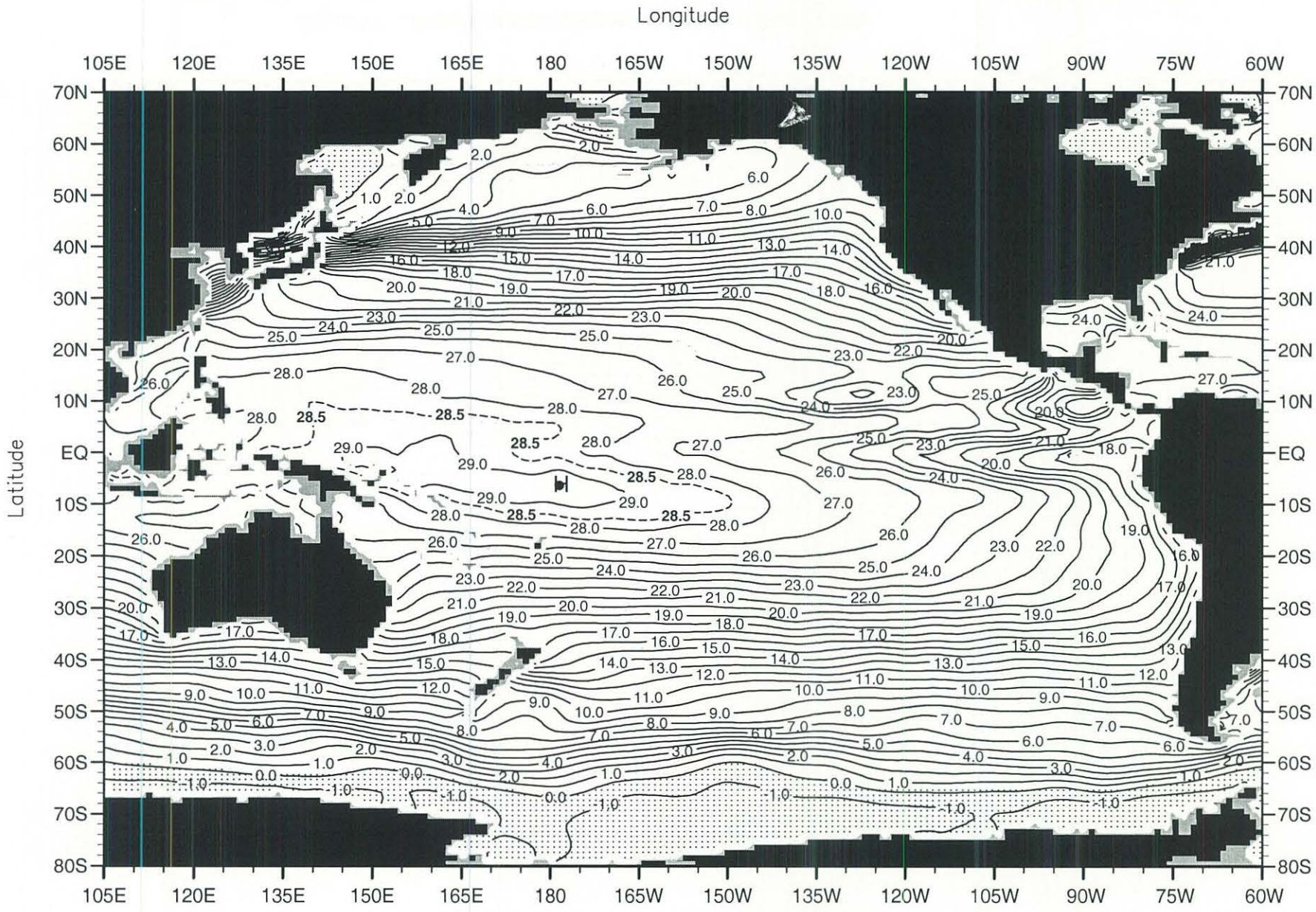


Fig. A18. Annual mean temperature (°C) at 50 m. depth .

Minimum Value= -1.93 Maximum Value= 29.35 Contour Interval: 1.00

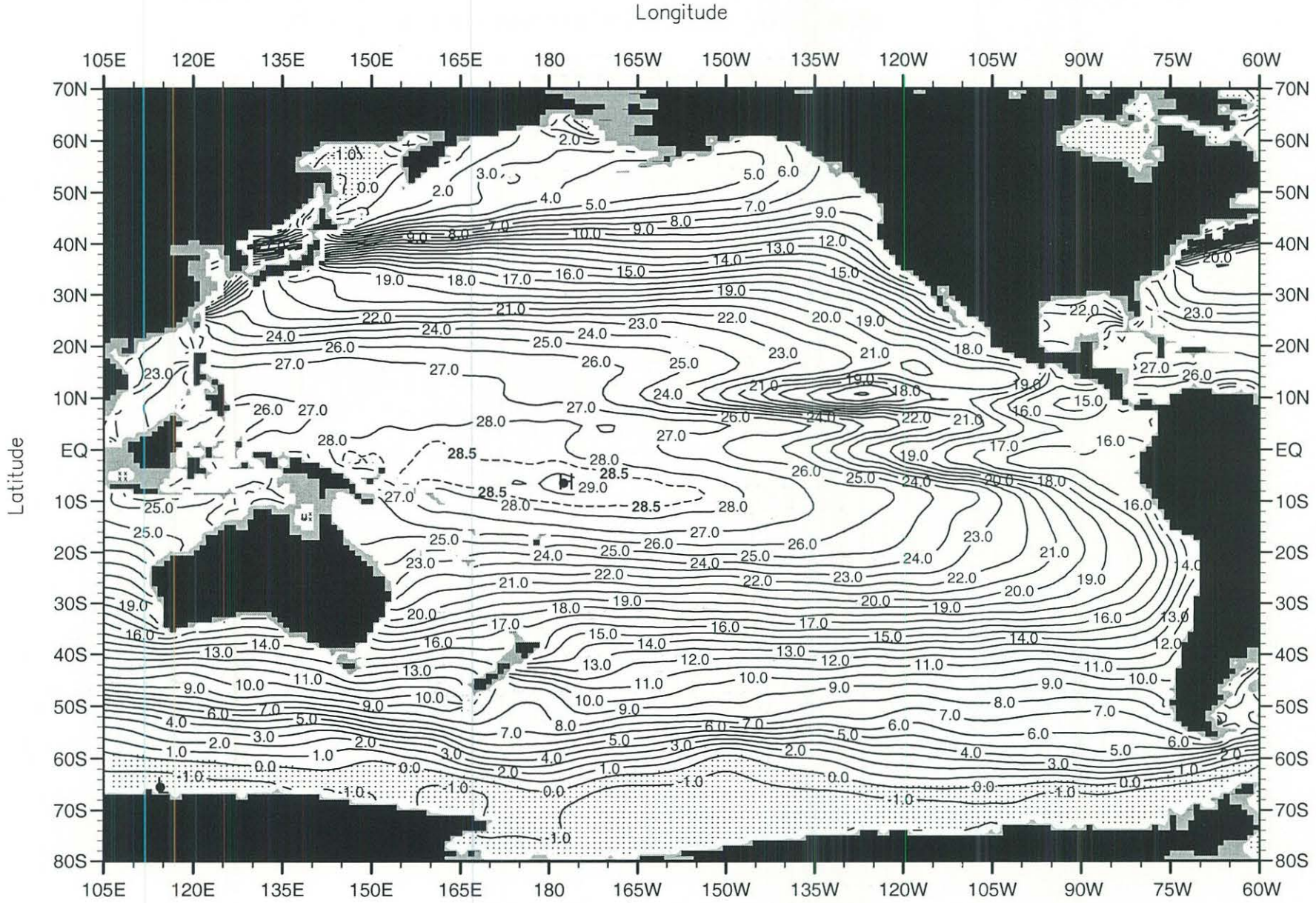


Fig. A19. Annual mean temperature (°C) at 75 m. depth .

Minimum Value= -1.92 Maximum Value= 29.17 Contour Interval: 1.00

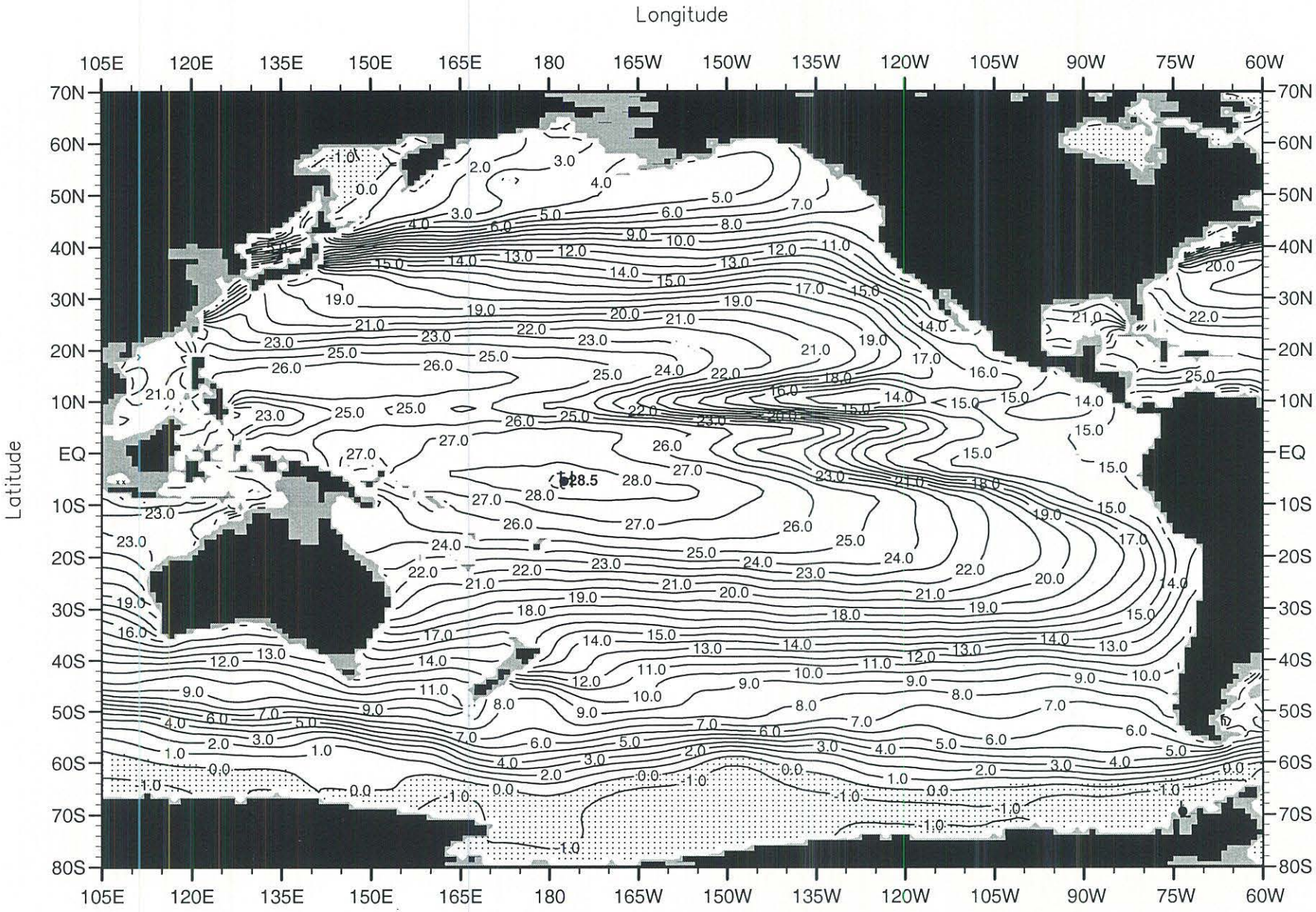


Fig. A20. Annual mean temperature (°C) at 100 m. depth .

Minimum Value= -1.91 Maximum Value= 28.64 Contour Interval: 1.00

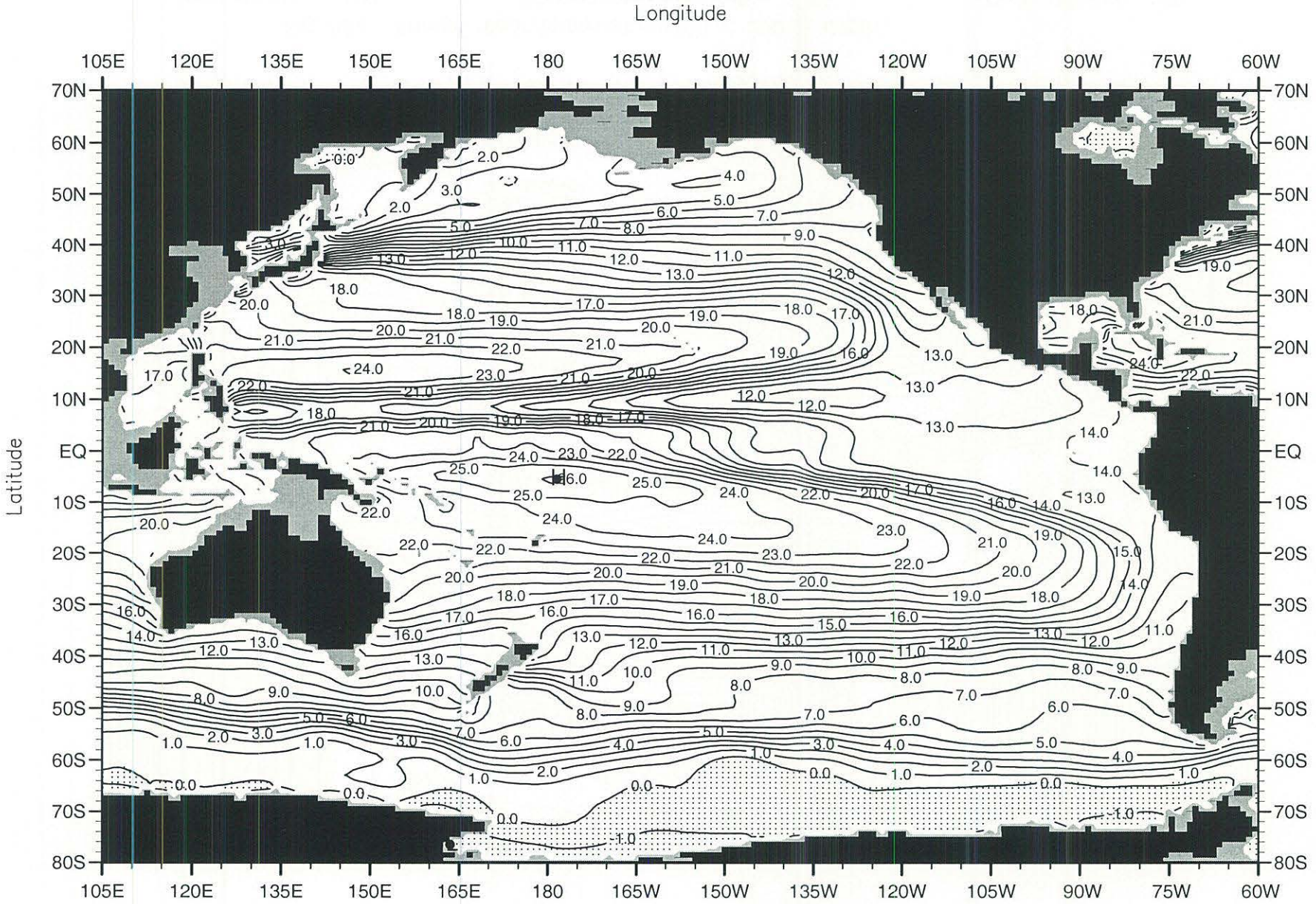


Fig. A21. Annual mean temperature (°C) at 150 m. depth .

Minimum Value= -1.91 Maximum Value= 26.09 Contour Interval: 1.00

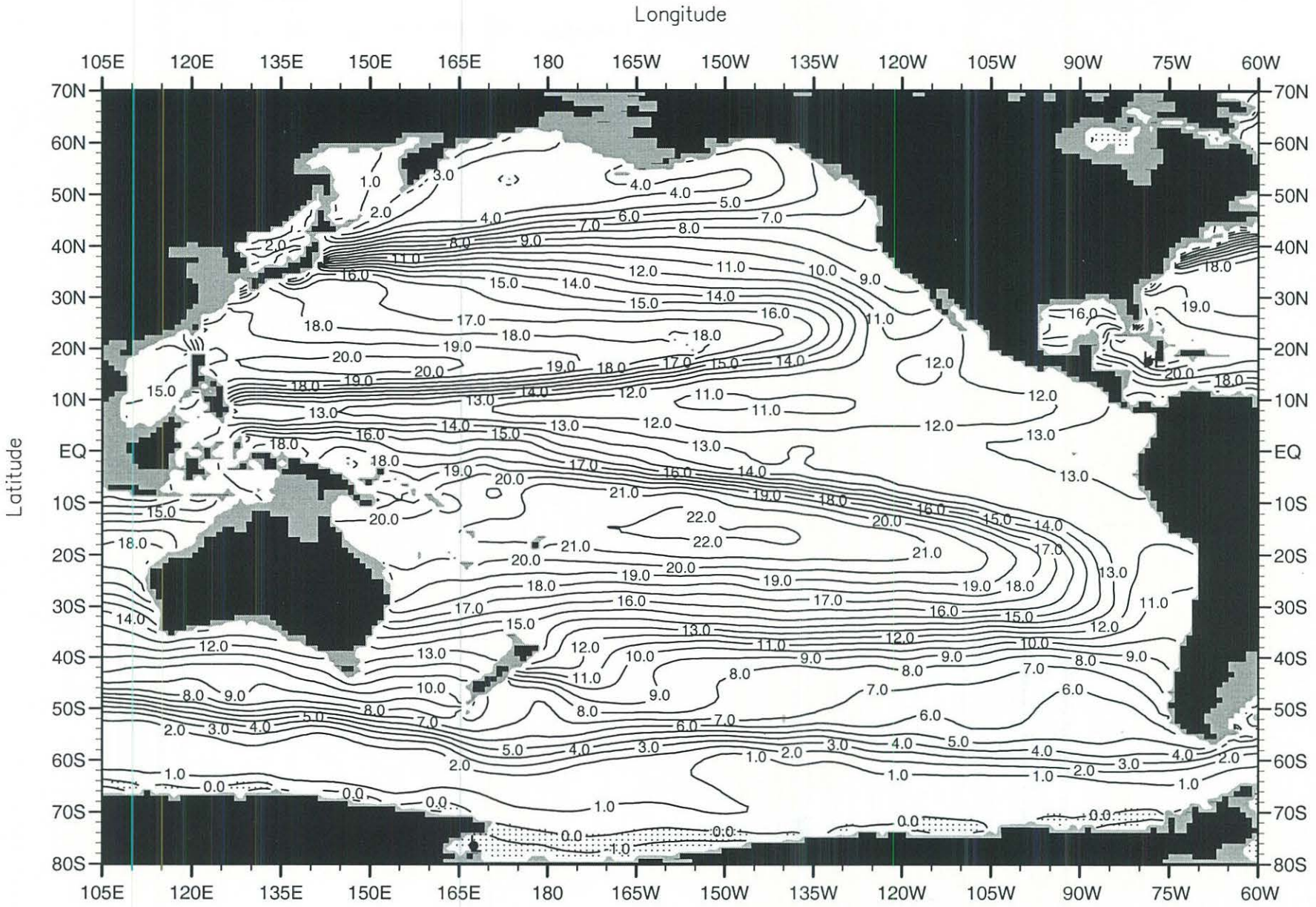


Fig. A22. Annual mean temperature (°C) at 200 m. depth .

Minimum Value= -1.98 Maximum Value= 22.63 Contour Interval: 1.00

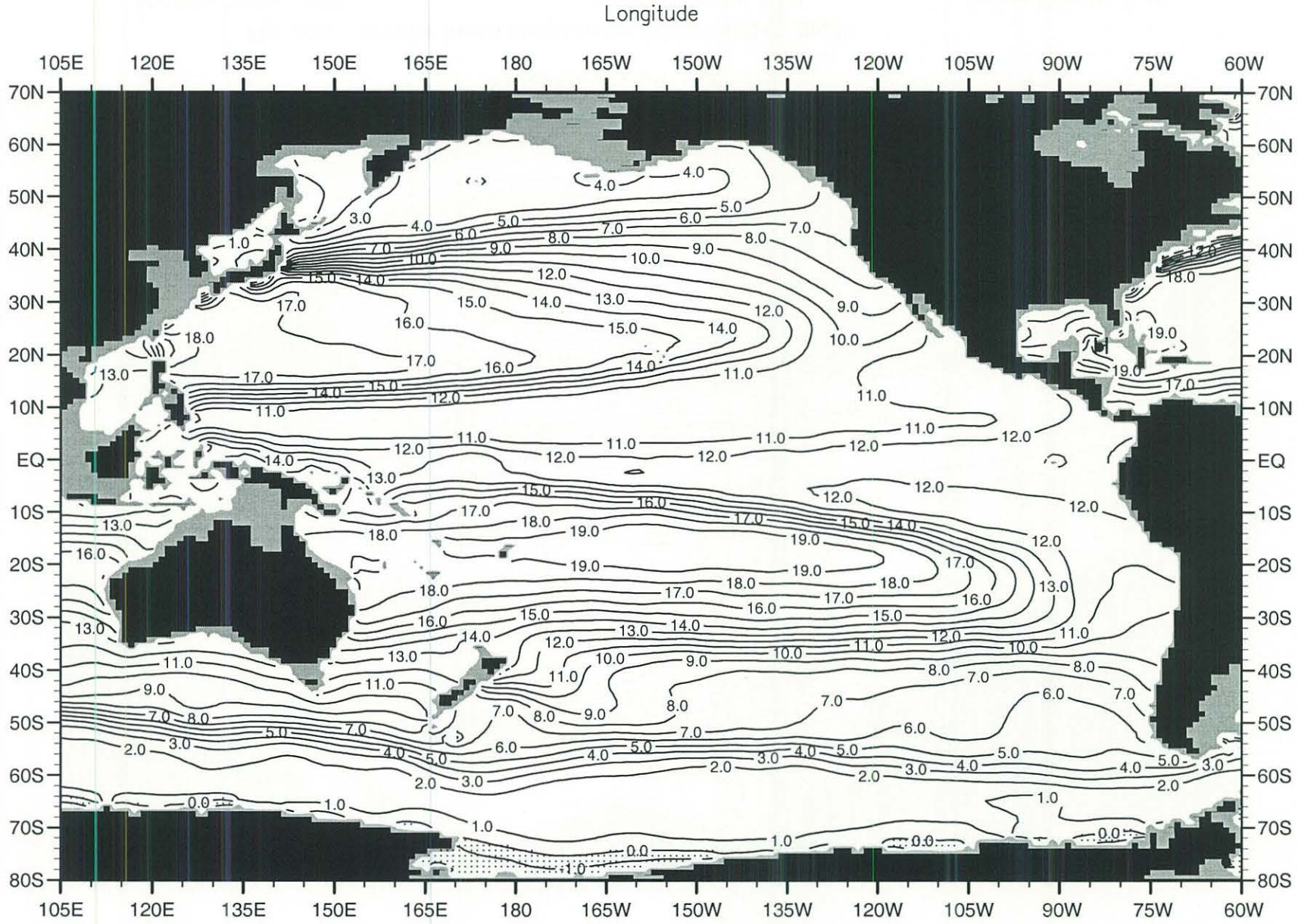


Fig. A23. Annual mean temperature (°C) at 250 m. depth .

Minimum Value= -2.07 Maximum Value= 20.01 Contour Interval: 1.00

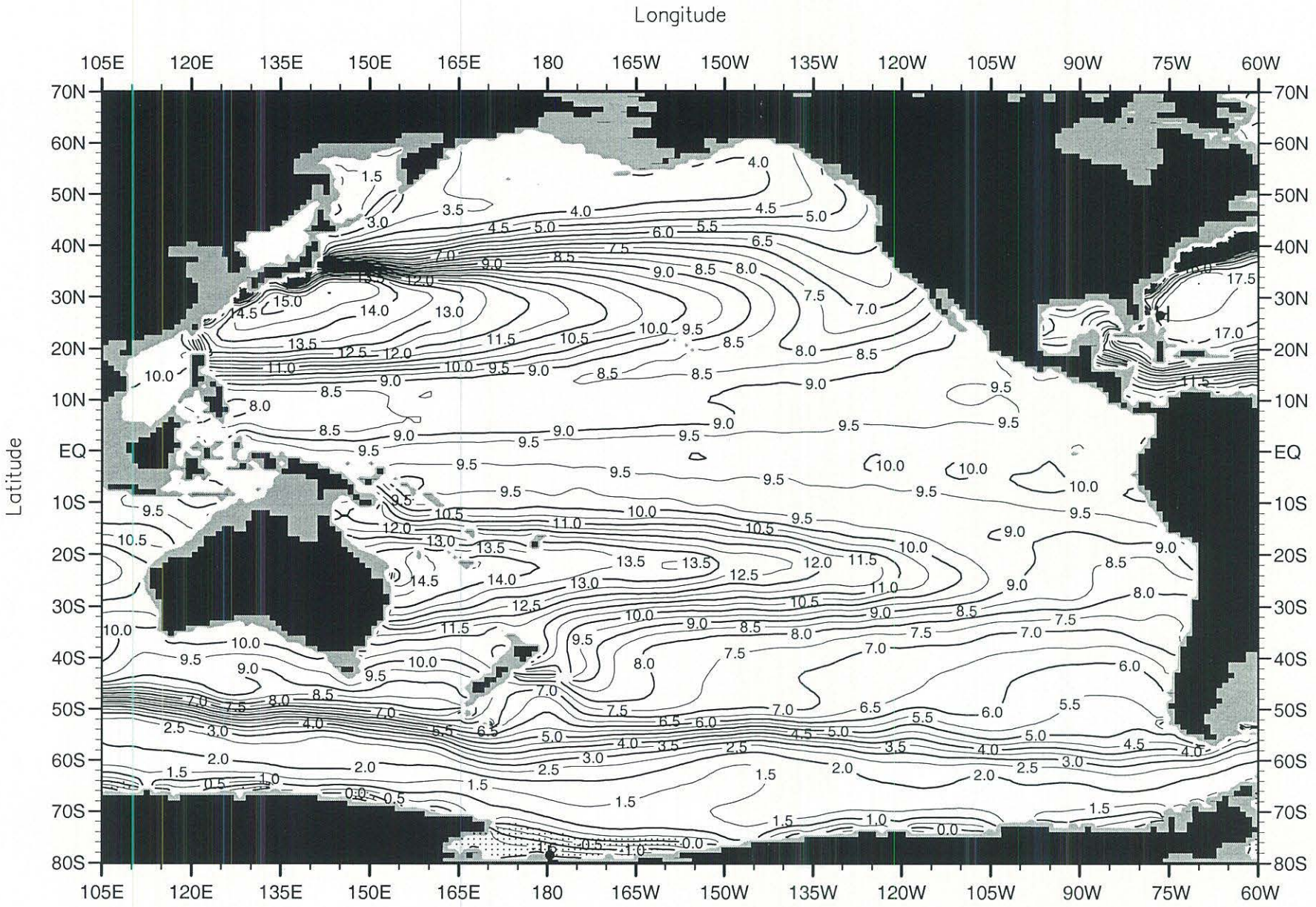


Fig. A24. Annual mean temperature (°C) at 400 m. depth .

Minimum Value= -2.09 Maximum Value= 18.11 Contour Interval: 0.50

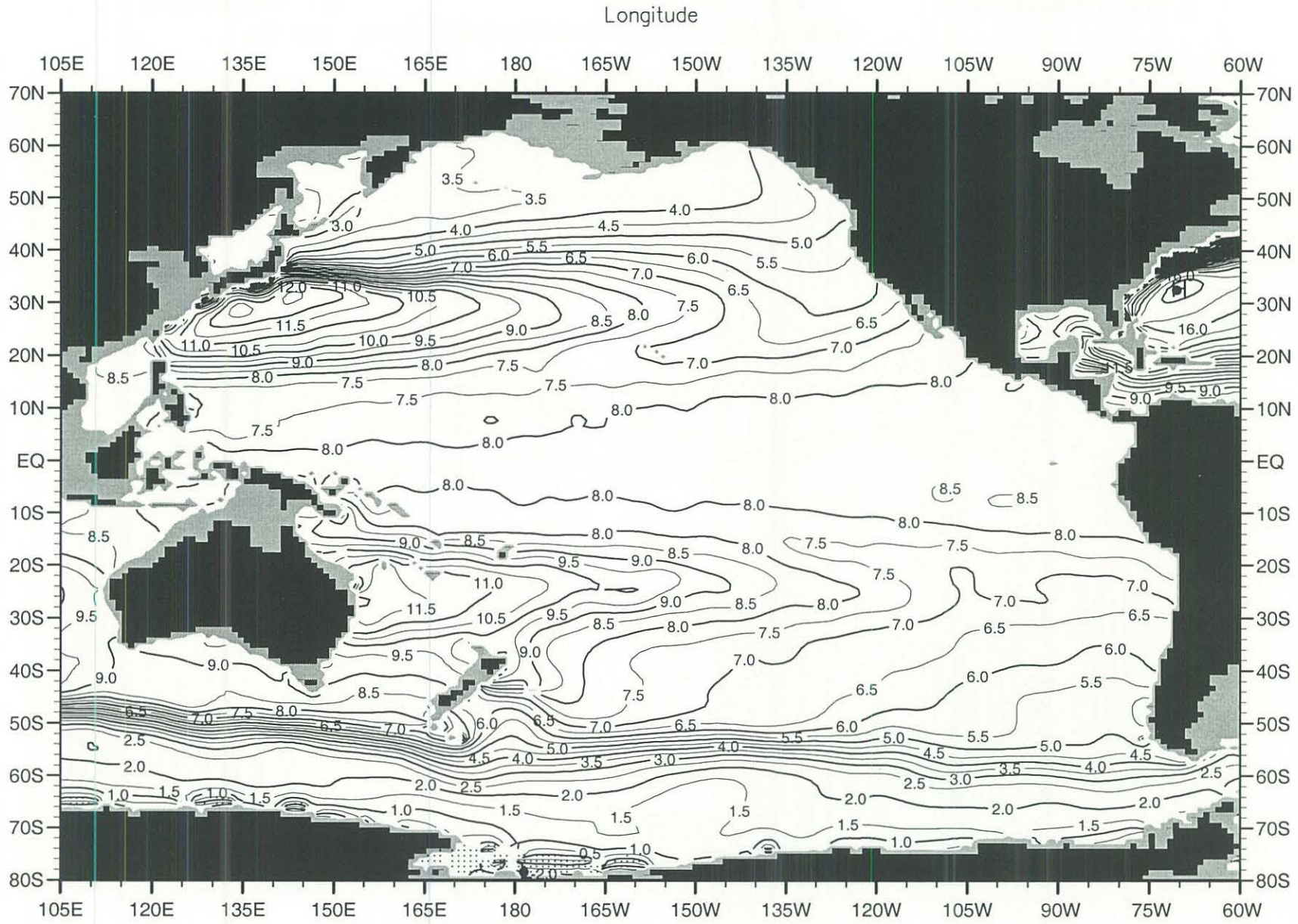


Fig. A25. Annual mean temperature (°C) at 500 m. depth .

Minimum Value= -2.10 Maximum Value= 17.29 Contour Interval: 0.50

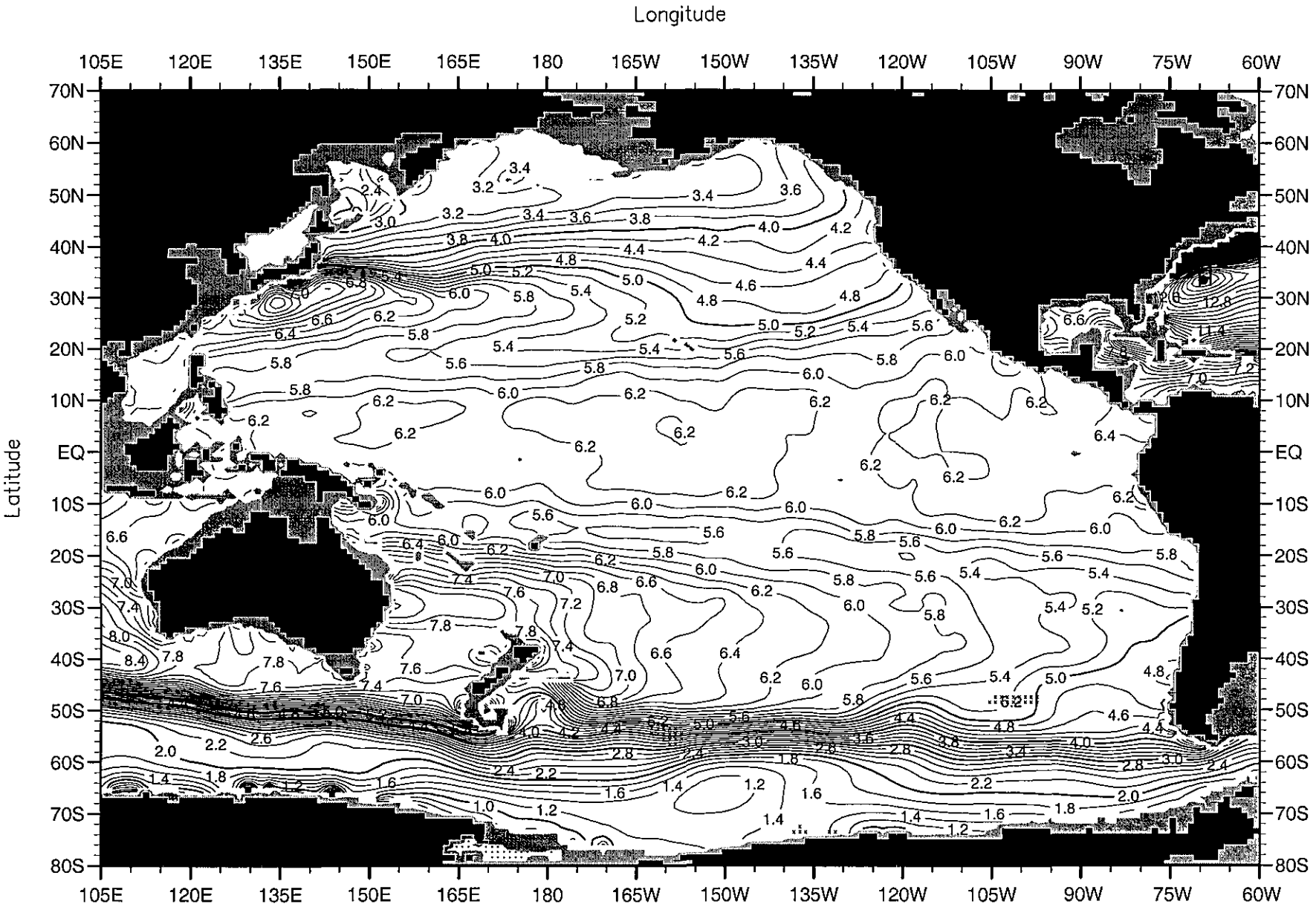


Fig. A26. Annual mean temperature (°C) at 700 m. depth .

Minimum Value= -1.99 Maximum Value= 14.04 Contour Interval: 0.20

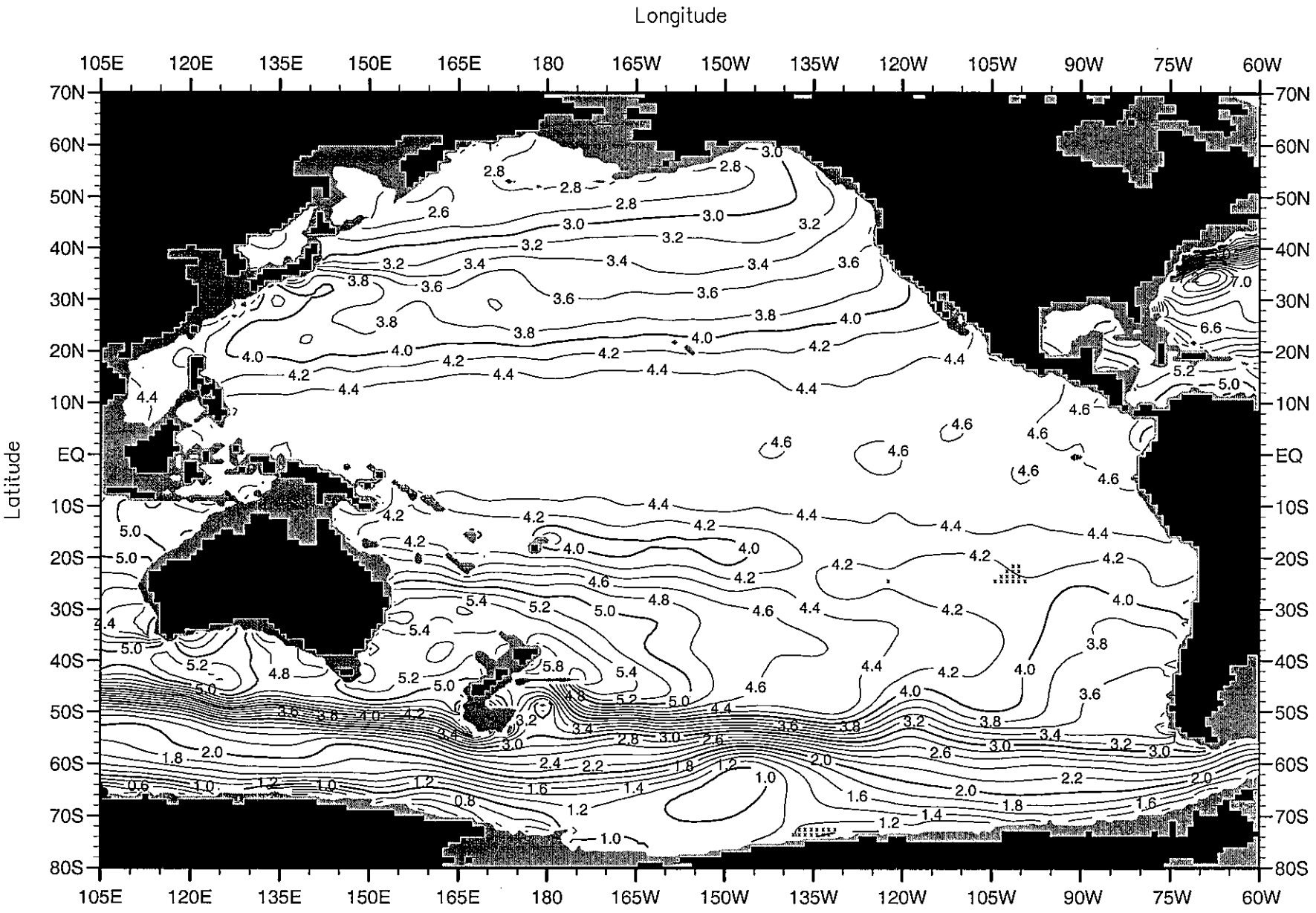


Fig. A27. Annual mean temperature (°C) at 1000 m. depth .

Minimum Value= -0.08 Maximum Value= 10.48 Contour Interval: 0.20

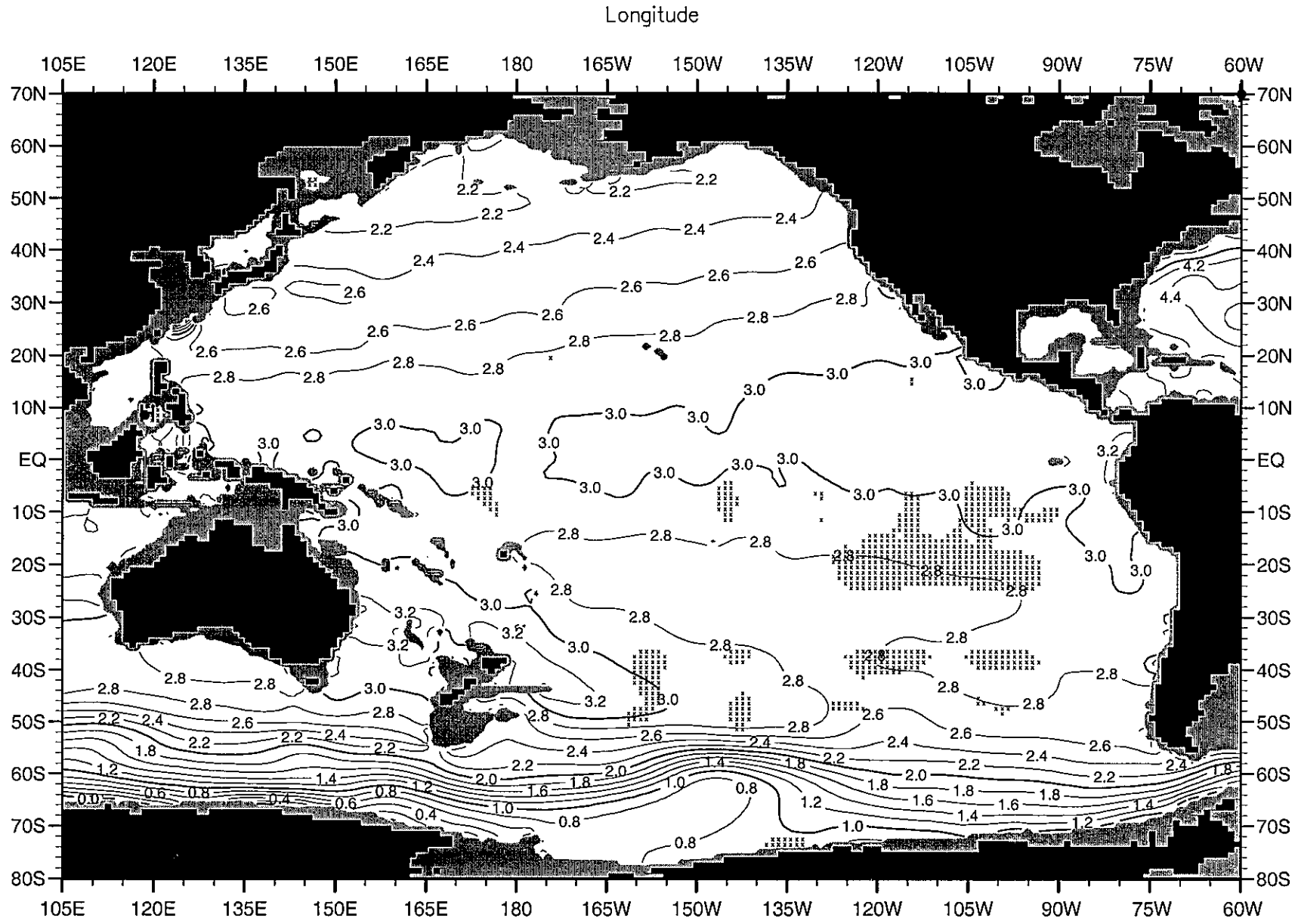


Fig. A28. Annual mean temperature (°C) at 1500 m. depth .

Minimum Value= -0.32 Maximum Value= 10.11 Contour Interval: 0.20

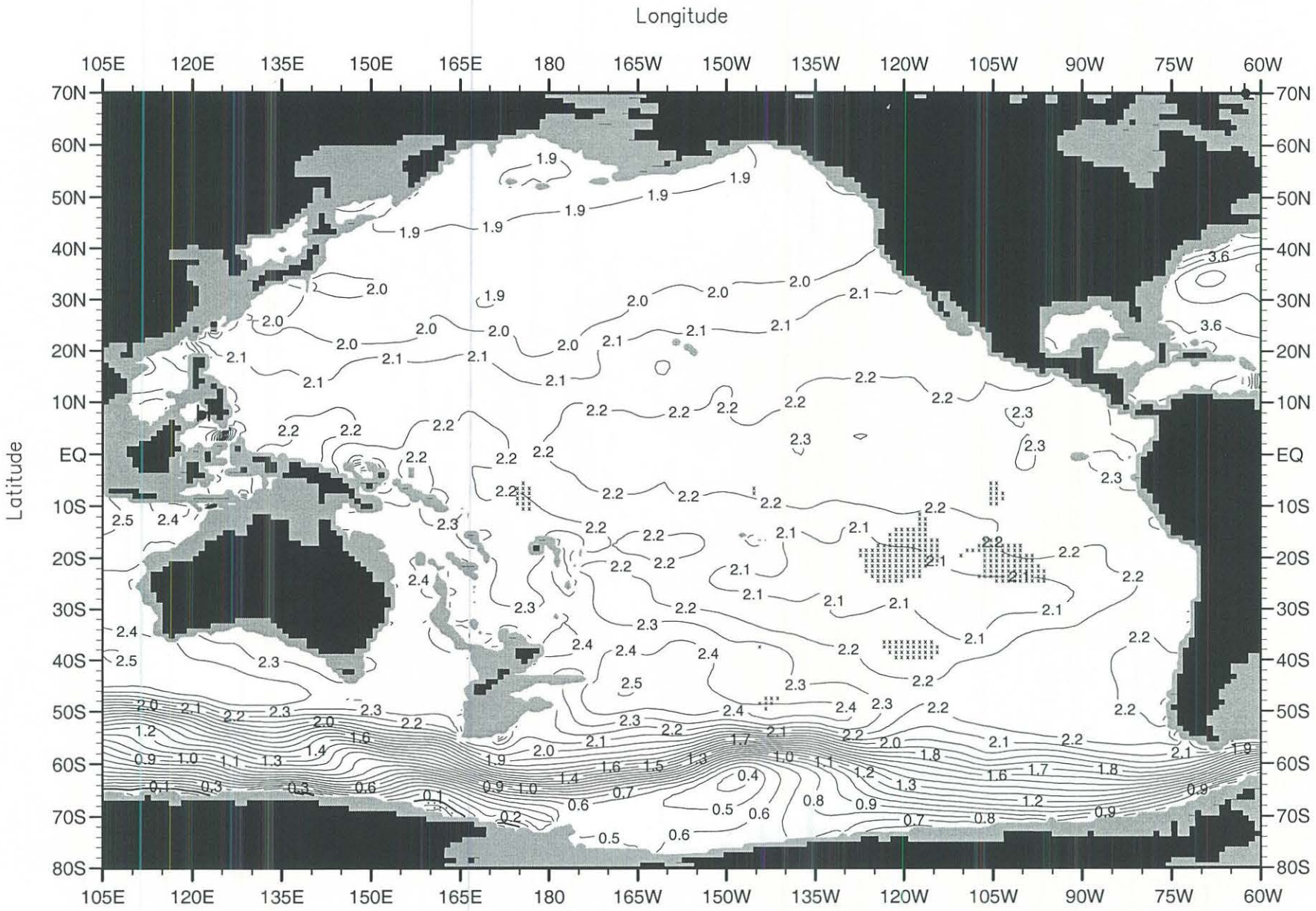


Fig. A29. Annual mean temperature (°C) at 2000 m. depth .

Minimum Value= -0.38 Maximum Value= 10.21 Contour Interval: 0.10

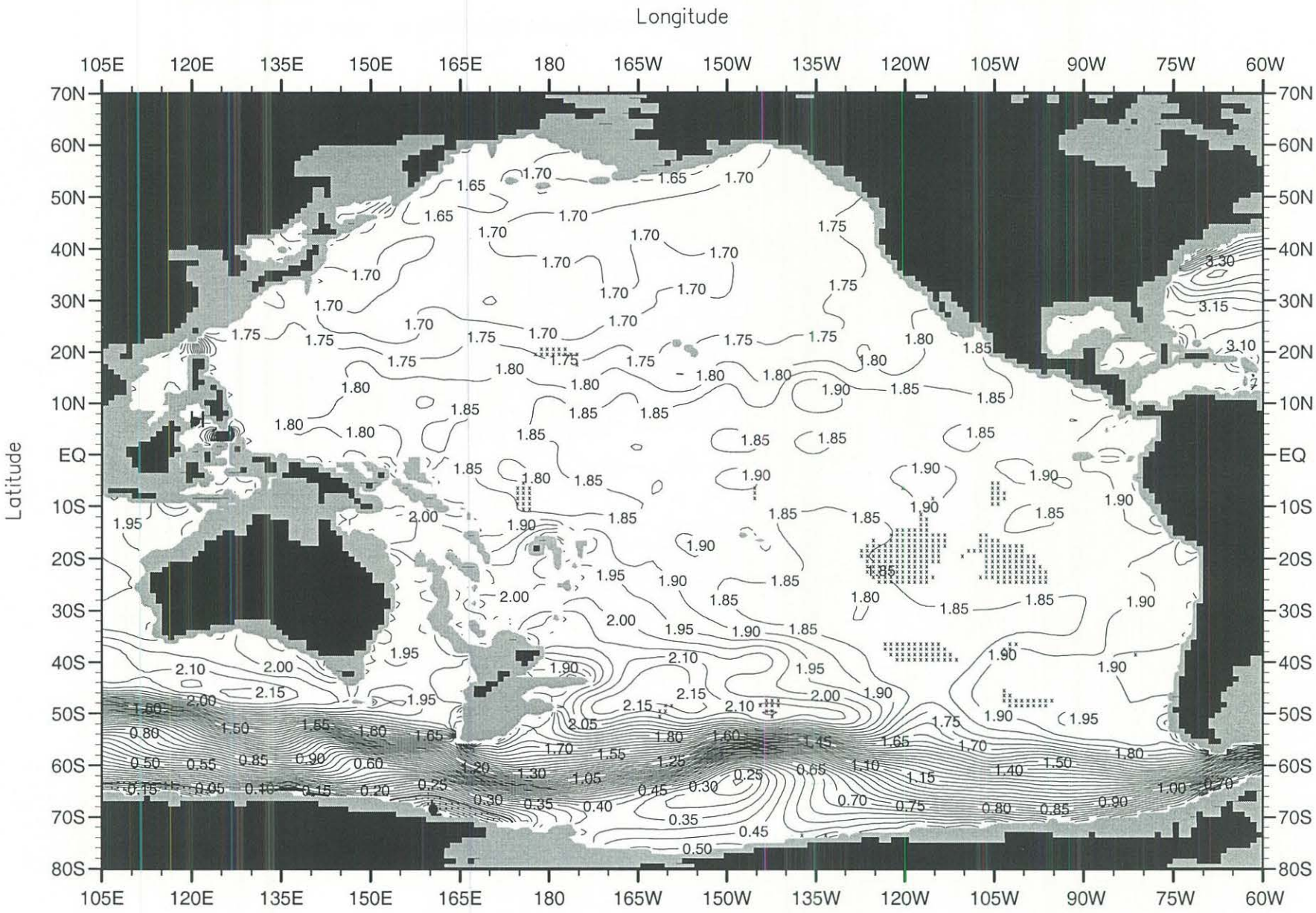


Fig. A30. Annual mean temperature (°C) at 2500 m. depth .

Minimum Value= -0.38 Maximum Value= 10.22 Contour Interval: 0.05

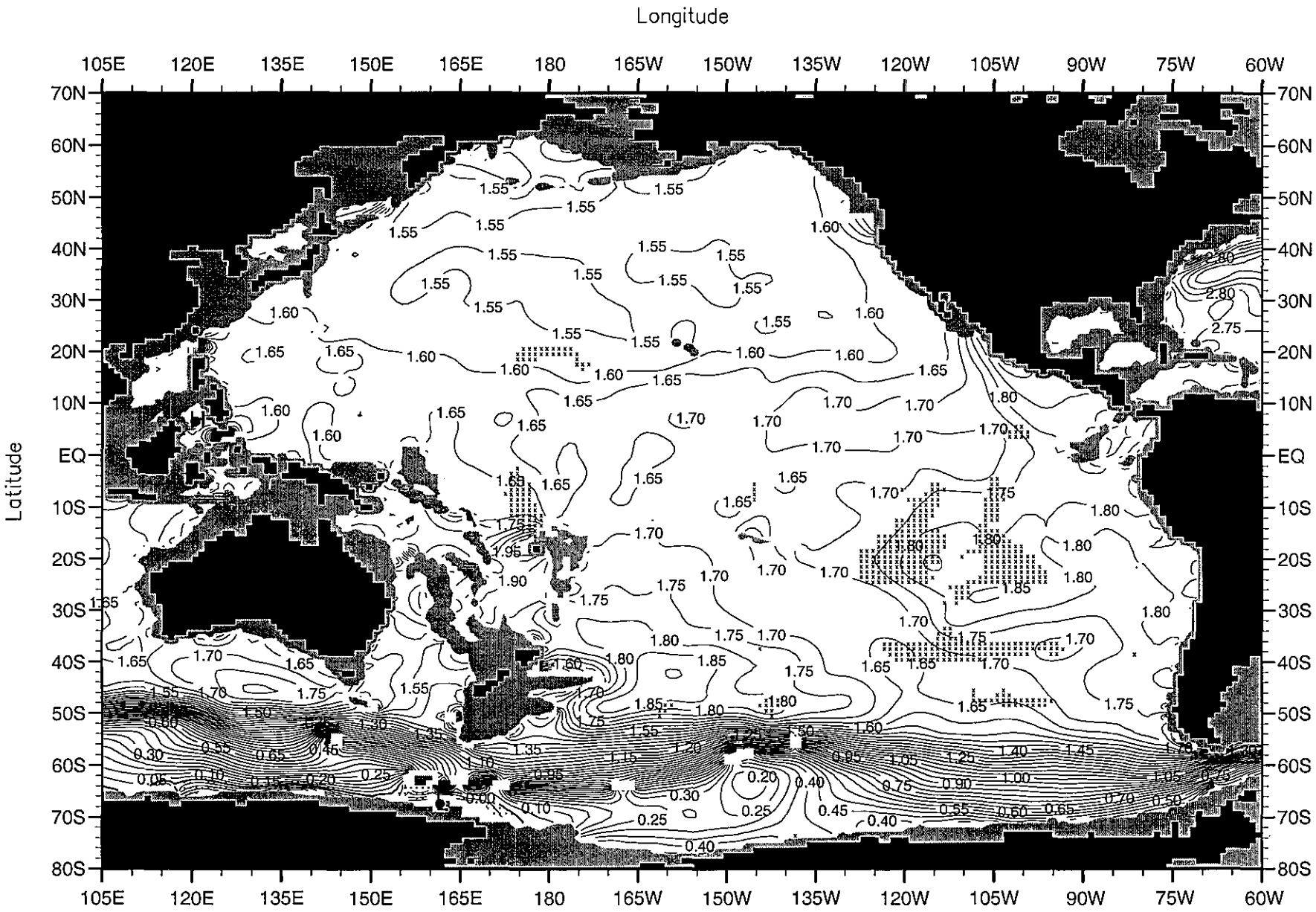


Fig. A31. Annual mean temperature (°C) at 3000 m. depth .

Minimum Value= -0.29 Maximum Value= 10.31 Contour Interval: 0.05

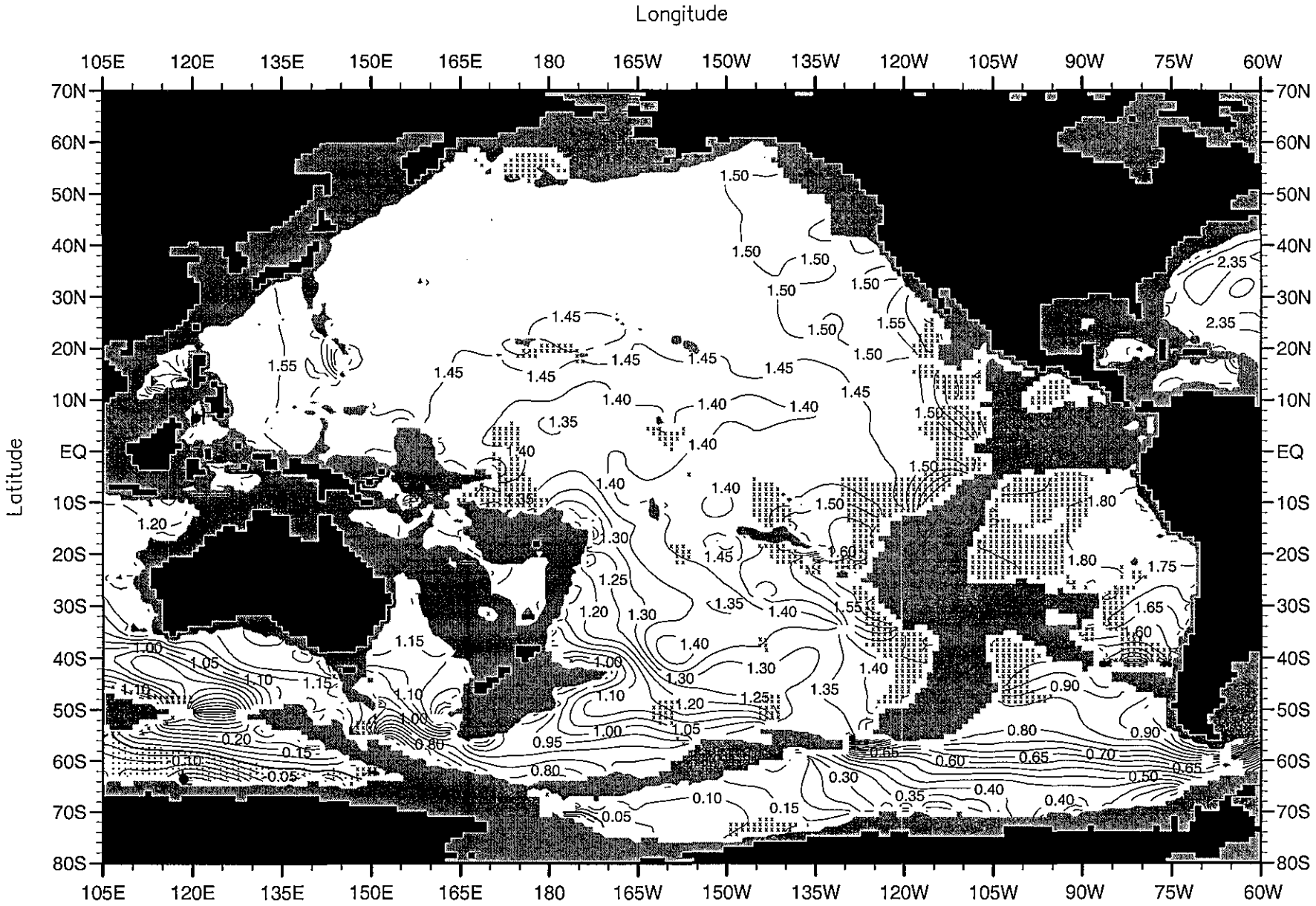


Fig. A32. Annual mean temperature (°C) at 4000 m. depth .

Minimum Value= -0.37 Maximum Value= 10.44 Contour Interval: 0.05

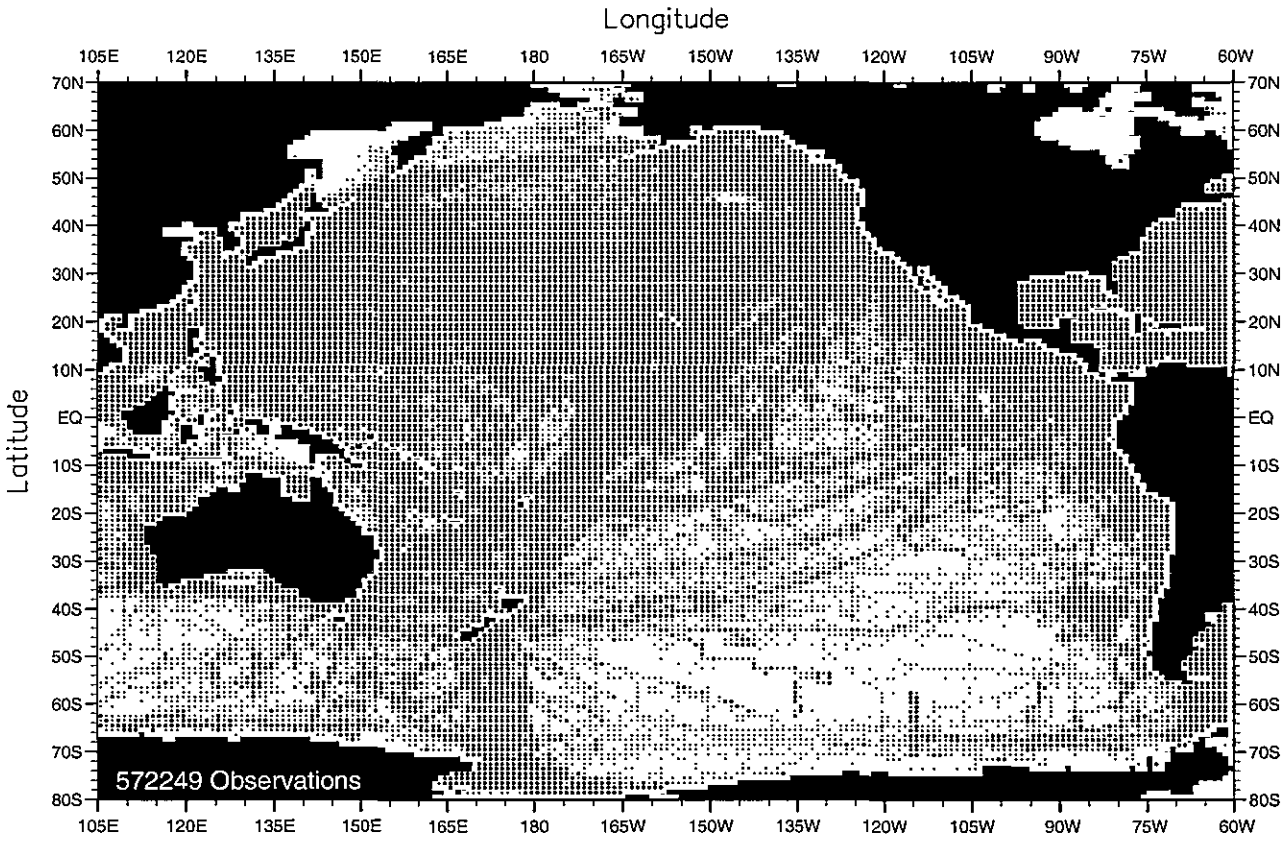


Fig. B1. Winter (Jan.-Mar.) temperature observations at the surface .

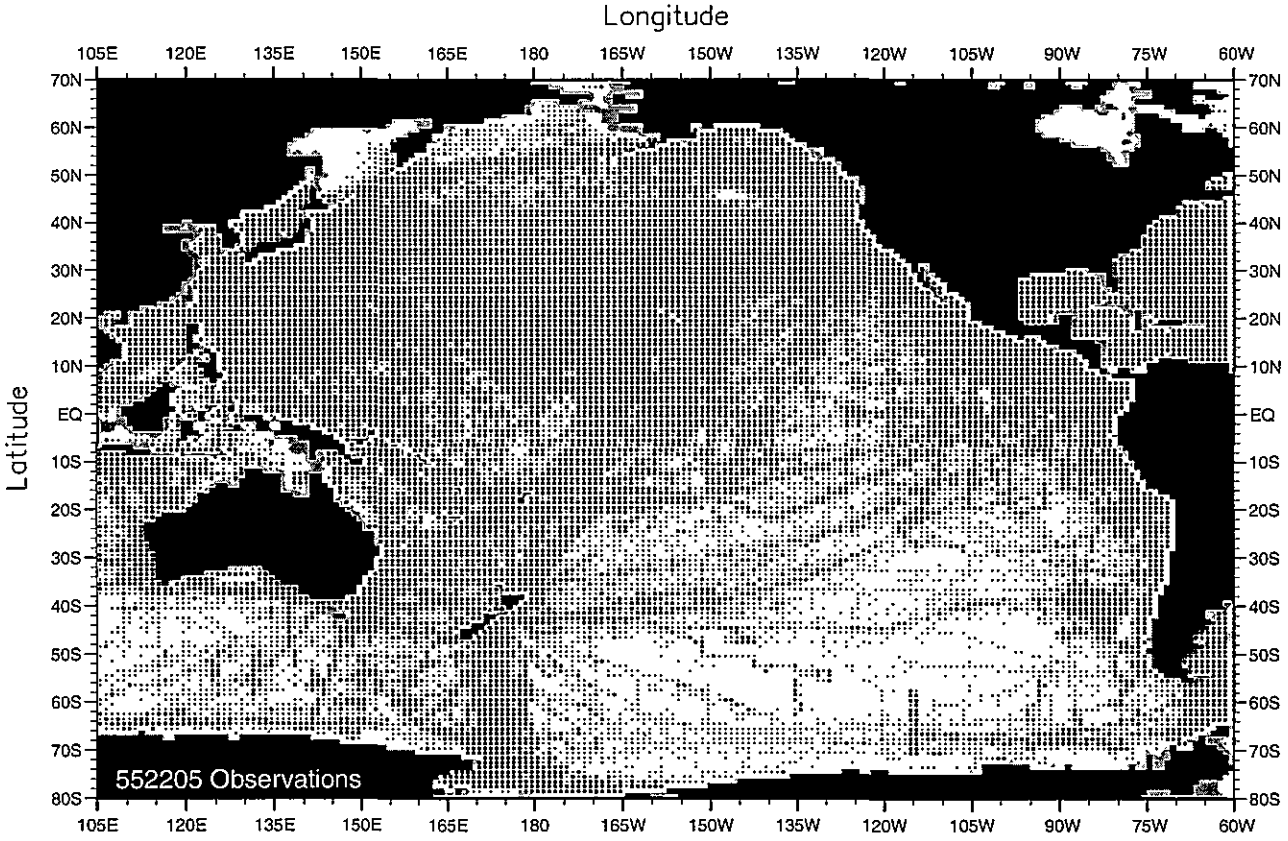


Fig. B2. Winter (Jan.-Mar.) temperature observations at 50 m. depth .

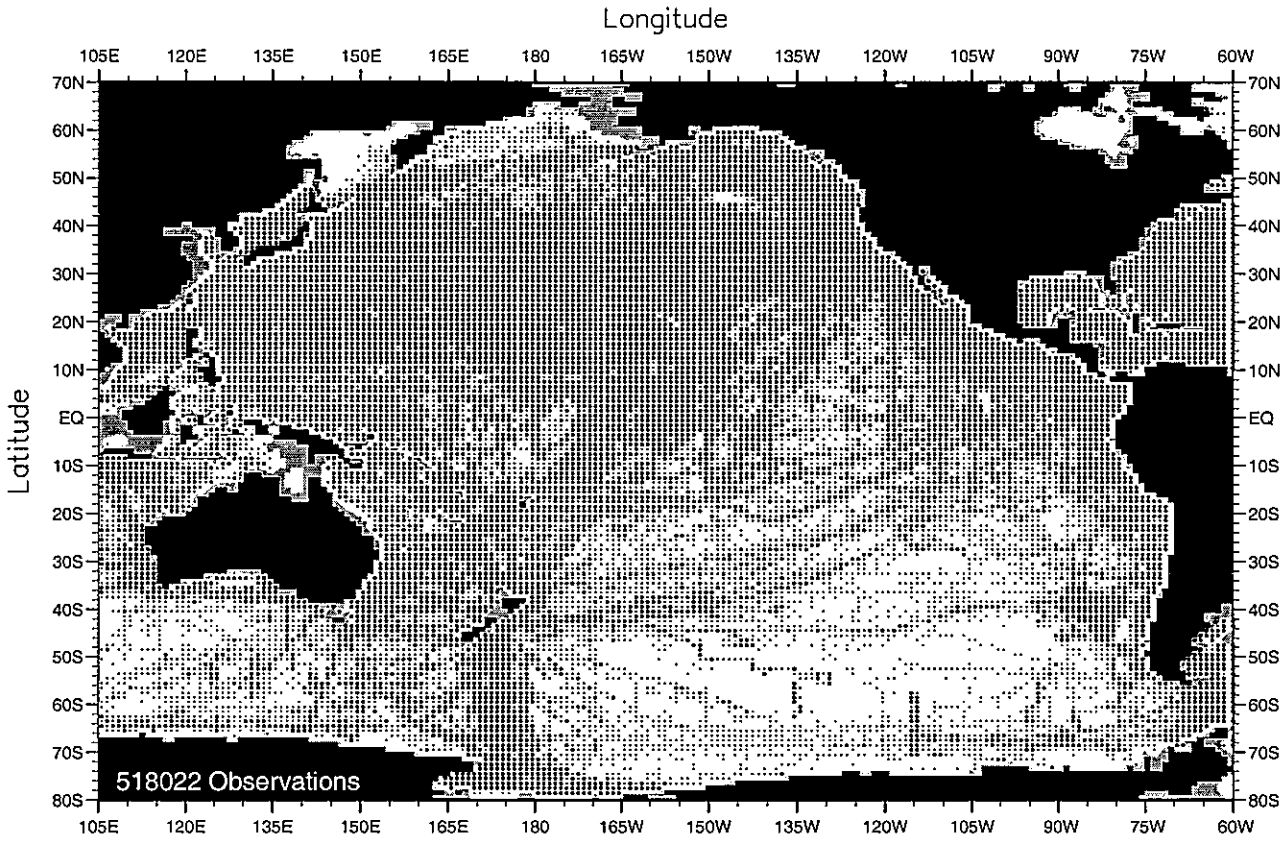


Fig. B3. Winter (Jan.-Mar.) temperature observations at 75 m. depth .

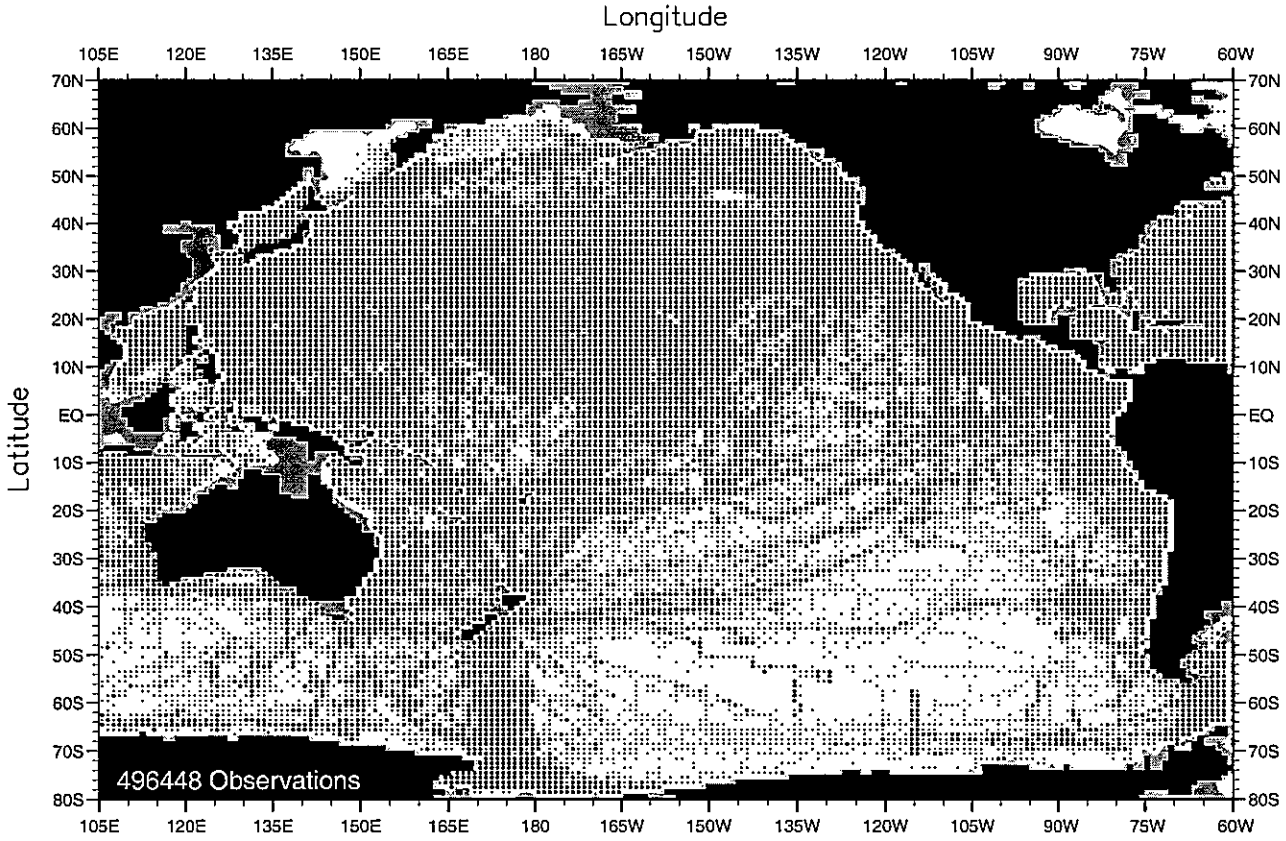


Fig. B4. Winter (Jan.-Mar.) temperature observations at 100 m. depth .

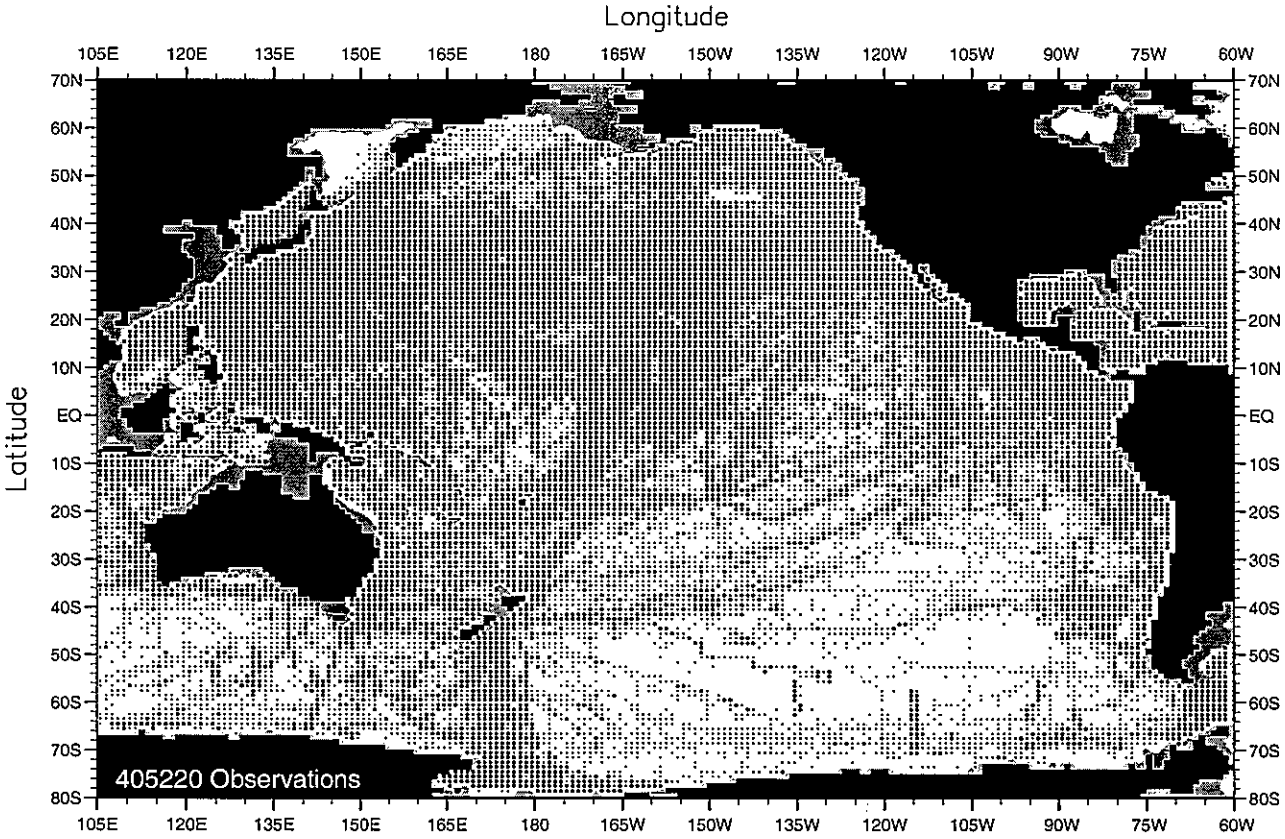


Fig. B5. Winter (Jan.-Mar.) temperature observations at 150 m. depth .

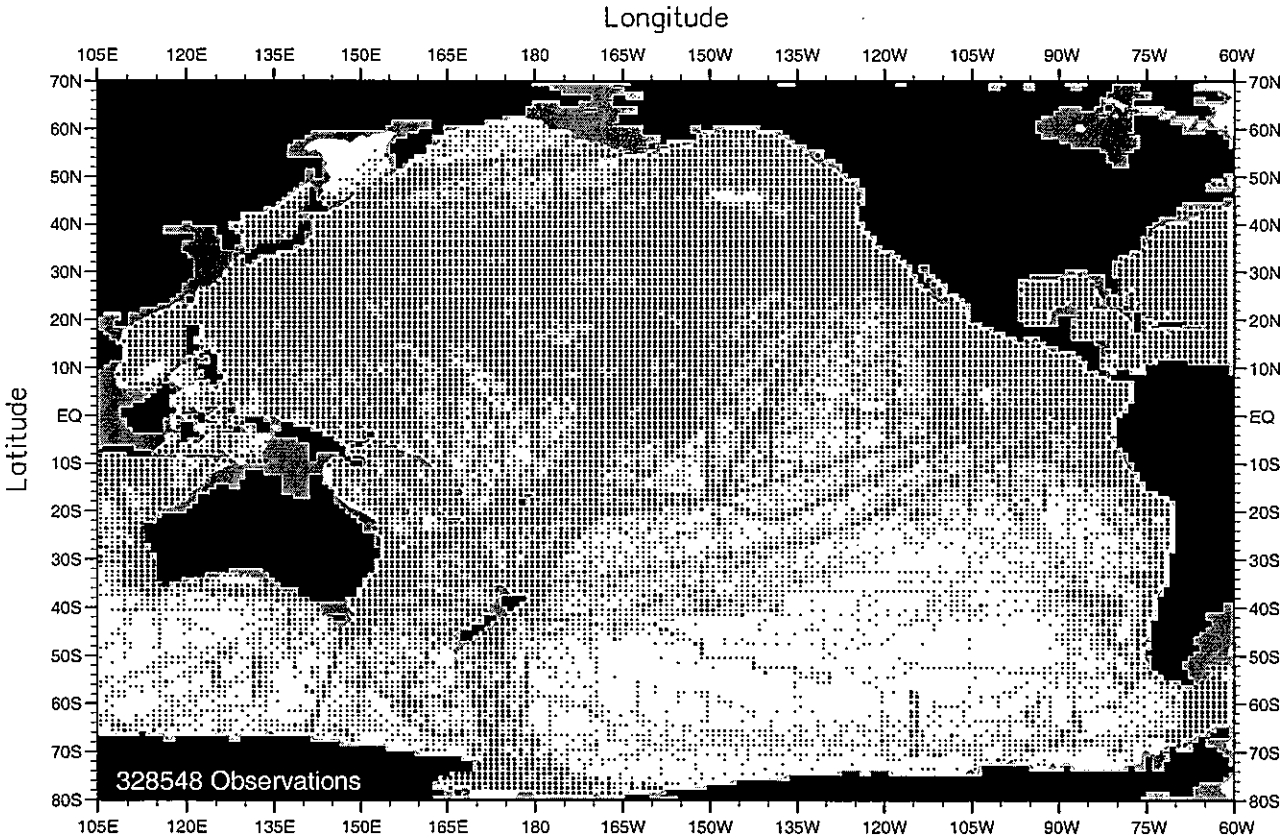


Fig. B6. Winter (Jan.-Mar.) temperature observations at 250 m. depth .

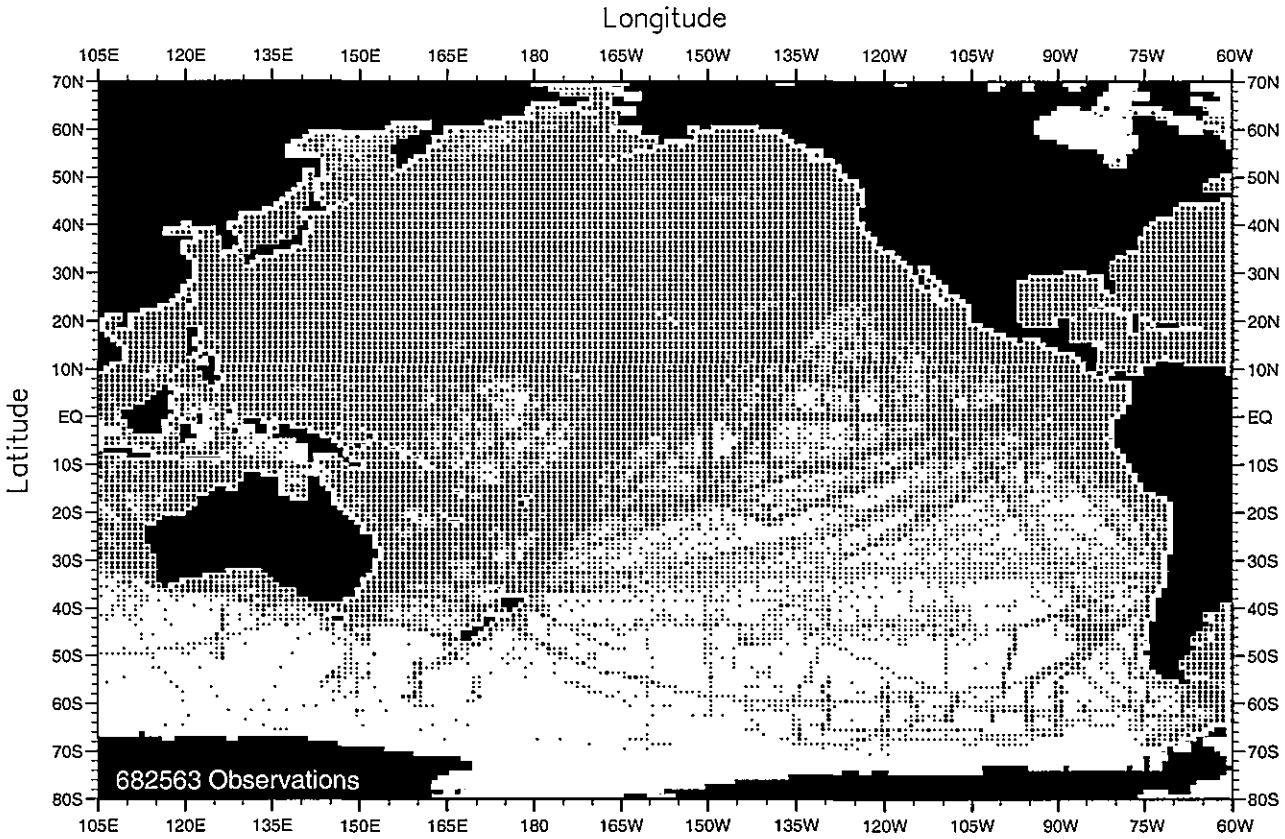


Fig. B7. Spring (Apr.-Jun.) temperature observations at the surface .

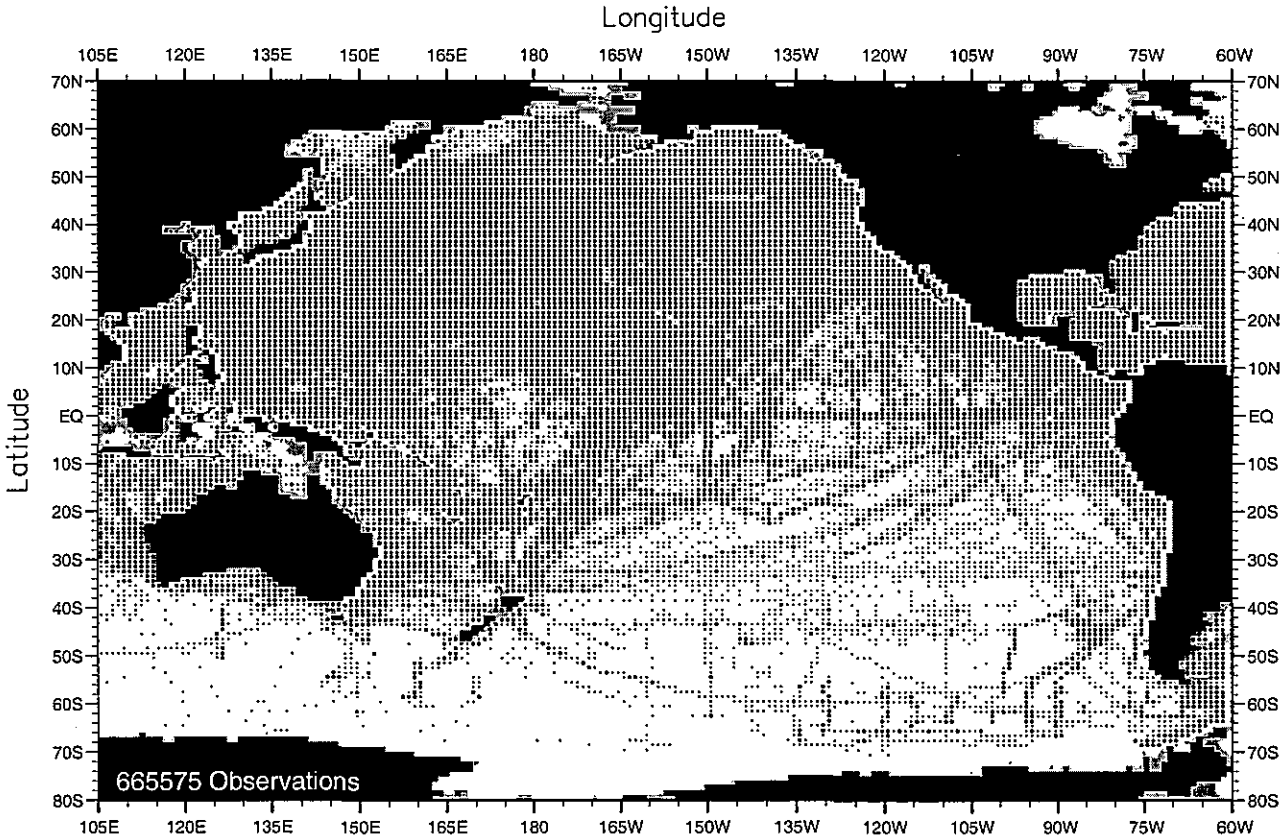


Fig. B8. Spring (Apr.-Jun.) temperature observations at 50 m. depth .

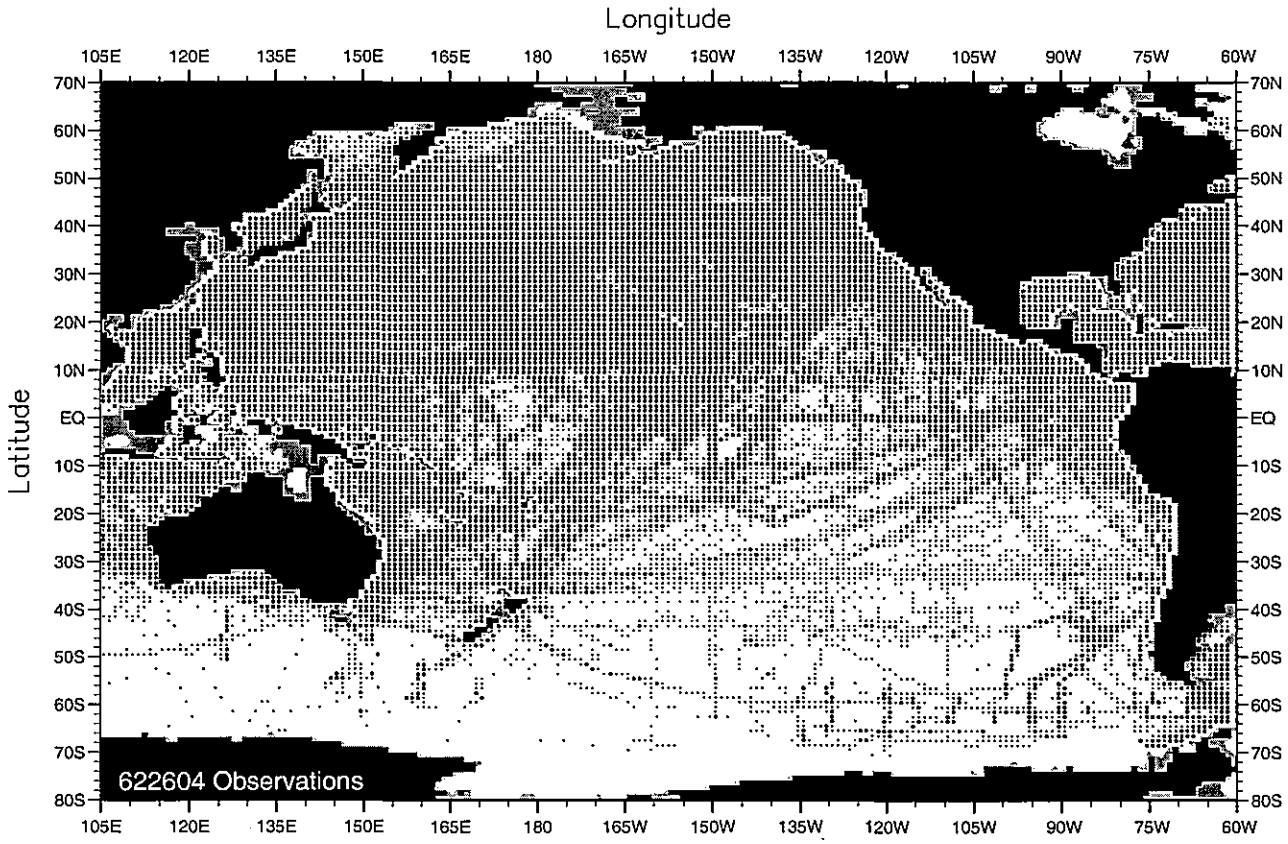


Fig. B9. Spring (Apr.-Jun.) temperature observations at 75 m. depth .

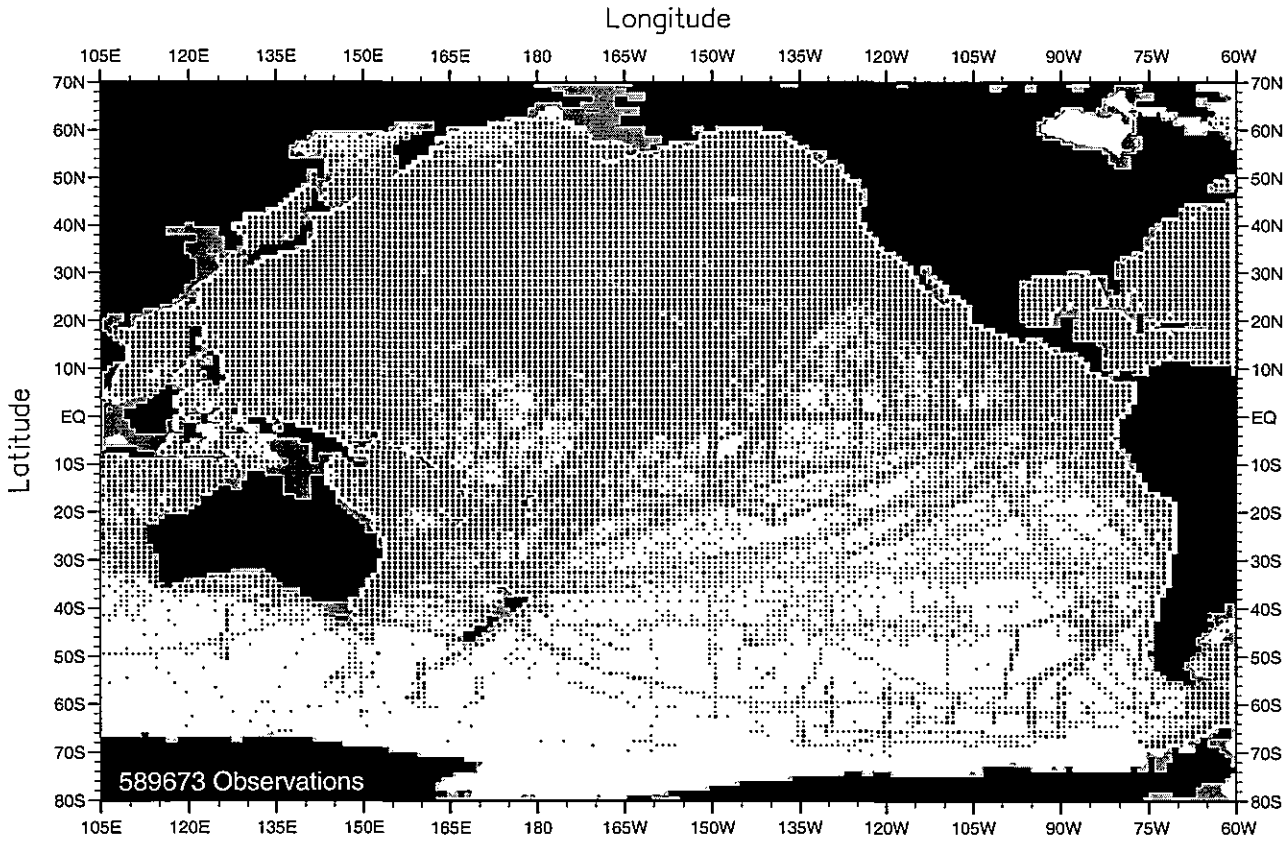


Fig. B10. Spring (Apr.-Jun.) temperature observations at 100 m. depth .

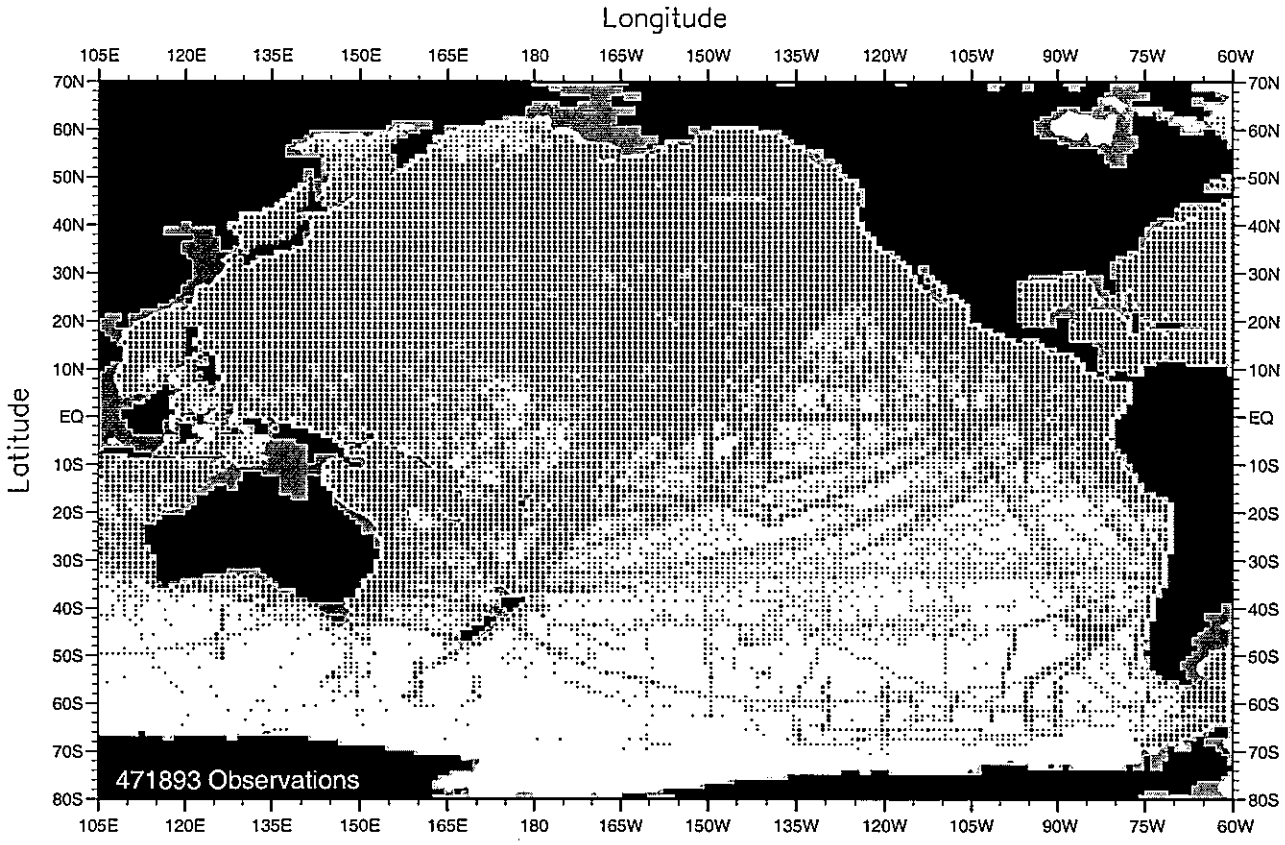


Fig. B11. Spring (Apr.-Jun.) temperature observations at 150 m. depth .

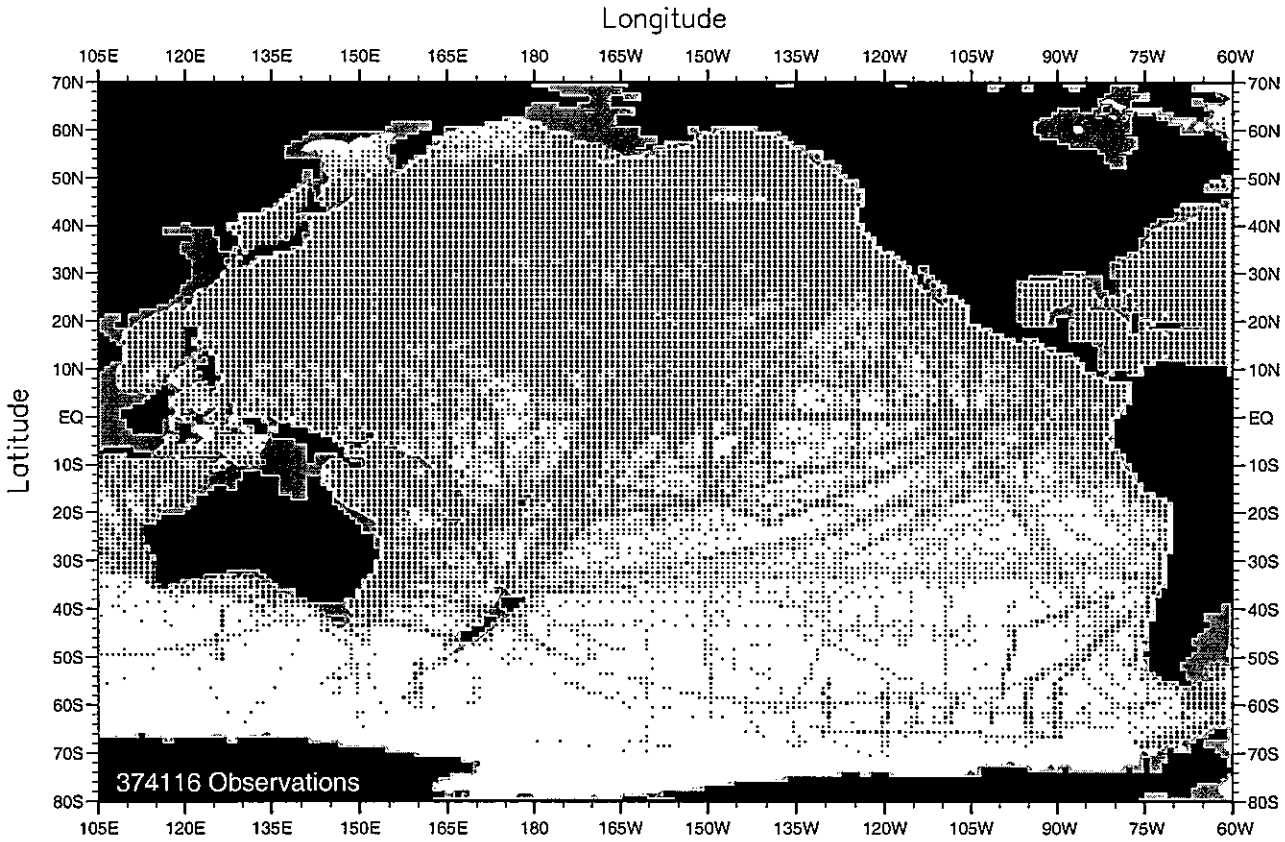


Fig. B12. Spring (Apr.-Jun.) temperature observations at 250 m. depth .

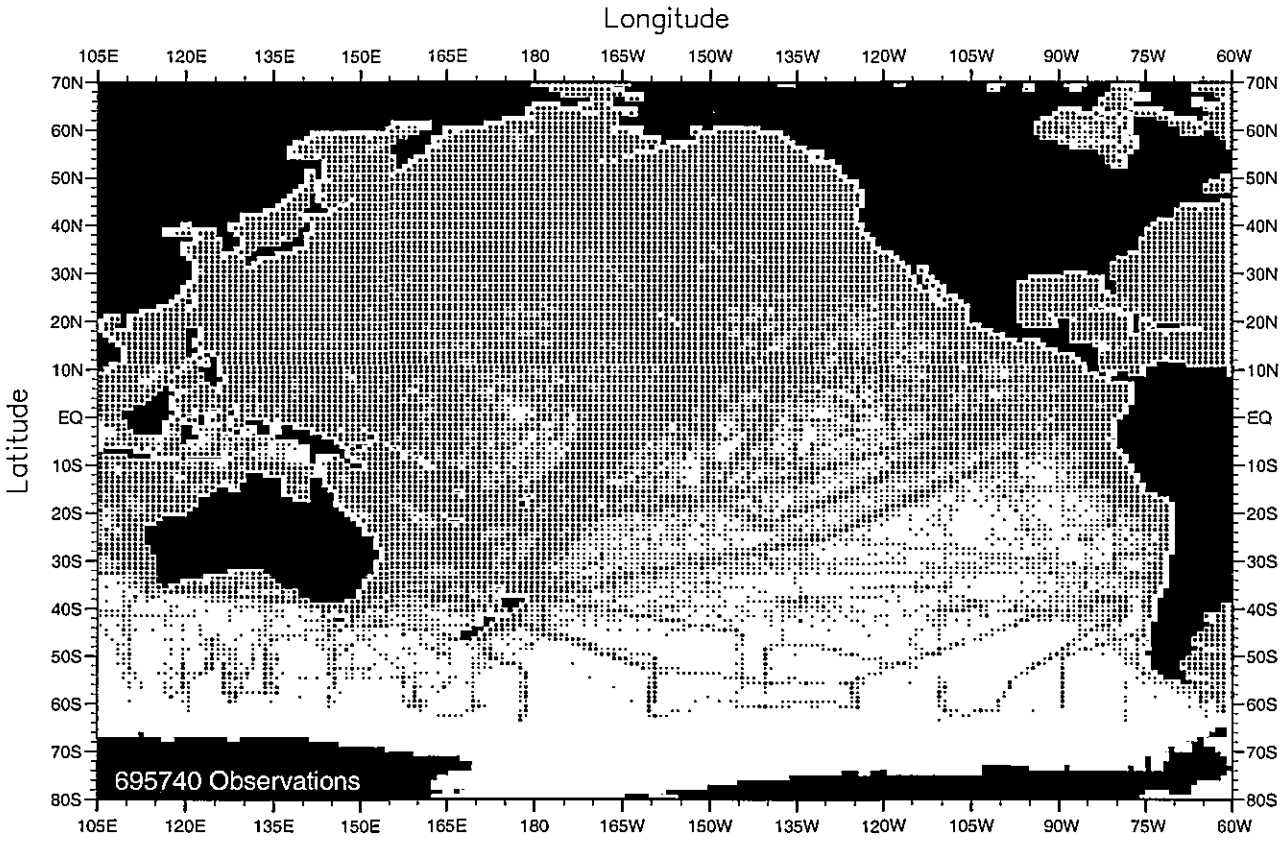


Fig. B13. Summer (Jul.-Sep.) temperature observations at the surface .

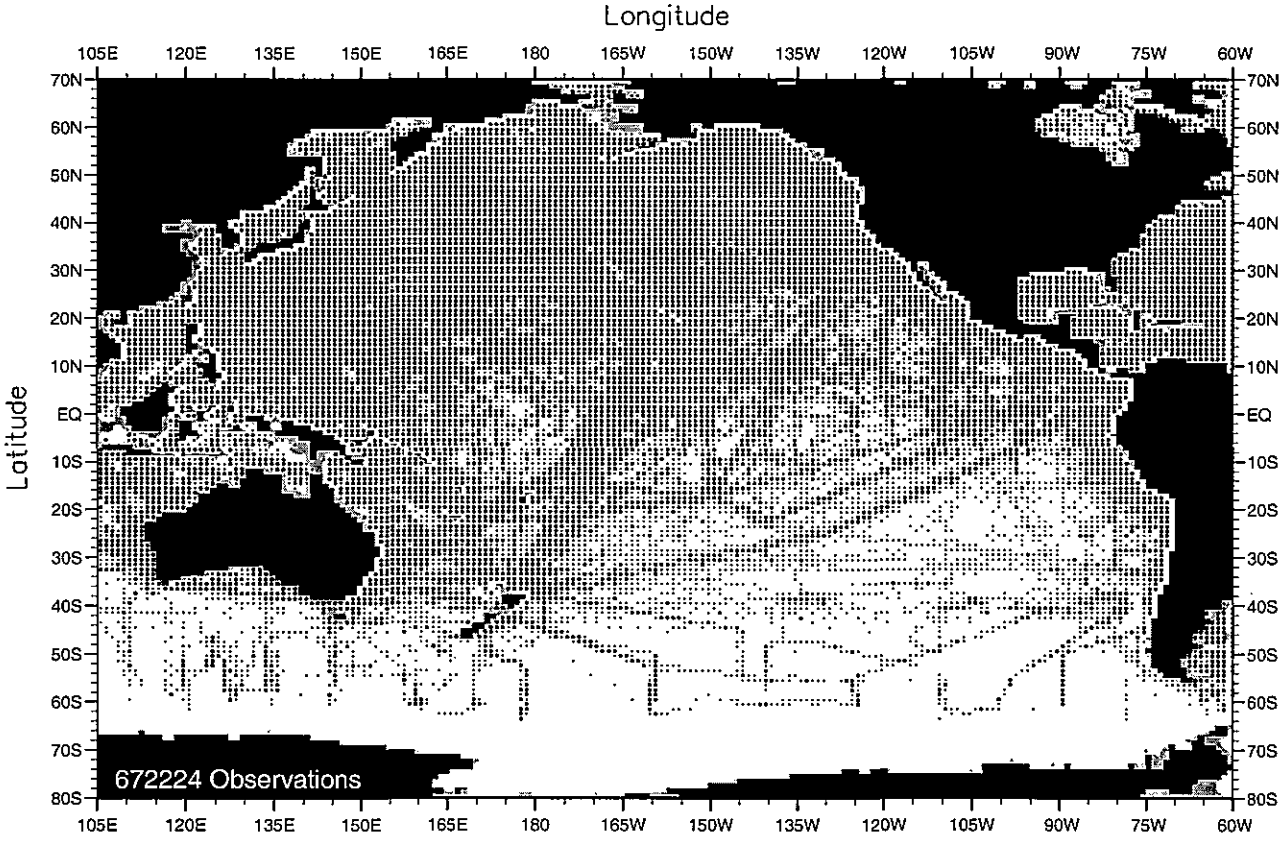


Fig. B14. Summer (Jul.-Sep.) temperature observations at 50 m. depth .

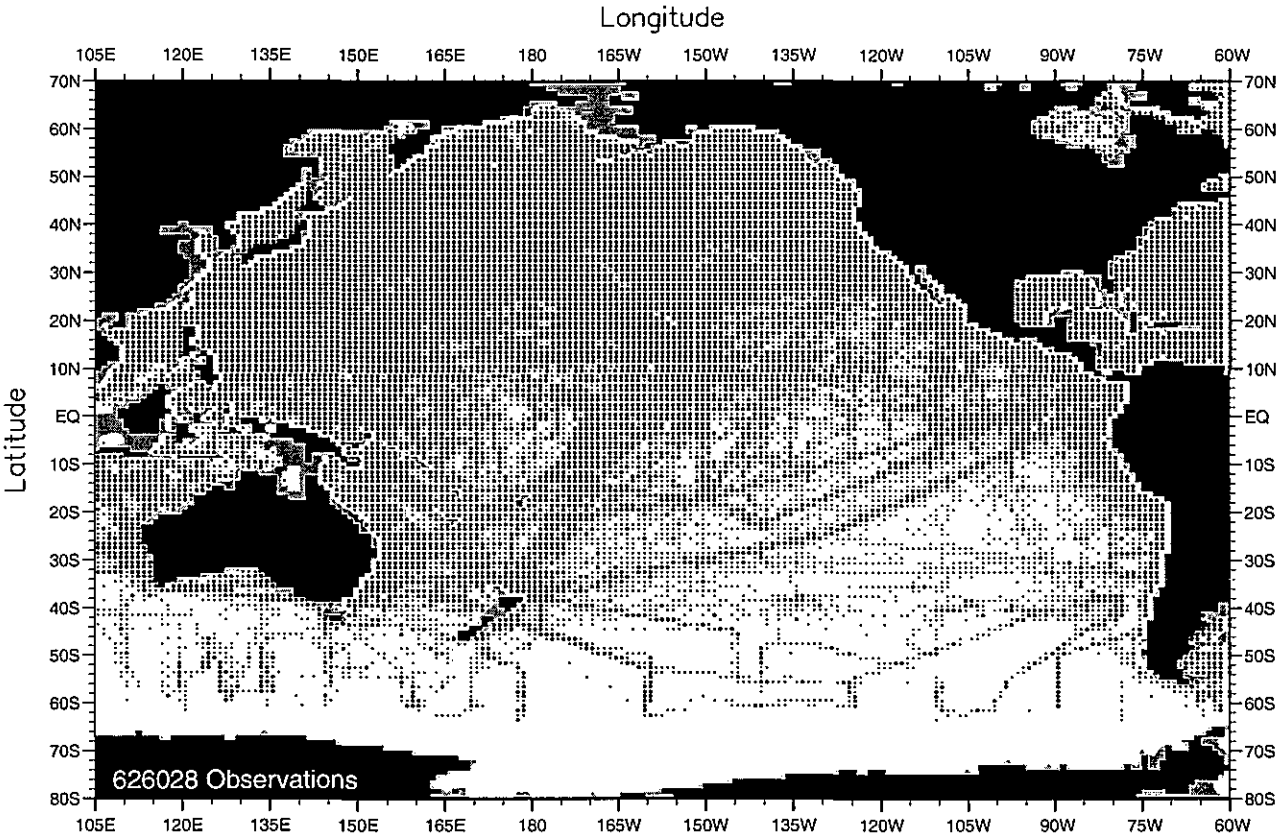


Fig. B15. Summer (Jul.-Sep.) temperature observations at 75 m. depth .

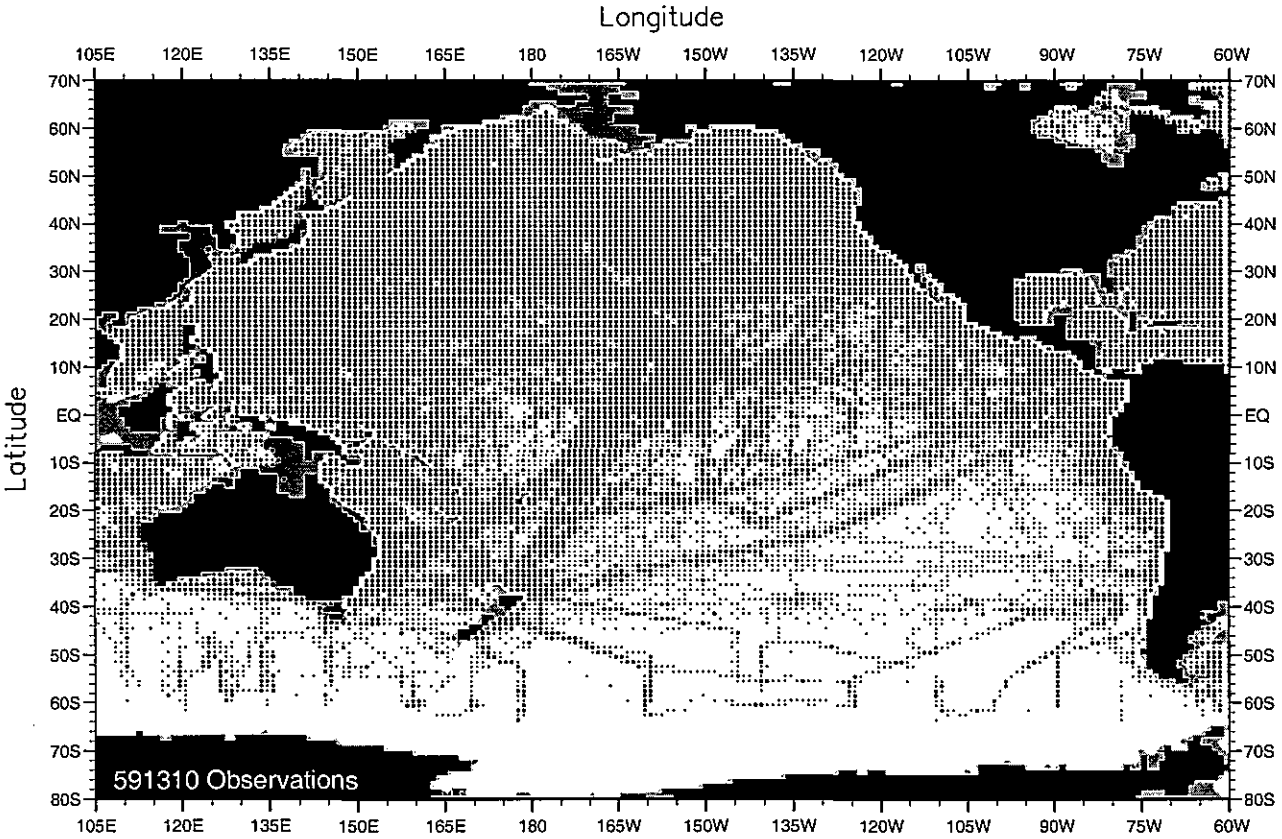


Fig. B16. Summer (Jul.-Sep.) temperature observations at 100 m. depth .

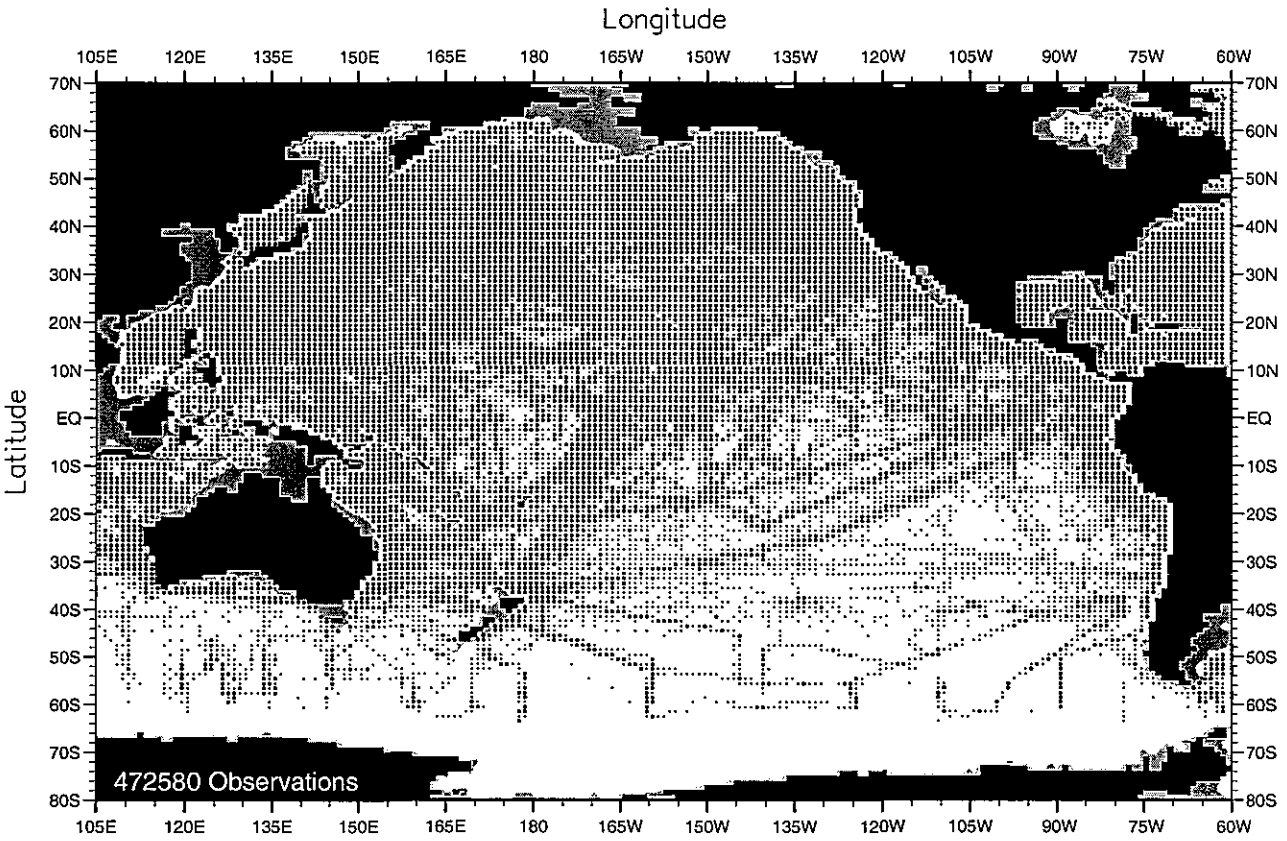


Fig. B17. Summer (Jul.-Sep.) temperature observations at 150 m. depth .

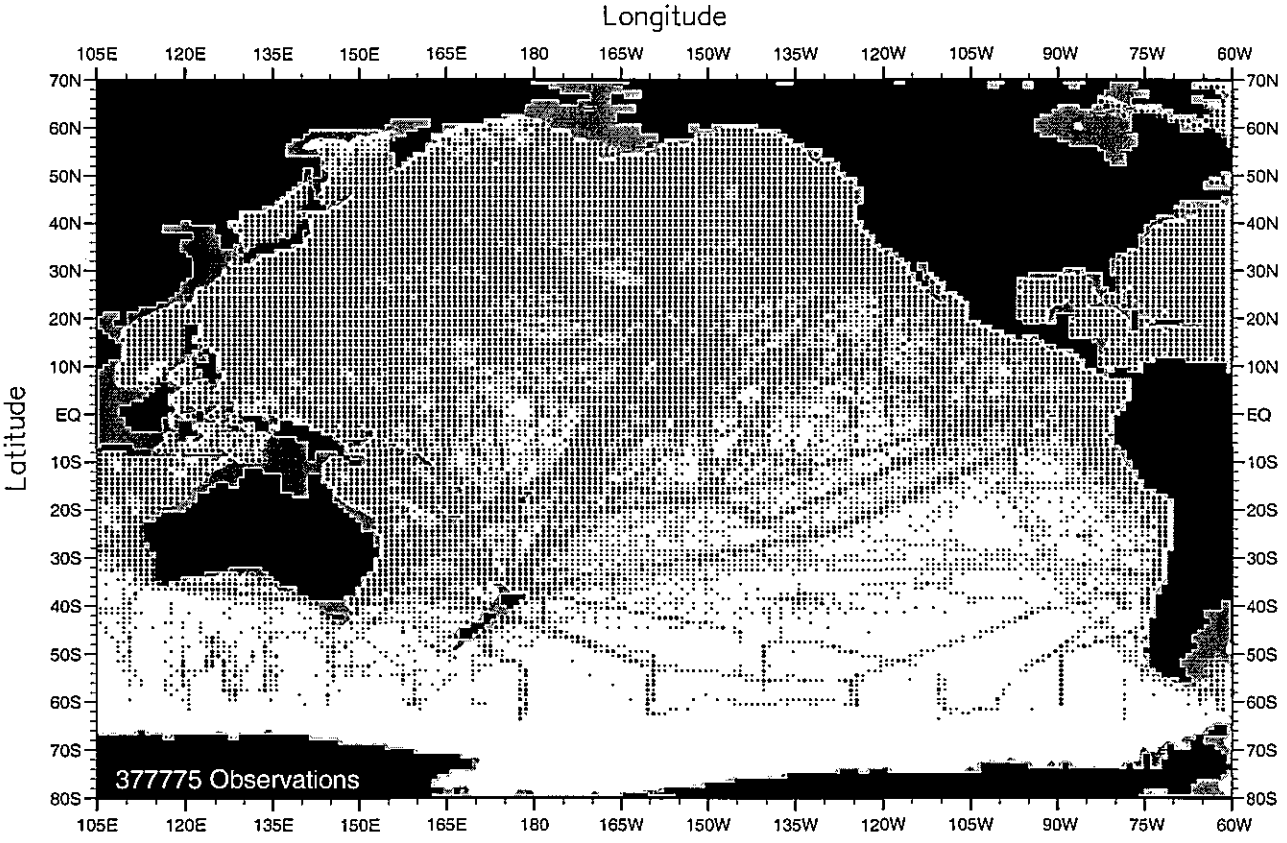


Fig. B18. Summer (Jul.-Sep.) temperature observations at 250 m. depth .

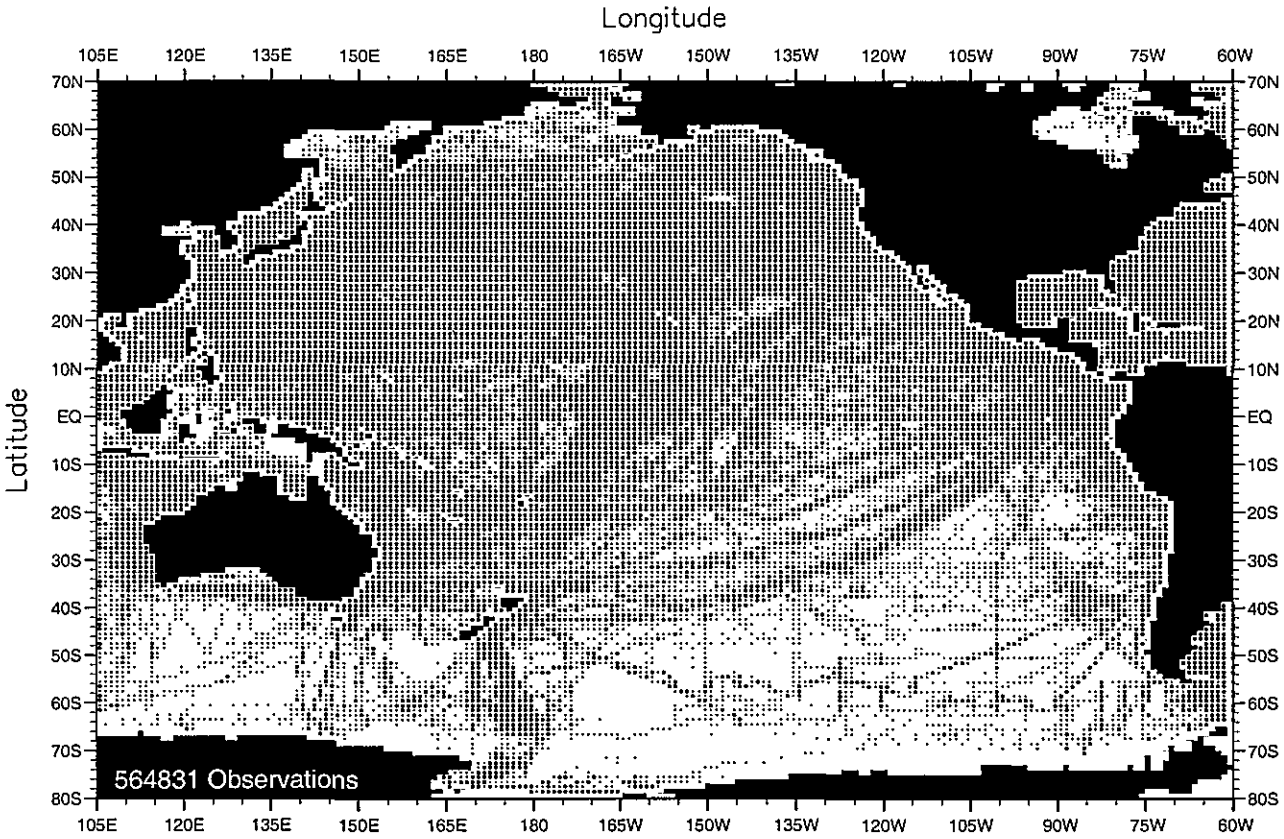


Fig. B19. Fall (Oct.-Dec.) temperature observations at the surface .

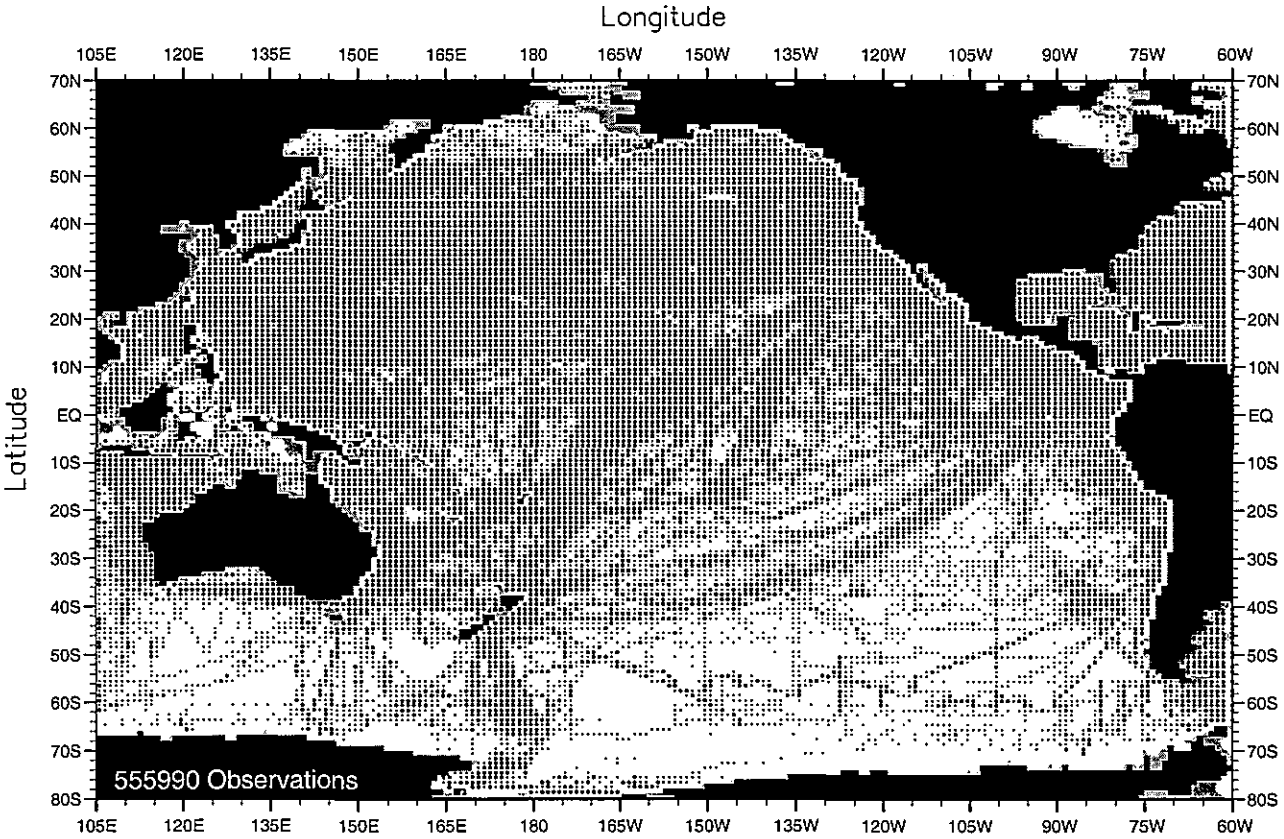


Fig. B20. Fall (Oct.-Dec.) temperature observations at 50 m. depth .

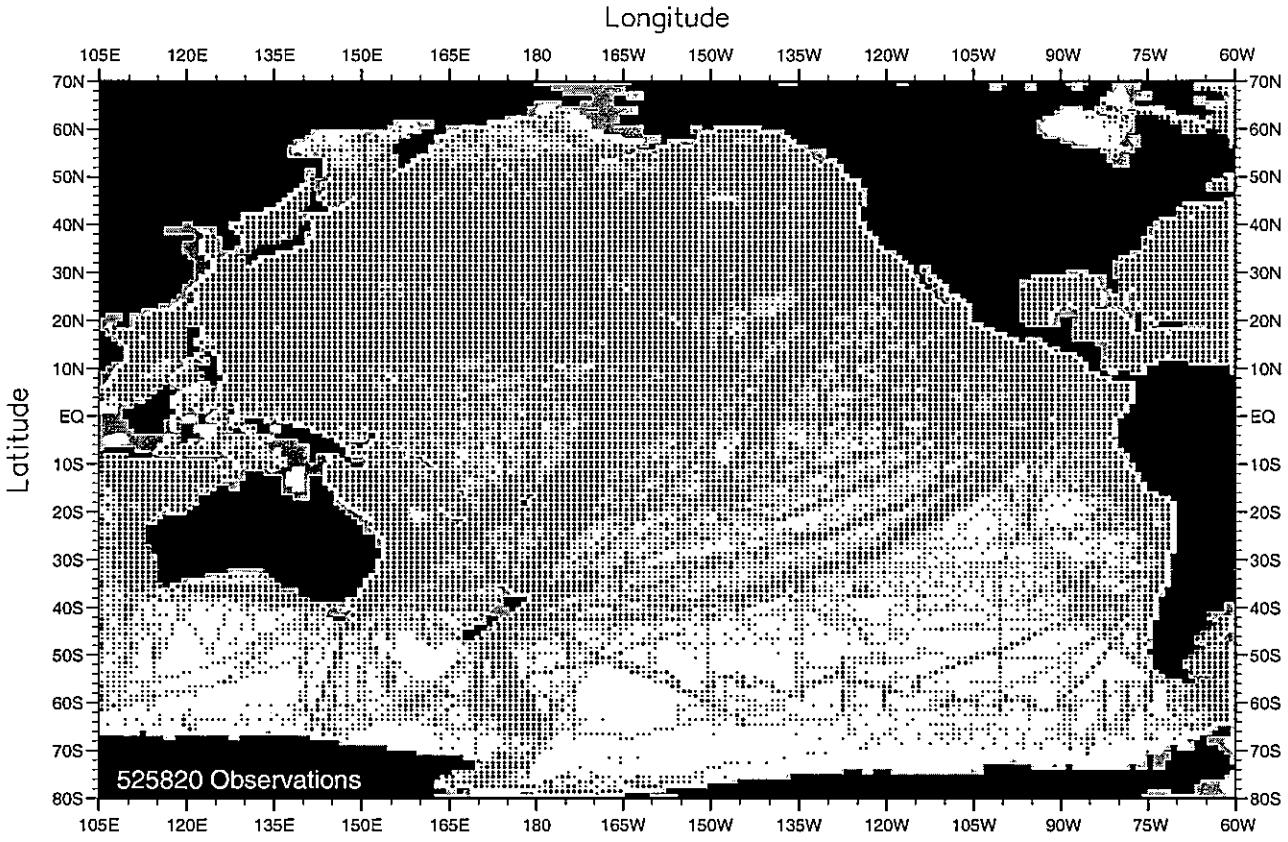


Fig. B21. Fall (Oct.-Dec.) temperature observations at 75 m. depth .

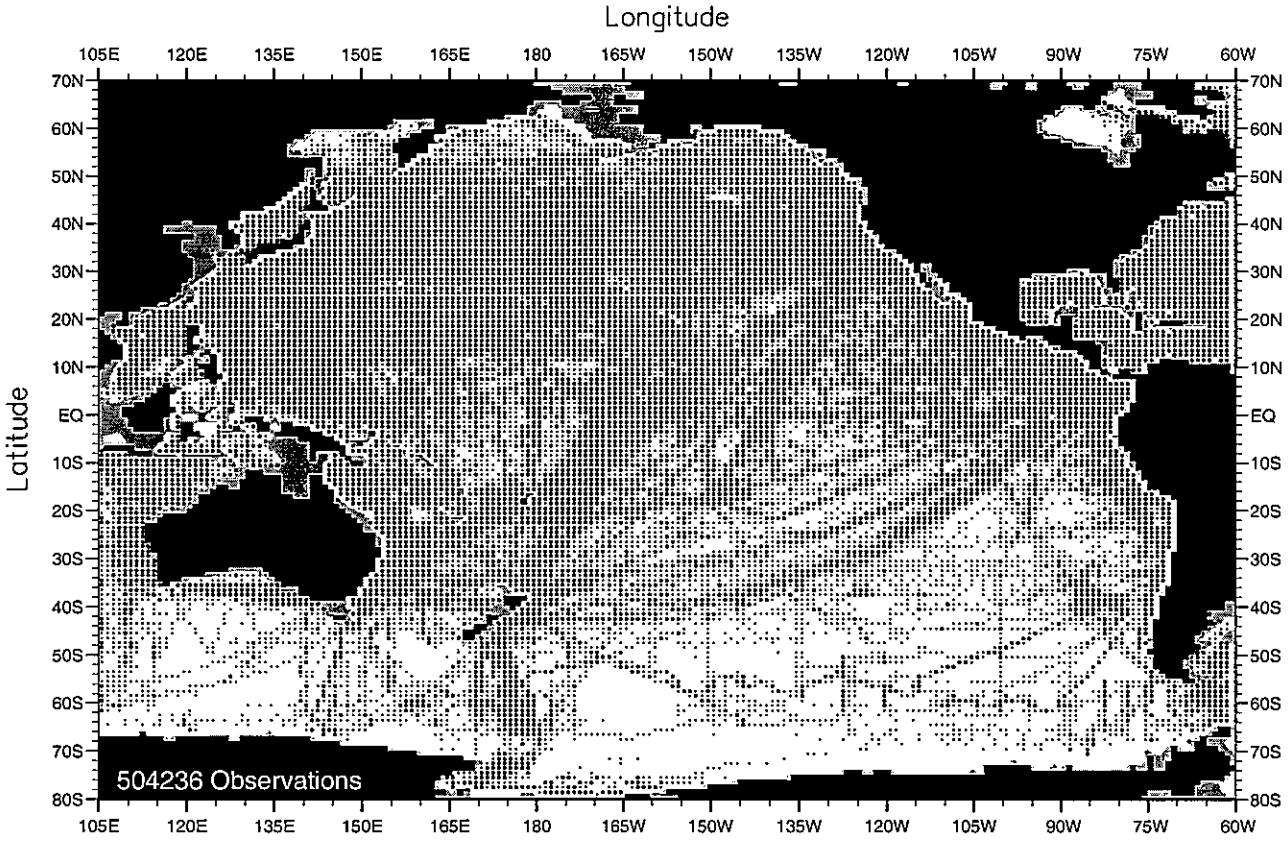


Fig. B22. Fall (Oct.-Dec.) temperature observations at 100 m. depth .

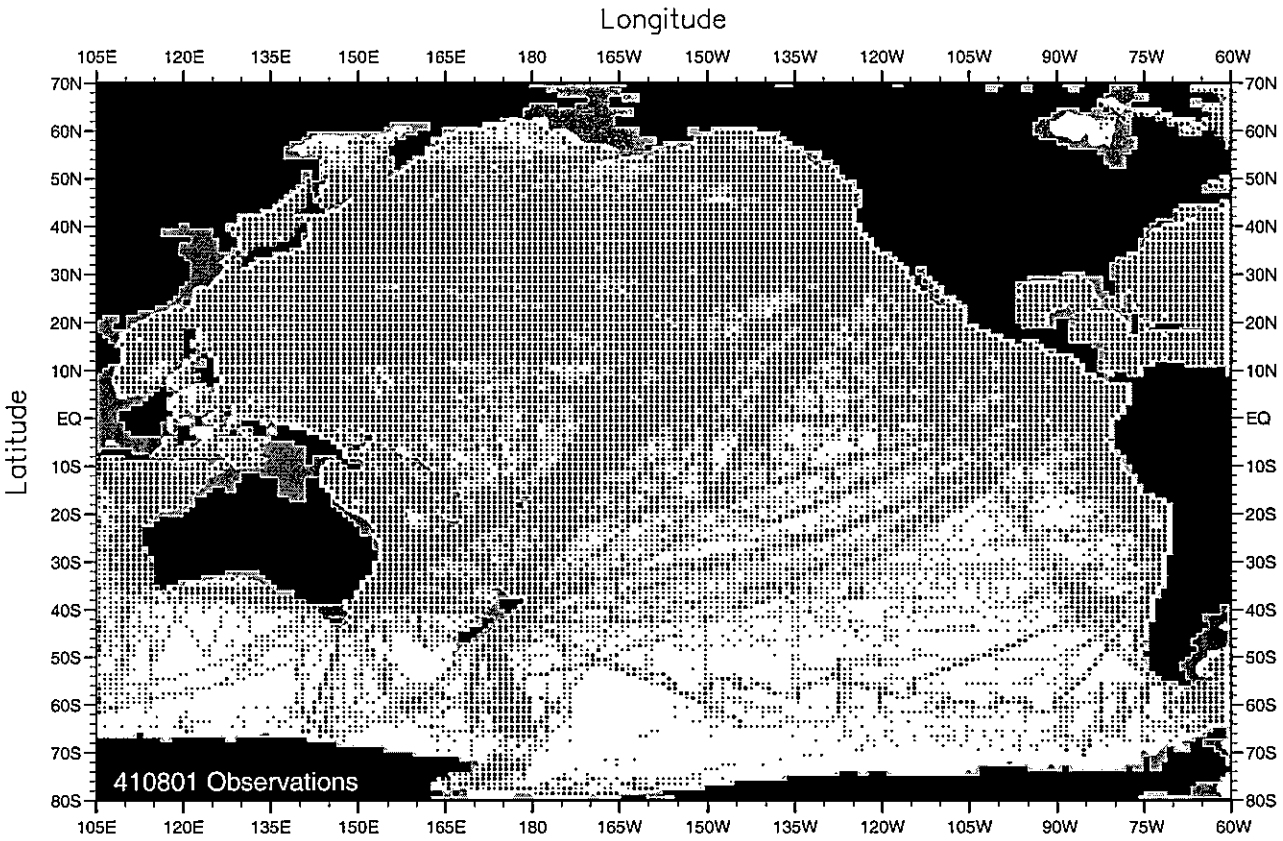


Fig. B23. Fall (Oct.-Dec.) temperature observations at 150 m. depth .

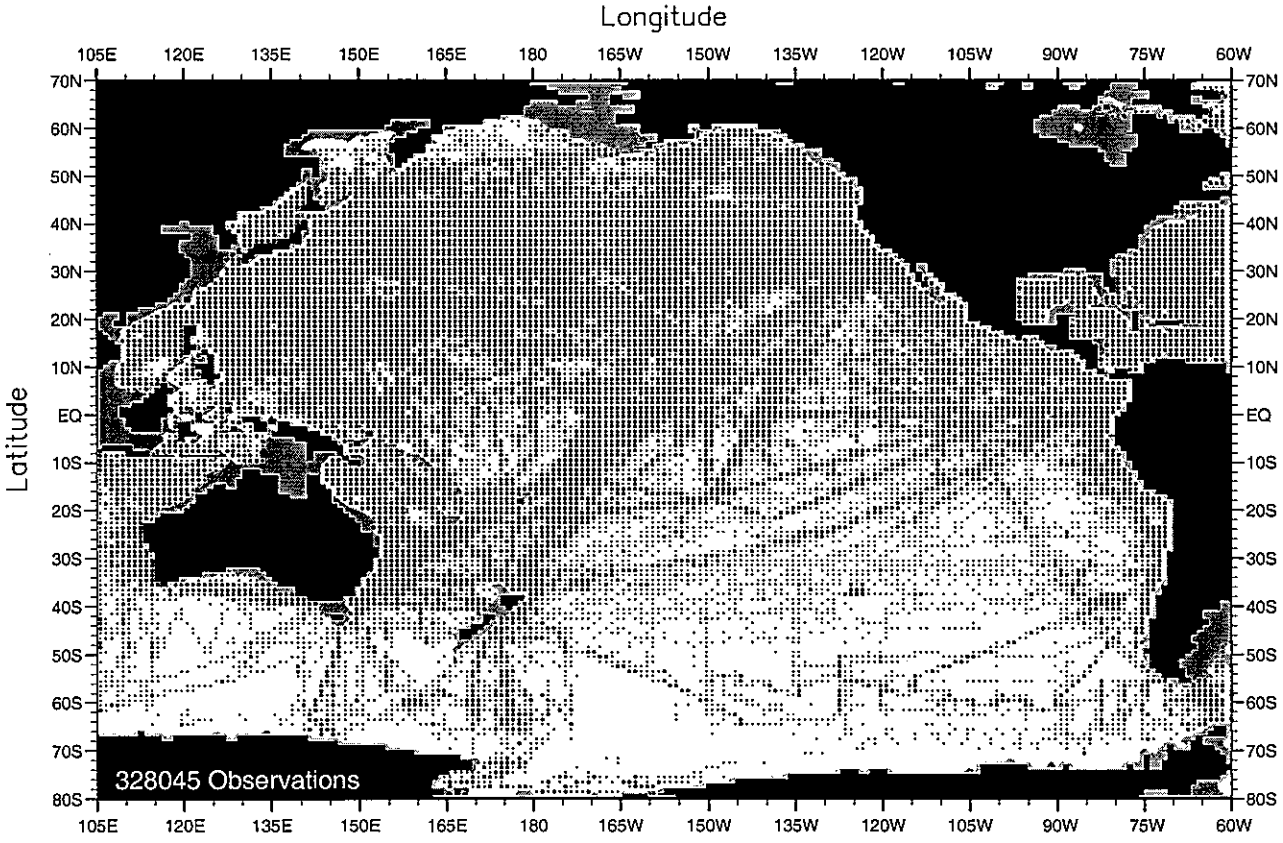


Fig. B24. Fall (Oct.-Dec.) temperature observations at 250 m. depth .

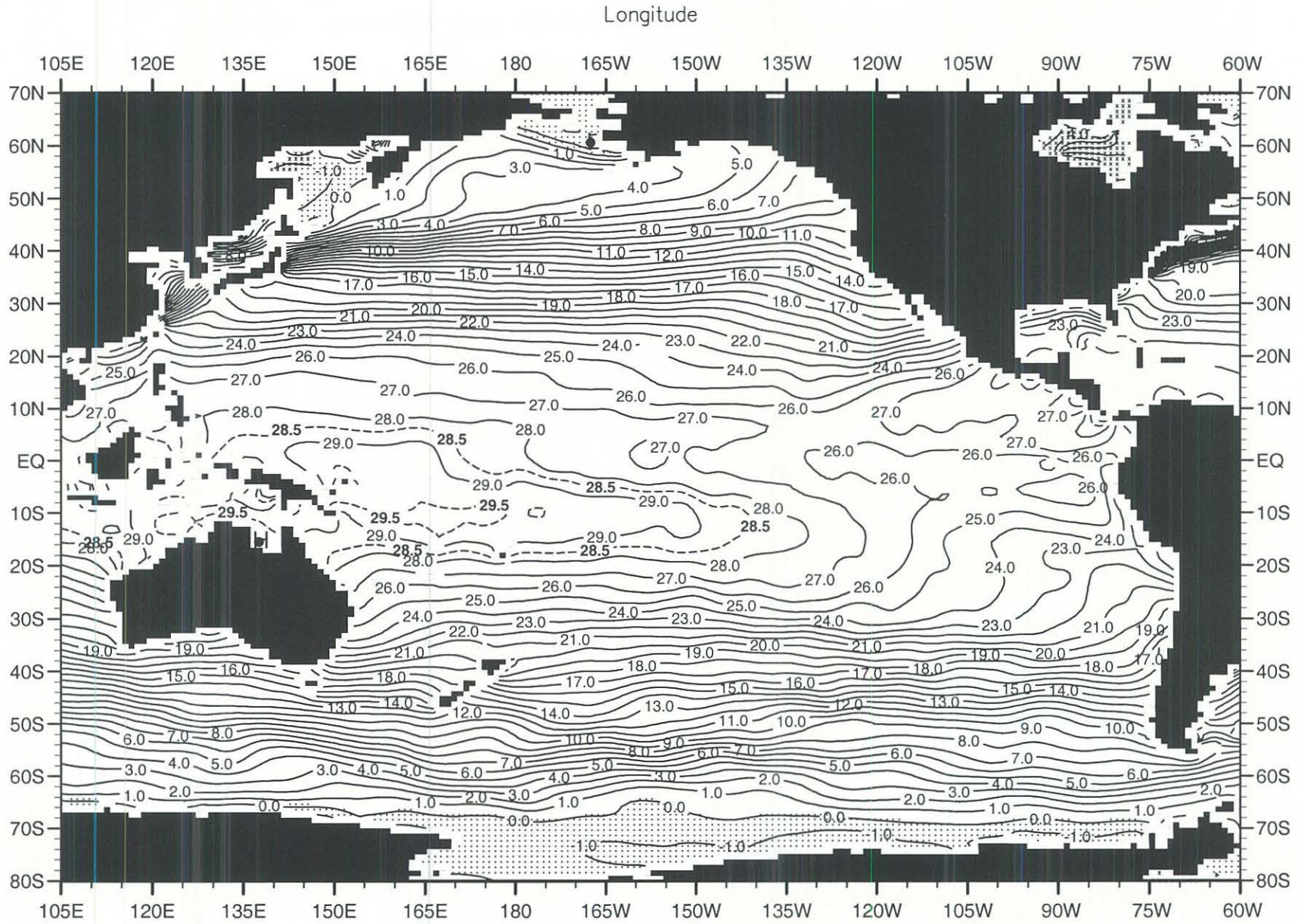


Fig. B25. Winter (Jan.-Mar.) mean temperature (°C) at the surface .

Minimum Value= -2.08 Maximum Value= 30.11 Contour Interval: 1.00

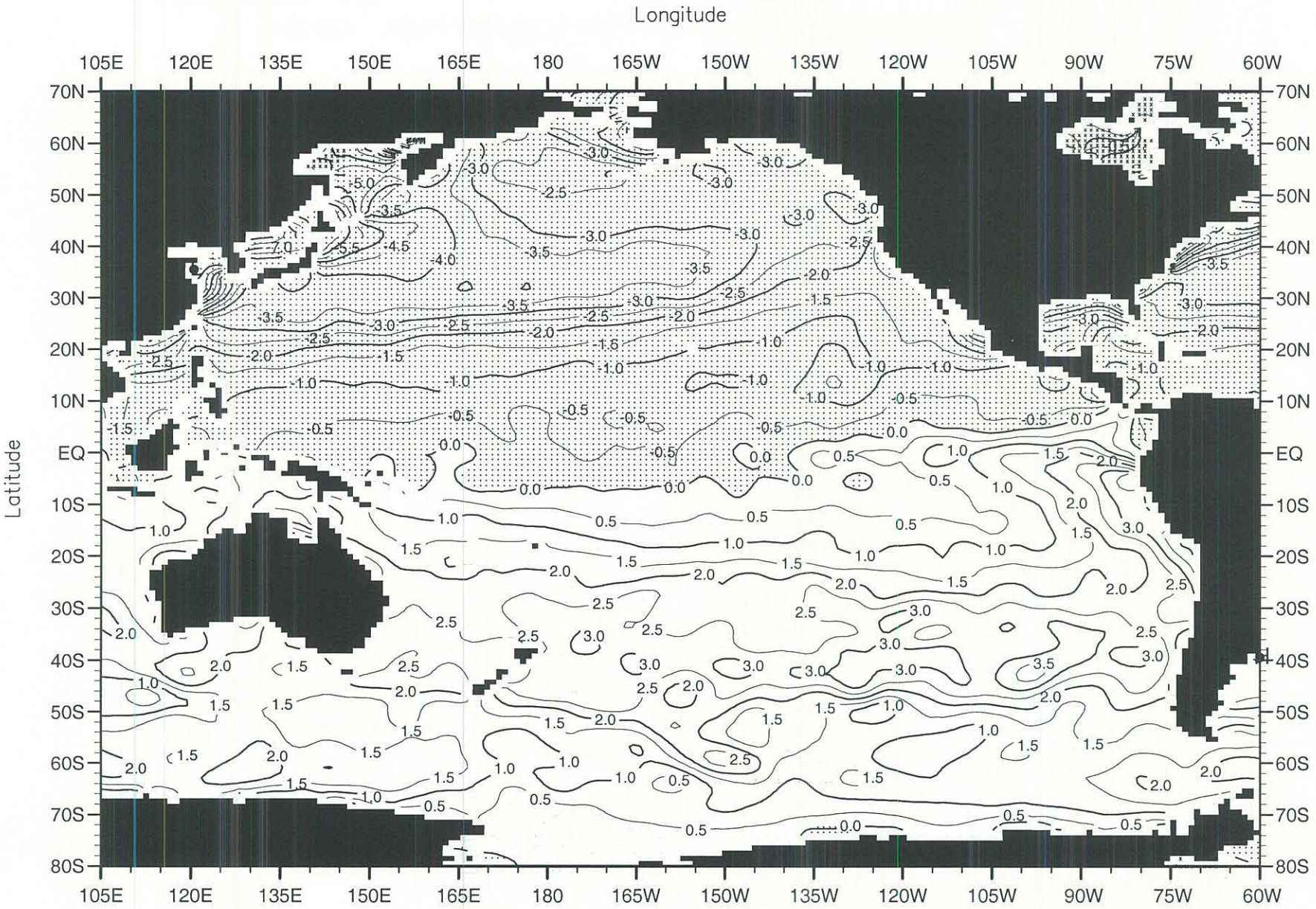


Fig. B26. Winter (Jan.-Mar.) minus annual temperature (°C) at the surface .

Minimum Value= -9.22 Maximum Value= 4.22 Contour Interval: 0.50

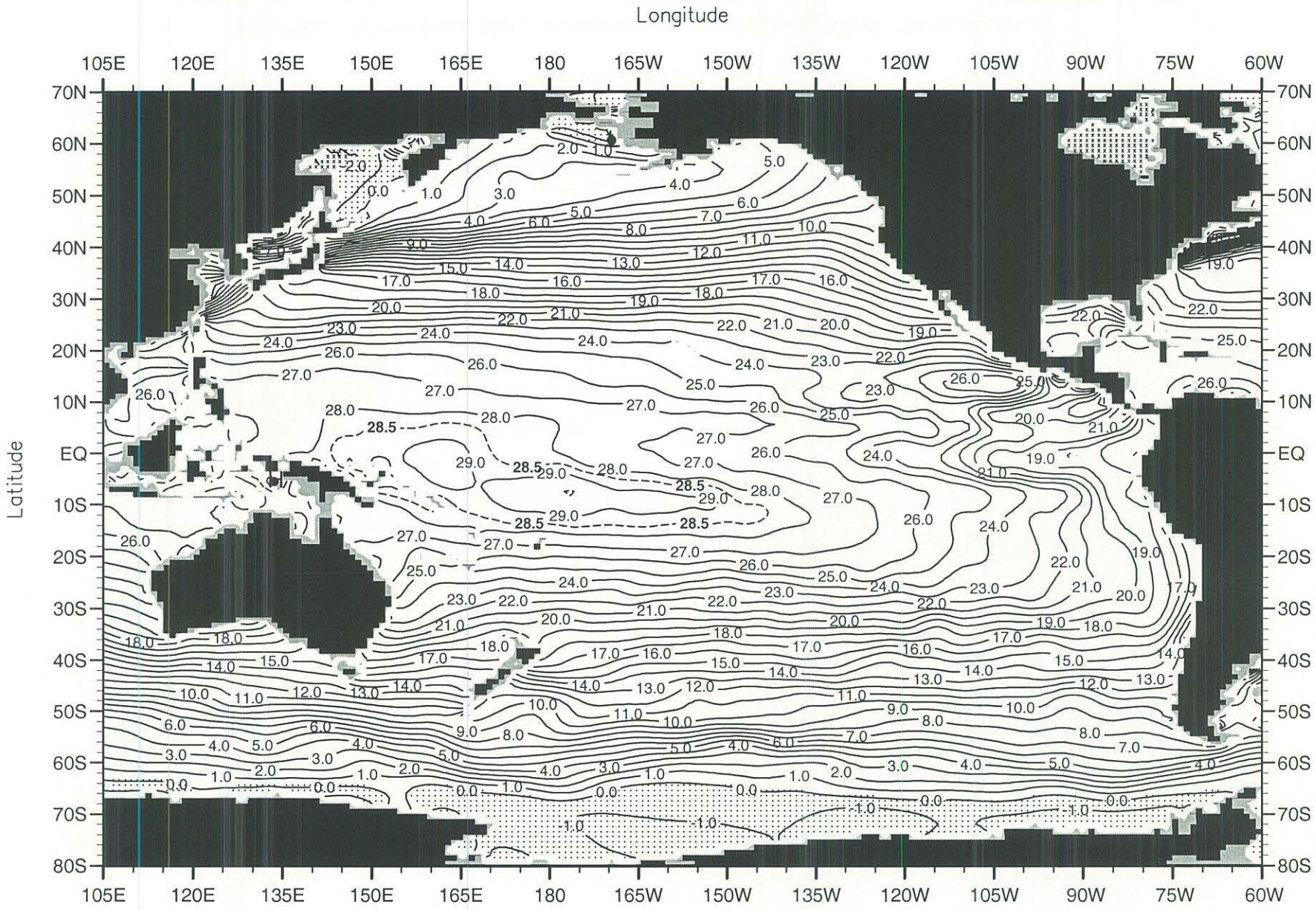


Fig. B27. Winter (Jan.-Mar.) mean temperature (°C) at 50 m. depth .

Minimum Value= -2.10 Maximum Value= 29.54 Contour Interval: 1.00

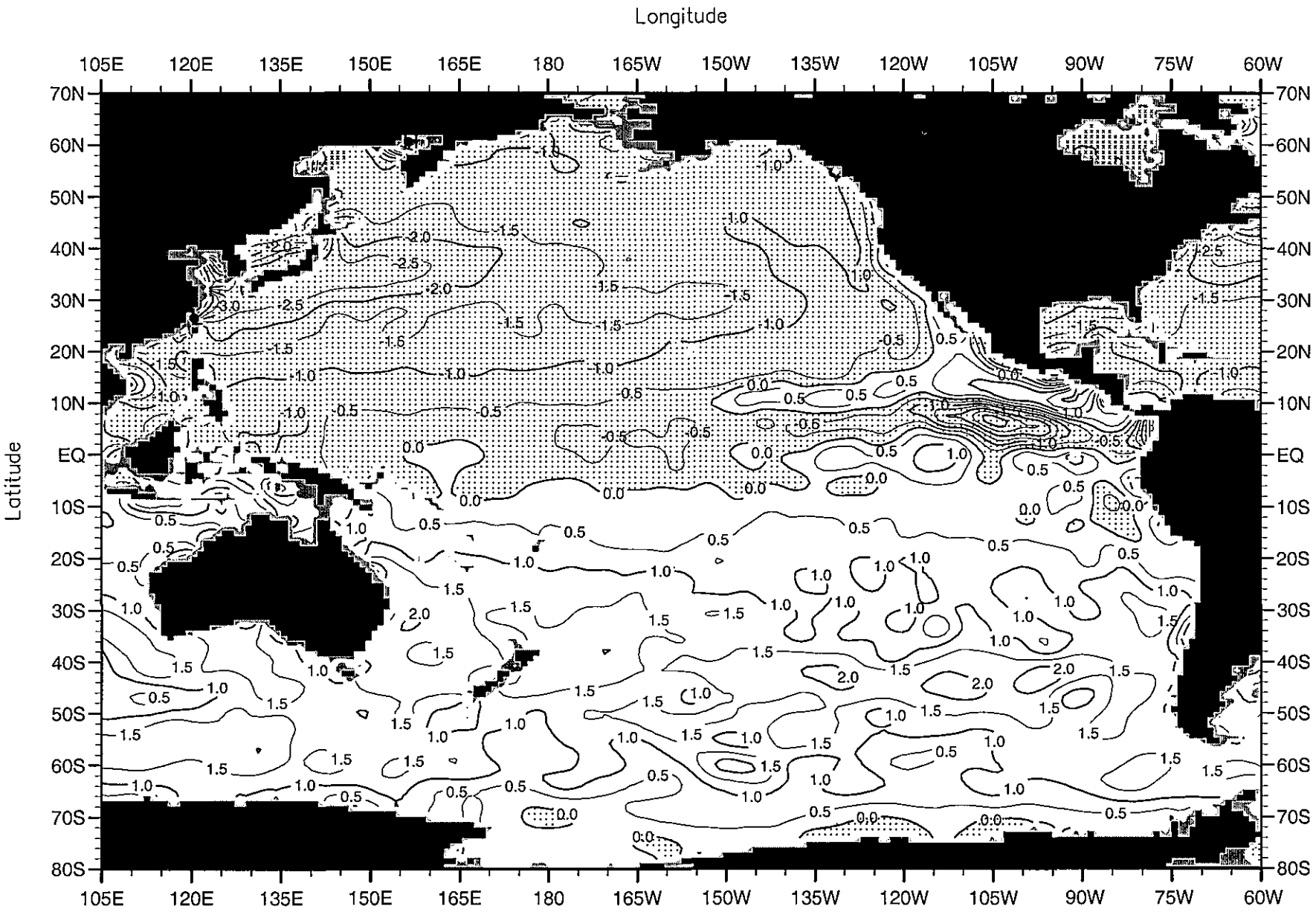


Fig. B28. Winter (Jan.-Mar.) minus annual temperature (°C) at 50 m. depth .

Minimum Value= -4.98 Maximum Value= 5.21 Contour Interval: 0.50

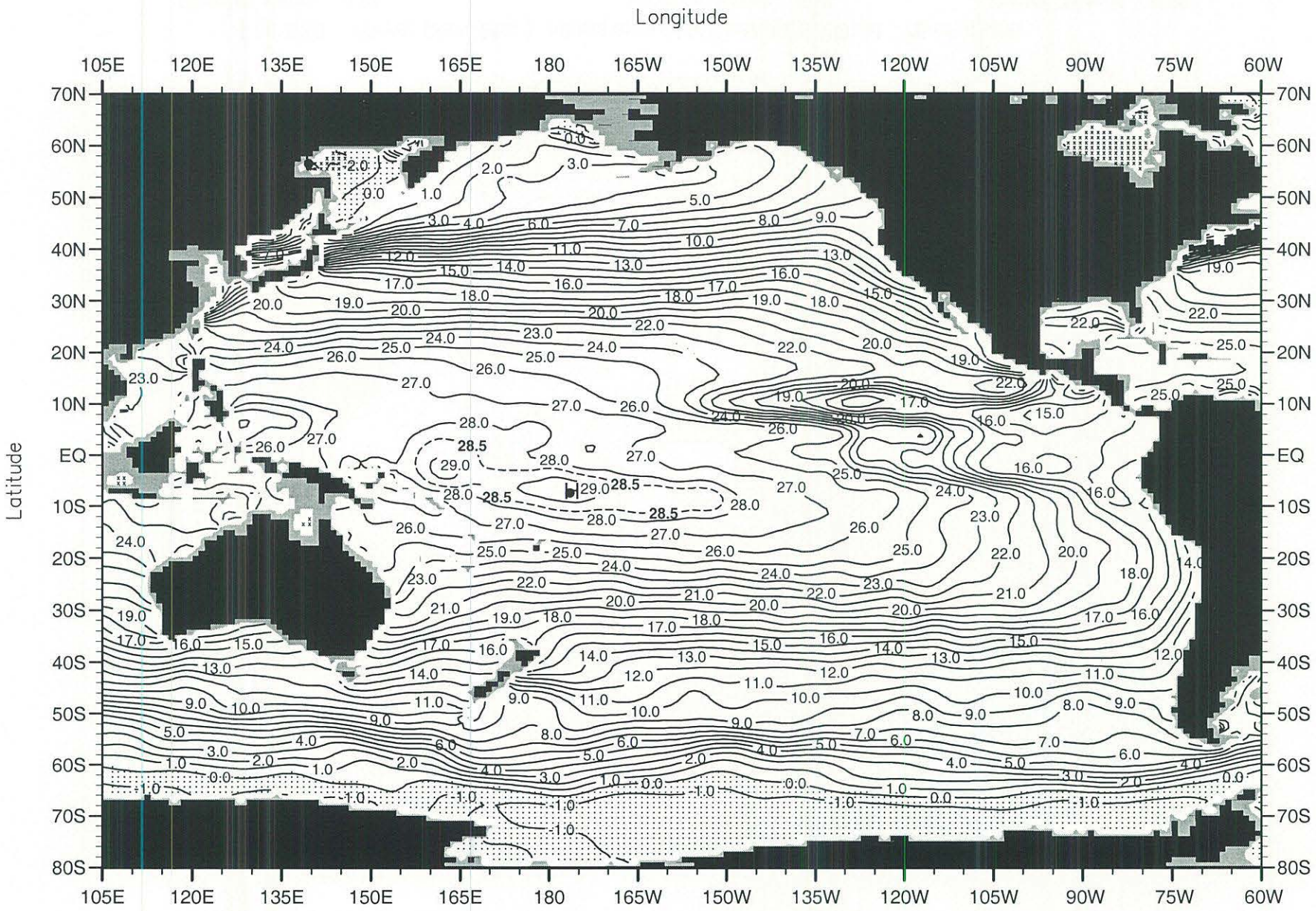


Fig. B29. Winter (Jan.-Mar.) mean temperature (°C) at 75 m. depth .

Minimum Value= -2.10 Maximum Value= 29.29 Contour Interval: 1.00

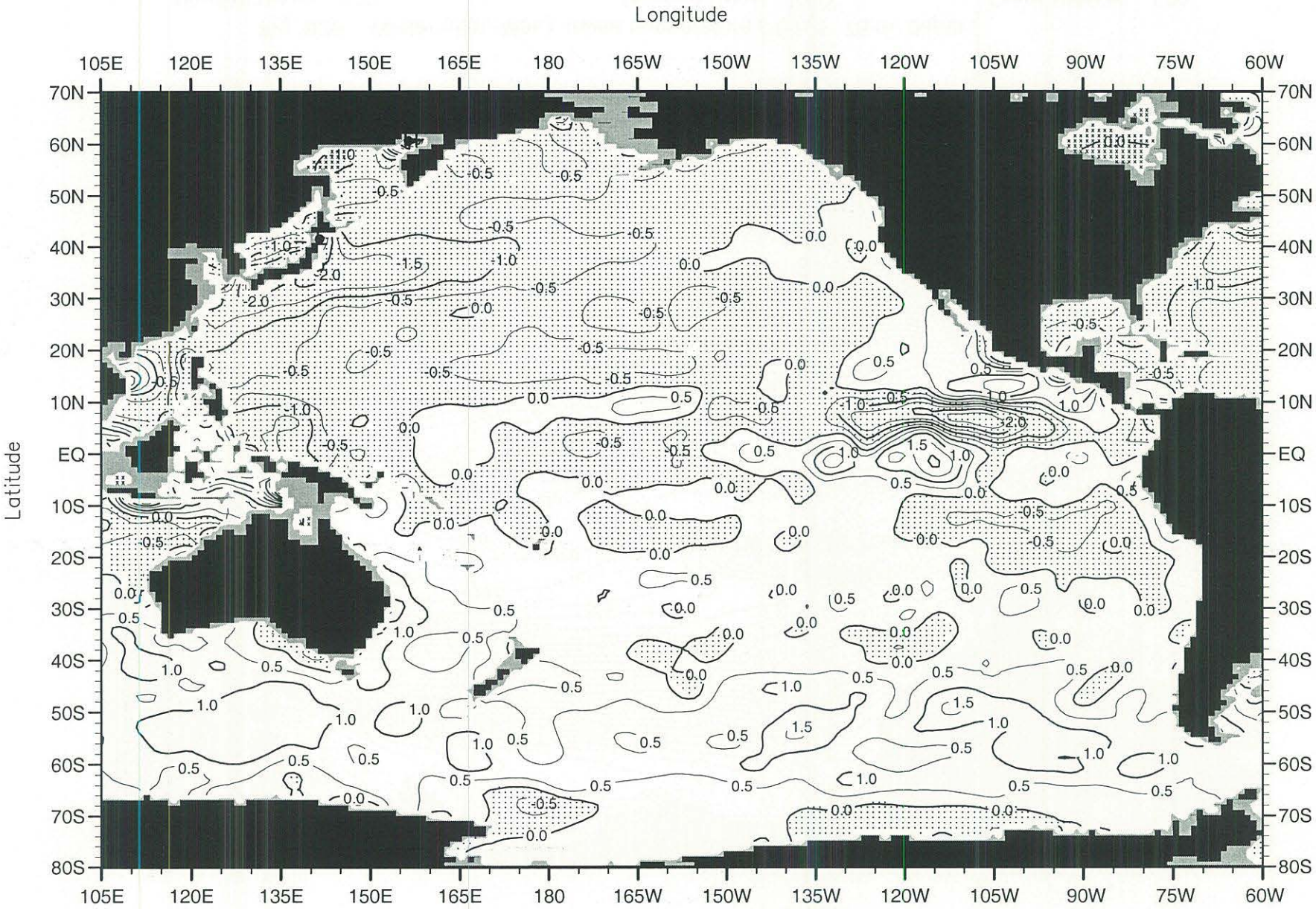


Fig. B30. Winter (Jan.-Mar.) minus annual temperature (°C) at 75 m. depth .

Minimum Value= -3.92 Maximum Value= 5.42 Contour Interval: 0.50

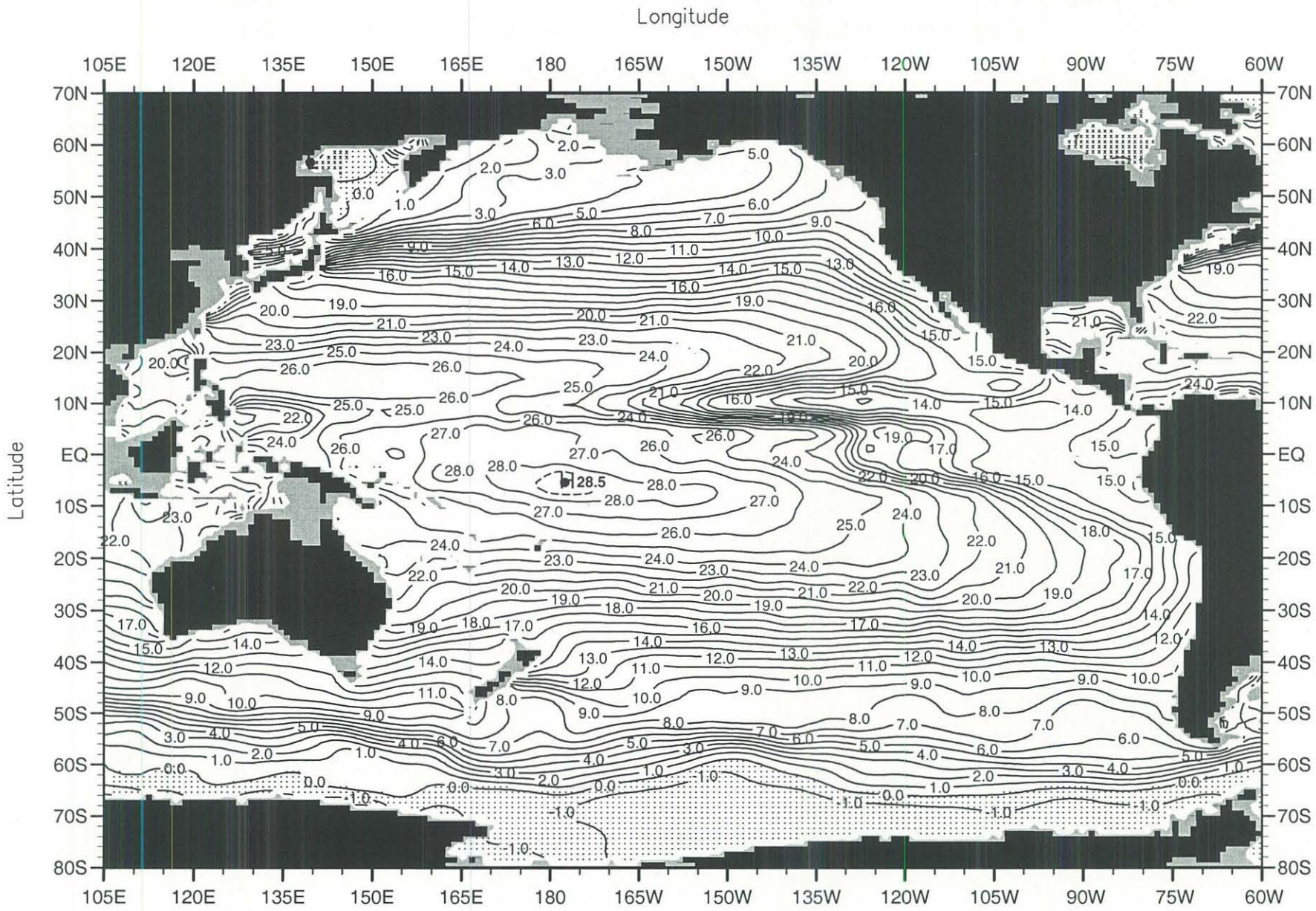


Fig. B31. Winter (Jan.-Mar.) mean temperature (°C) at 100 m. depth .

Minimum Value= -2.10 Maximum Value= 28.87 Contour Interval: 1.00

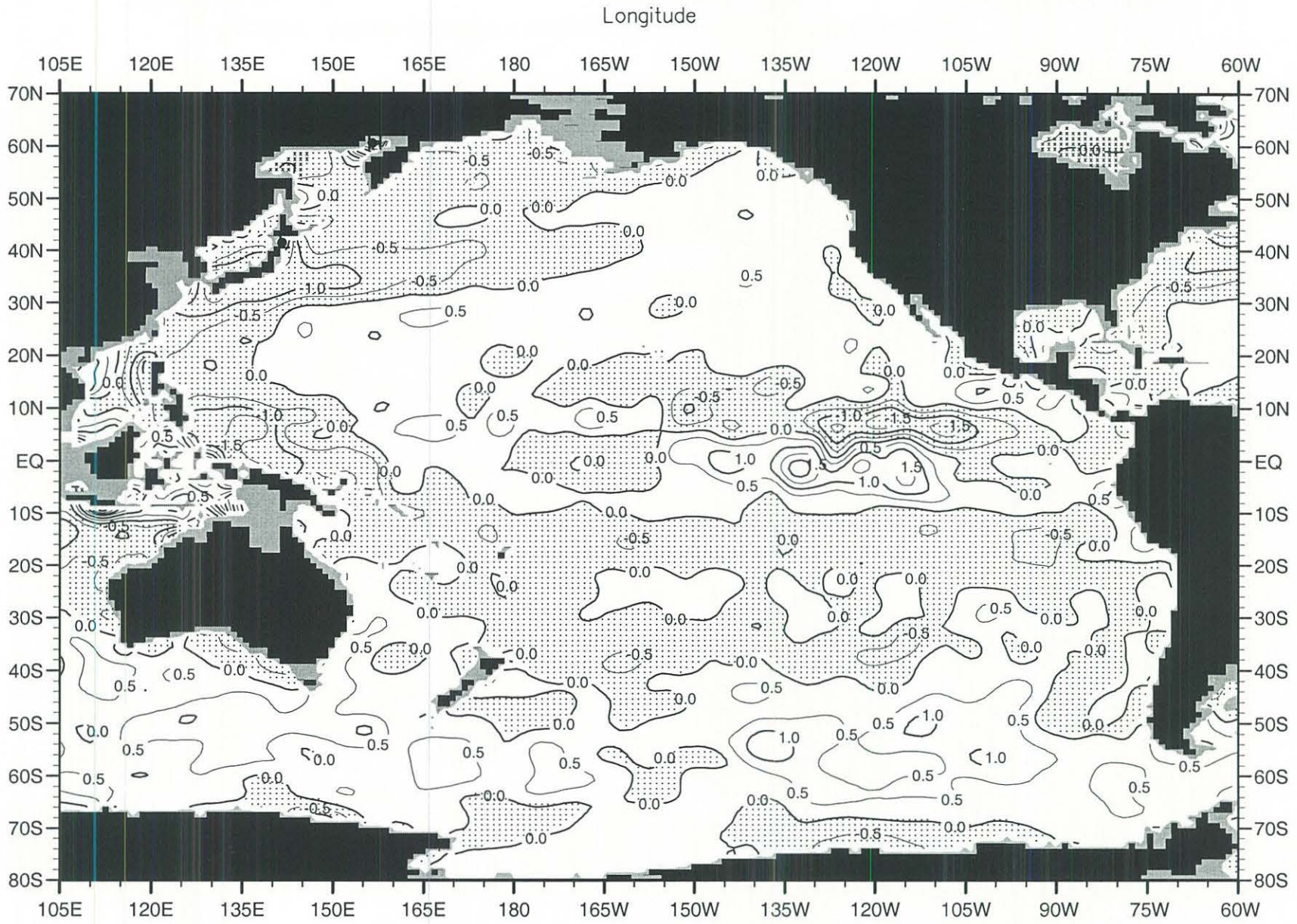


Fig. B32. Winter (Jan.-Mar.) minus annual temperature (°C) at 100 m. depth .

Minimum Value= -3.16 Maximum Value= 5.11 Contour Interval: 0.50

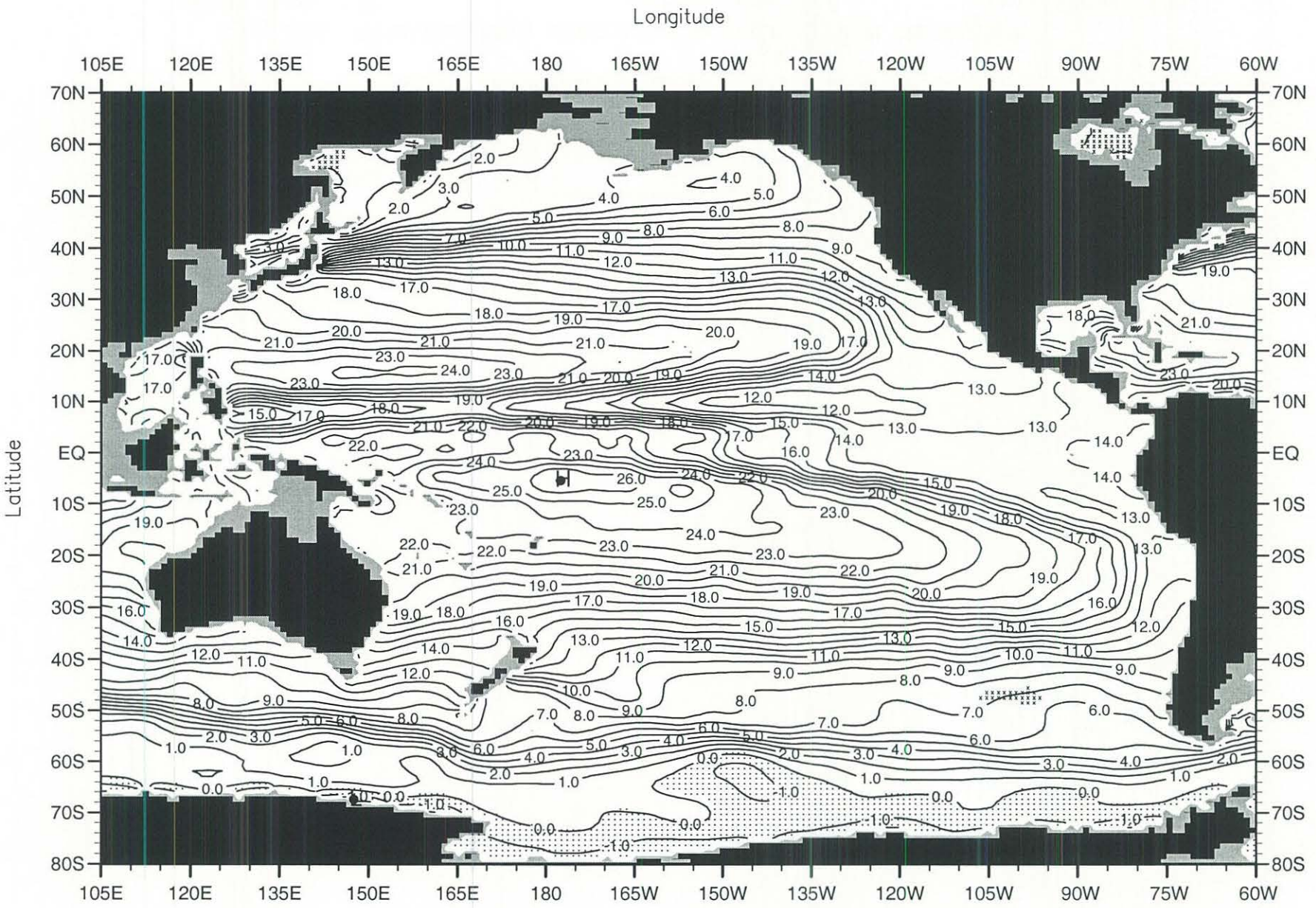


Fig. B33. Winter (Jan.-Mar.) mean temperature (°C) at 150 m. depth .

Minimum Value= -2.10 Maximum Value= 27.04 Contour Interval: 1.00

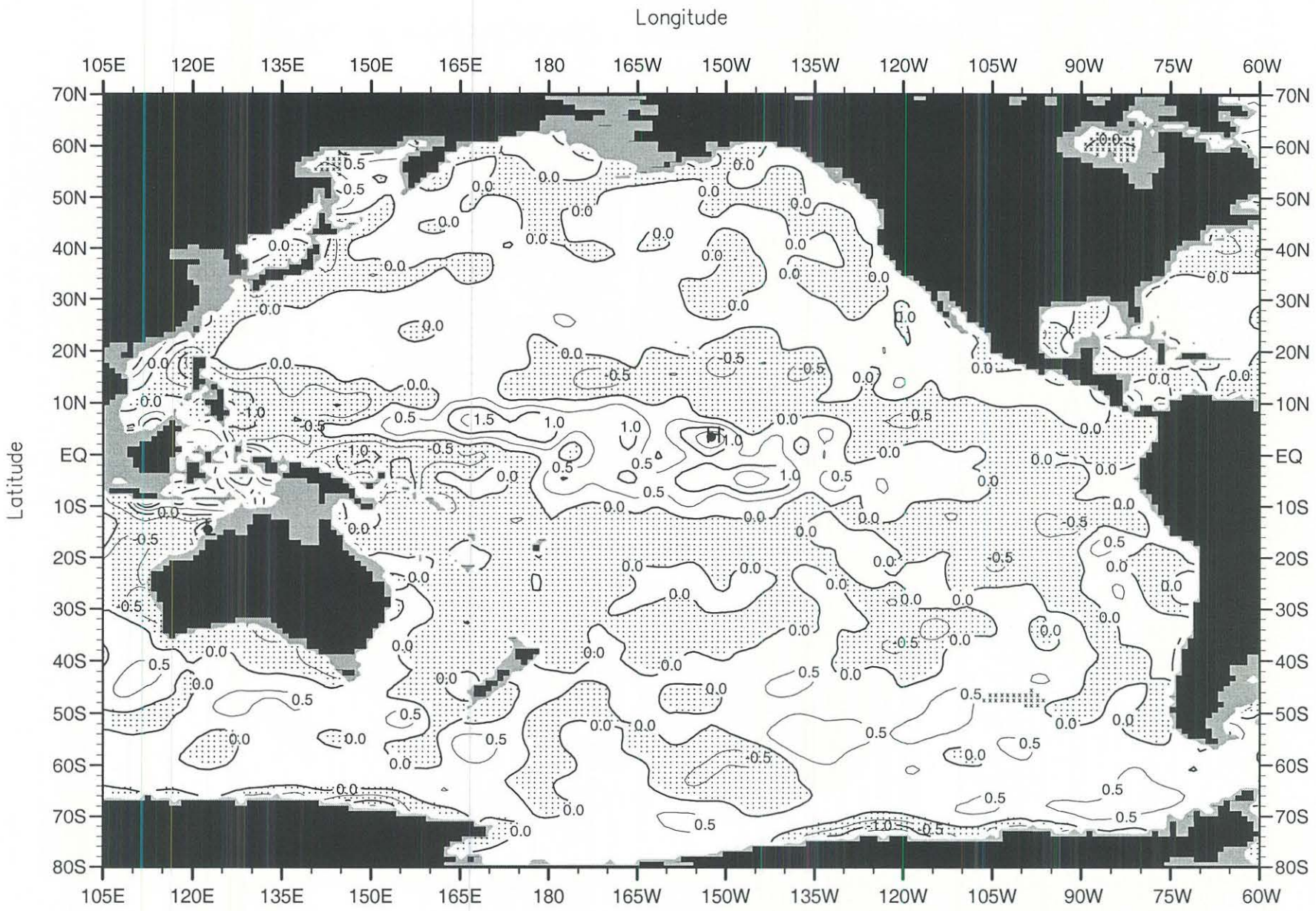


Fig. B34. Winter (Jan.-Mar.) minus annual temperature (°C) at 150 m. depth .

Minimum Value= -2.02 Maximum Value= 1.94 Contour Interval: 0.50

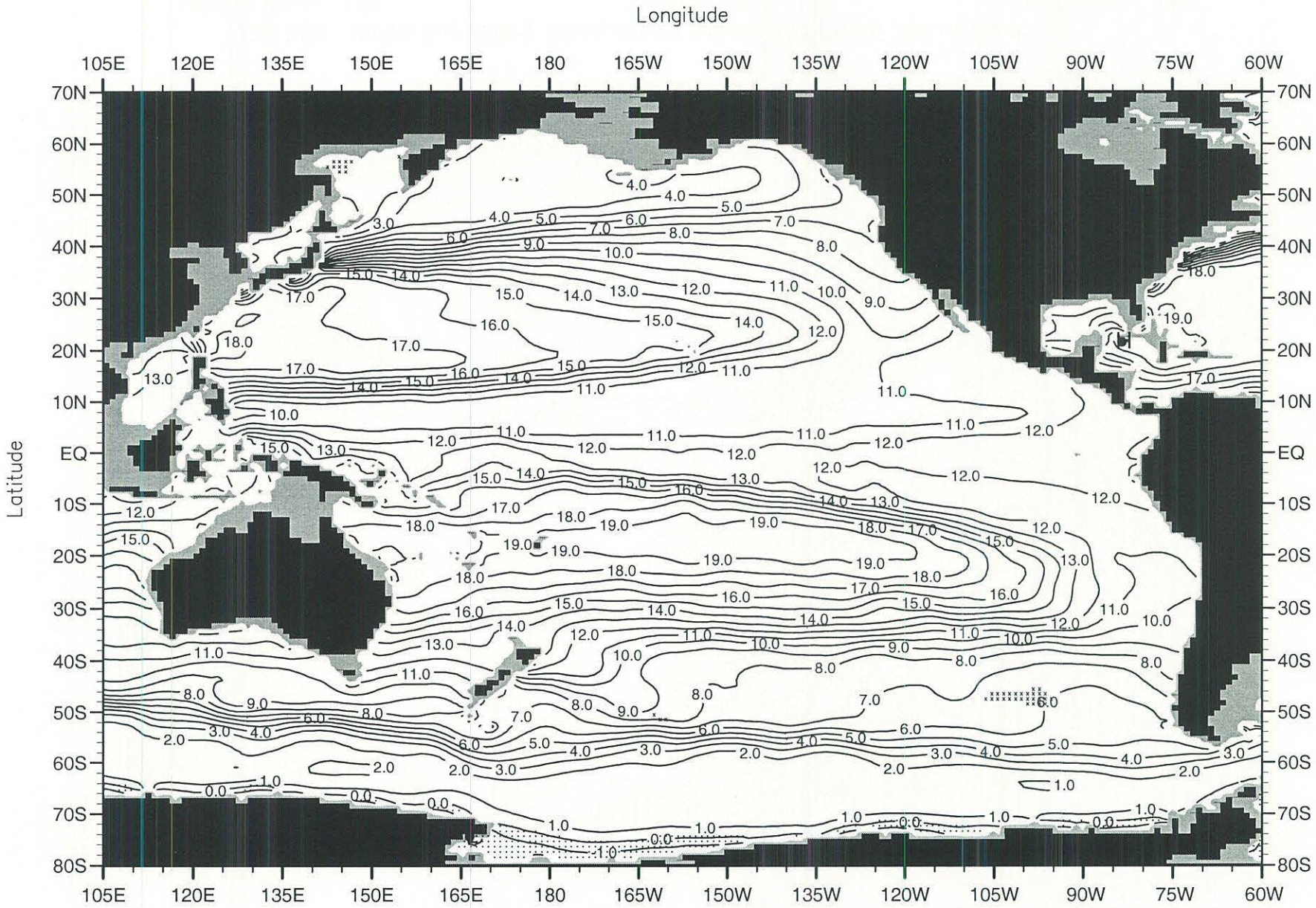


Fig. B35. Winter (Jan.-Mar.) mean temperature (°C) at 250 m. depth .

Minimum Value= -2.08 Maximum Value= 20.11 Contour Interval: 1.00

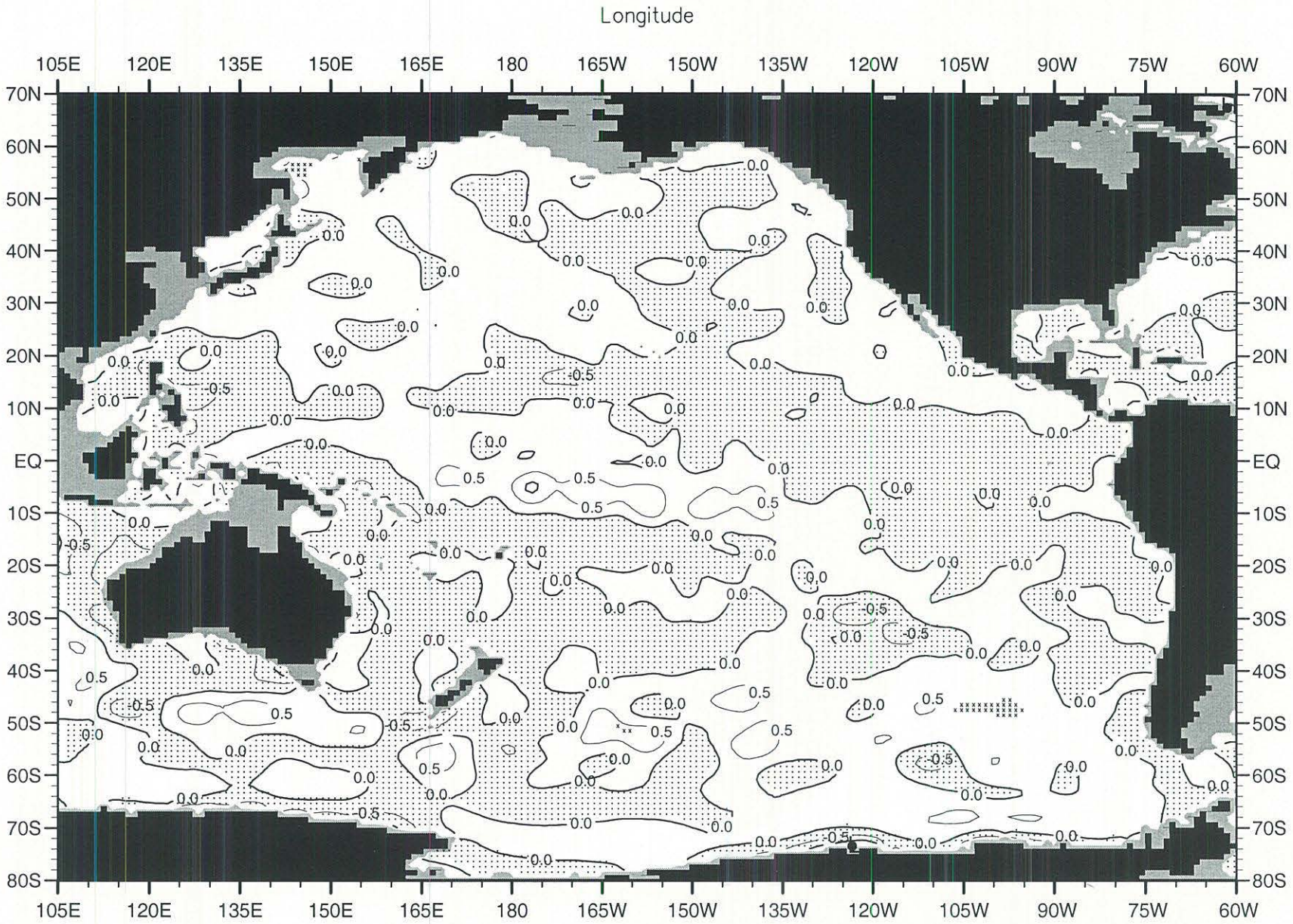


Fig. B36. Winter (Jan.-Mar.) minus annual temperature (°C) at 250 m. depth .

Minimum Value= -1.63 Maximum Value= 1.67 Contour Interval: 0.50

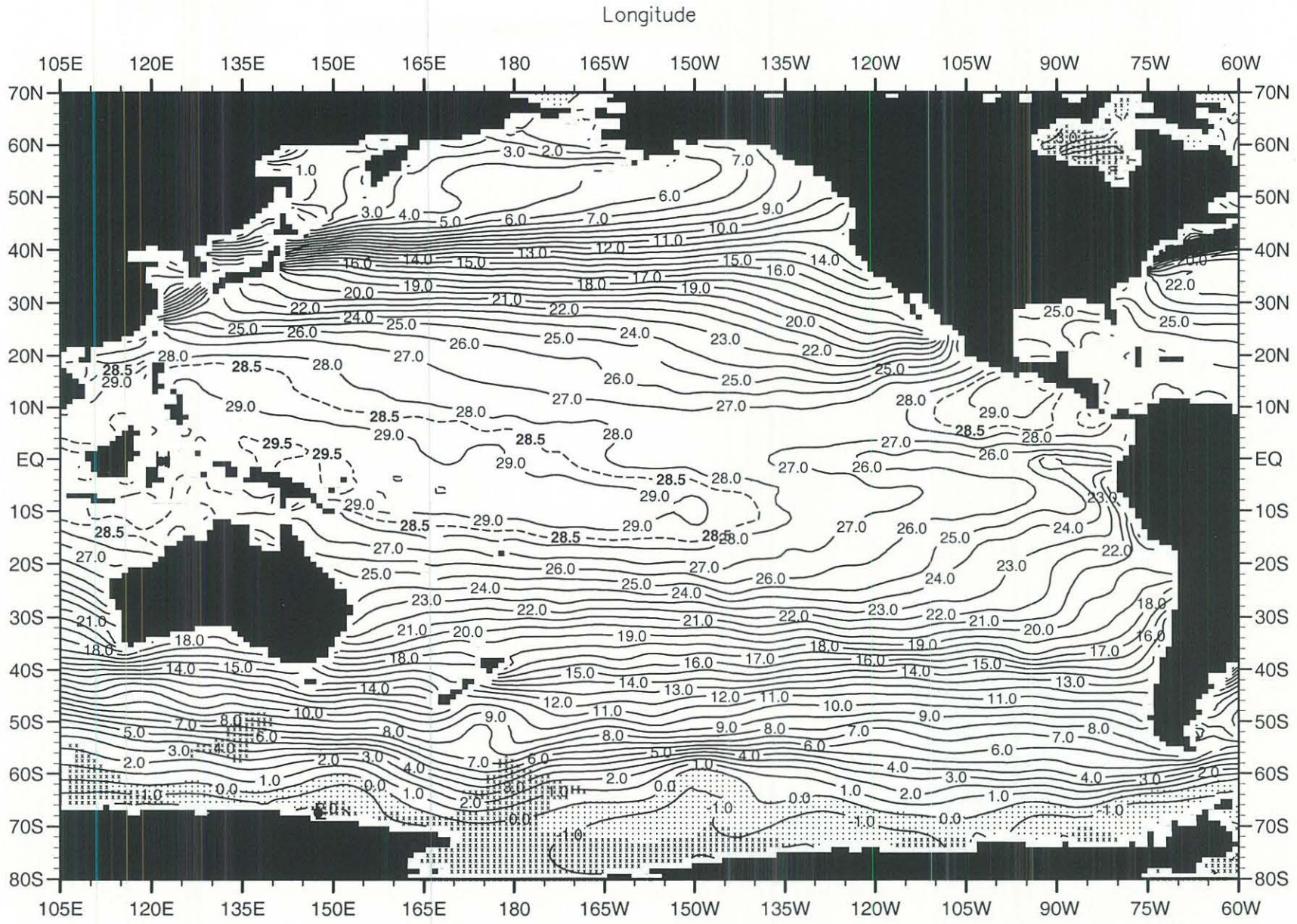


Fig. B37. Spring (Apr.-Jun.) mean temperature (°C) at the surface .

Minimum Value= -2.10 Maximum Value= 30.34 Contour Interval: 1.00

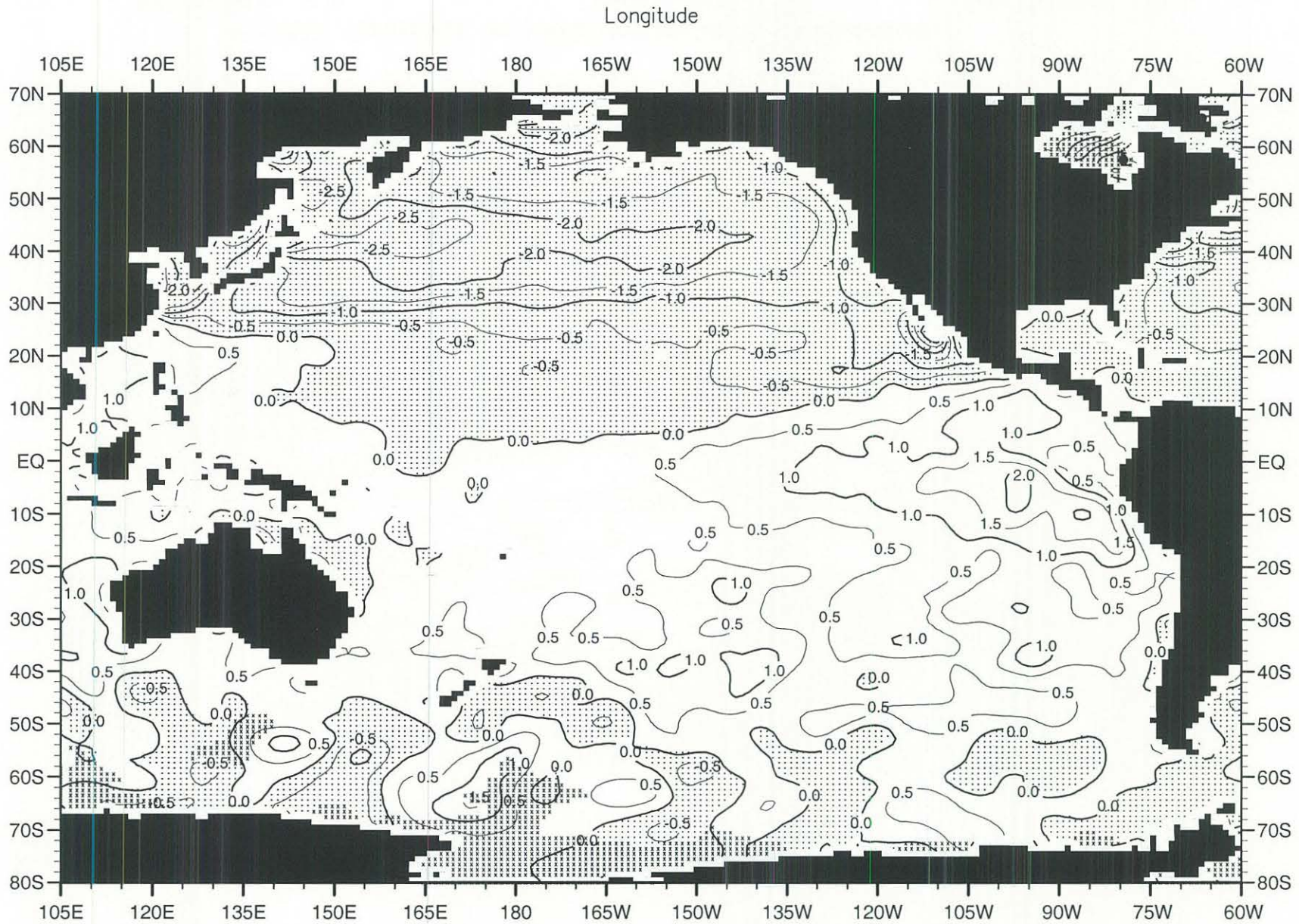


Fig. B38. Spring (Apr.-Jun.) minus annual temperature (°C) at the surface .

Minimum Value= -4.16 Maximum Value= 5.70 Contour Interval: 0.50

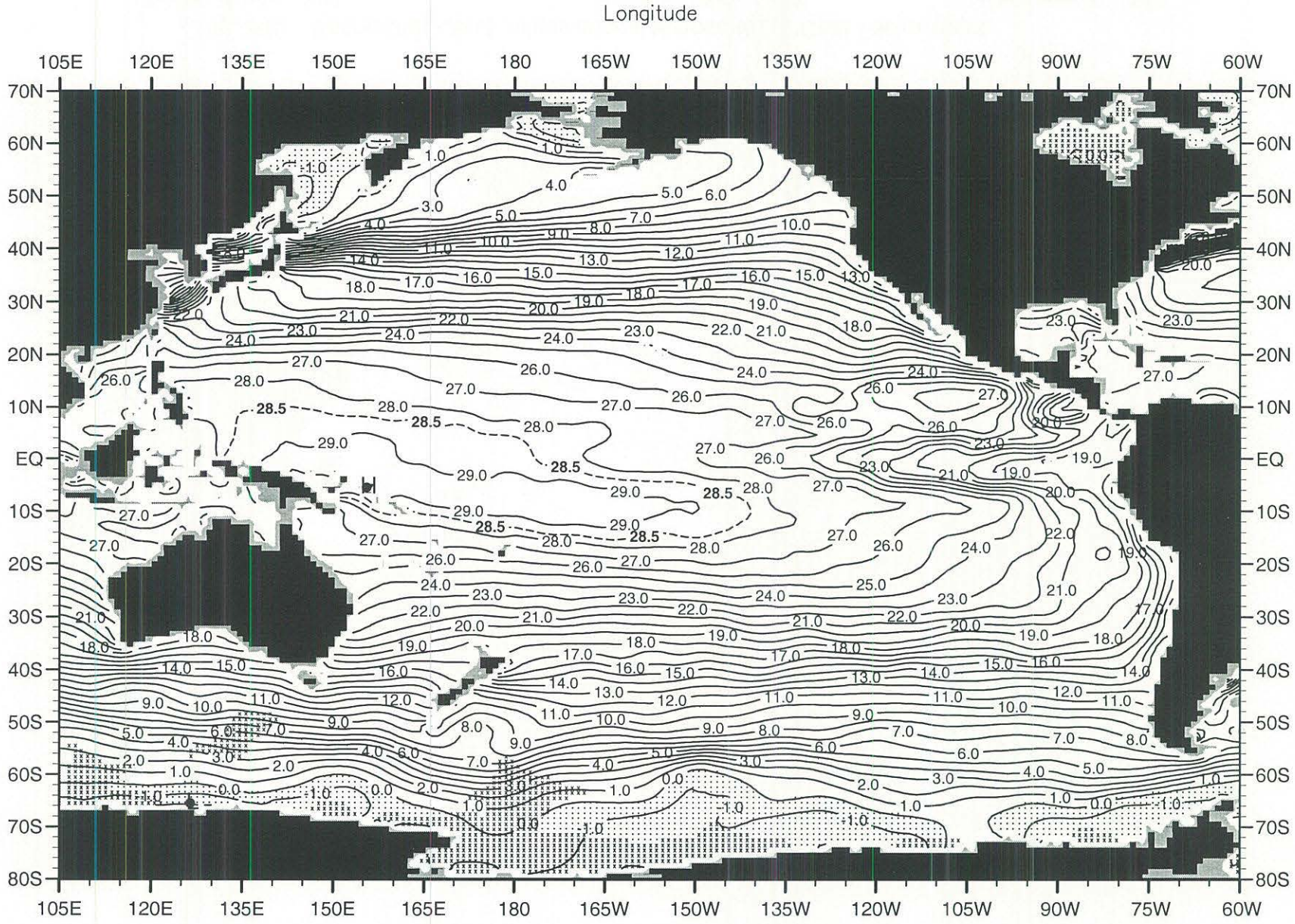


Fig. B39. Spring (Apr.-Jun.) mean temperature (°C) at 50 m. depth .

Minimum Value= -2.10 Maximum Value= 29.57 Contour Interval: 1.00

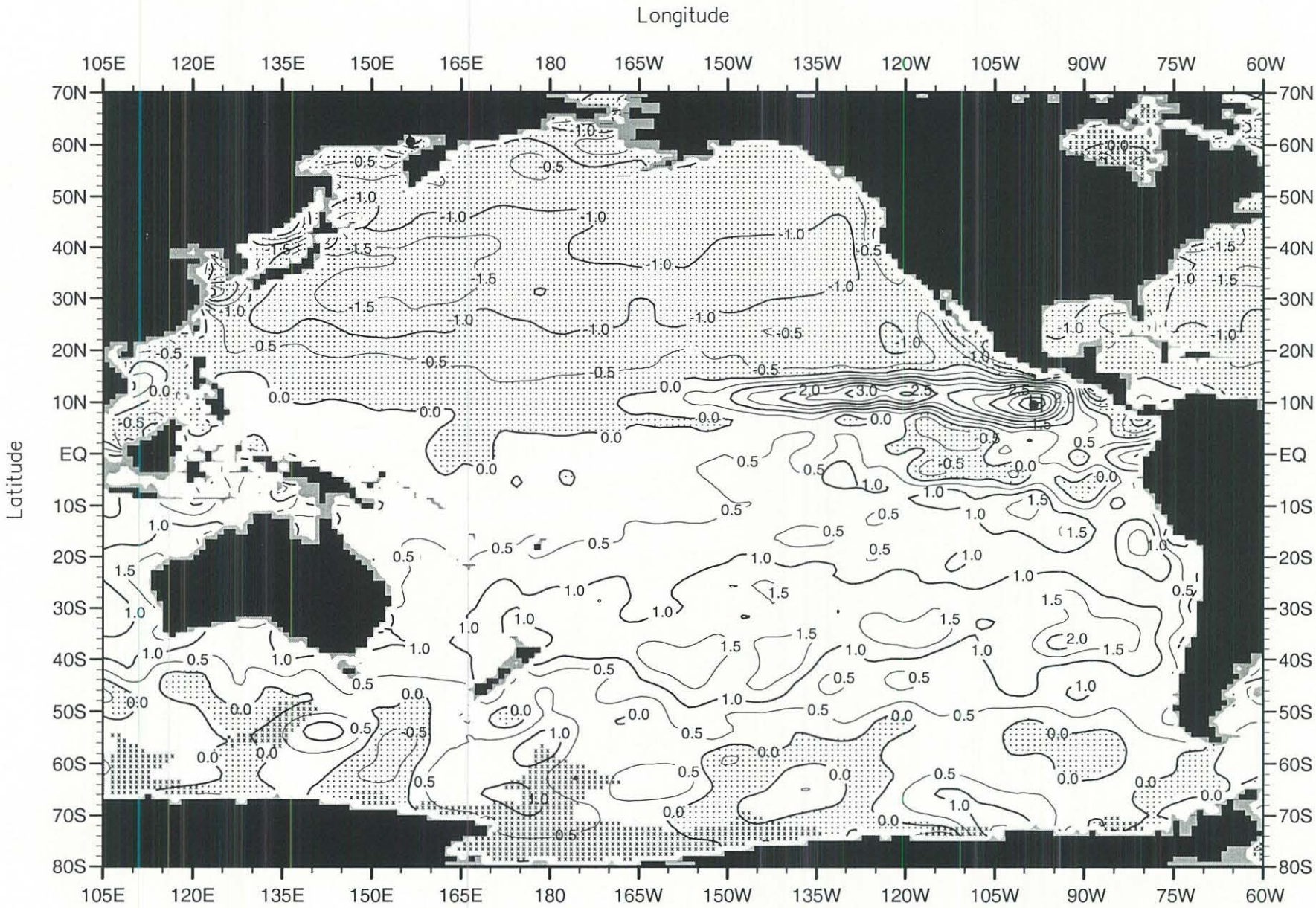


Fig. B40. Spring (Apr.-Jun.) minus annual temperature (°C) at 50 m. depth .

Minimum Value= -3.60 Maximum Value= 4.40 Contour Interval: 0.50

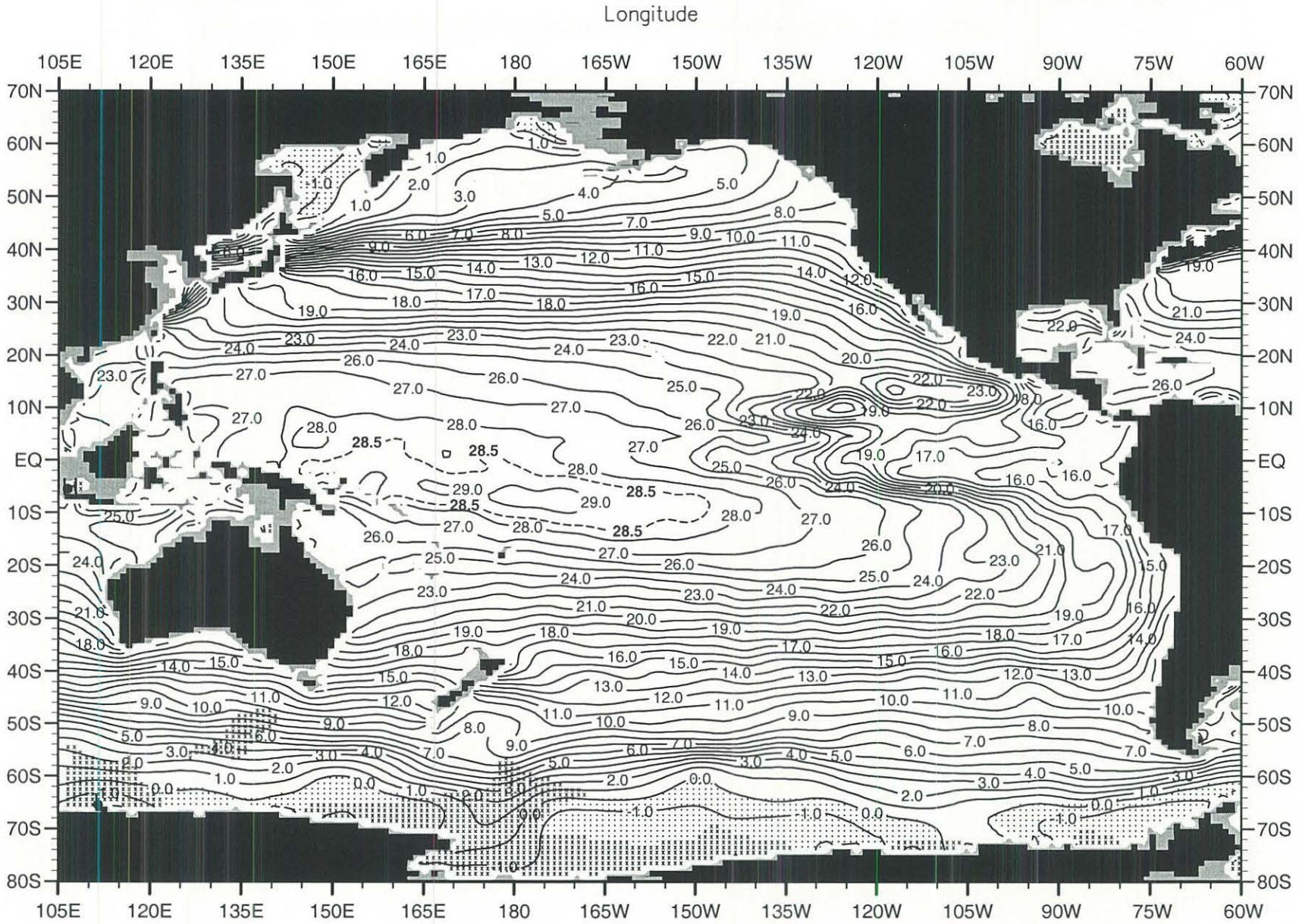


Fig. B41. Spring (Apr.-Jun.) mean temperature (°C) at 75 m. depth .

Minimum Value= -2.10 Maximum Value= 29.52 Contour Interval: 1.00

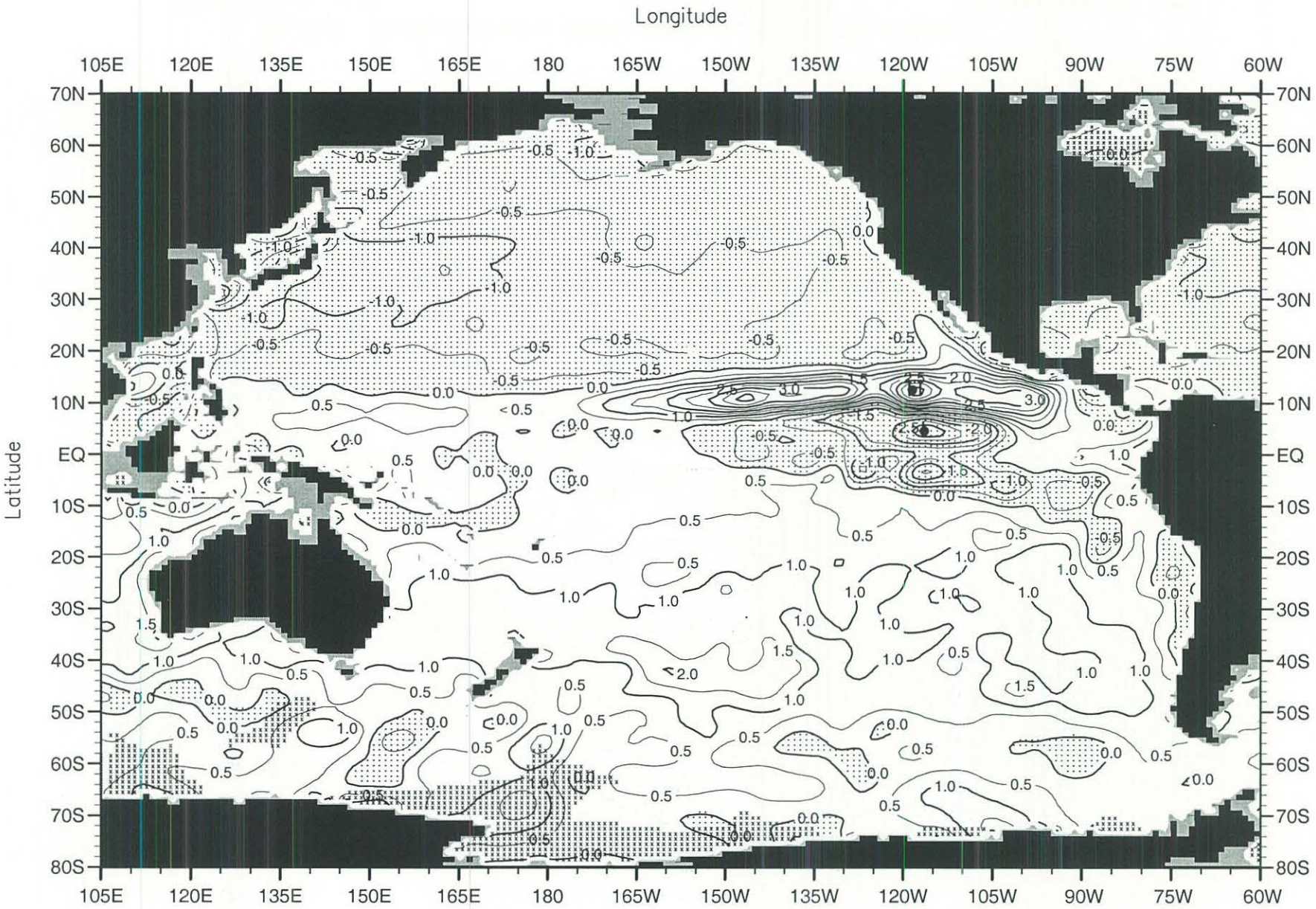


Fig. B42. Spring (Apr.-Jun.) minus annual temperature (°C) at 75 m. depth .

Minimum Value= -3.38 Maximum Value= 4.22 Contour Interval: 0.50

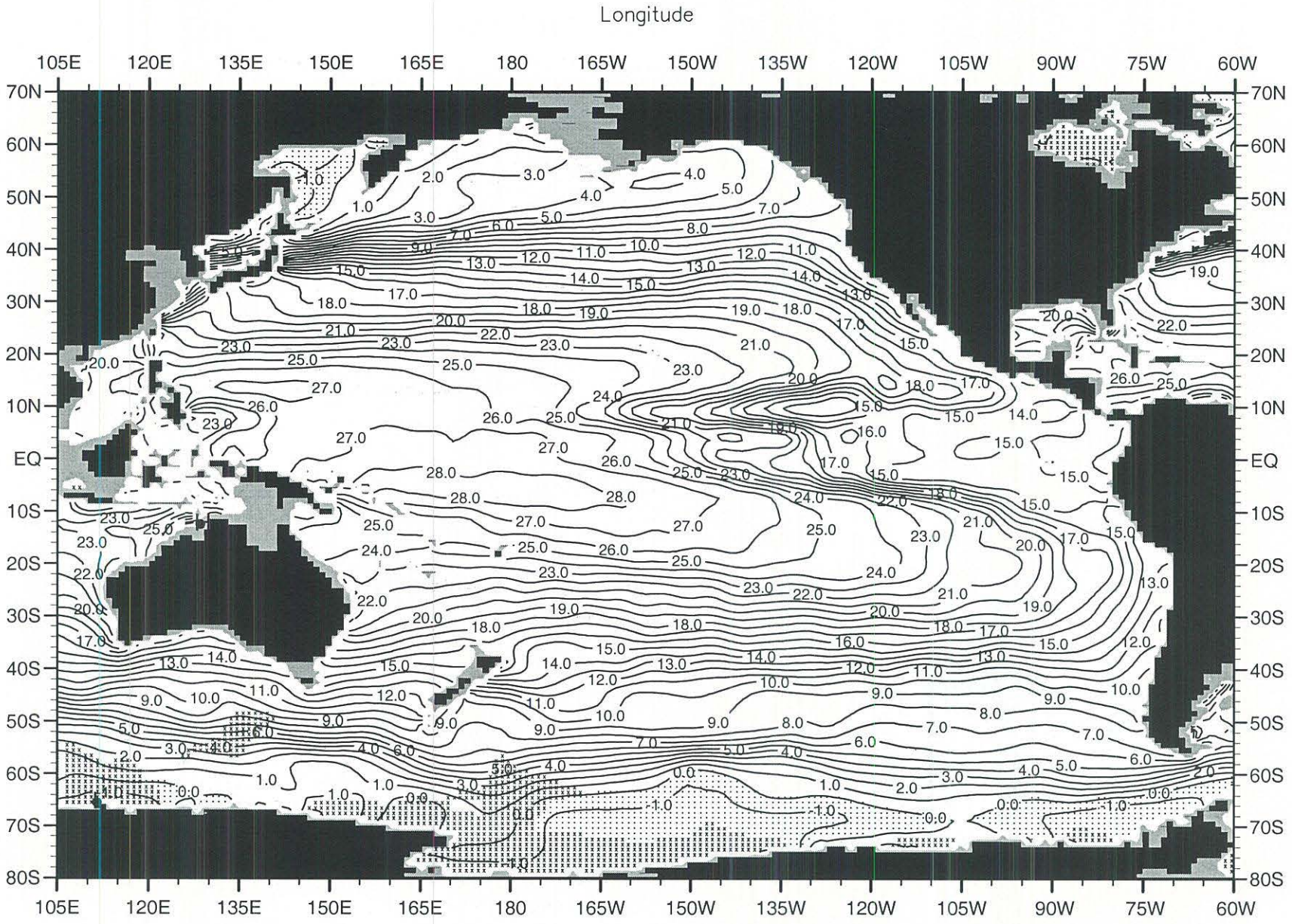


Fig. B43. Spring (Apr.-Jun.) mean temperature (°C) at 100 m. depth .

Minimum Value= -2.10 Maximum Value= 29.22 Contour Interval: 1.00

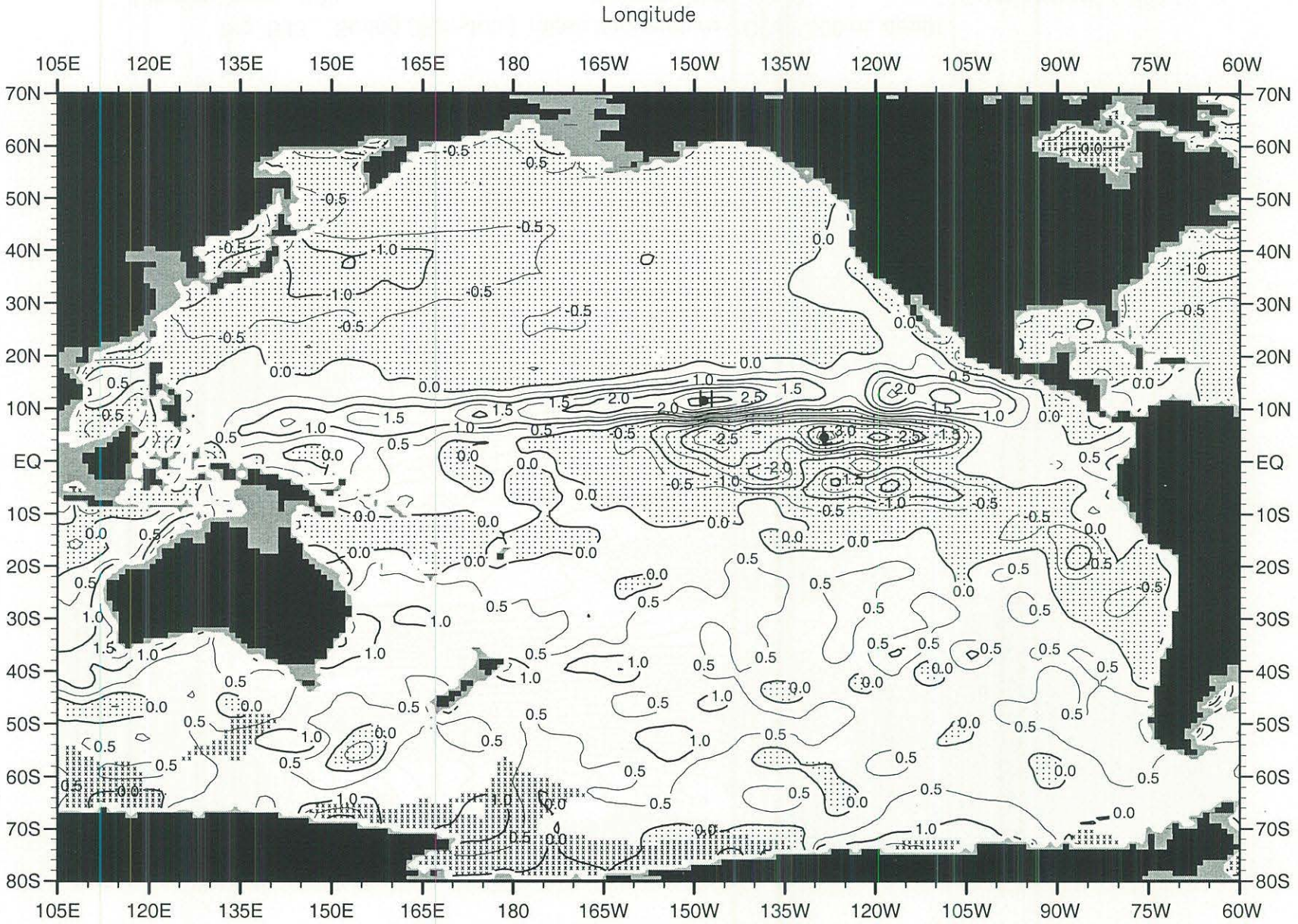


Fig. B44. Spring (Apr.-Jun.) minus annual temperature (°C) at 100 m. depth .

Minimum Value= -3.72 Maximum Value= 3.15 Contour Interval: 0.50

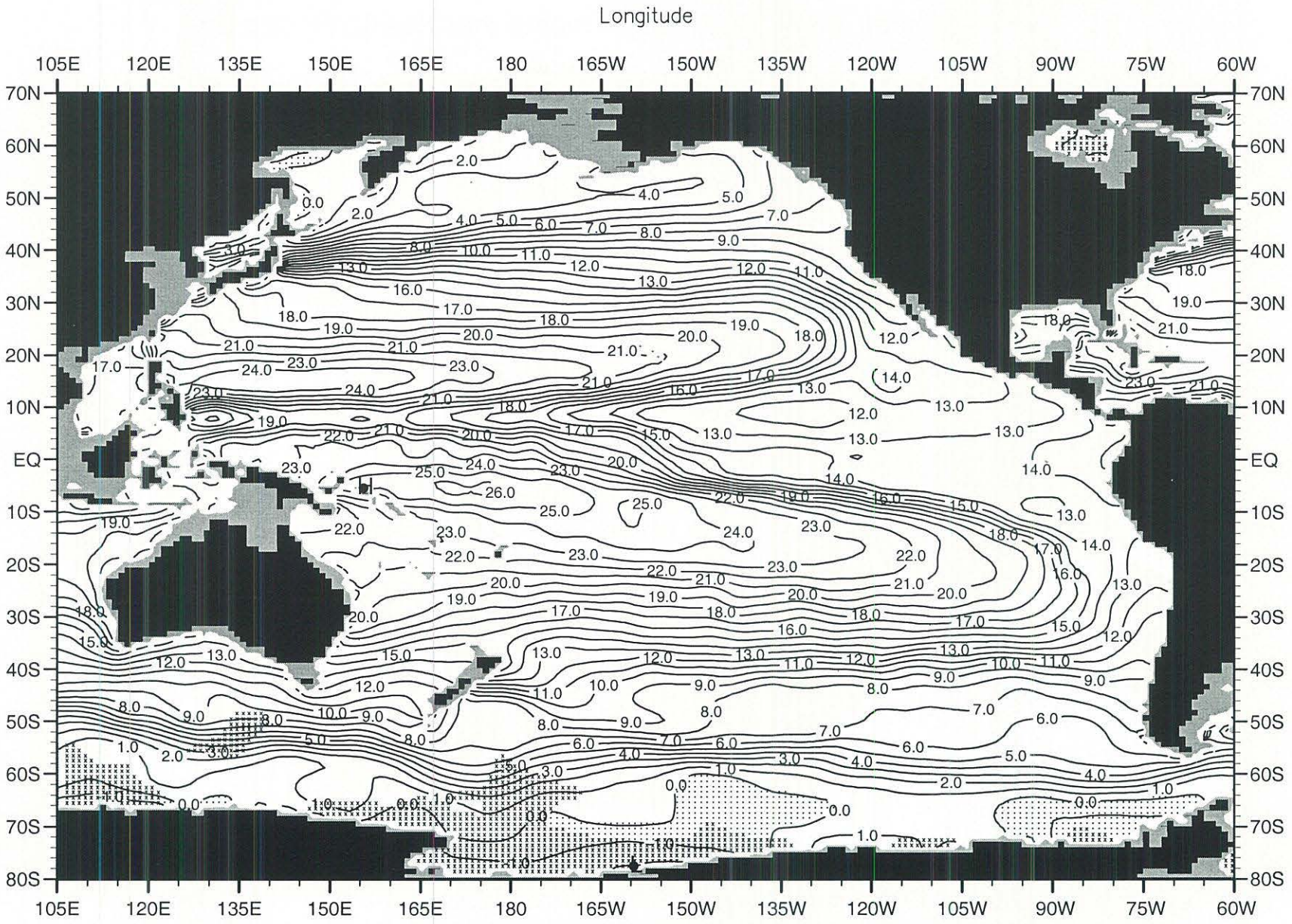


Fig. B45. Spring (Apr.-Jun.) mean temperature (°C) at 150 m. depth .

Minimum Value= -2.10 Maximum Value= 26.27 Contour Interval: 1.00

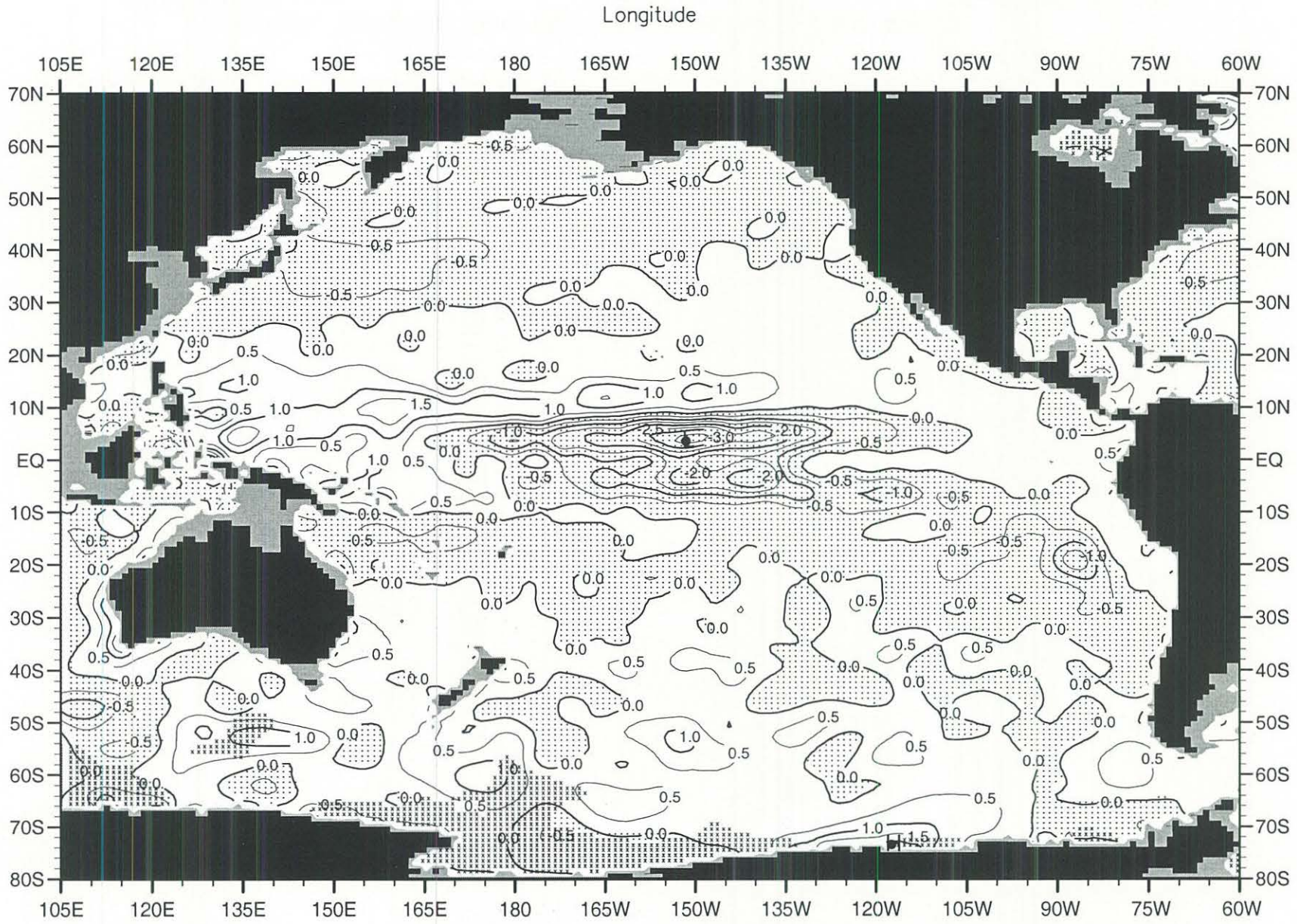


Fig. B46. Spring (Apr.-Jun.) minus annual temperature (°C) at 150 m. depth .

Minimum Value= -3.68 Maximum Value= 2.51 Contour Interval: 0.50

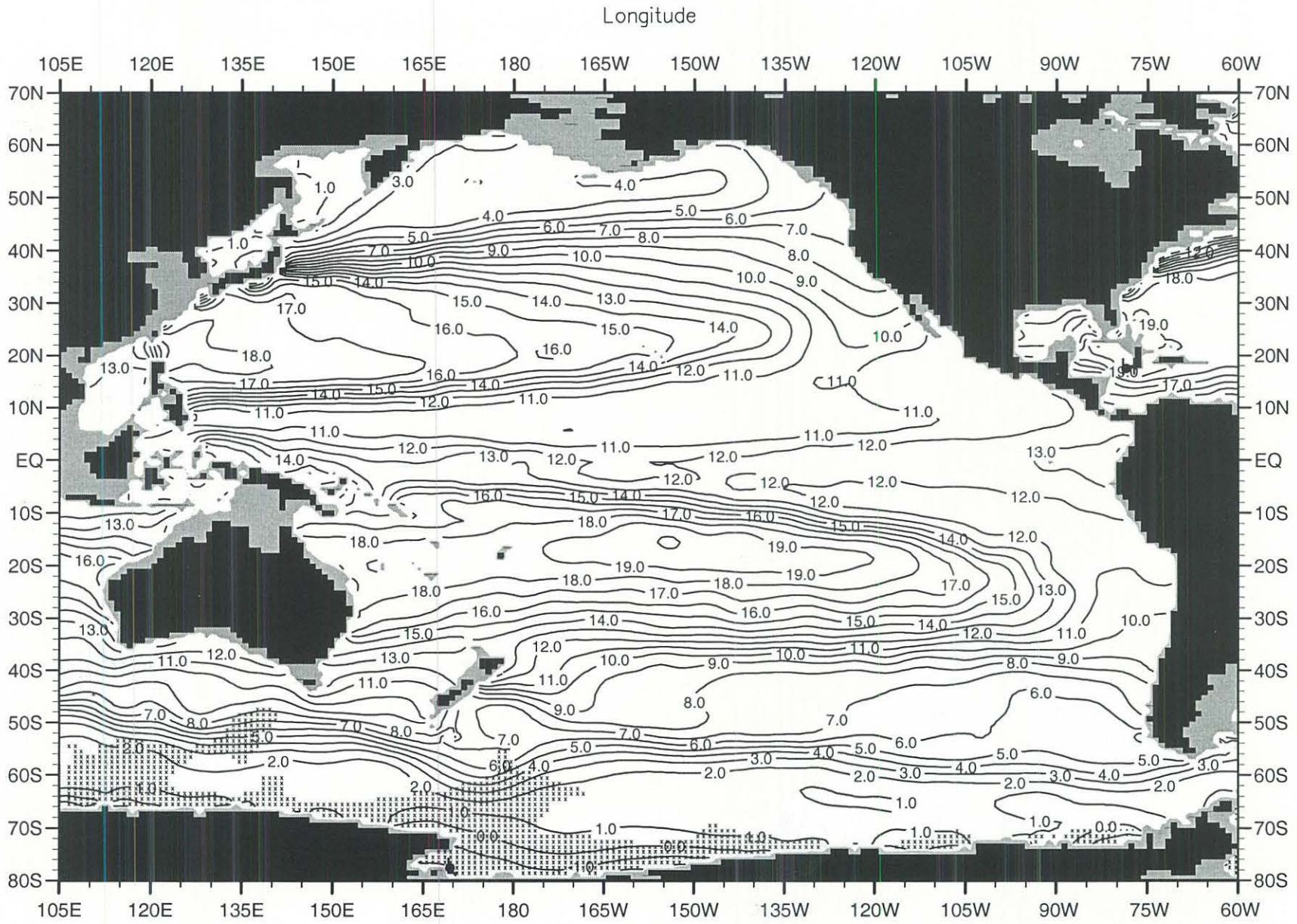


Fig. B47. Spring (Apr.-Jun.) mean temperature (°C) at 250 m. depth .

Minimum Value= -2.10 Maximum Value= 20.13 Contour Interval: 1.00

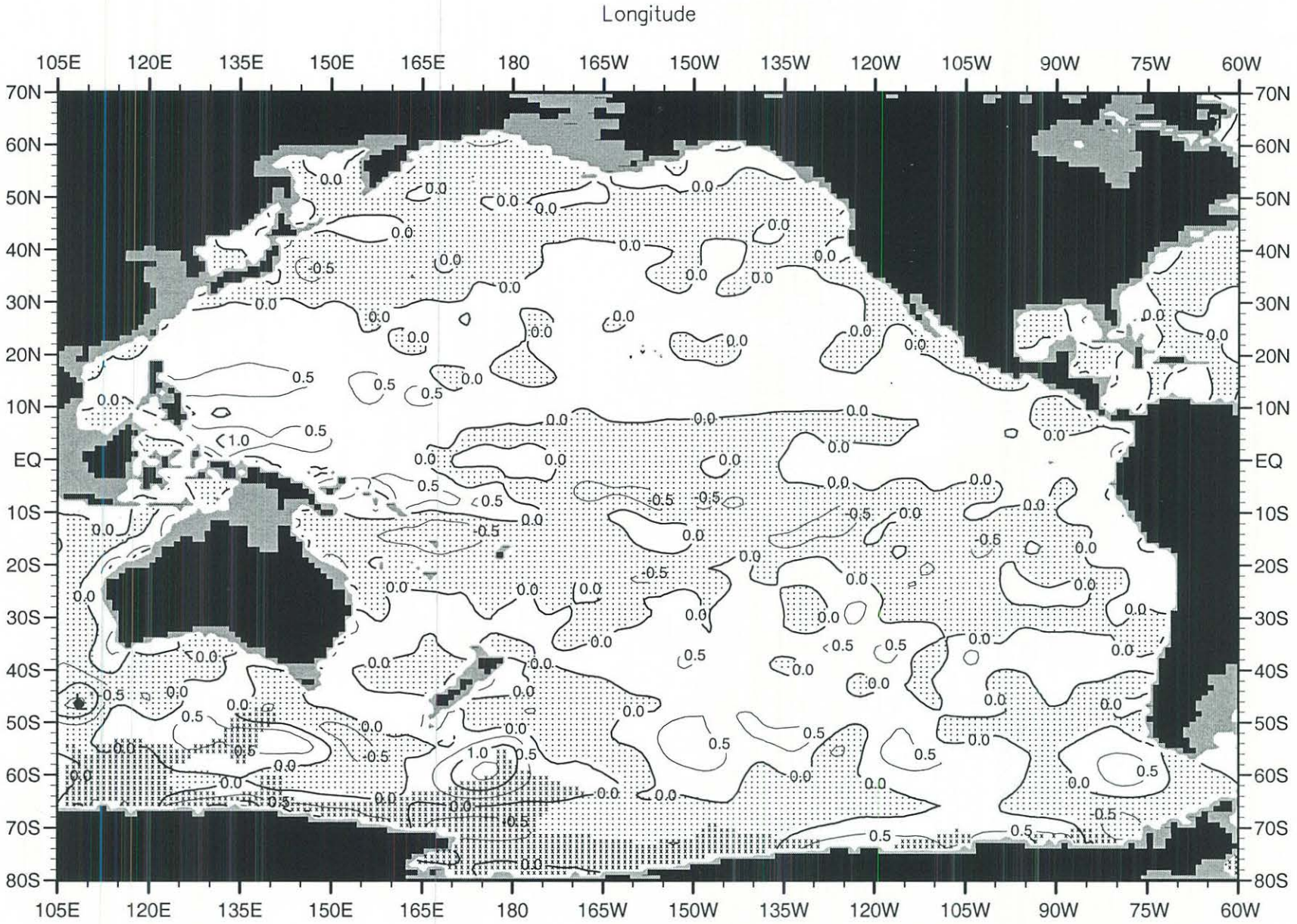


Fig. B48. Spring (Apr.-Jun.) minus annual temperature (°C) at 250 m. depth .

Minimum Value= -1.60 Maximum Value= 1.89 Contour Interval: 0.50

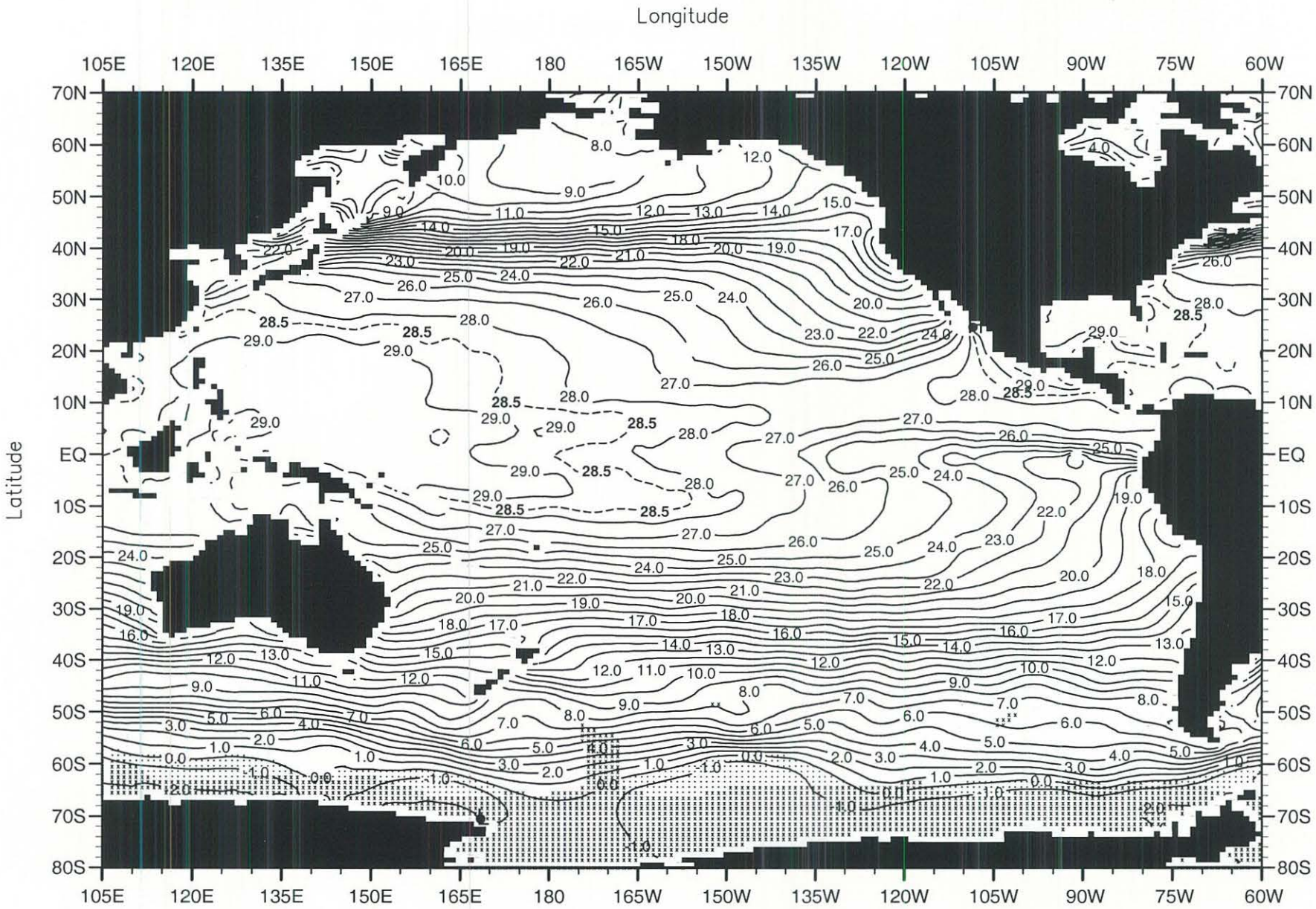


Fig. B49. Summer (Jul.-Sep.) mean temperature (°C) at the surface .

Minimum Value= -2.10 Maximum Value= 29.99 Contour Interval: 1.00

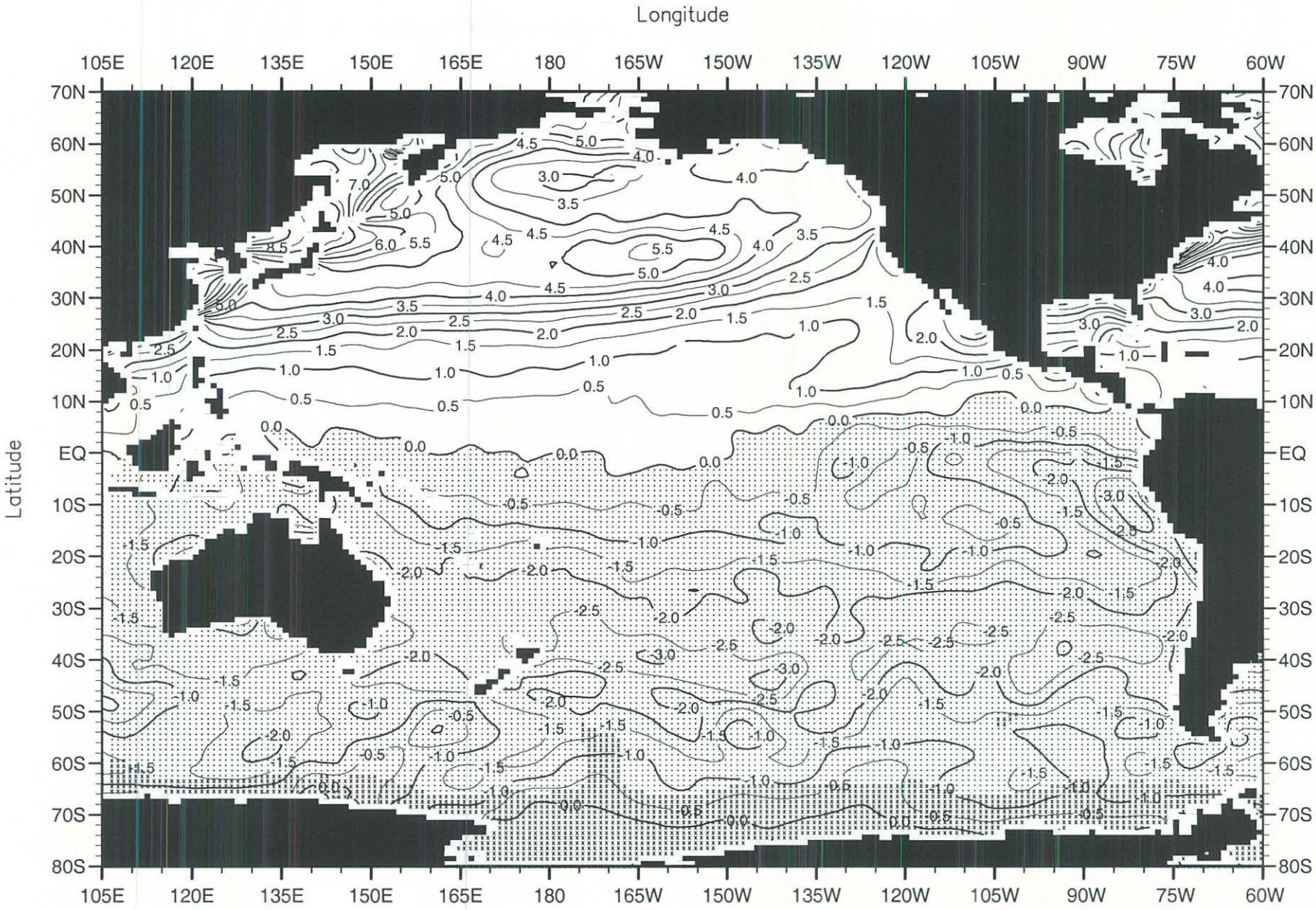


Fig. B50. Summer (Jul.-Sep.) minus annual temperature (°C) at the surface .

Minimum Value= -4.17 Maximum Value= 10.55 Contour Interval: 0.50

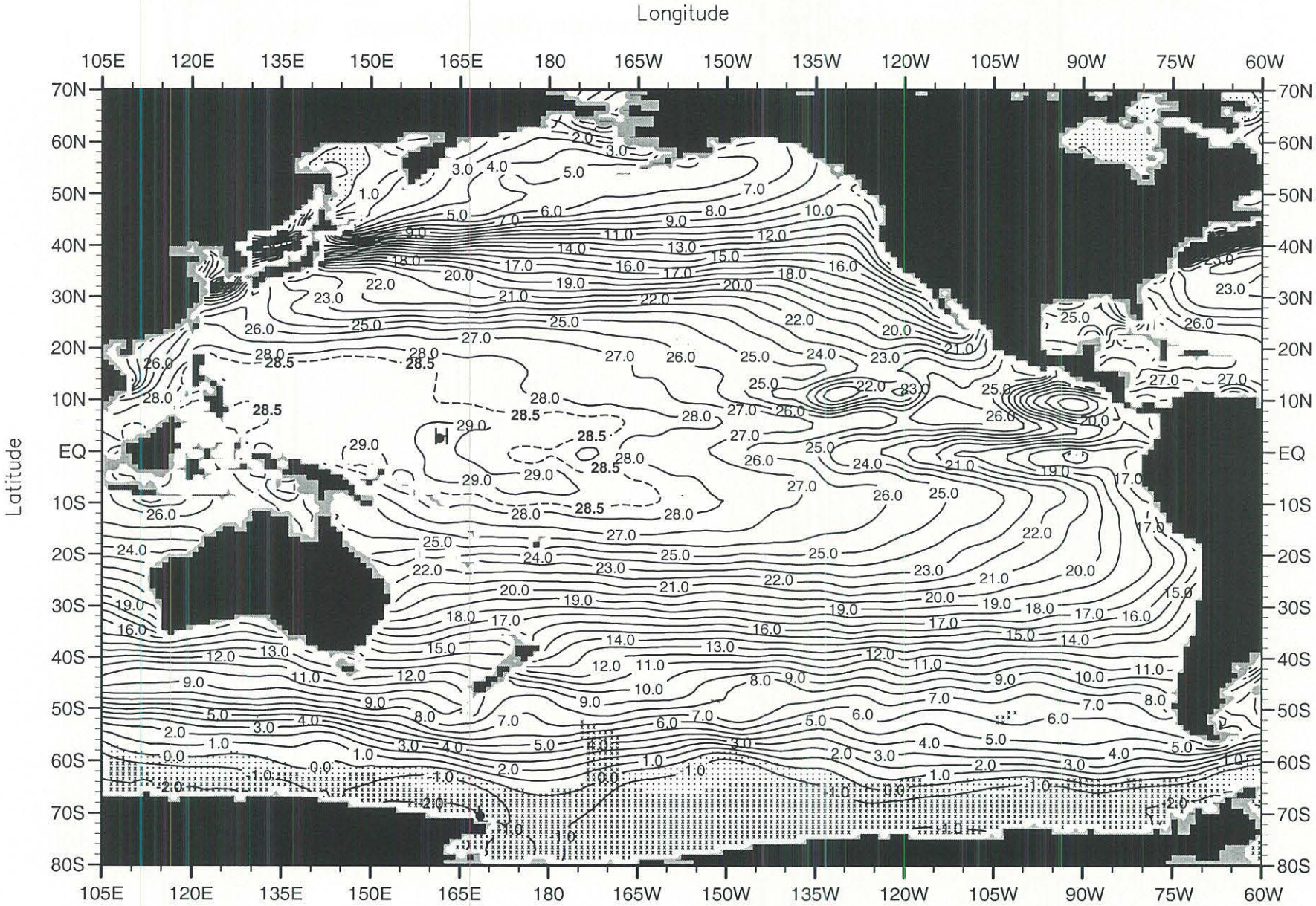


Fig. B51. Summer (Jul.-Sep.) mean temperature (°C) at 50 m. depth .

Minimum Value= -2.10 Maximum Value= 29.30 Contour Interval: 1.00

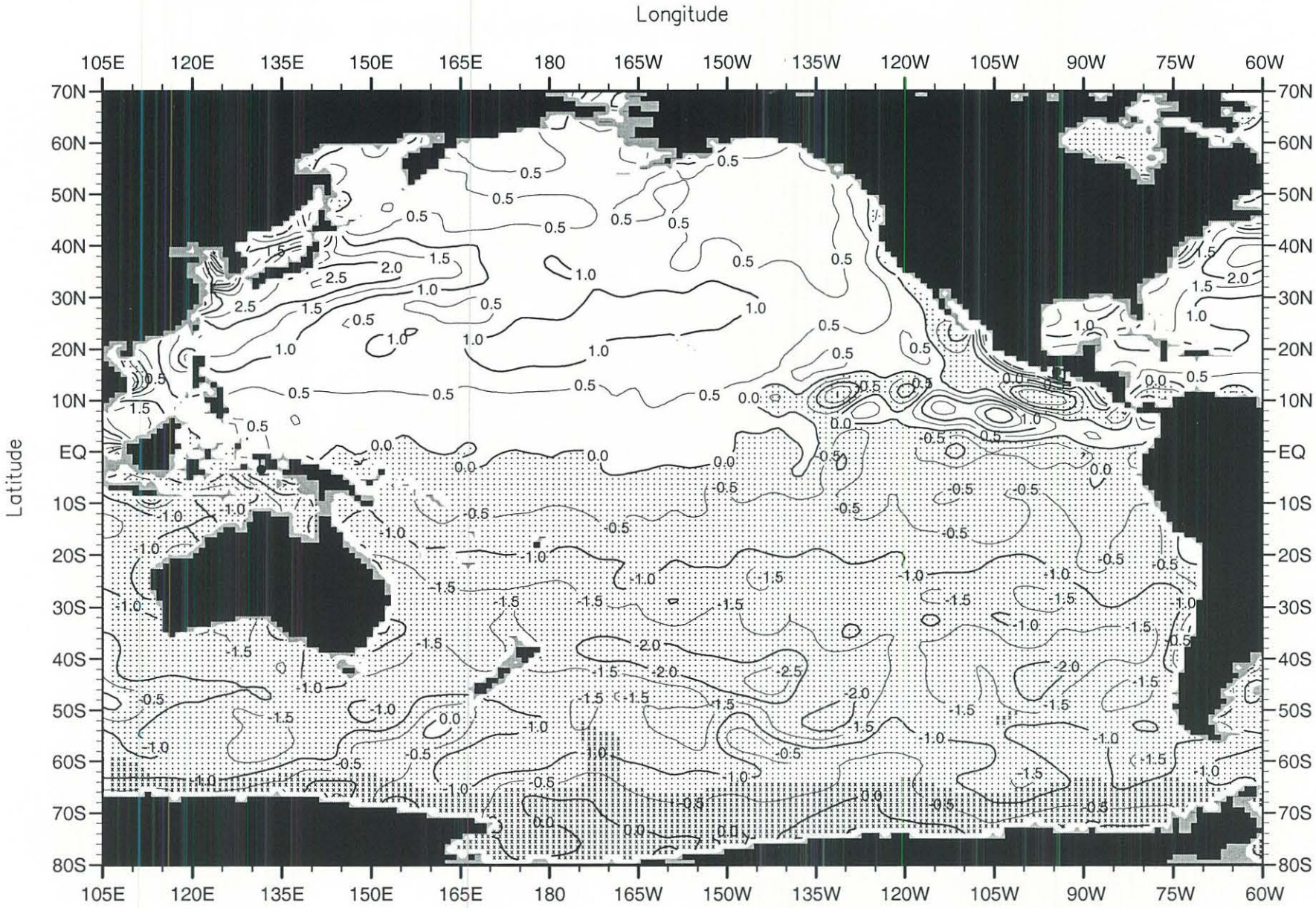


Fig. B52. Summer (Jul.-Sep.) minus annual temperature (°C) at 50 m. depth .

Minimum Value= -2.98 Maximum Value= 4.67 Contour Interval: 0.50

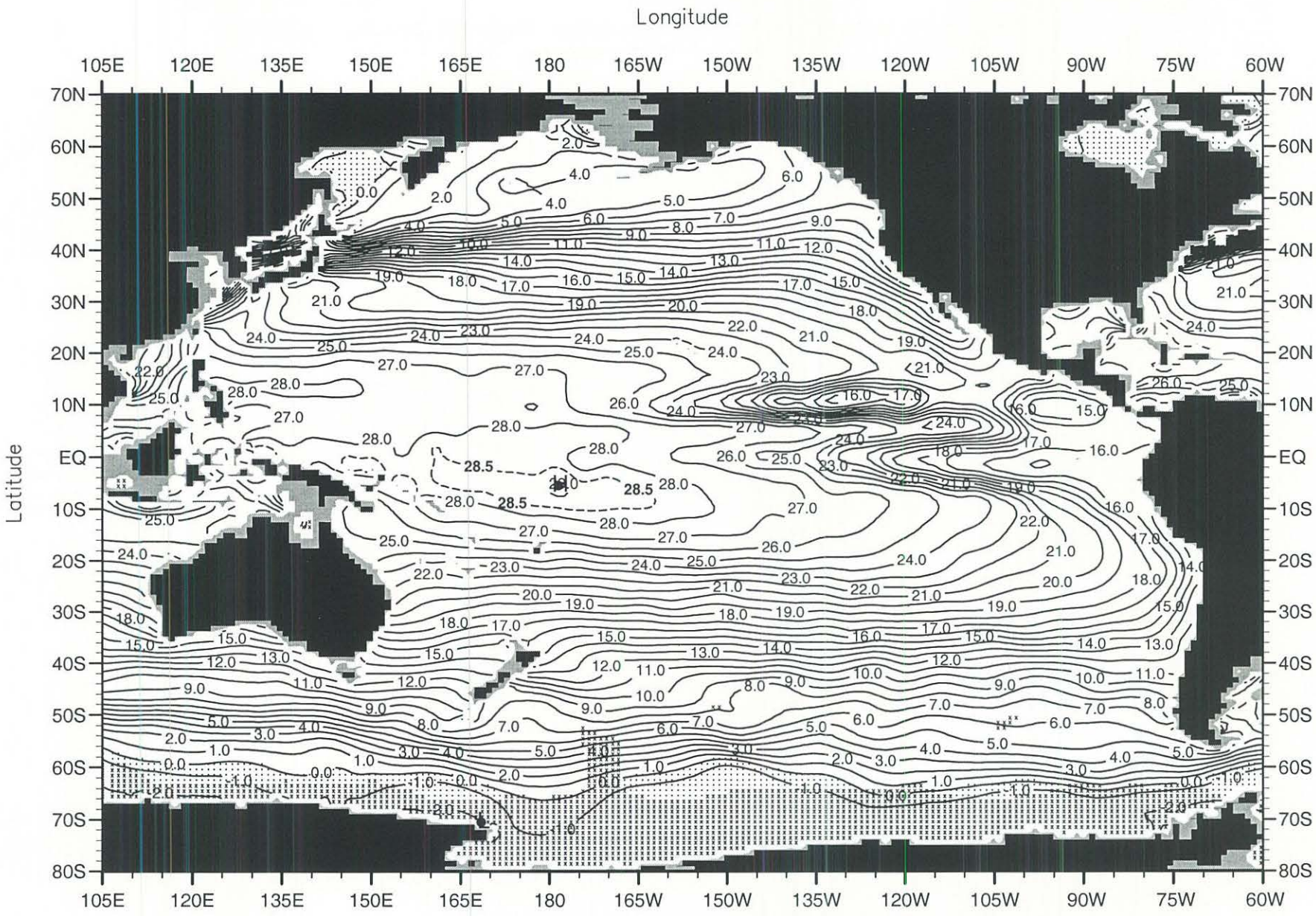


Fig. B53. Summer (Jul.-Sep.) mean temperature (°C) at 75 m. depth .

Minimum Value= -2.10 Maximum Value= 29.10 Contour Interval: 1.00

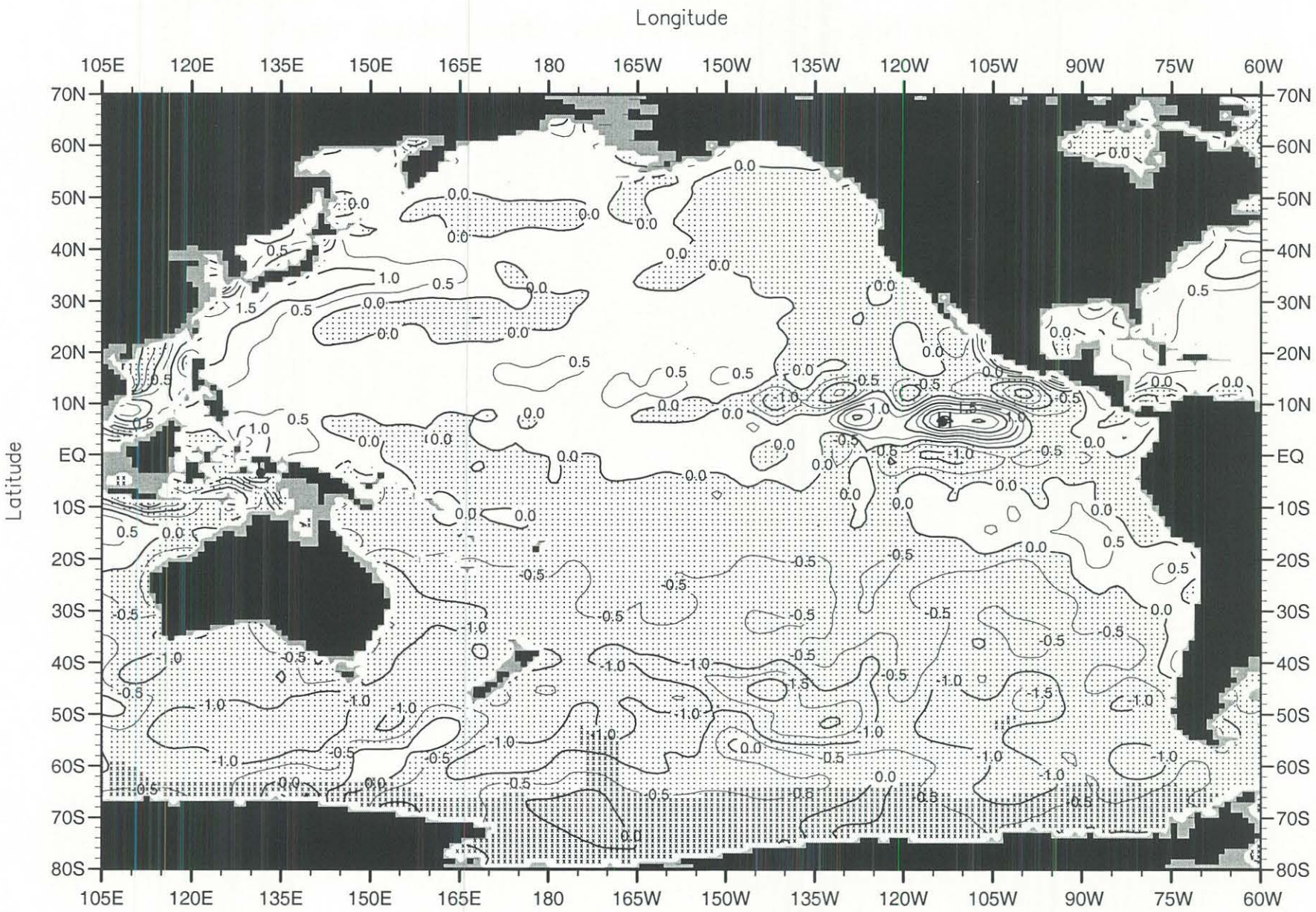


Fig. B54. Summer (Jul.-Sep.) minus annual temperature (°C) at 75 m. depth .

Minimum Value= -3.05 Maximum Value= 3.14 Contour Interval: 0.50

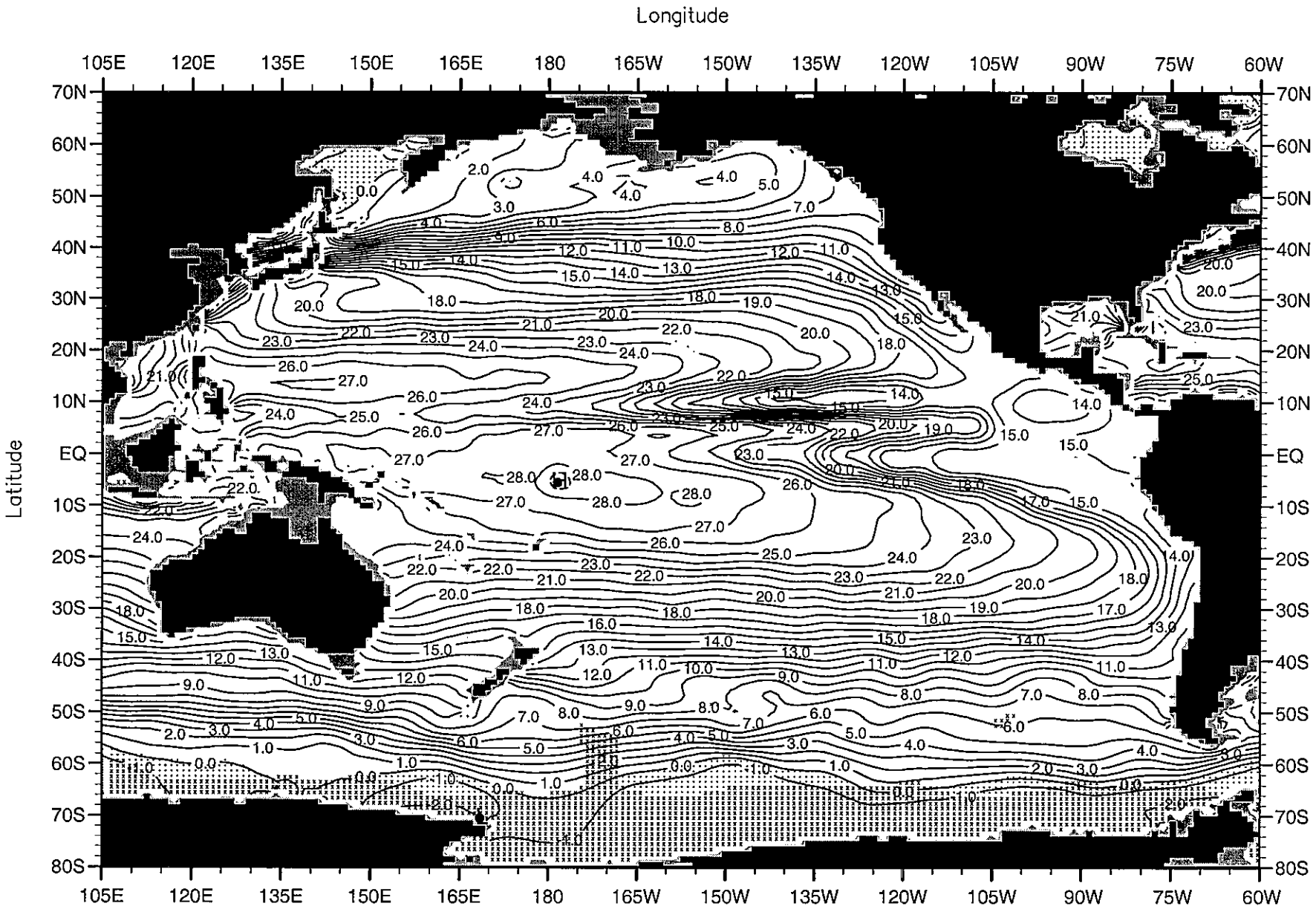


Fig. B55. Summer (Jul.-Sep.) mean temperature (°C) at 100 m. depth .

Minimum Value= -2.10 Maximum Value= 28.67 Contour Interval: 1.00

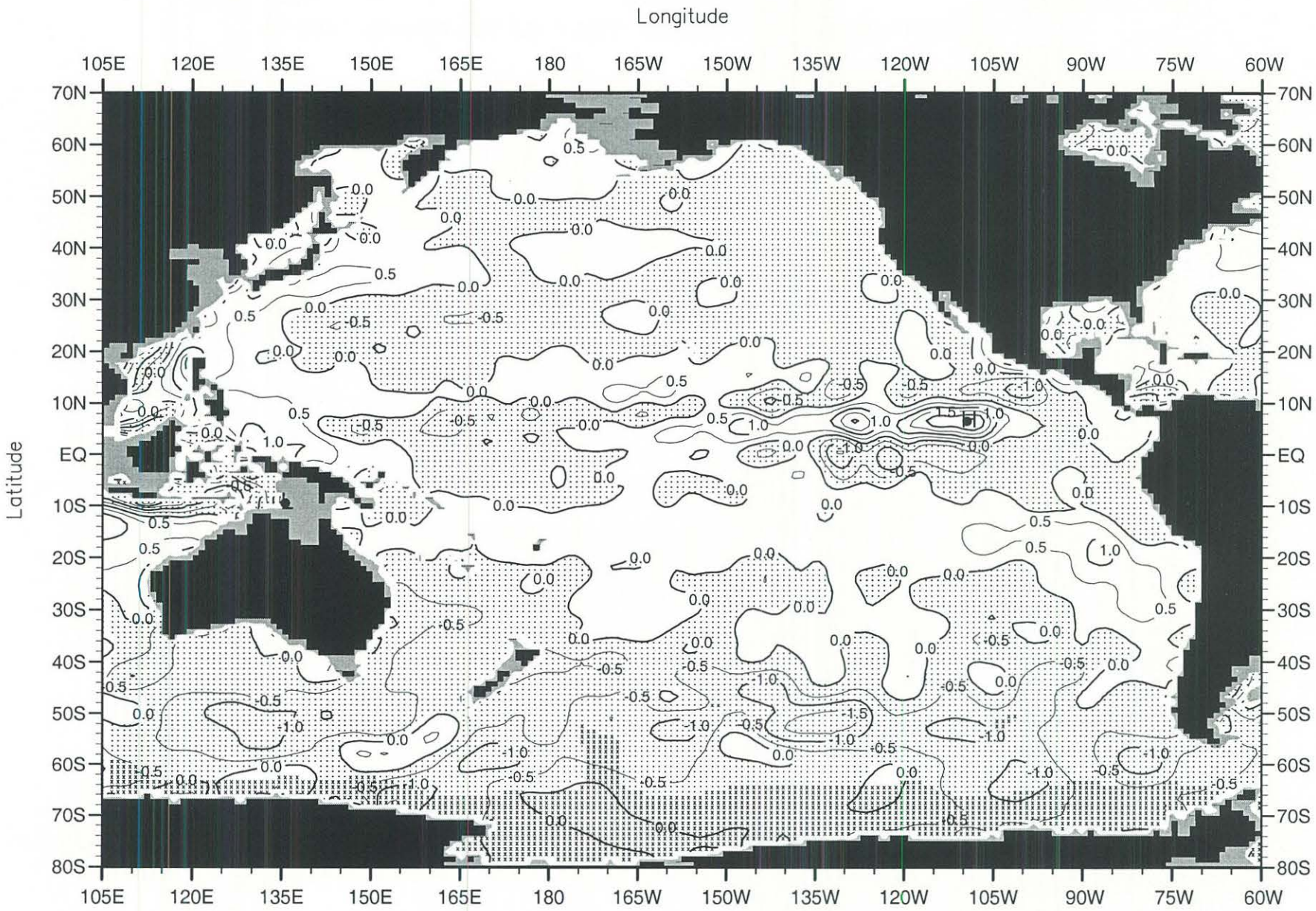


Fig. B56. Summer (Jul.-Sep.) minus annual temperature (°C) at 100 m. depth .

Minimum Value= -2.79 Maximum Value= 2.47 Contour Interval: 0.50

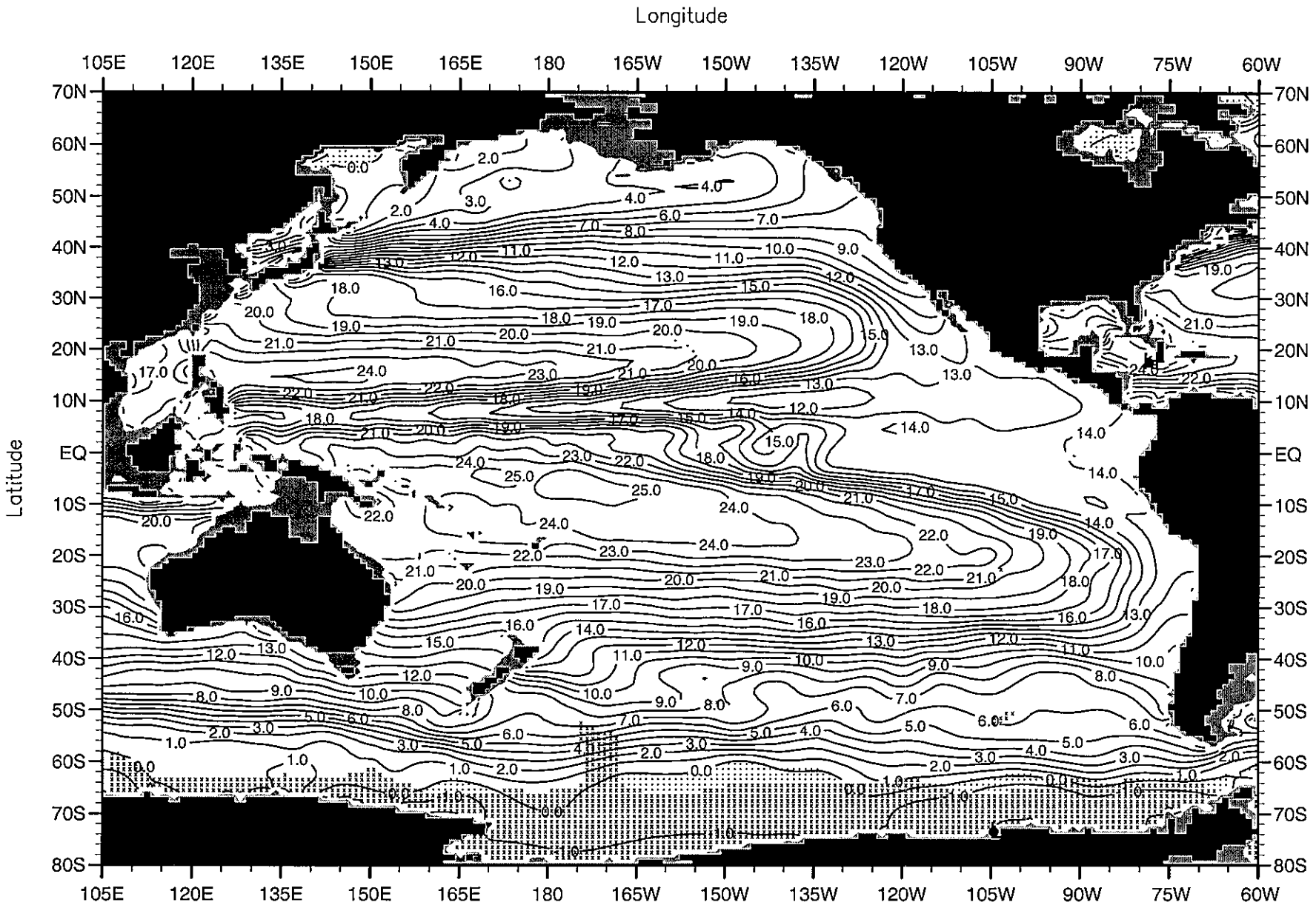


Fig. B57. Summer (Jul.-Sep.) mean temperature (°C) at 150 m. depth .

Minimum Value= -2.10 Maximum Value= 26.17 Contour Interval: 1.00

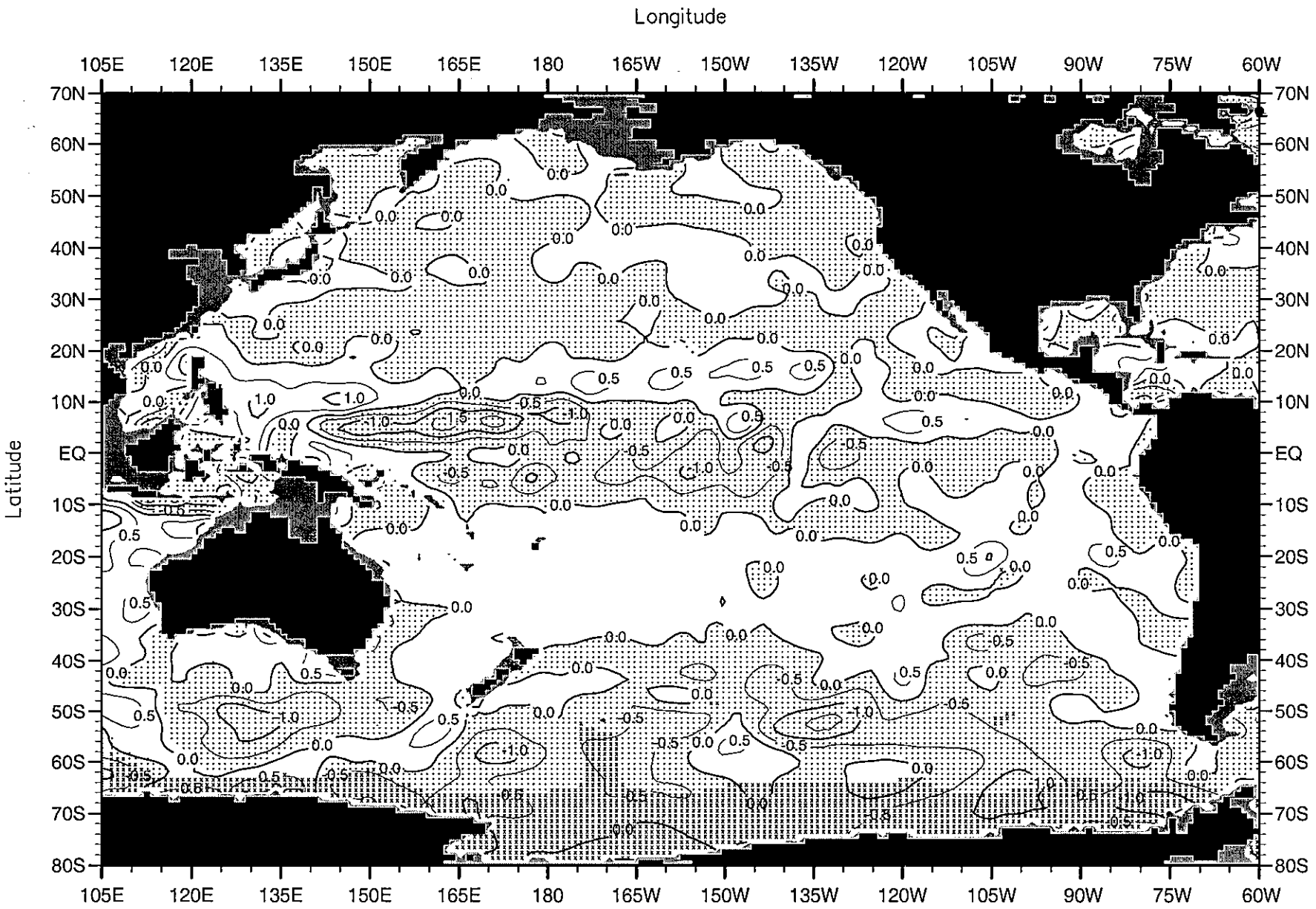


Fig. B58. Summer (Jul.-Sep.) minus annual temperature (°C) at 150 m. depth .

Minimum Value= -1.98 Maximum Value= 1.58 Contour Interval: 0.50

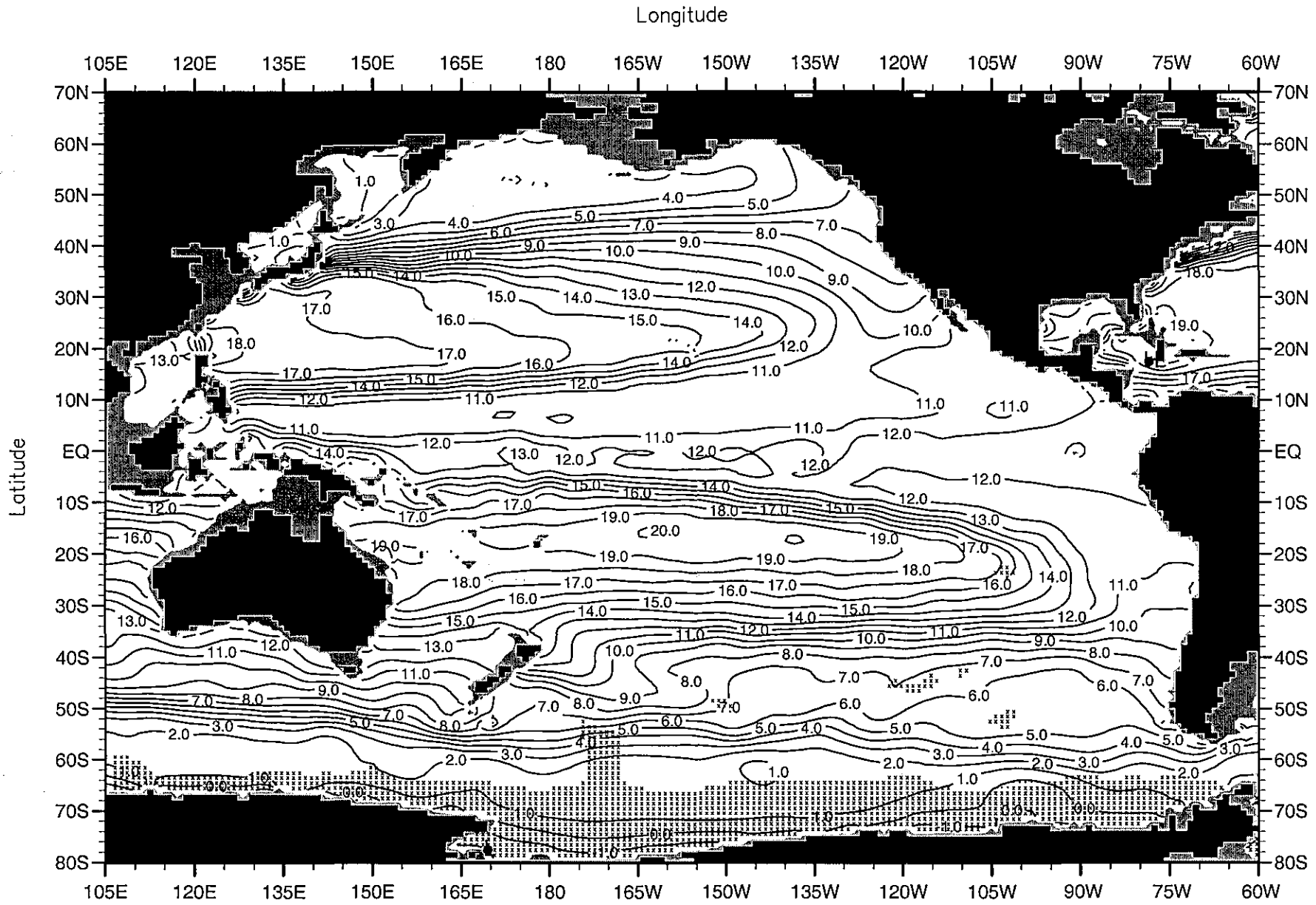


Fig. B59. Summer (Jul.-Sep.) mean temperature (°C) at 250 m. depth .

Minimum Value= -2.10 Maximum Value= 20.33 Contour Interval: 1.00

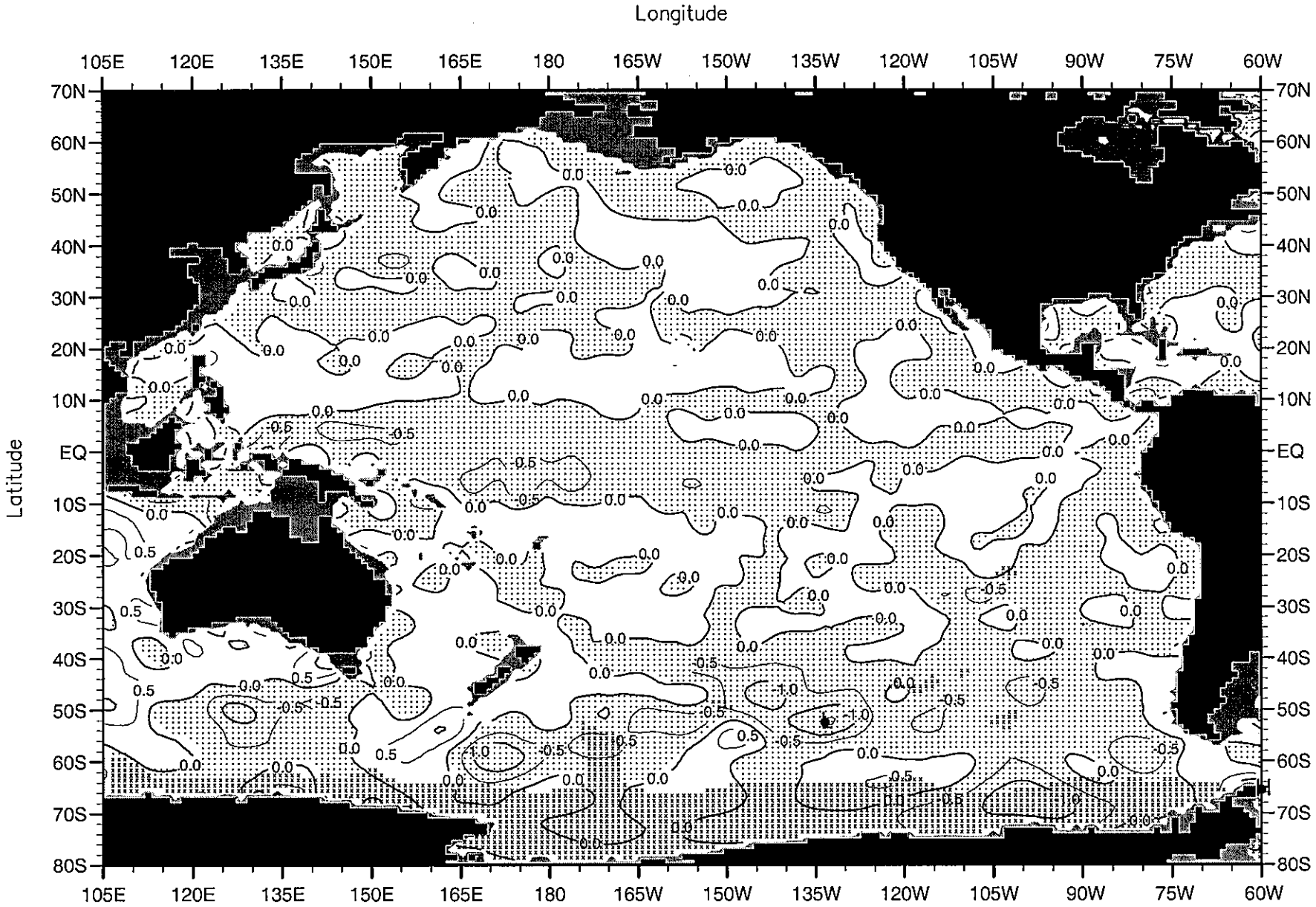


Fig. B60. Summer (Jul.-Sep.) minus annual temperature (°C) at 250 m. depth .

Minimum Value= -1.54 Maximum Value= 1.53 Contour Interval: 0.50

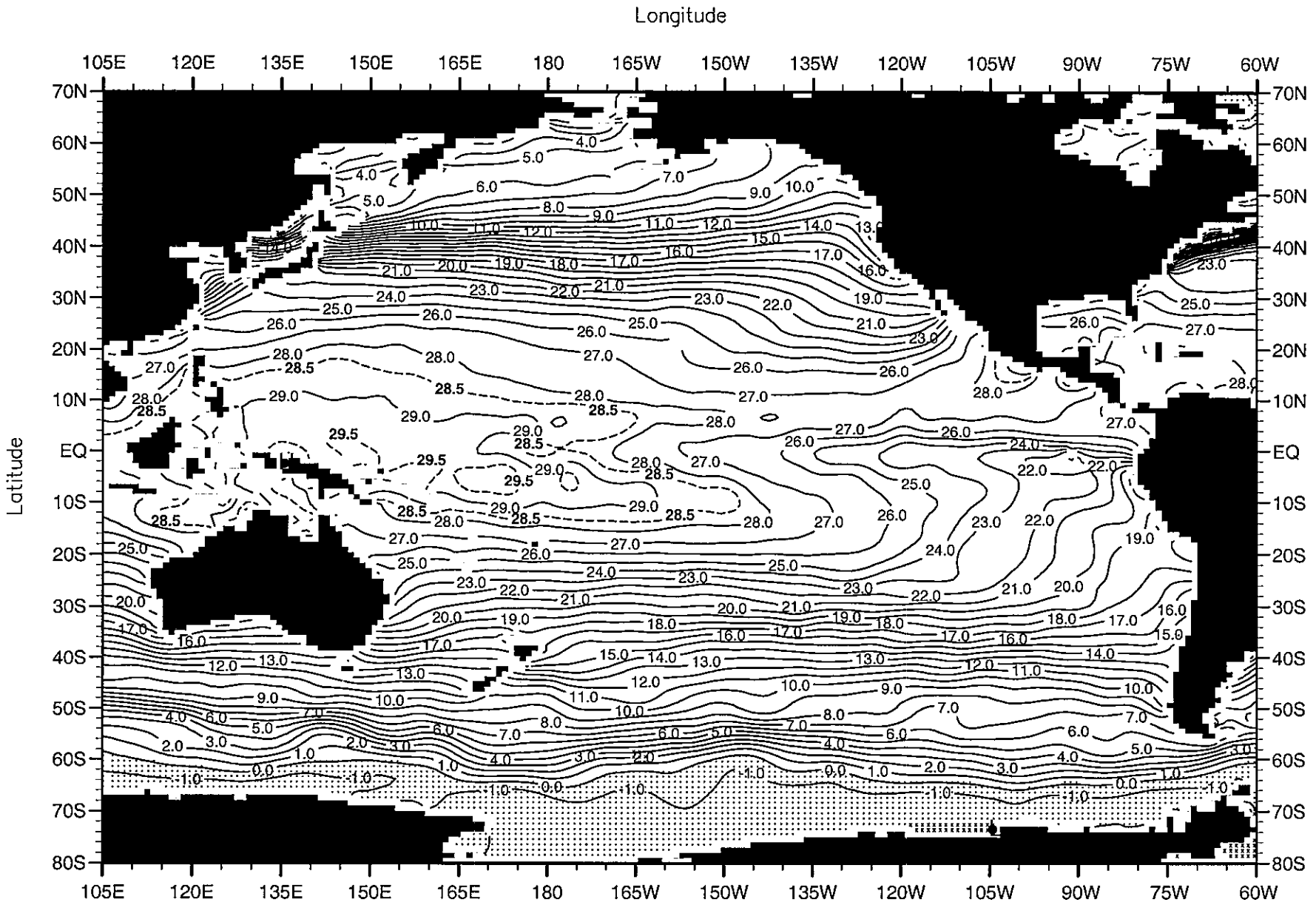


Fig. B61. Fall (Oct.-Dec.) mean temperature (°C) at the surface .

Minimum Value= -2.10 Maximum Value= 30.12 Contour Interval: 1.00

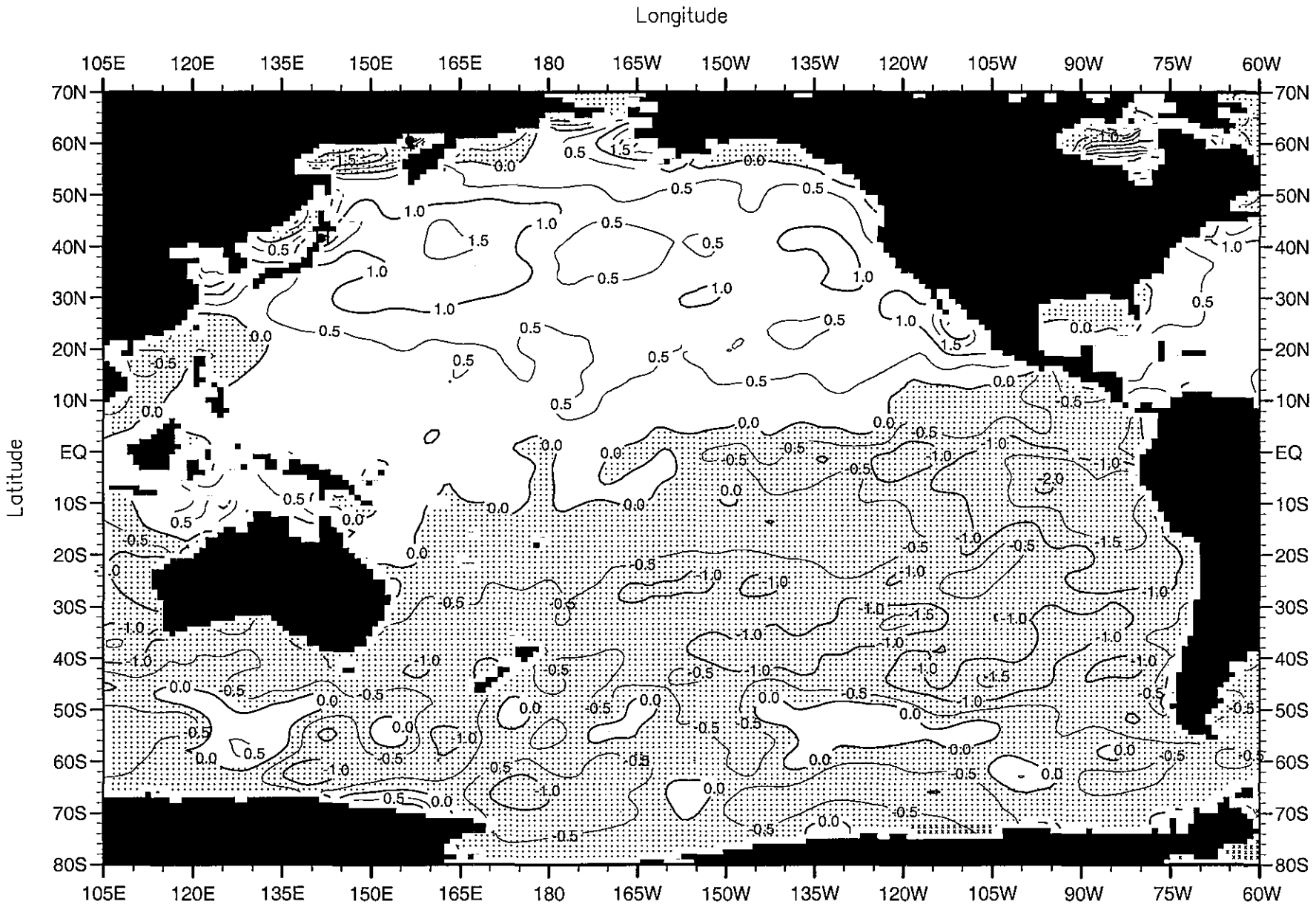


Fig. B62. Fall (Oct.-Dec.) minus annual temperature (°C) at the surface .

Minimum Value= -2.79 Maximum Value= 3.17 Contour Interval: 0.50

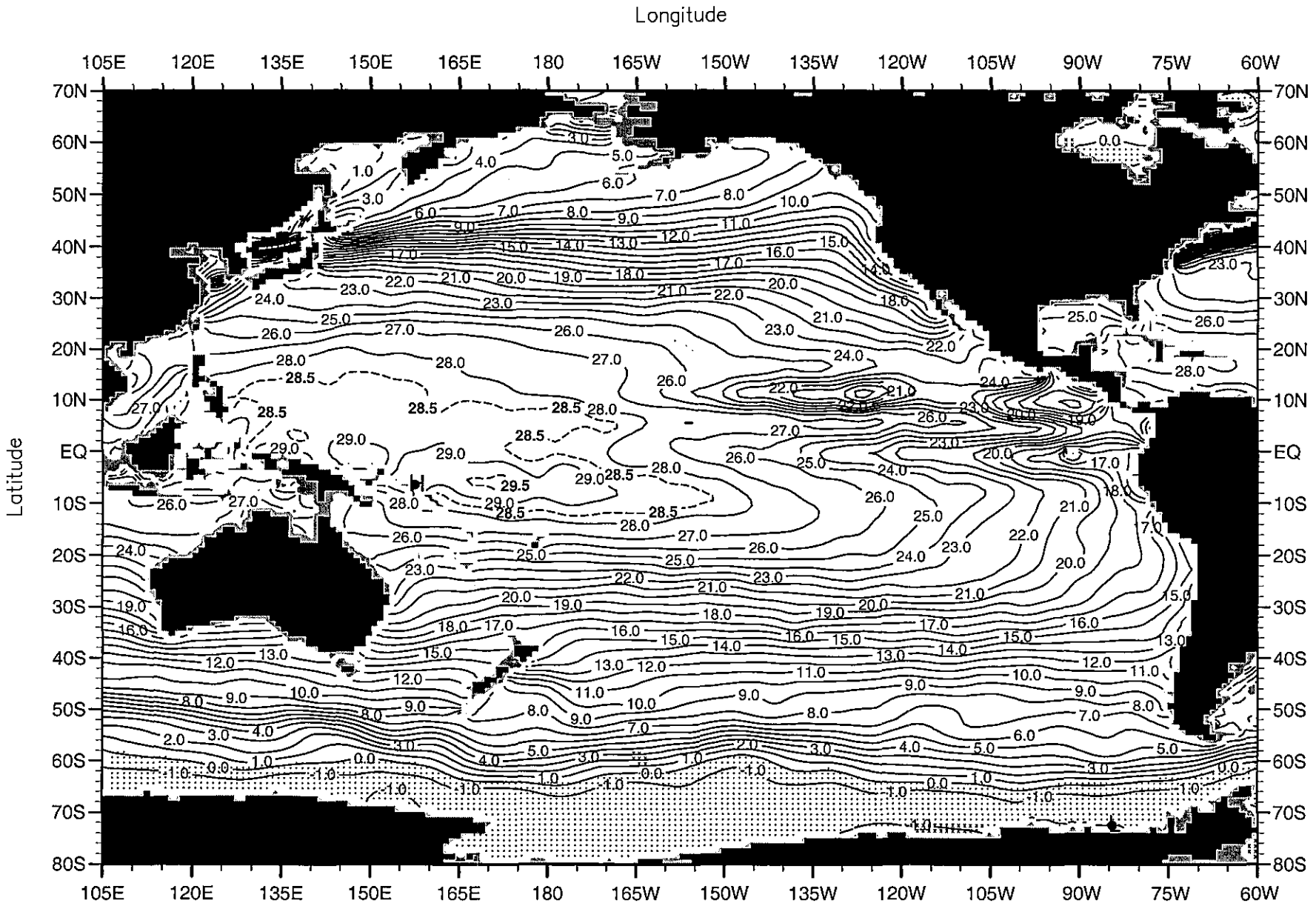


Fig. B63. Fall (Oct.-Dec.) mean temperature (°C) at 50 m. depth .

Minimum Value= -2.06 Maximum Value= 29.66 Contour Interval: 1.00

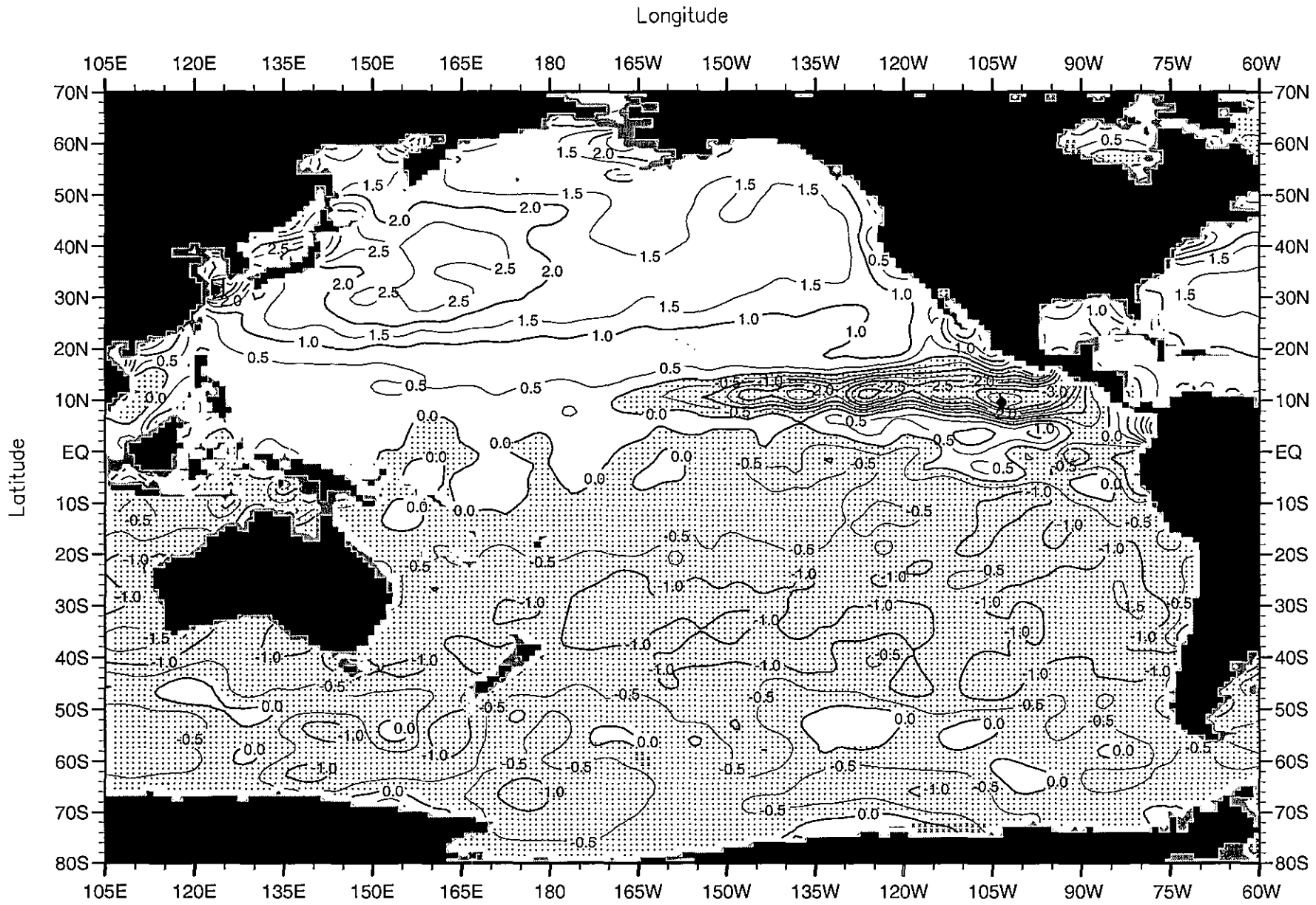


Fig. B64. Fall (Oct.-Dec.) minus annual temperature (°C) at 50 m. depth .

Minimum Value= -3.86 Maximum Value= 4.68 Contour Interval: 0.50

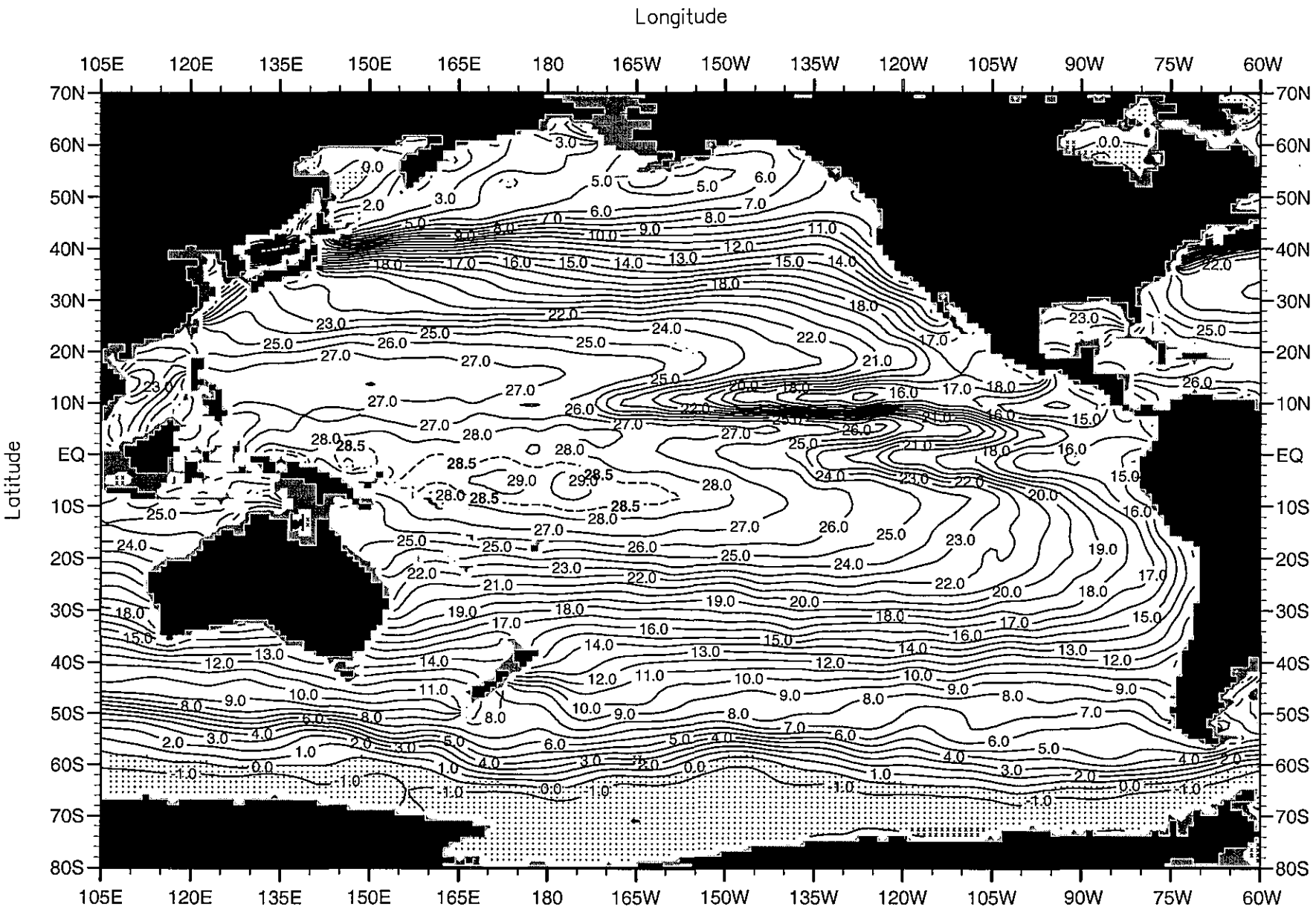


Fig. B65. Fall (Oct.-Dec.) mean temperature (°C) at 75 m. depth .

Minimum Value= -2.10 Maximum Value= 32.61 Contour Interval: 1.00

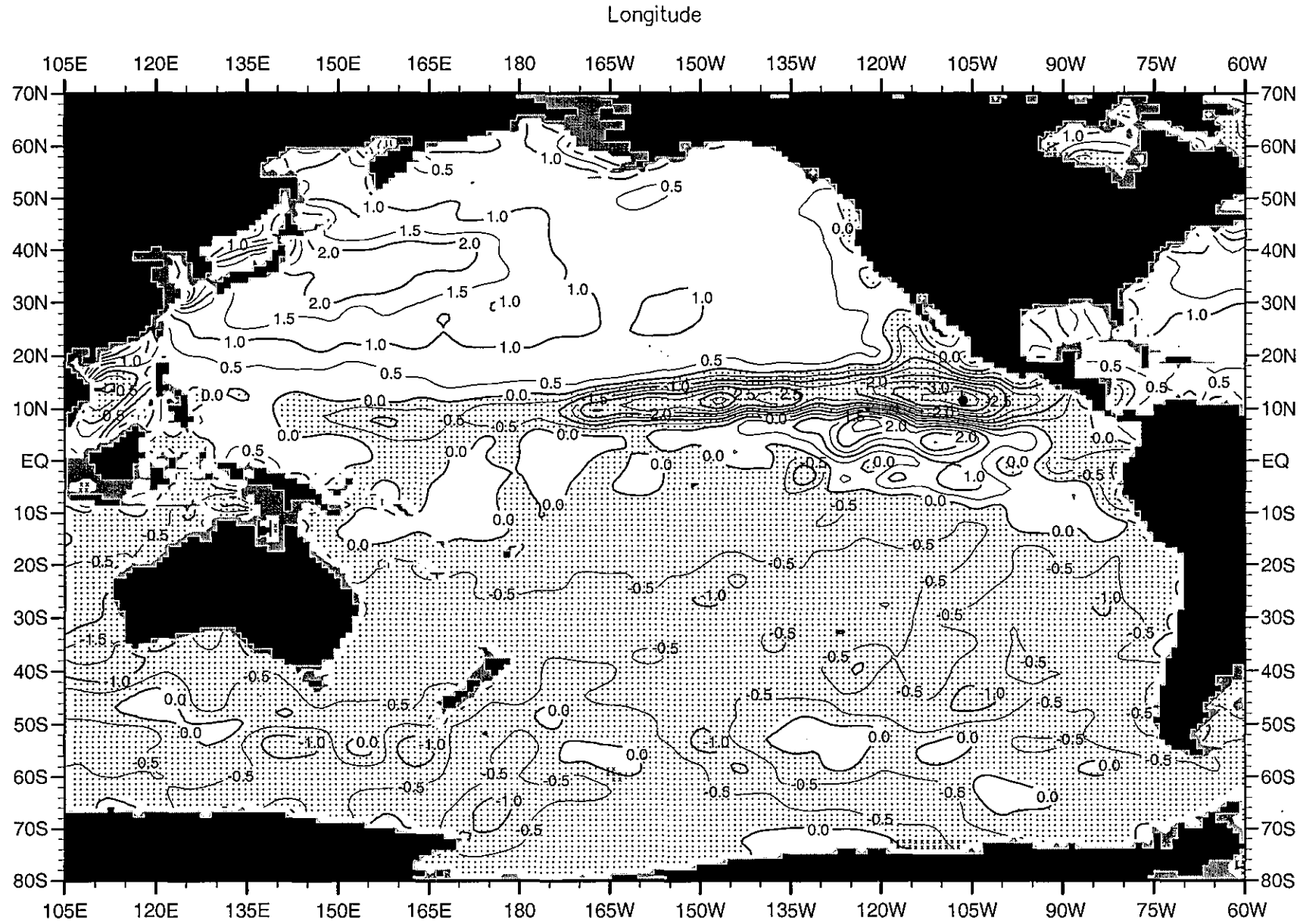


Fig. B66. Fall (Oct.-Dec.) minus annual temperature (°C) at 75 m. depth .

Minimum Value= -3.91 Maximum Value= 4.25 Contour Interval: 0.50

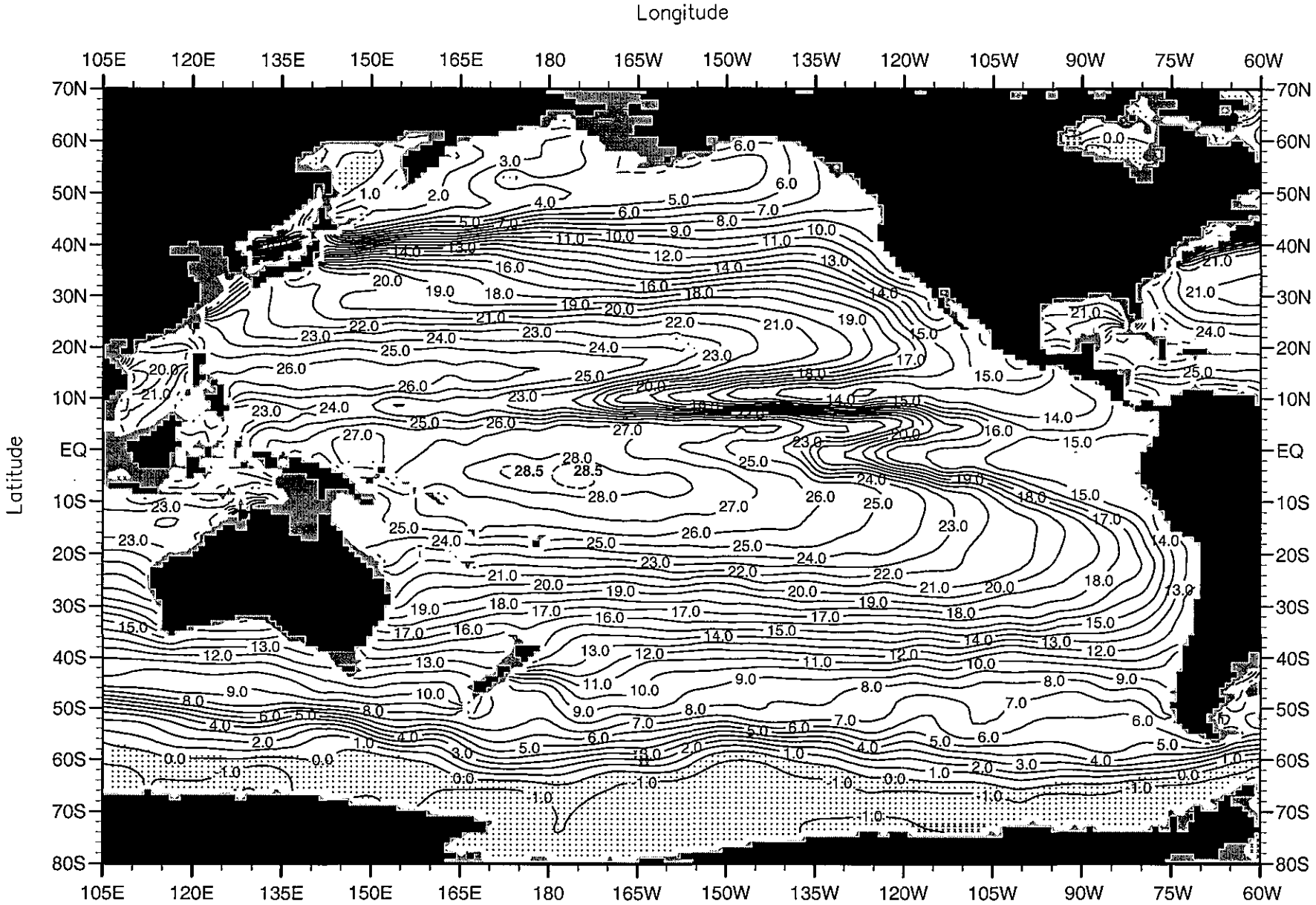


Fig. B67. Fall (Oct.-Dec.) mean temperature (°C) at 100 m. depth .

Minimum Value= -2.10 Maximum Value= 28.88 Contour Interval: 1.00

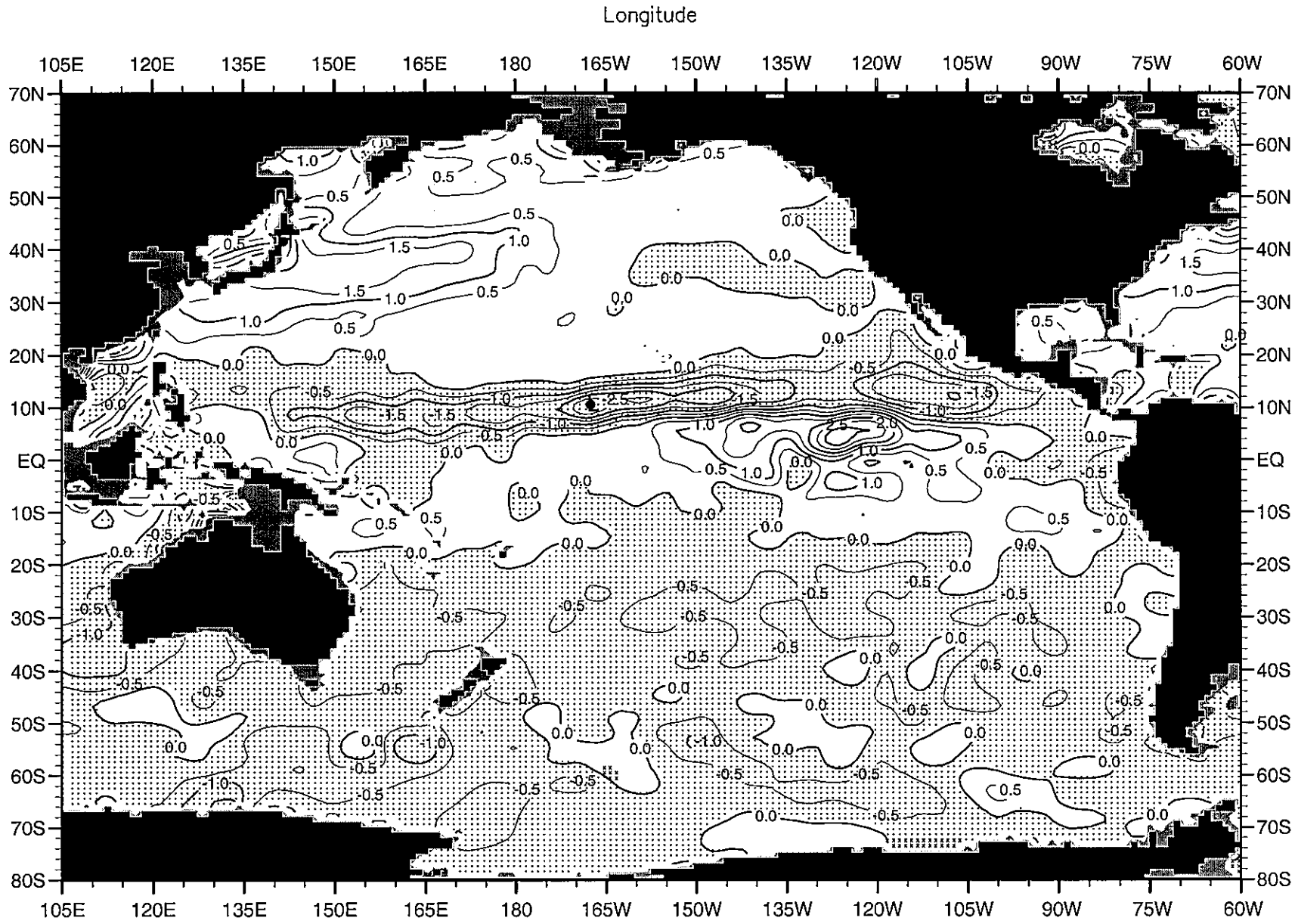


Fig. B68. Fall (Oct.-Dec.) minus annual temperature (°C) at 100 m. depth .

Minimum Value= -2.98 Maximum Value= 3.64 Contour Interval: 0.50

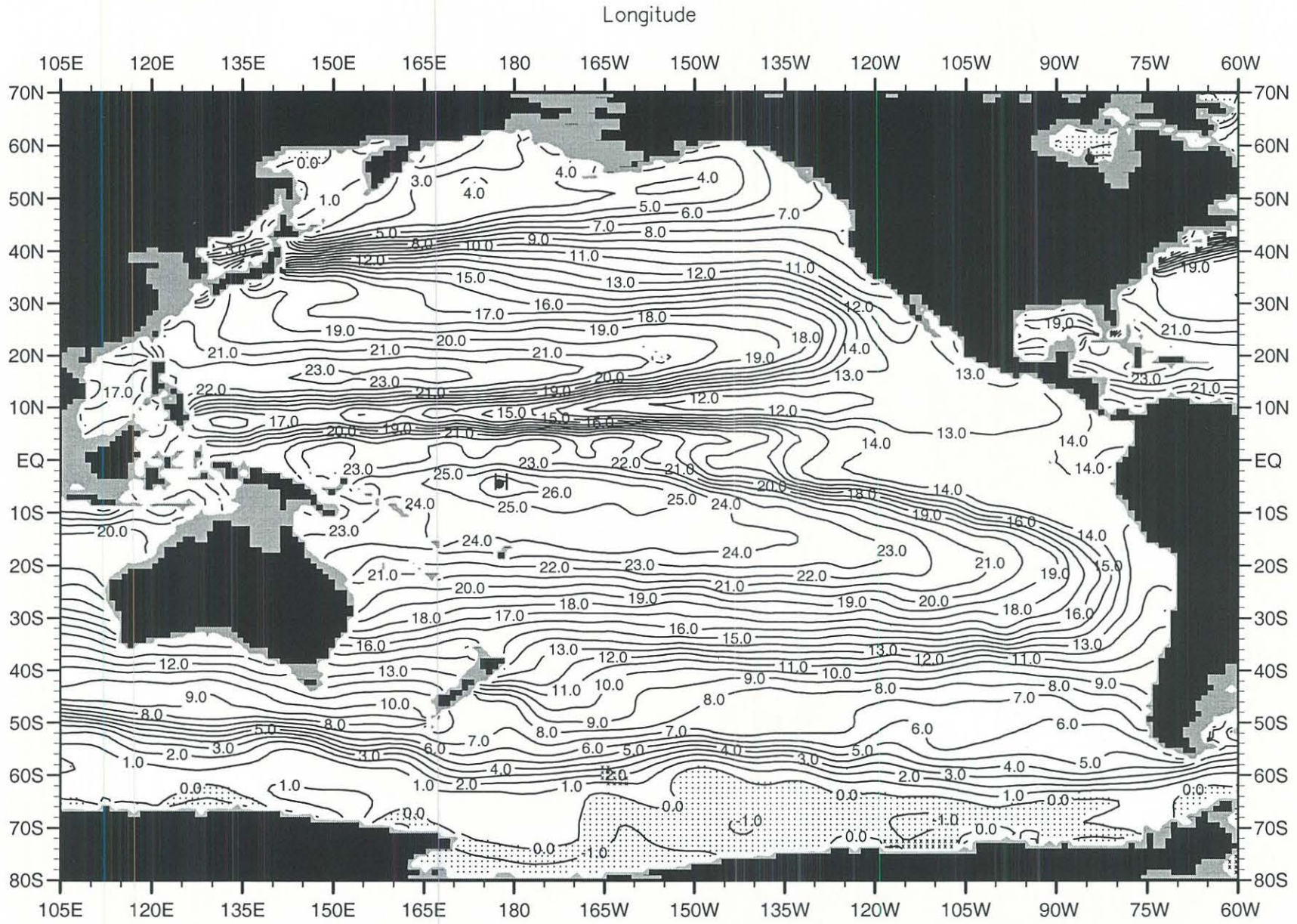


Fig. B69. Fall (Oct.-Dec.) mean temperature (°C) at 150 m. depth .

Minimum Value= -2.10 Maximum Value= 26.67 Contour Interval: 1.00

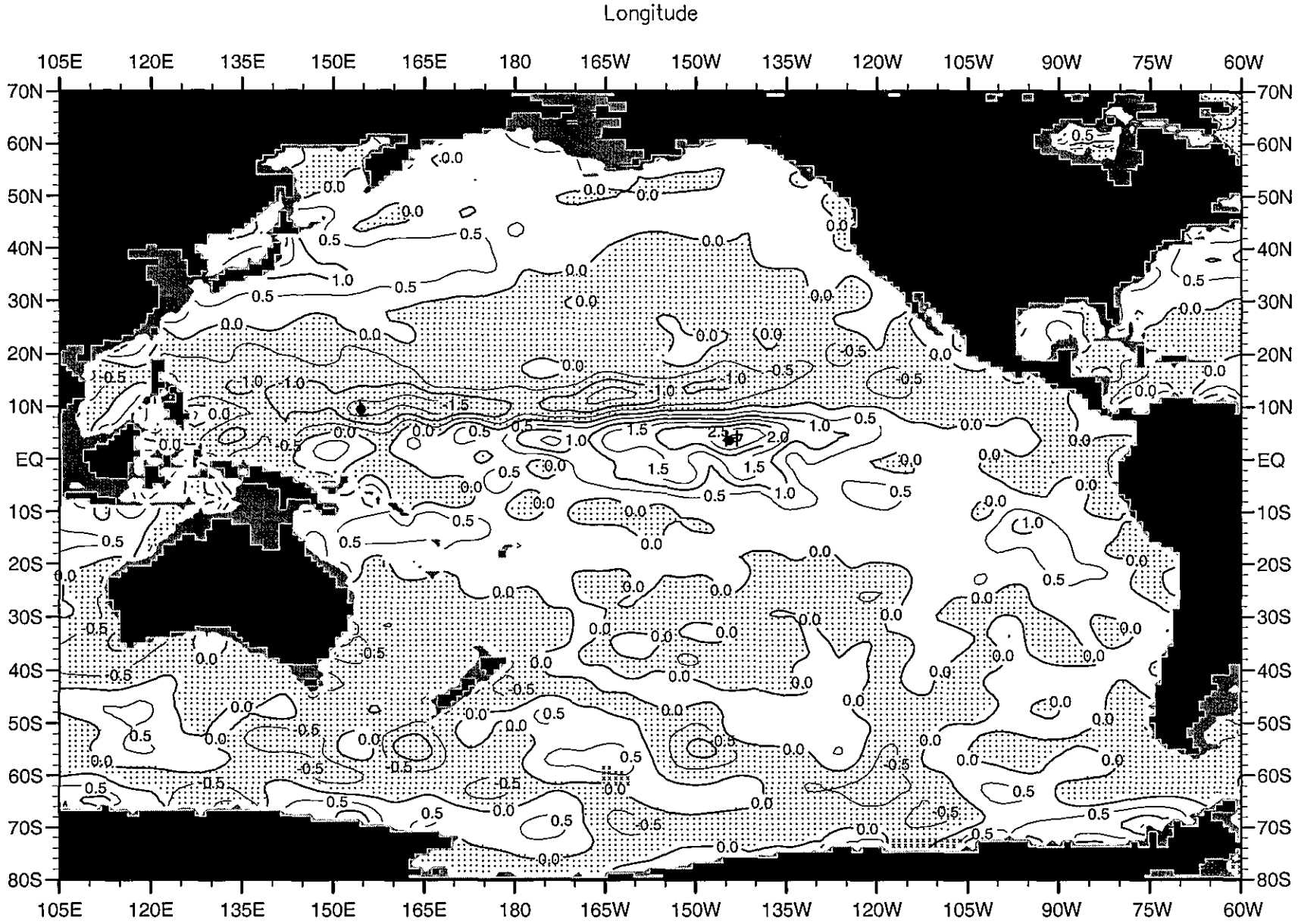


Fig. B70. Fall (Oct.-Dec.) minus annual temperature (°C) at 150 m. depth .

Minimum Value= -1.73 Maximum Value= 3.09 Contour Interval: 0.50

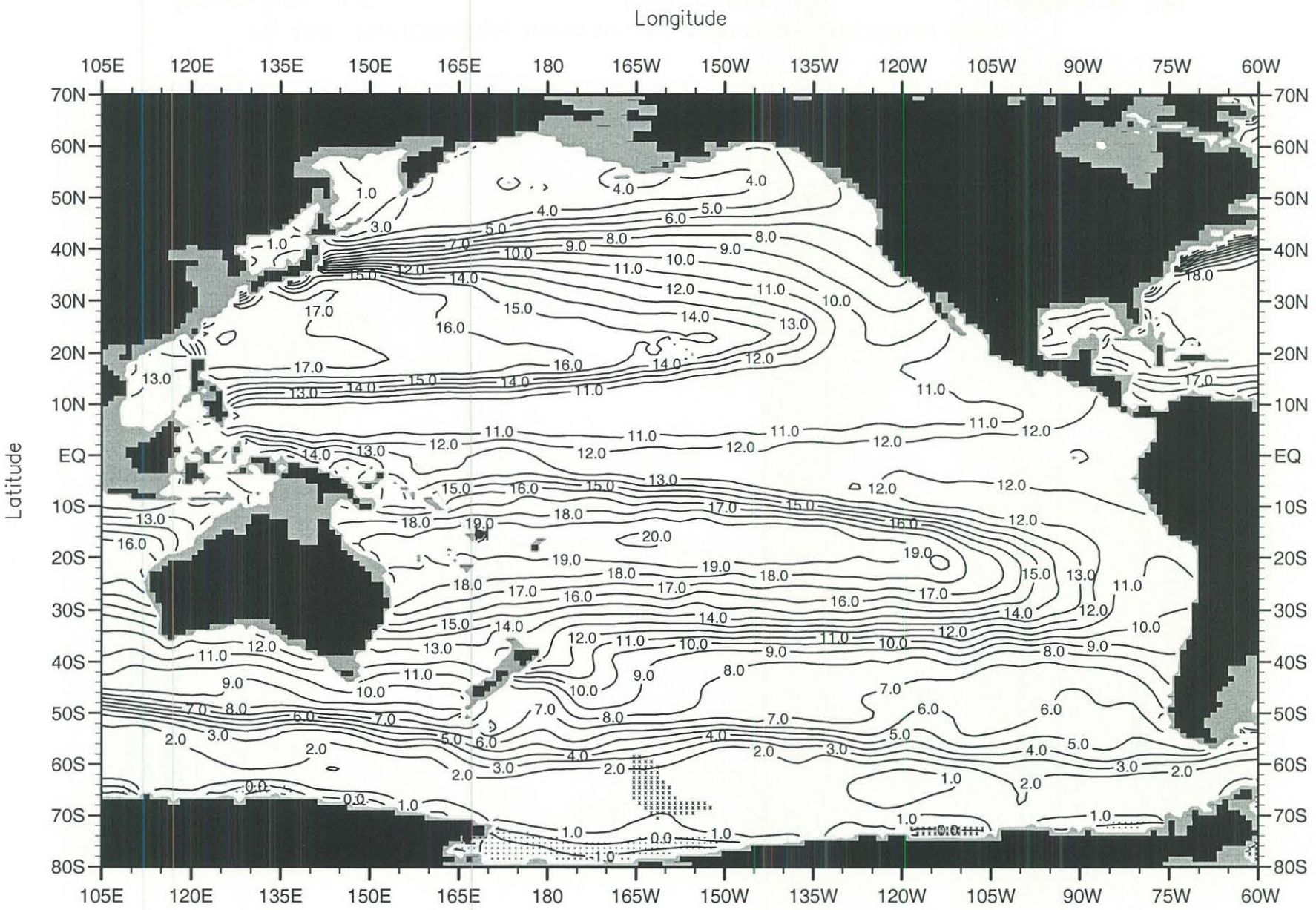


Fig. B71. Fall (Oct.-Dec.) mean temperature (°C) at 250 m. depth .

Minimum Value= -2.09 Maximum Value= 20.63 Contour Interval: 1.00

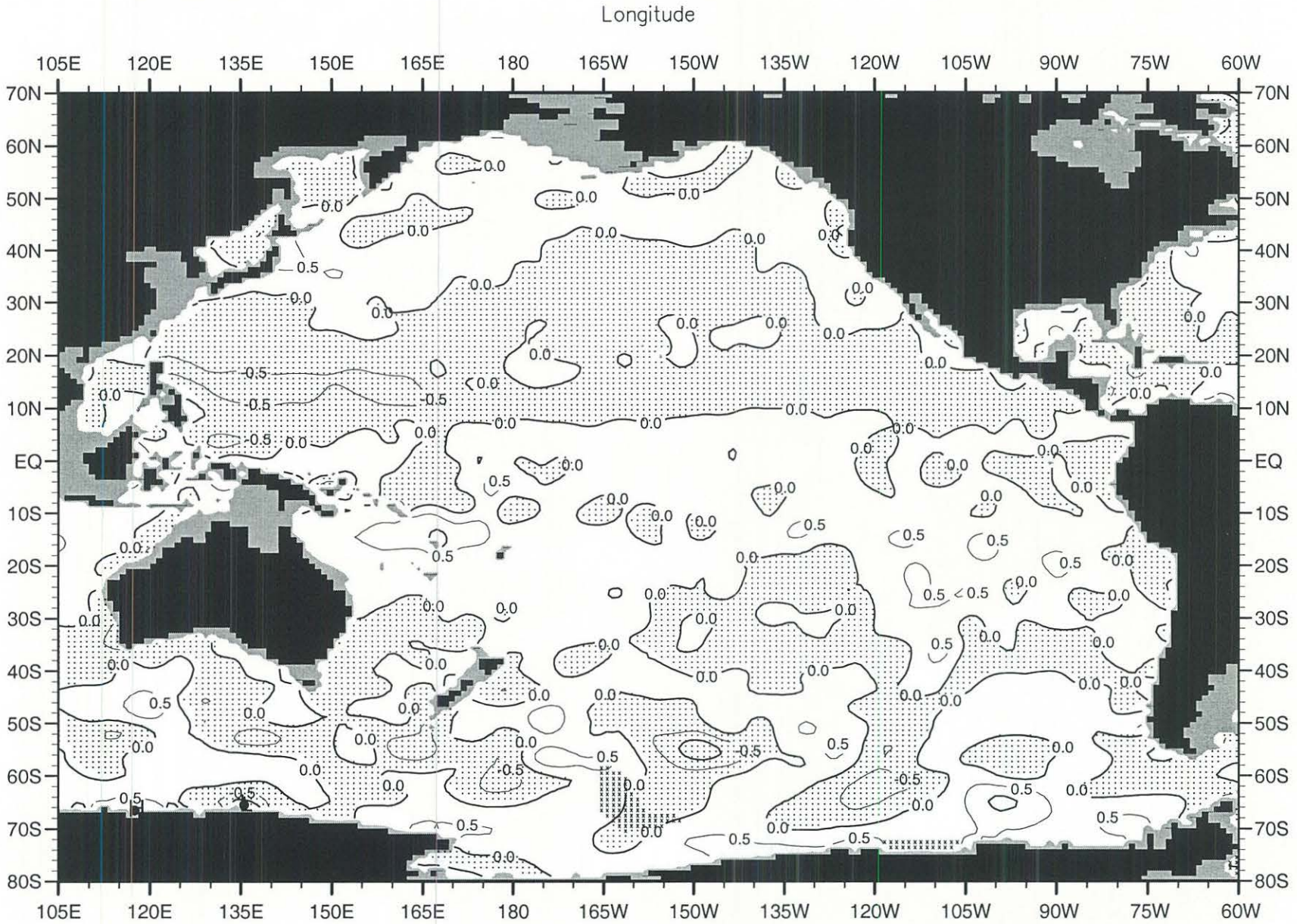


Fig. B72. Fall (Oct.-Dec.) minus annual temperature (°C) at 250 m. depth .

Minimum Value= -1.70 Maximum Value= 1.22 Contour Interval: 0.50

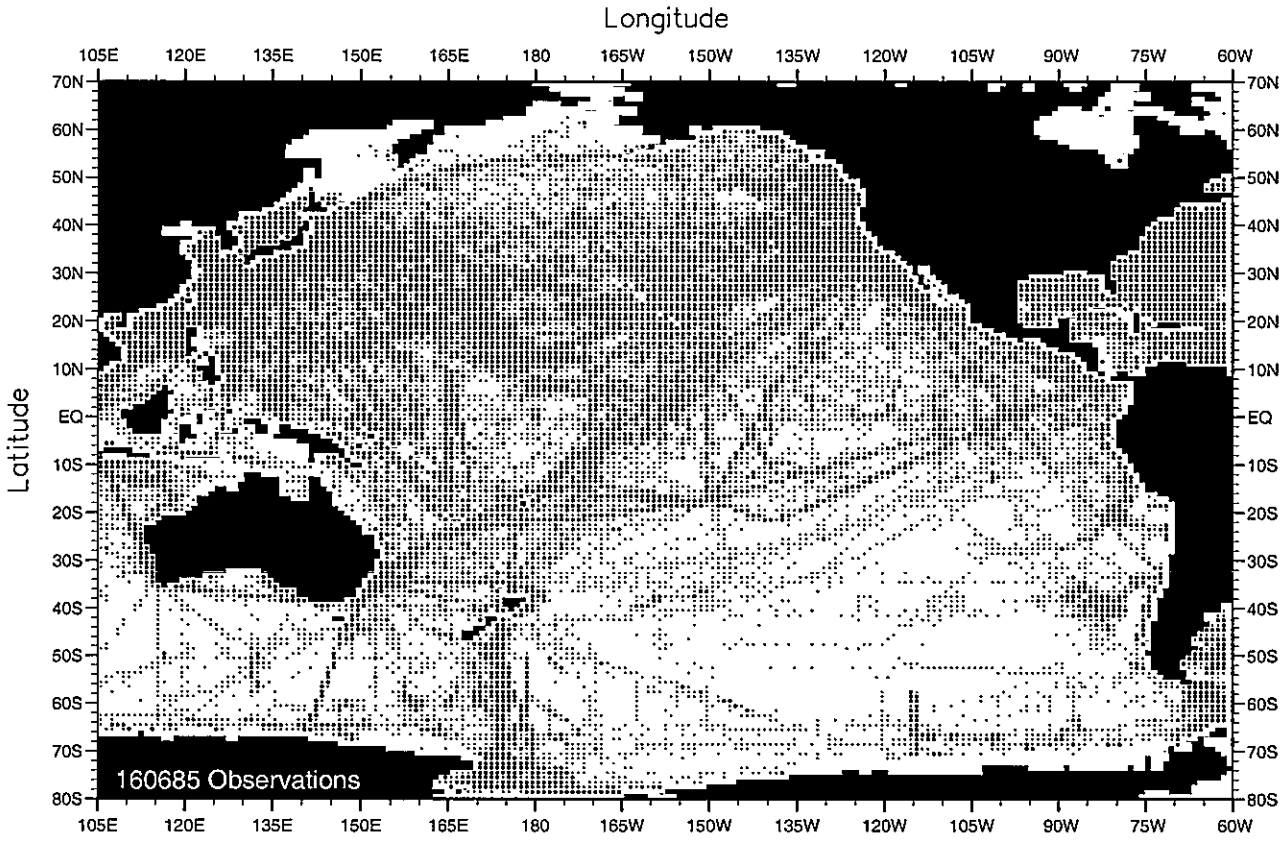


Fig. C1. January temperature observations at the surface .

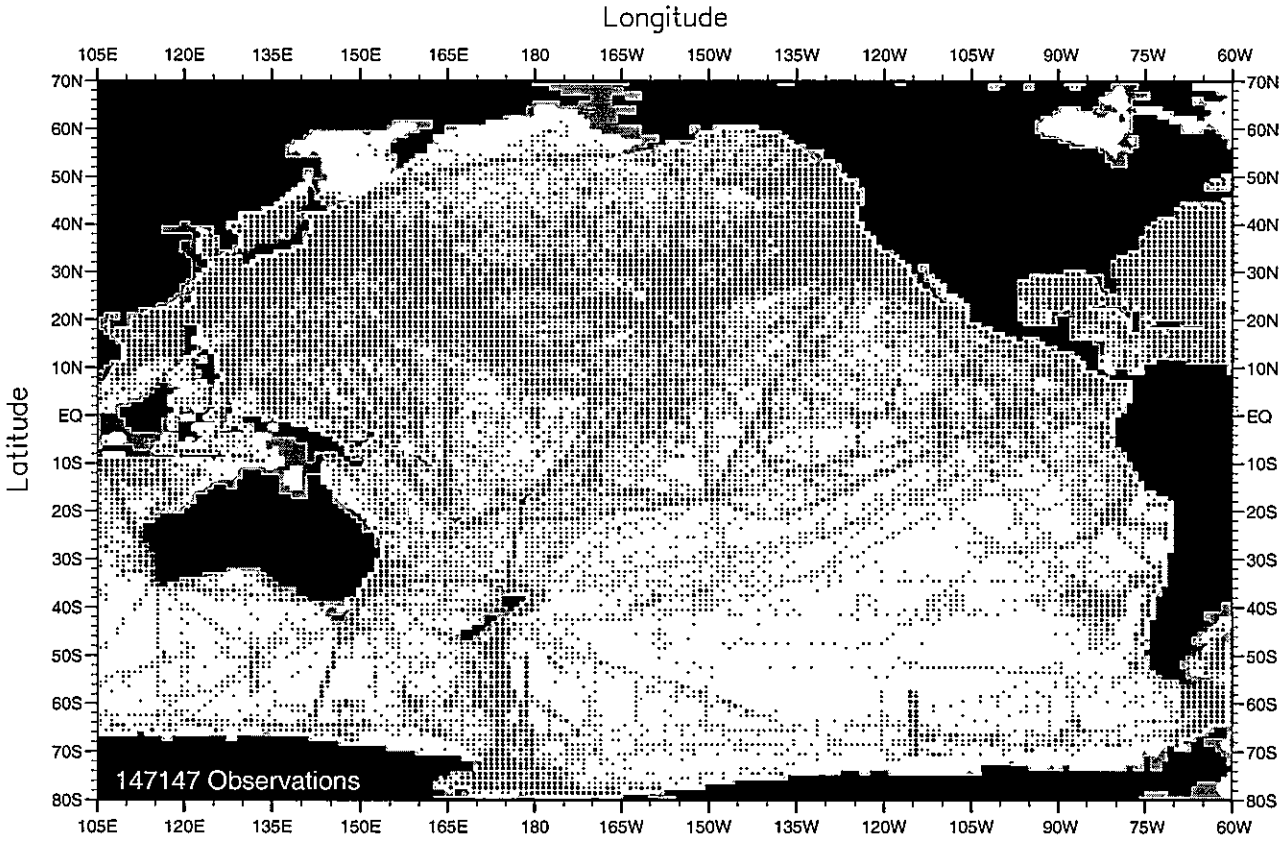


Fig. C2. January temperature observations at 75 m. depth .

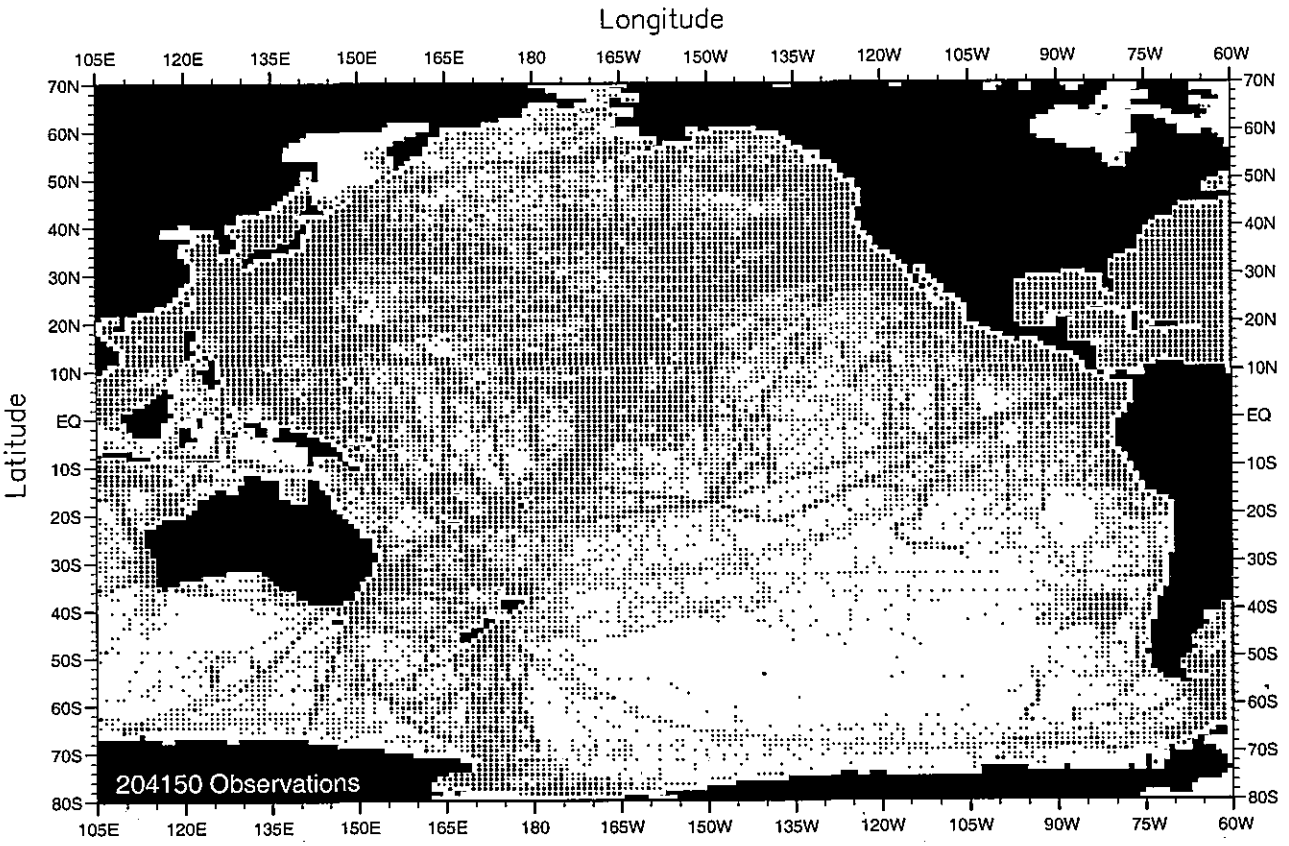


Fig. C3. February temperature observations at the surface .

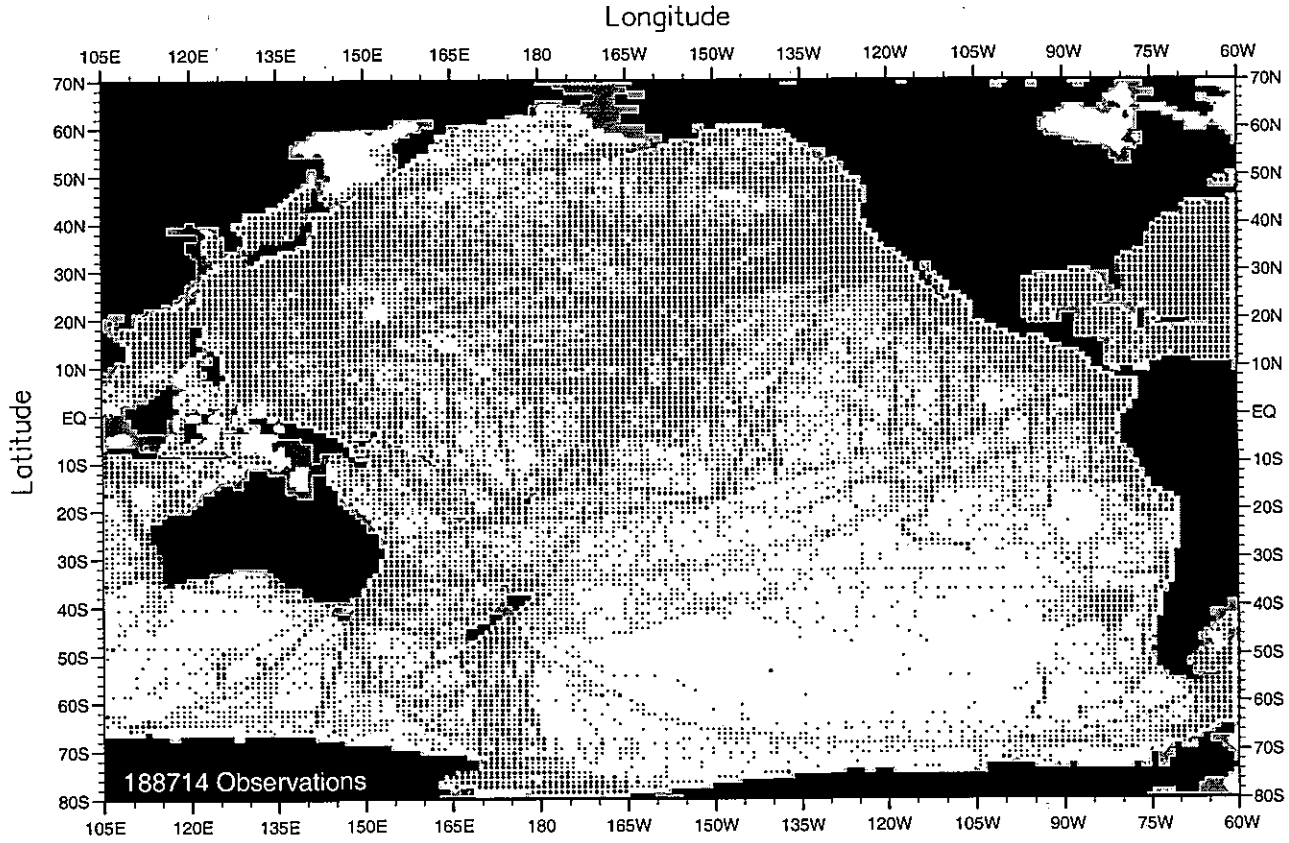


Fig. C4. February temperature observations at 75 m. depth .

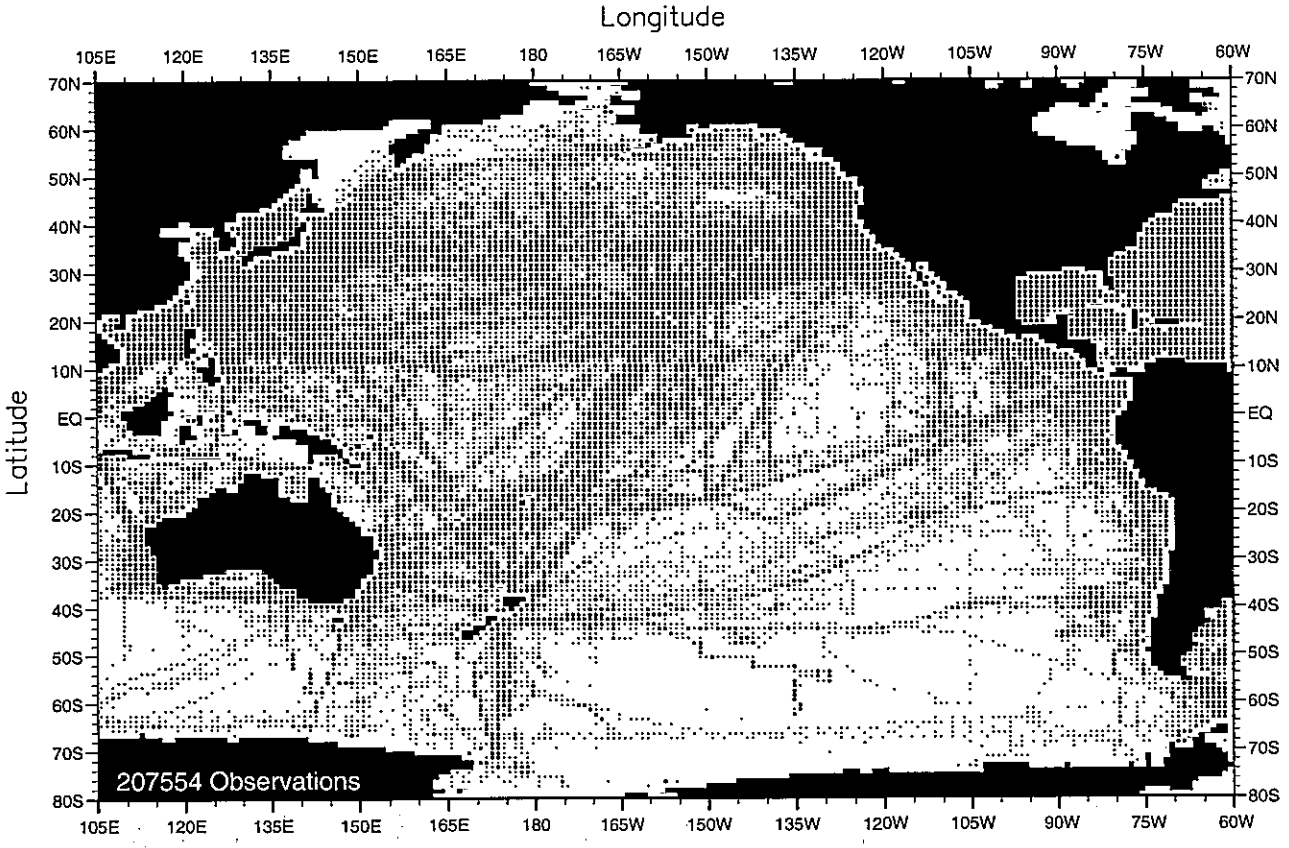


Fig. C5. March temperature observations at the surface .

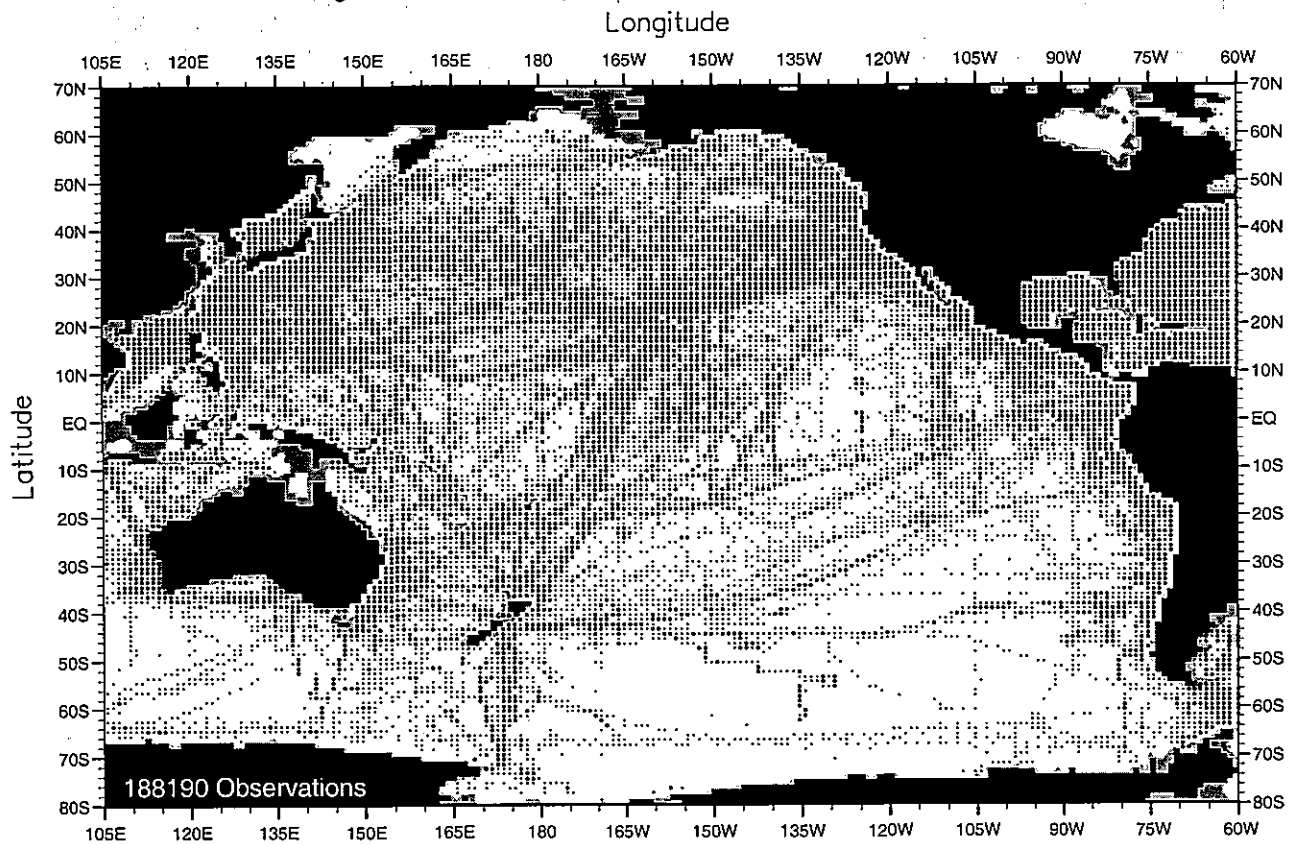


Fig. C6. March temperature observations at 75 m. depth .

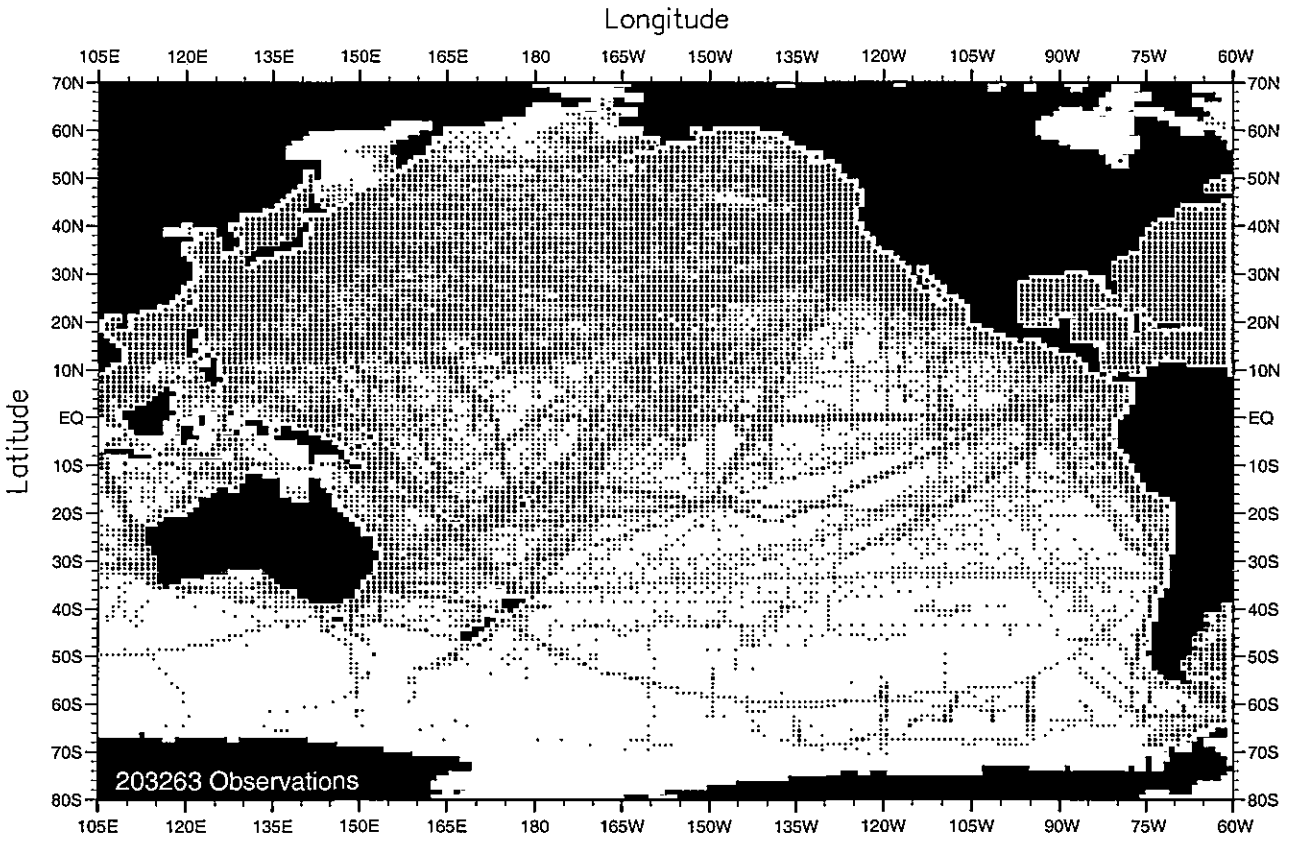


Fig. C7. April temperature observations at the surface .

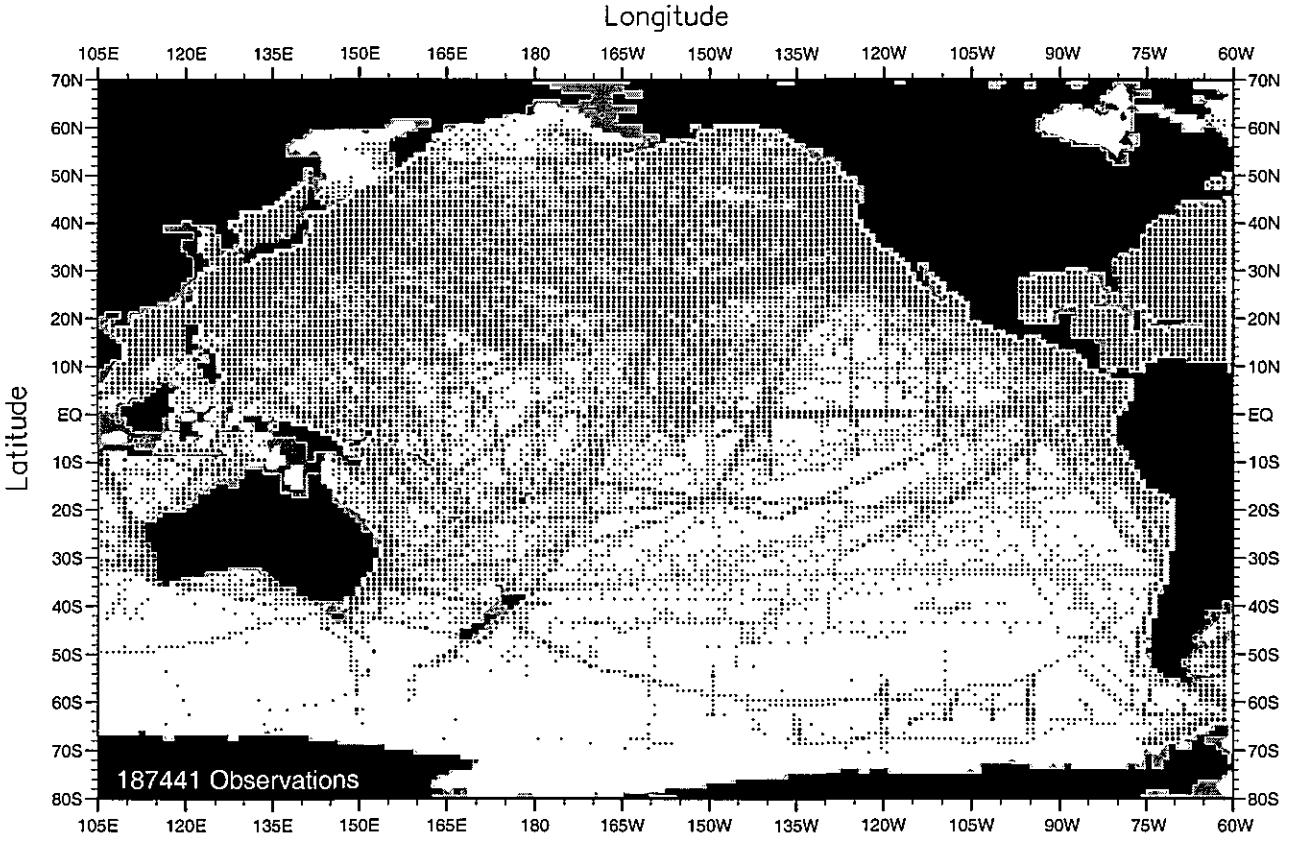


Fig. C8. April temperature observations at 75 m. depth .

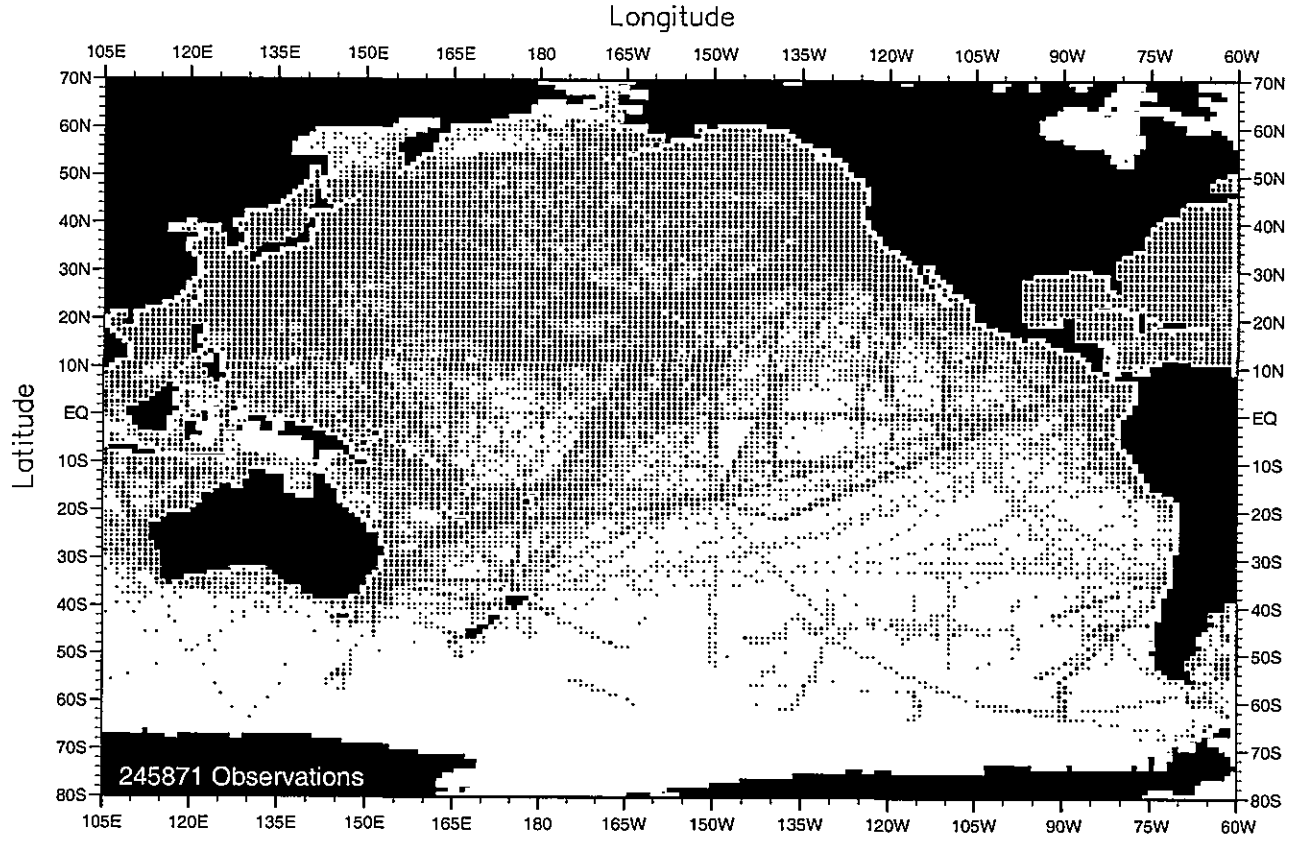


Fig. C9. May temperature observations at the surface .

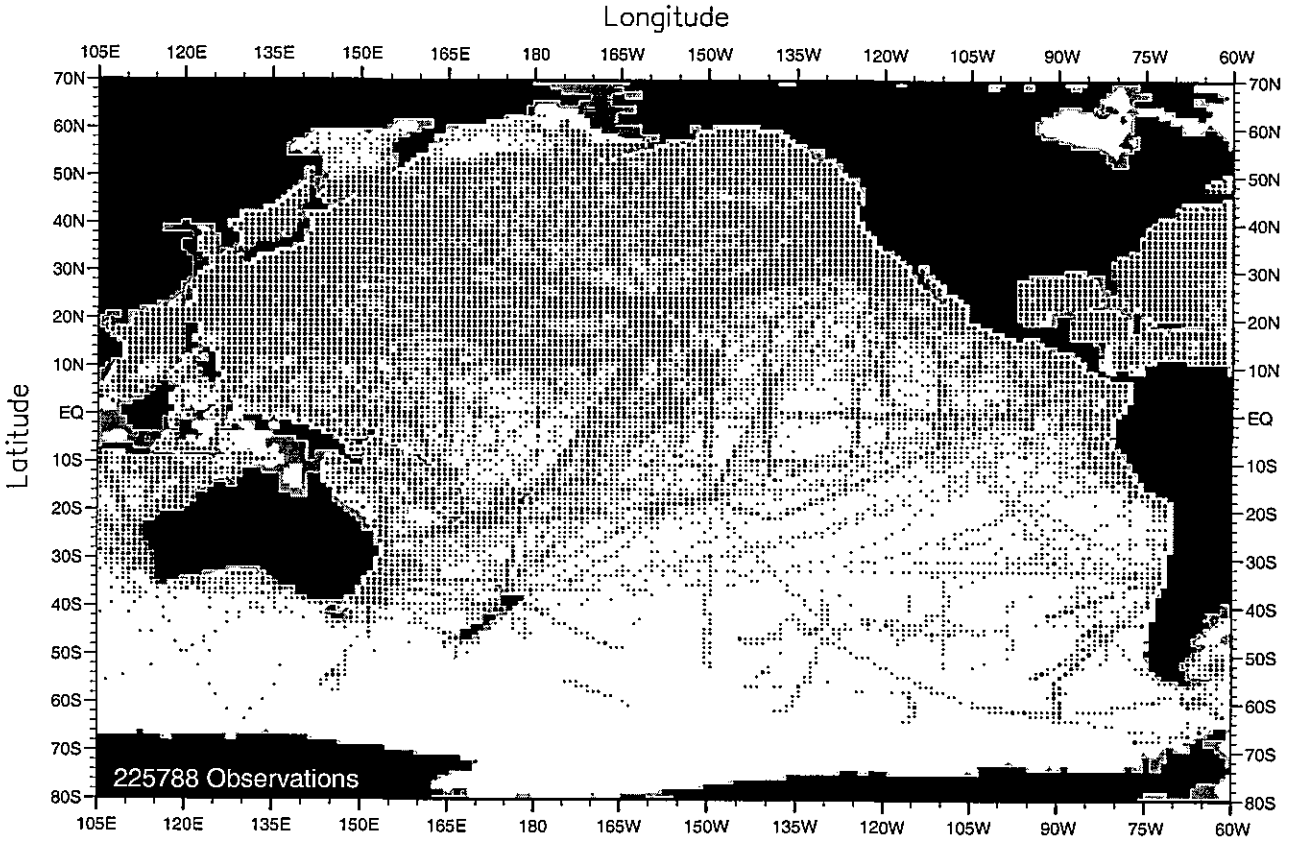


Fig. C10. May temperature observations at 75 m. depth .

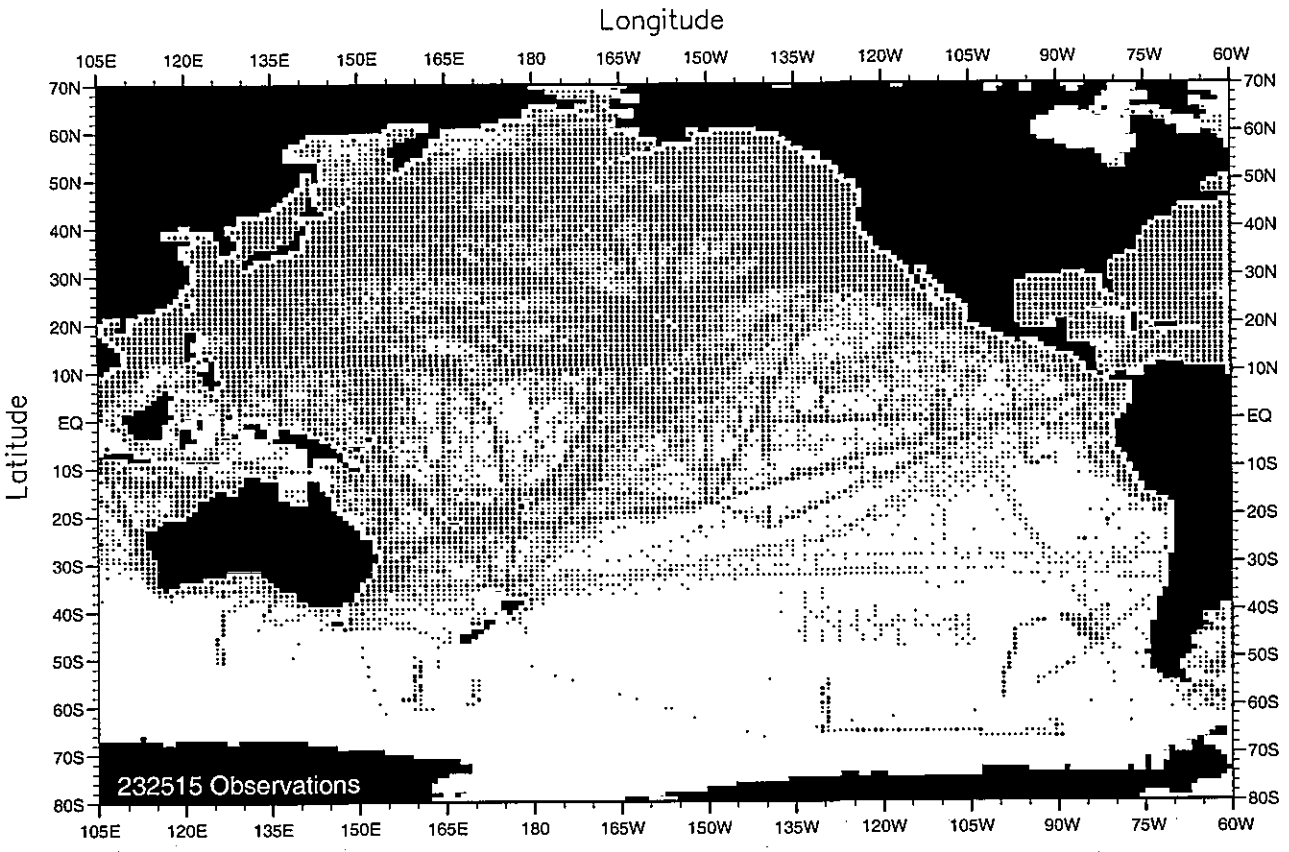


Fig. C11. June temperature observations at the surface .

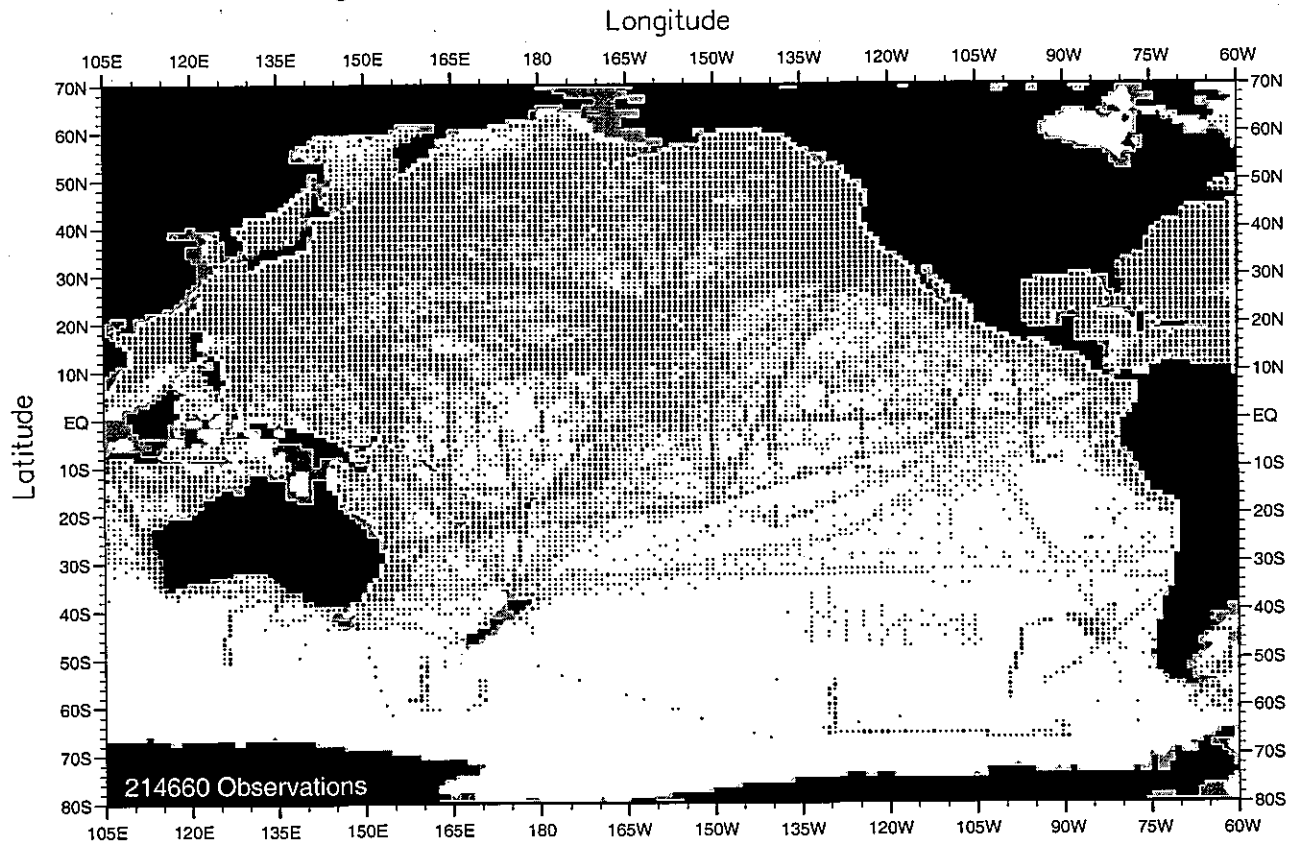


Fig. C12. June temperature observations at 75 m. depth .

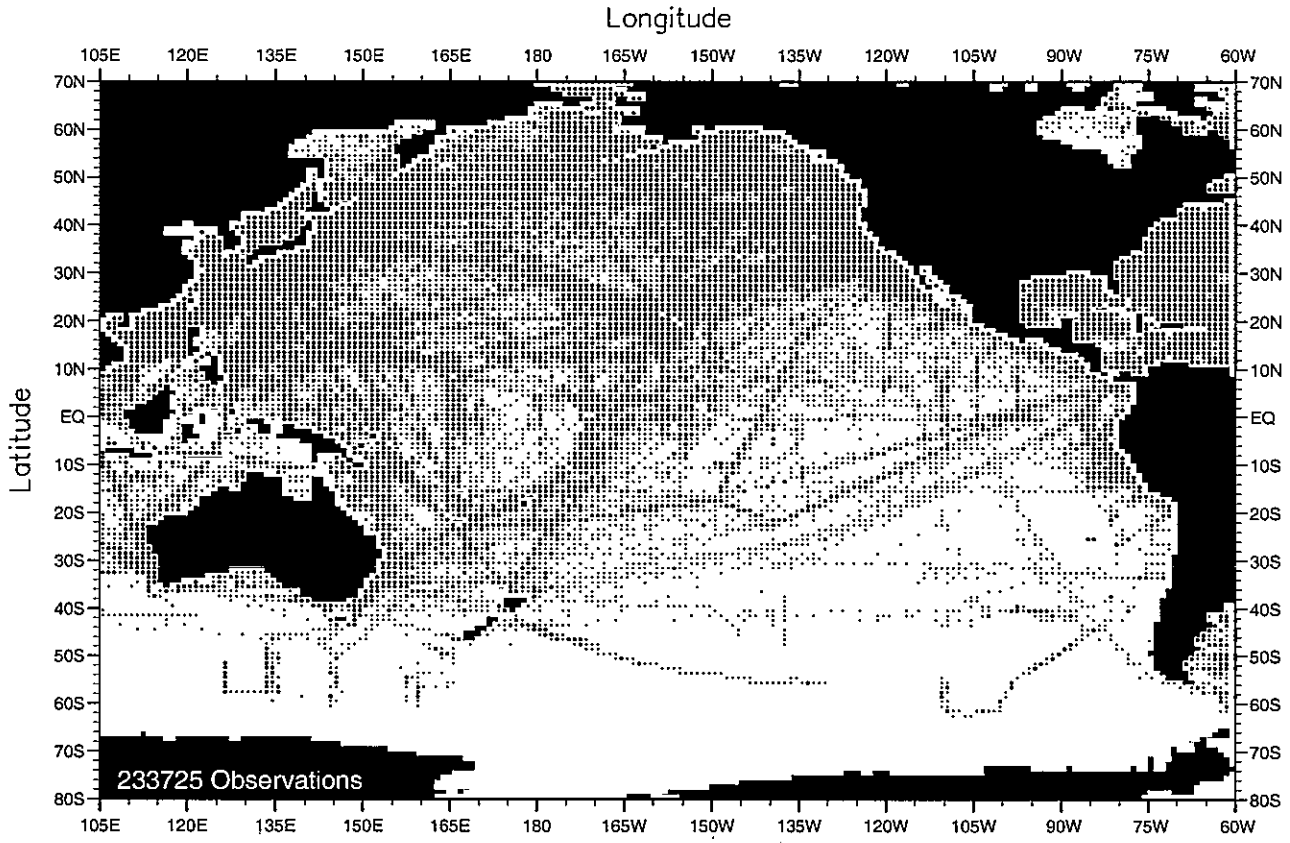


Fig. C13. July temperature observations at the surface .

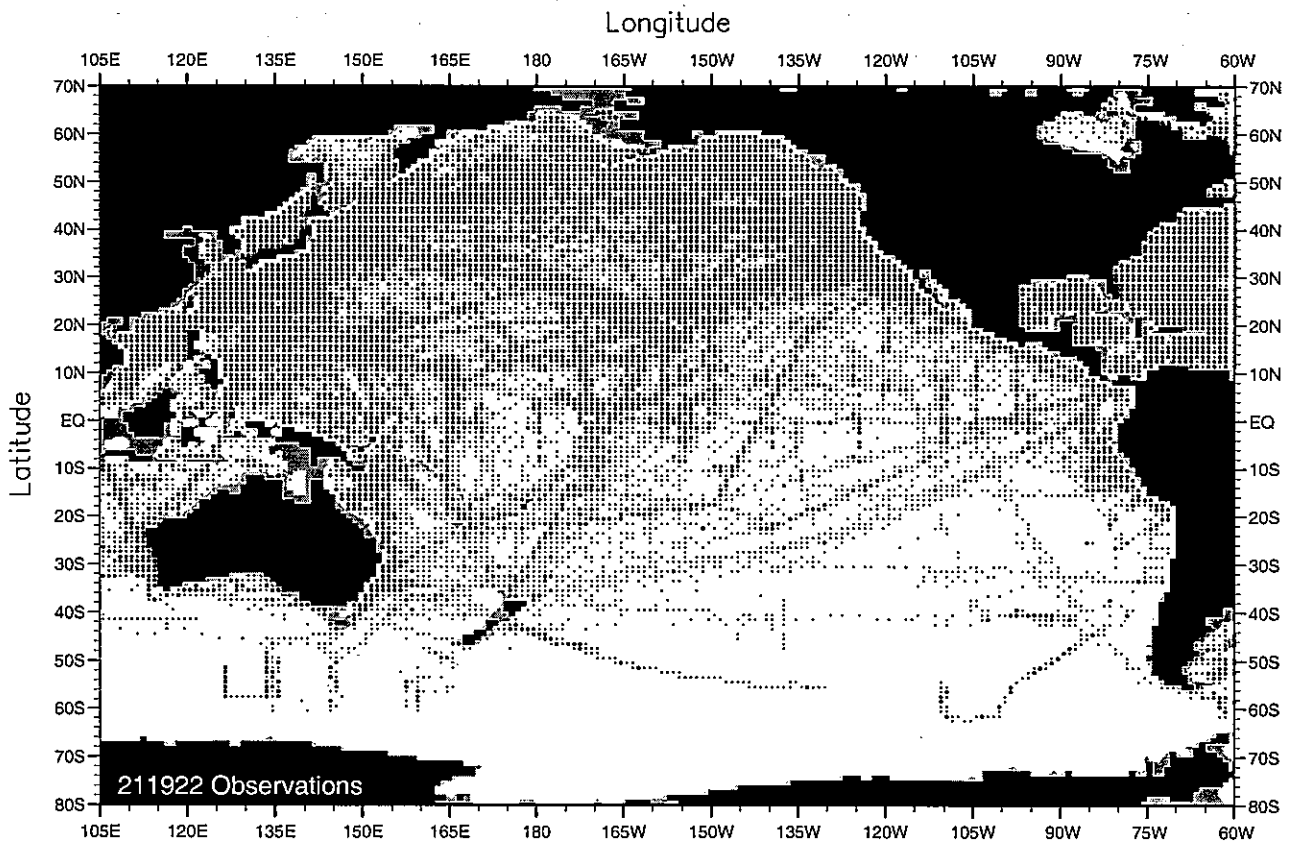


Fig. C14. July temperature observations at 75 m. depth .

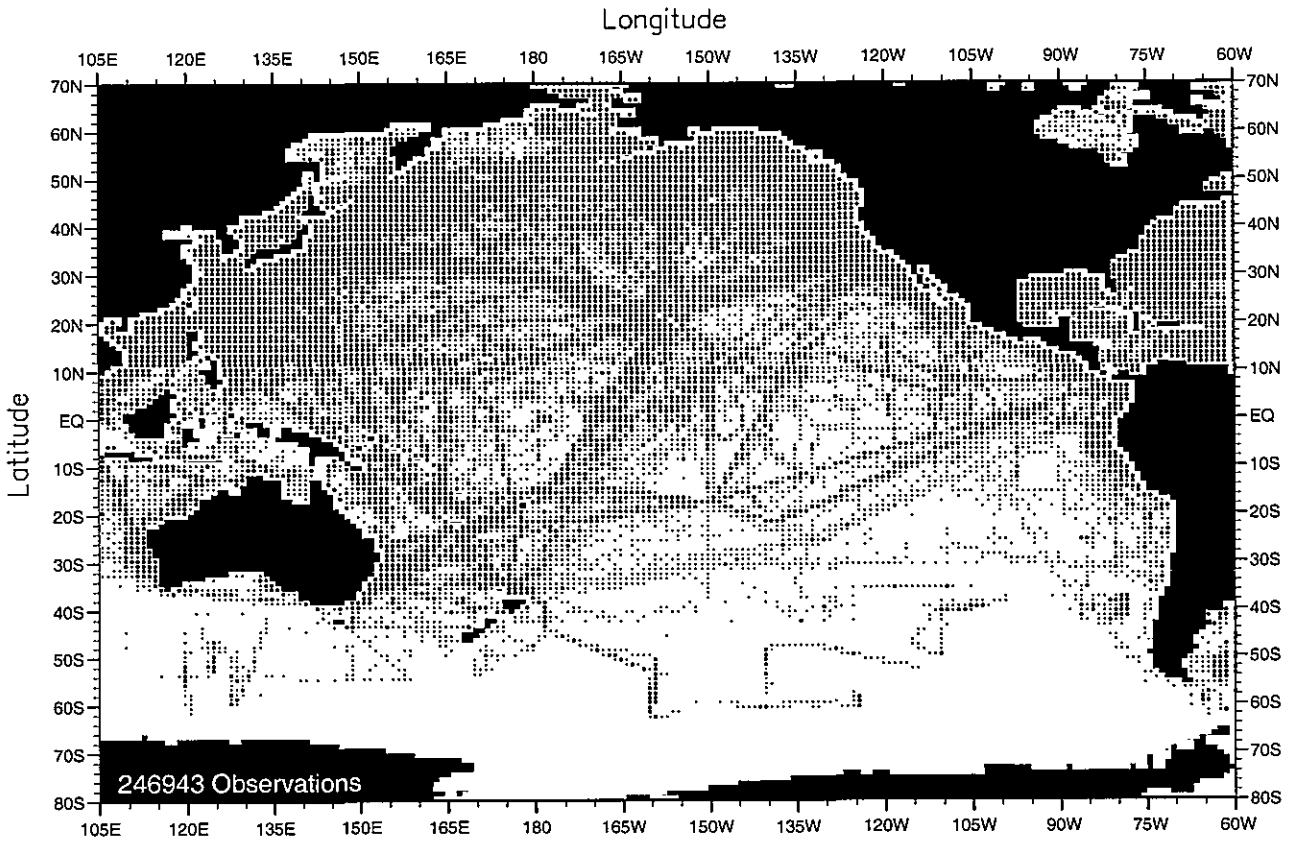


Fig. C15. August temperature observations at the surface .

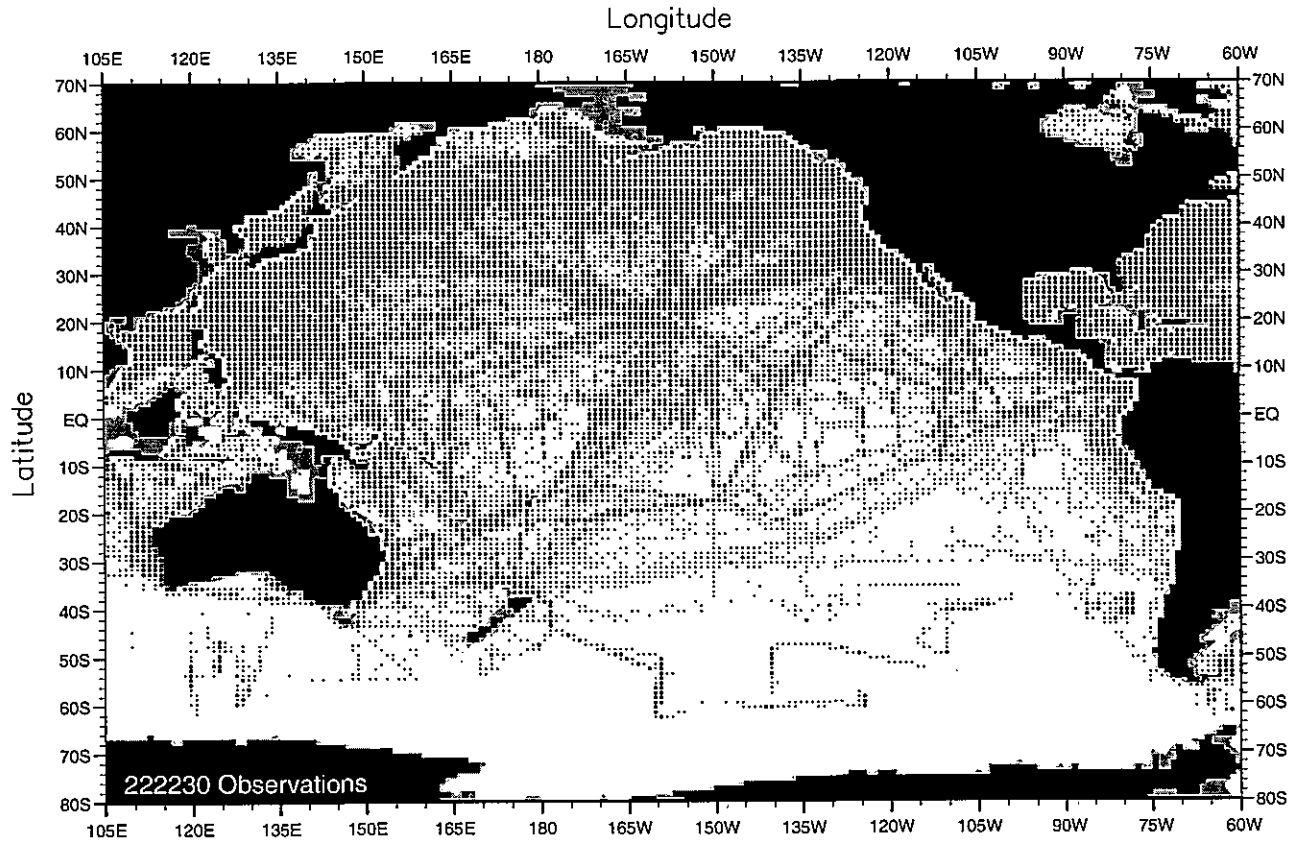


Fig. C16. August temperature observations at 75 m. depth .

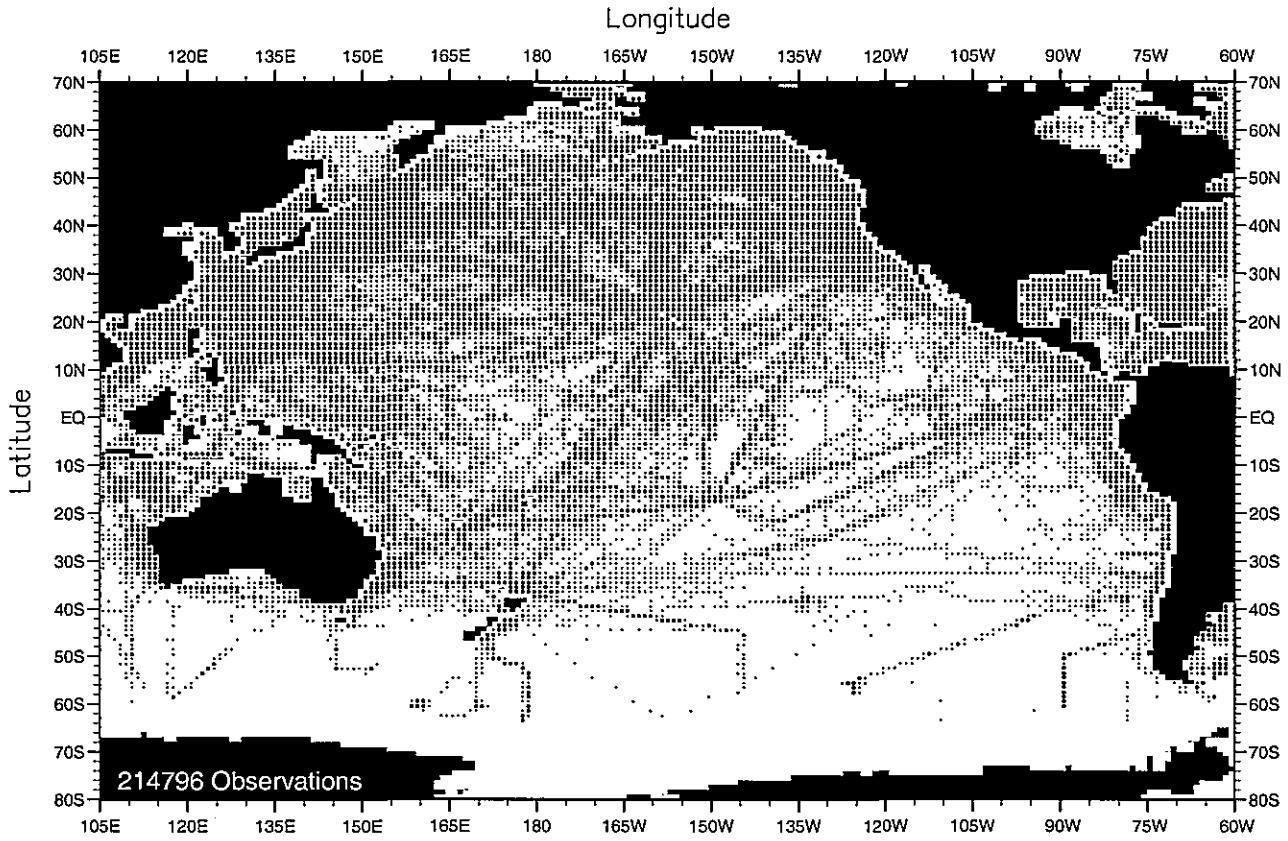


Fig. C17. September temperature observations at the surface .

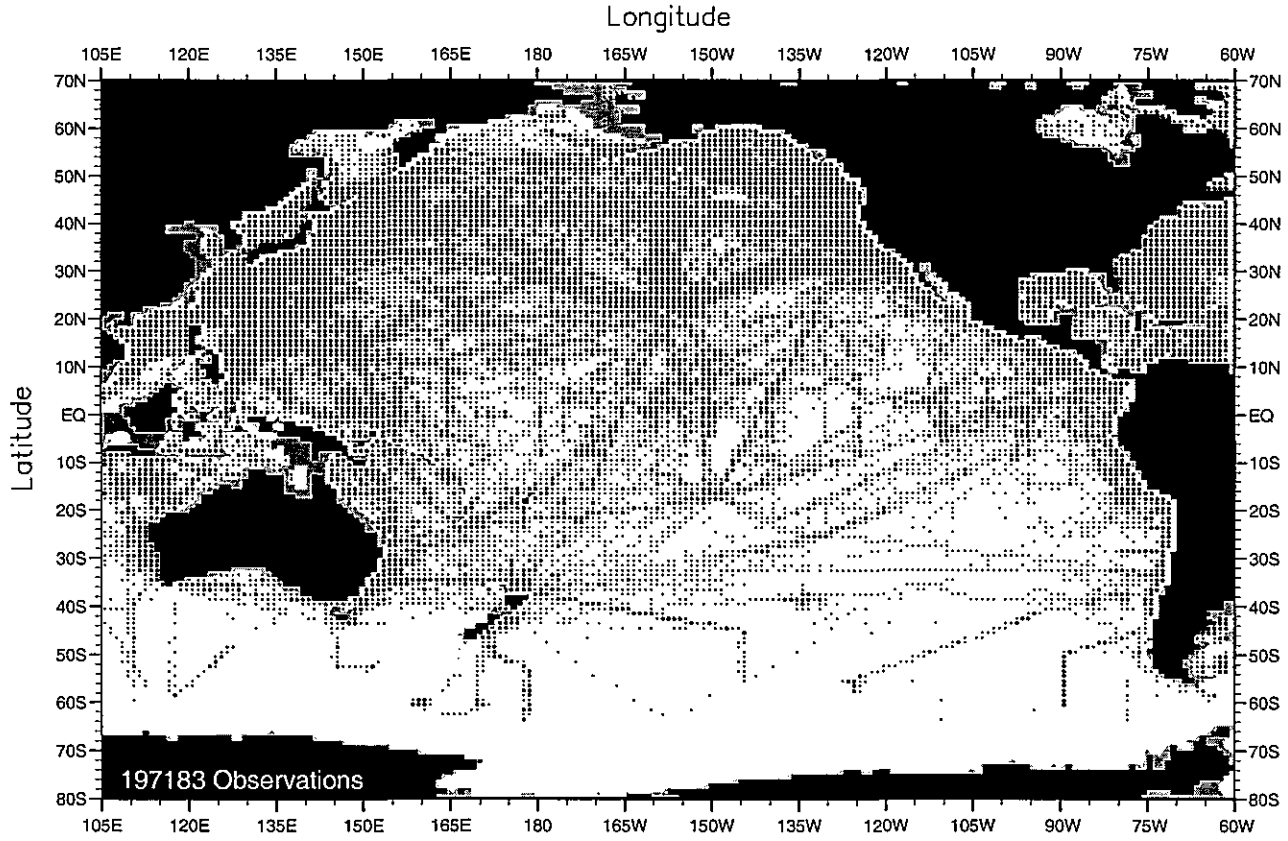


Fig. C18. September temperature observations at 75 m. depth .

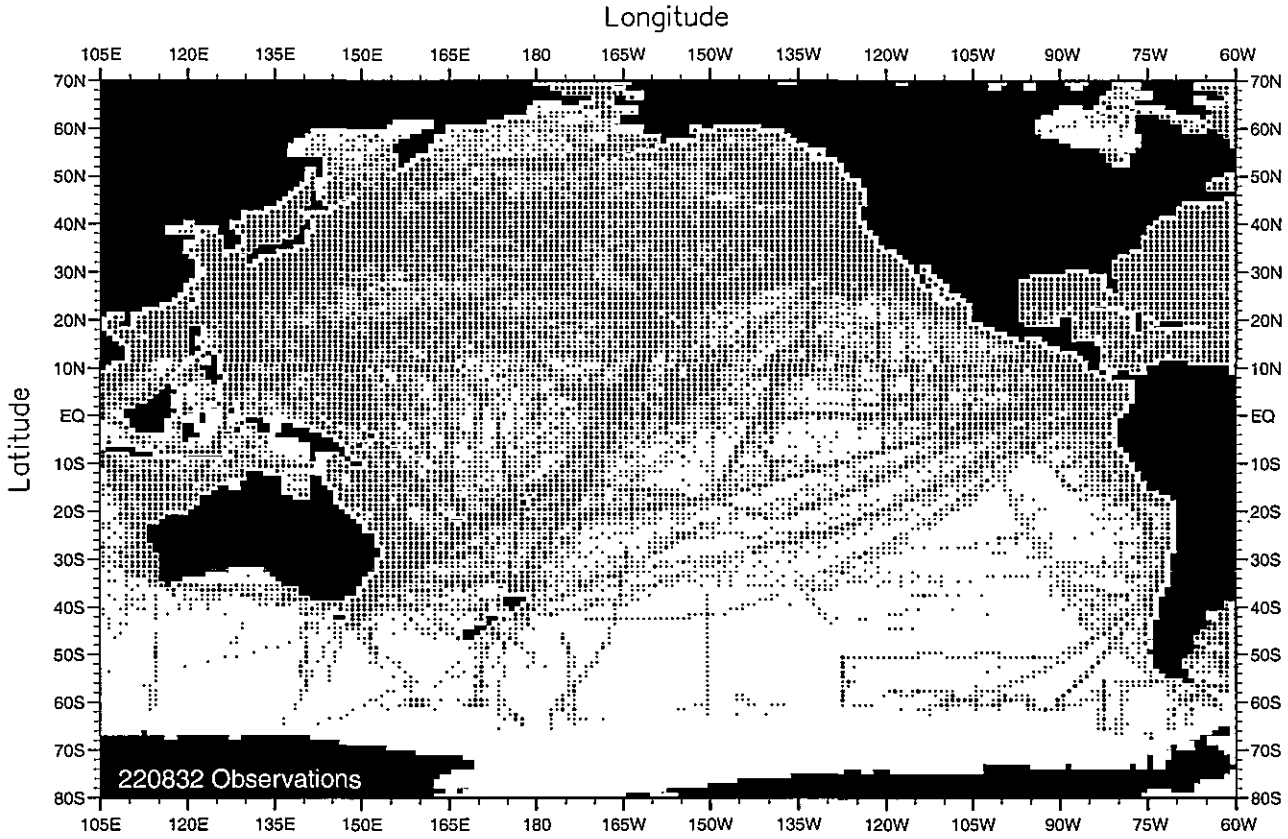


Fig. C19. October temperature observations at the surface .

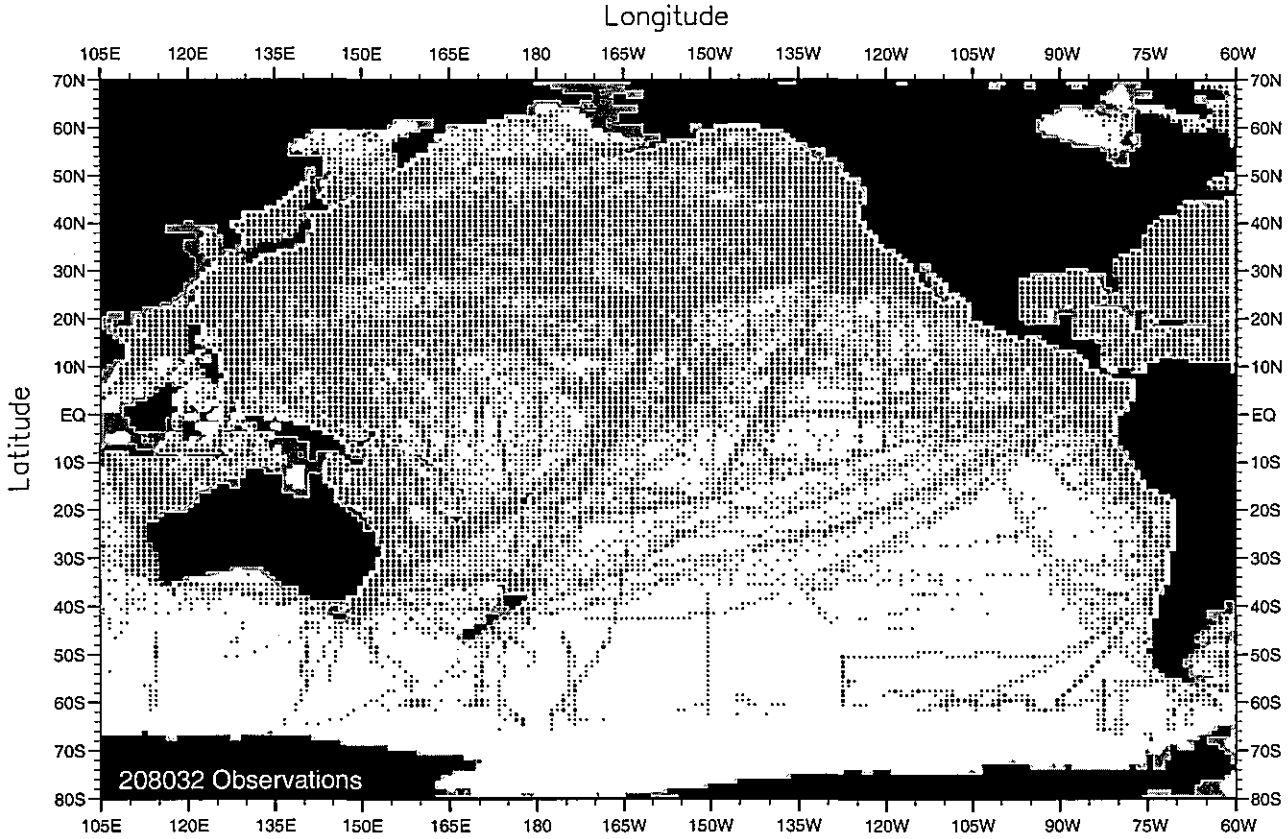


Fig. C20. October temperature observations at 75 m. depth .

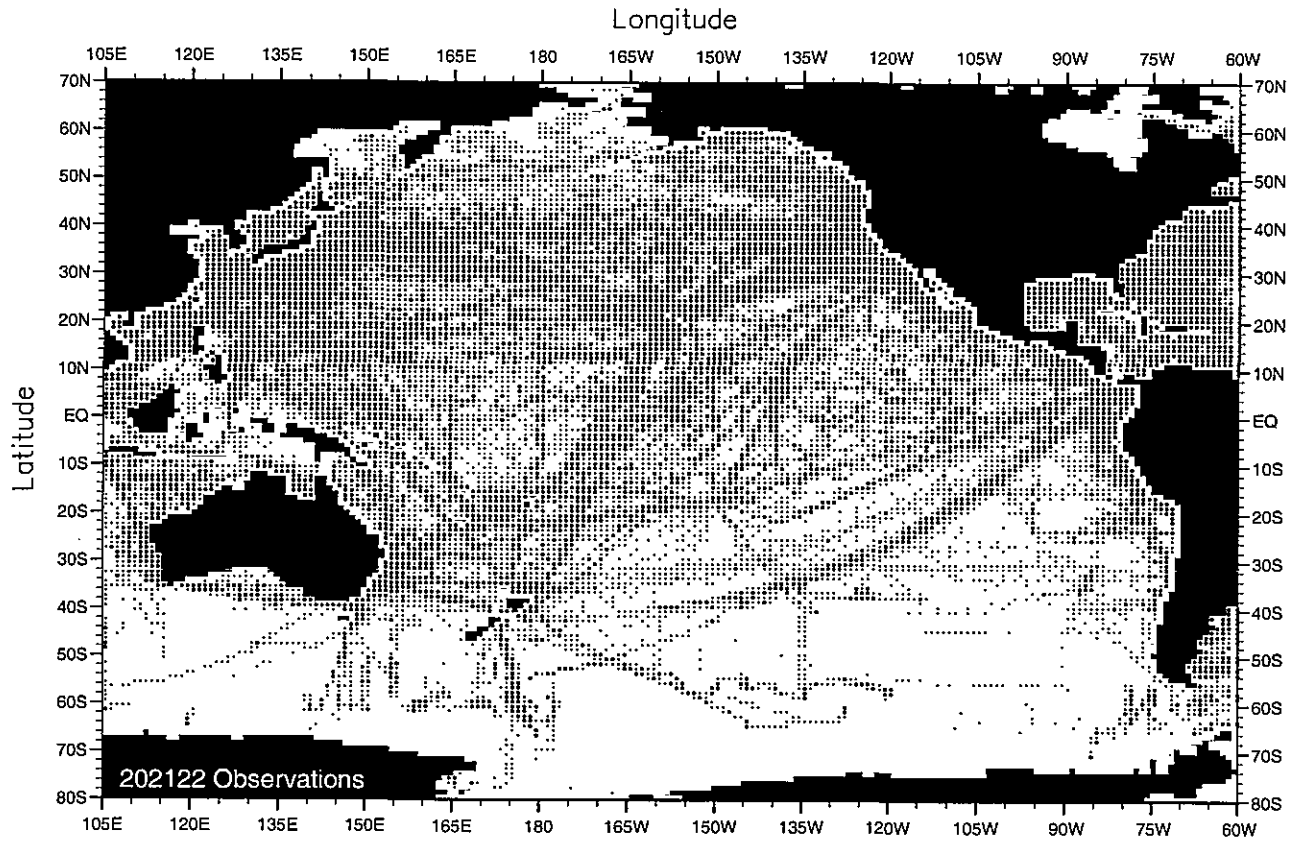


Fig. C21. November temperature observations at the surface .

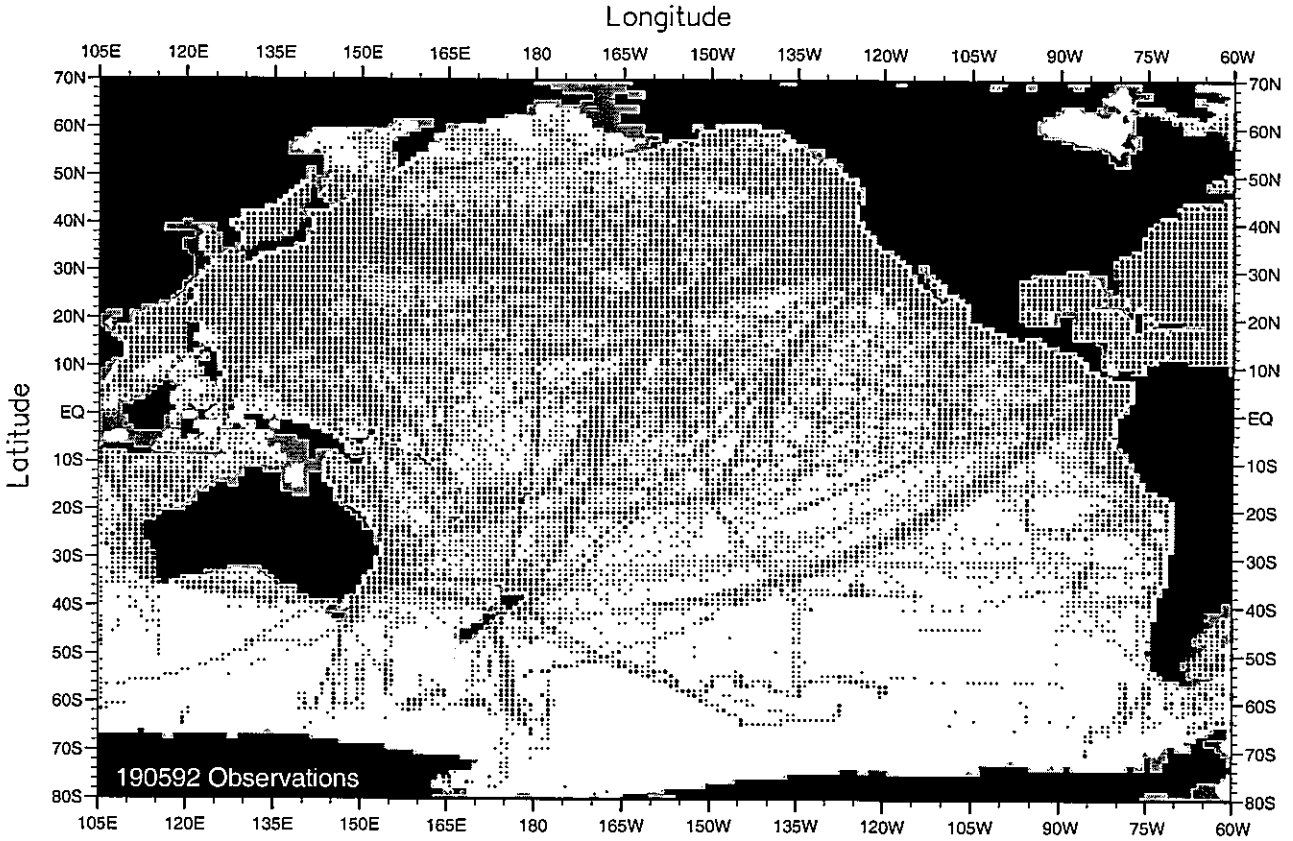


Fig. C22. November temperature observations at 75 m. depth .

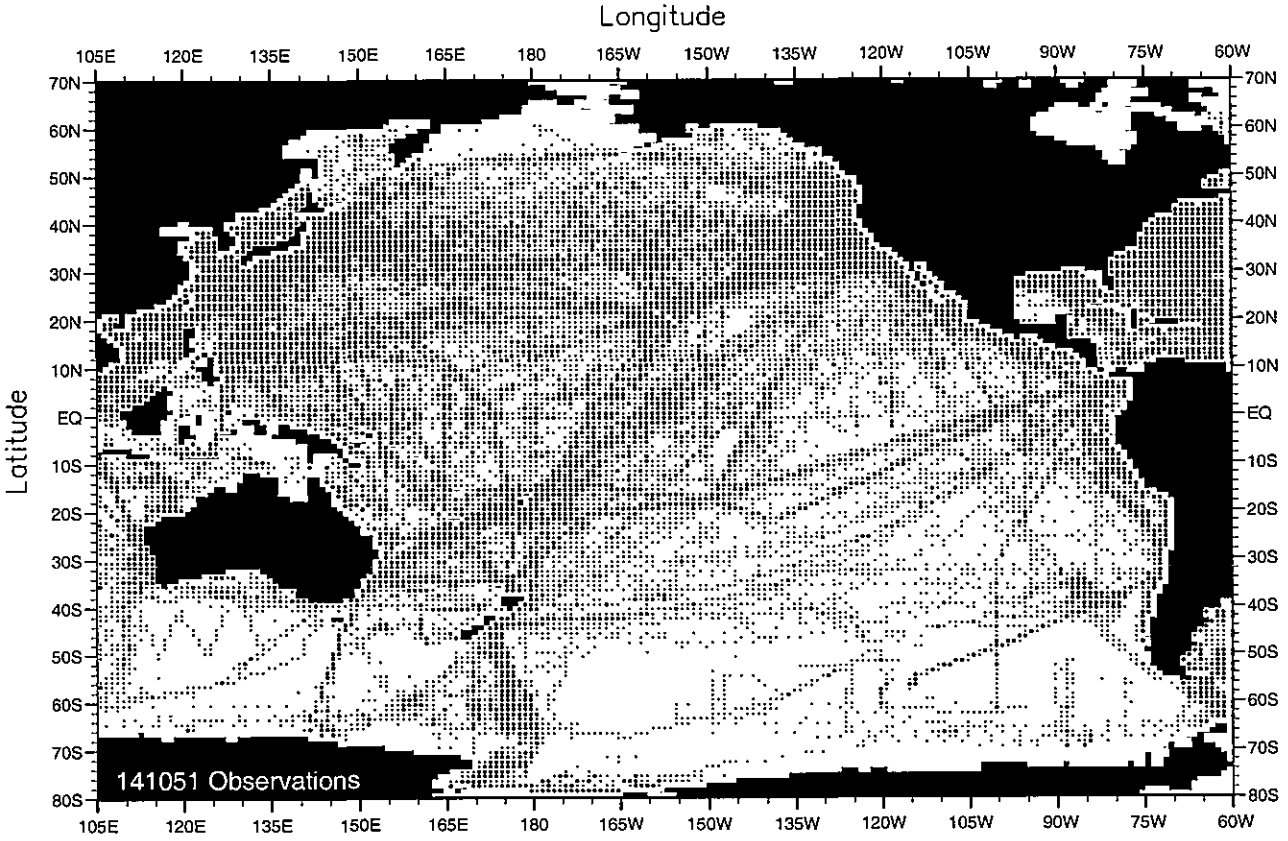


Fig. C23. December temperature observations at the surface .

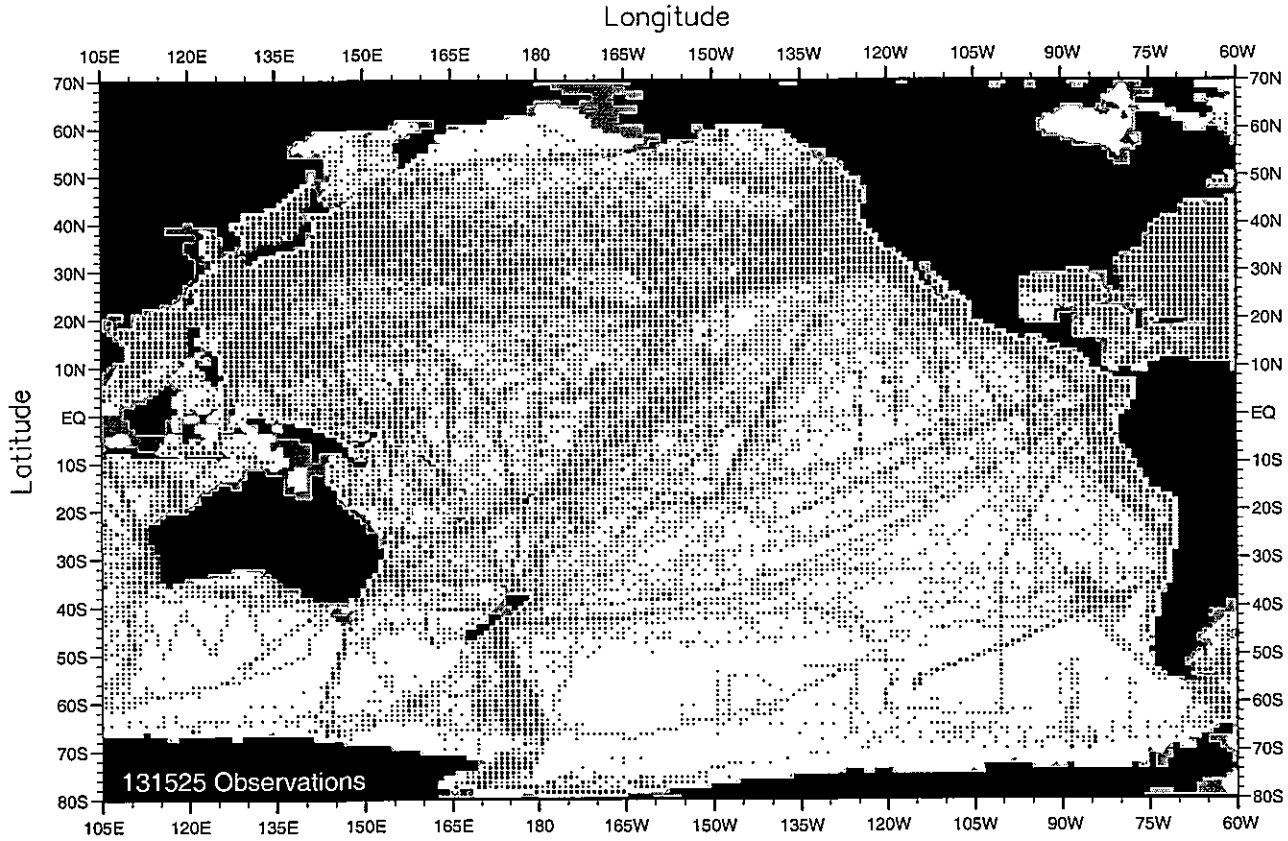


Fig. C24. December temperature observations at 75 m. depth .

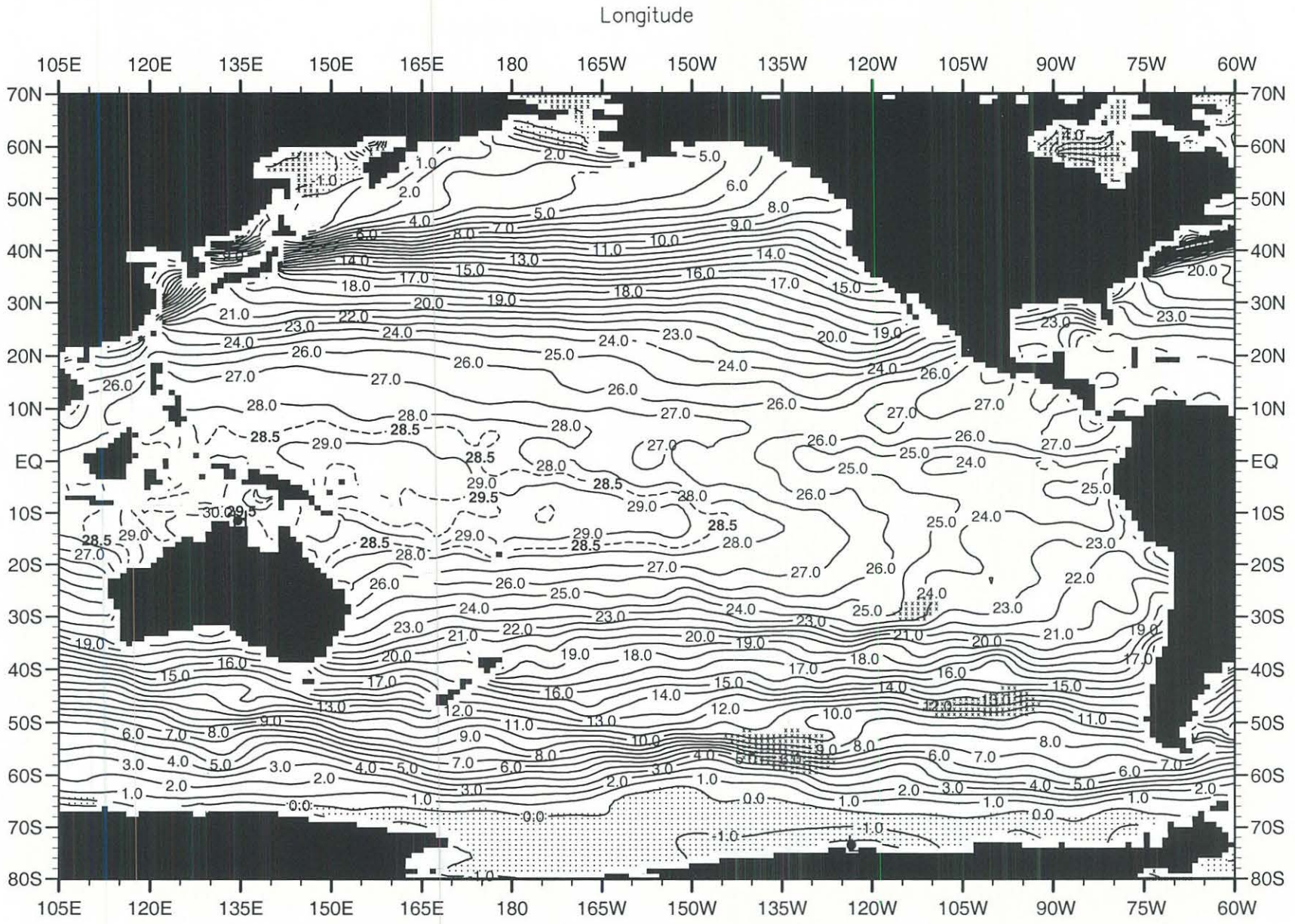


Fig. C25. January mean temperature (°C) at the surface .

Minimum Value= -2.10 Maximum Value= 30.59 Contour Interval: 1.00

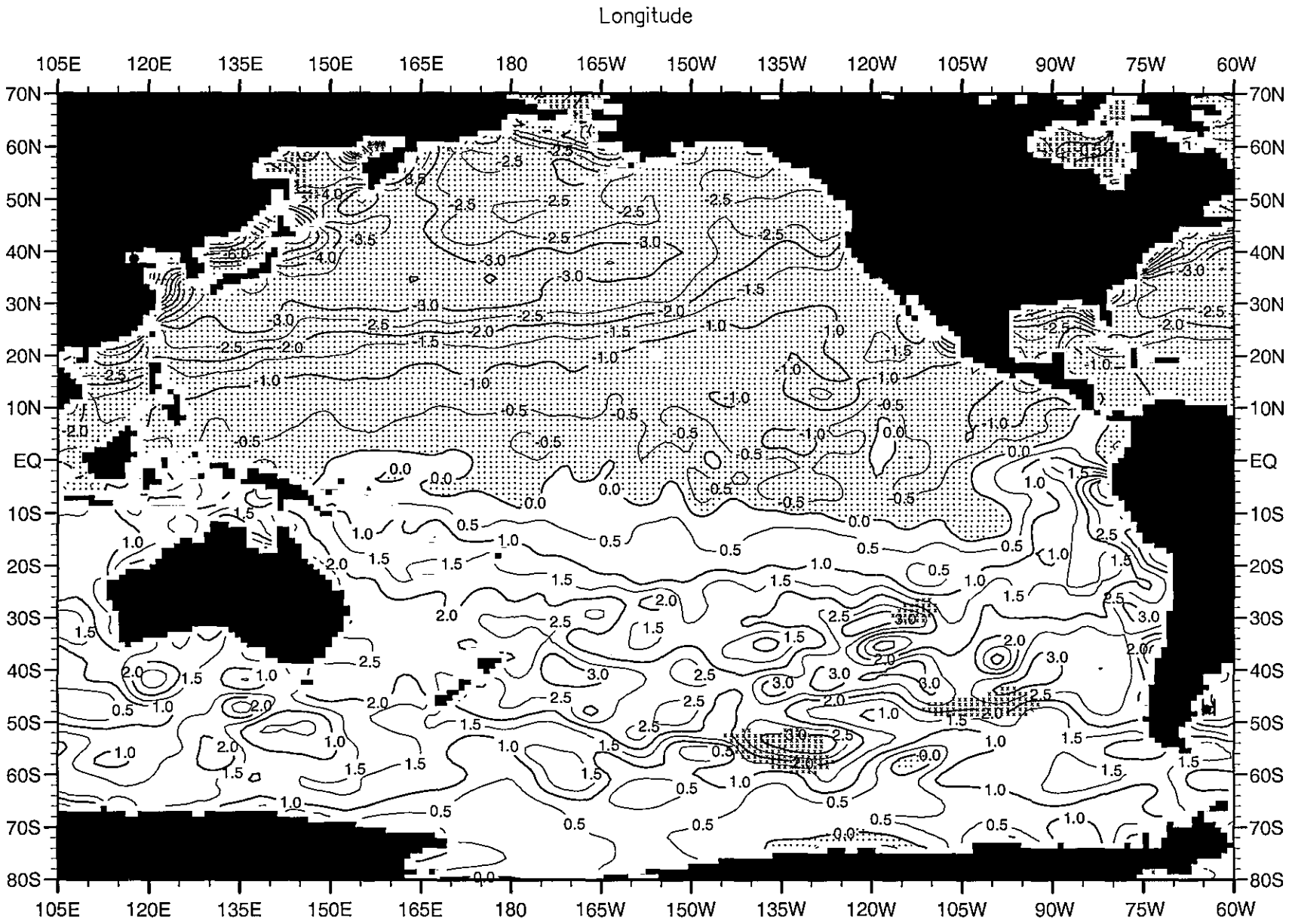


Fig. C26. January minus annual temperature (°C) at the surface .

Minimum Value= -8.74 Maximum Value= 4.20 Contour Interval: 0.50

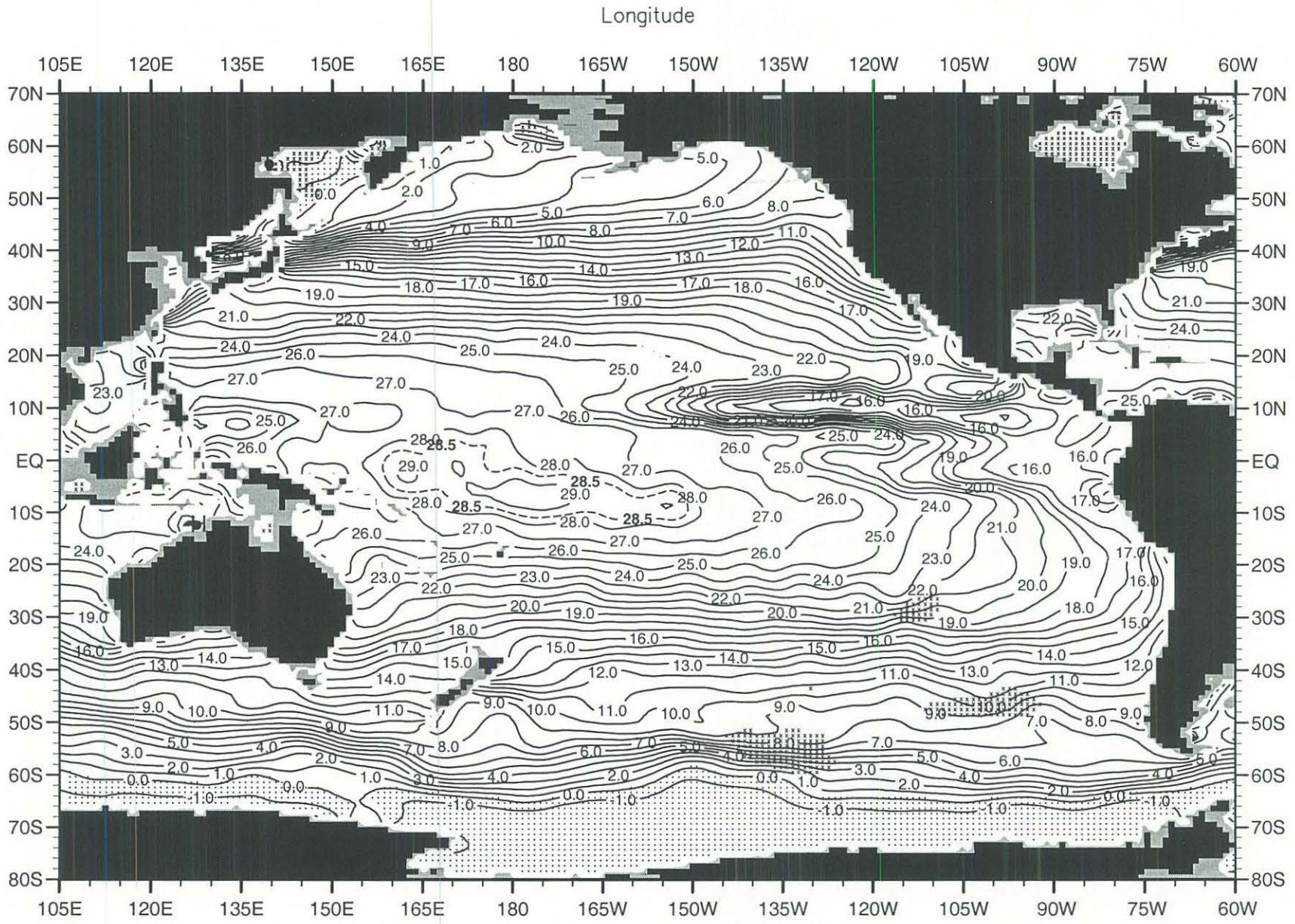


Fig. C27. January mean temperature (°C) at 75 m. depth .

Minimum Value= -2.10 Maximum Value= 29.68 Contour Interval: 1.00

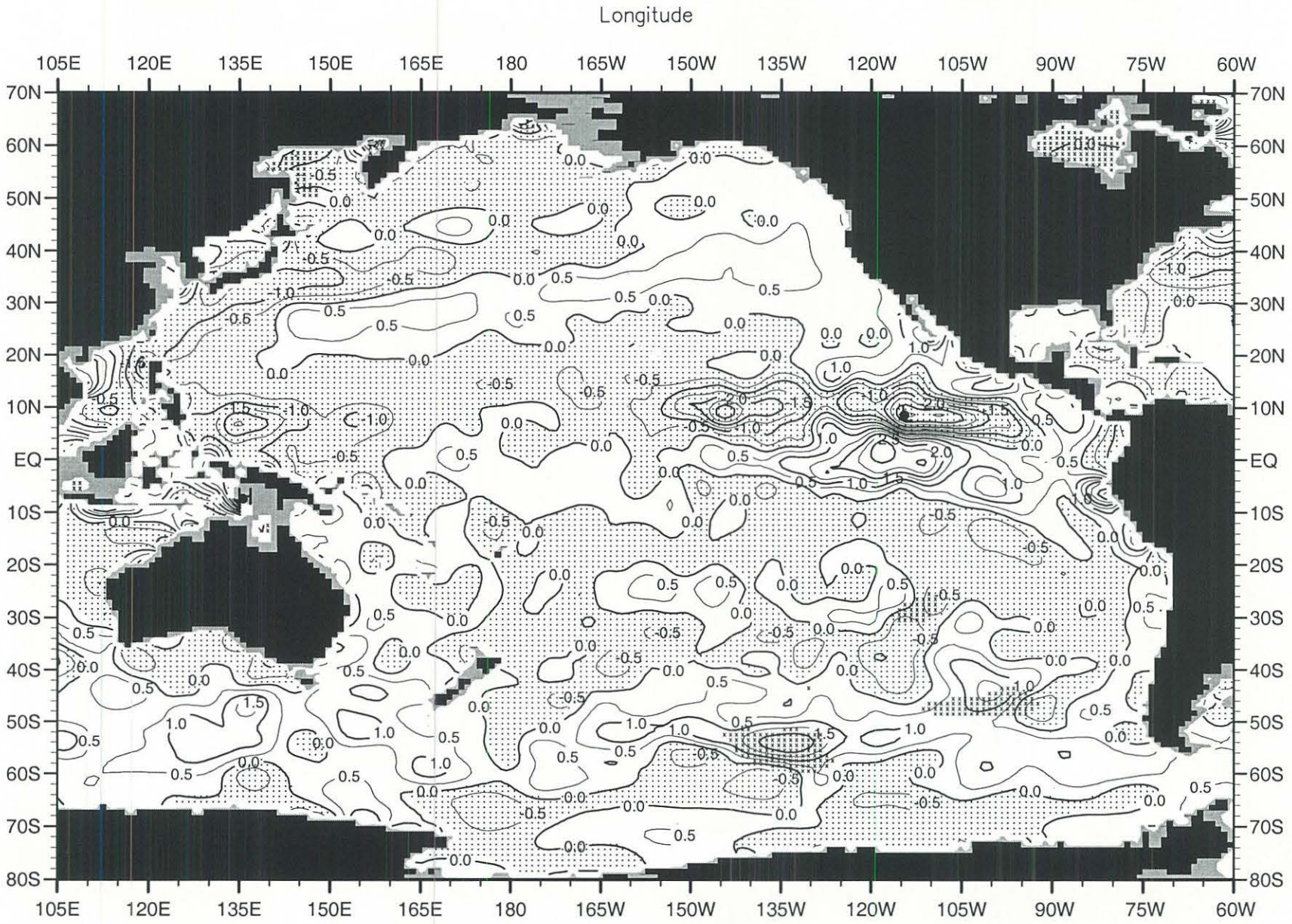


Fig. C28. January minus annual temperature (°C) at 75 m. depth .

Minimum Value= -3.59 Maximum Value= 4.32 Contour Interval: 0.50

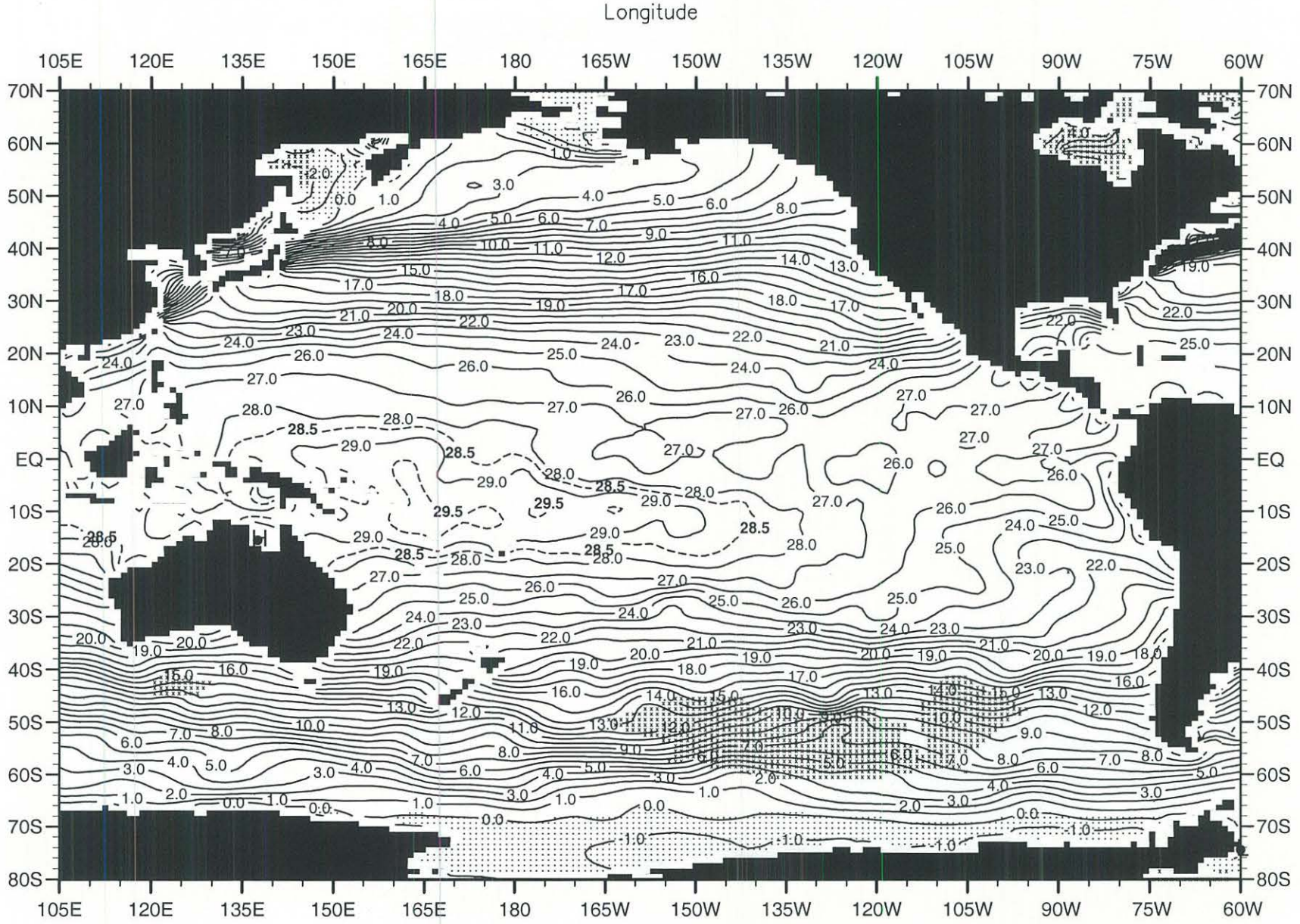


Fig. C29. February mean temperature (°C) at the surface .

Minimum Value= -2.10 Maximum Value= 30.98 Contour Interval: 1.00

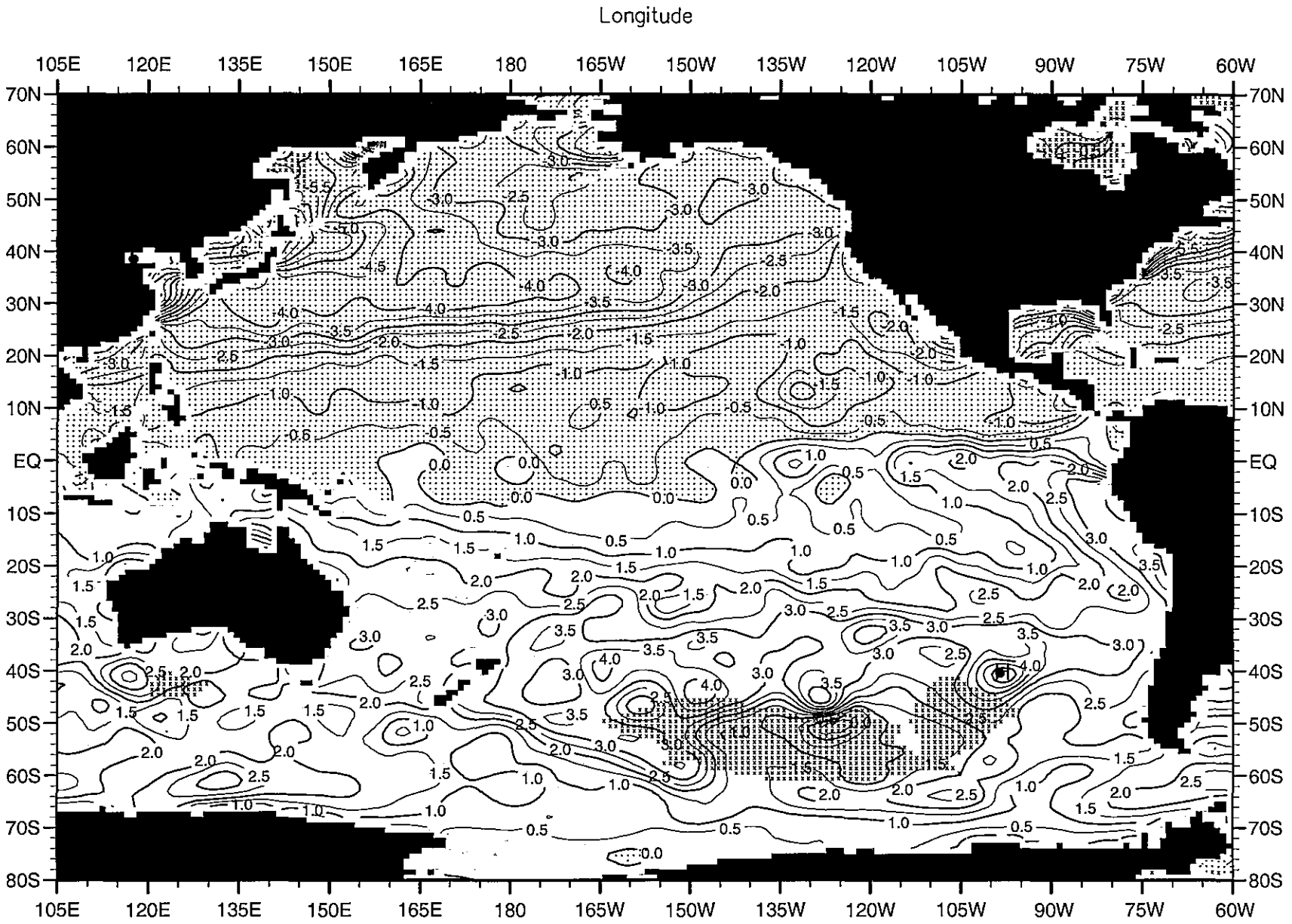


Fig. C30. February minus annual temperature (°C) at the surface .

Minimum Value= -9.45 Maximum Value= 5.43 Contour Interval: 0.50

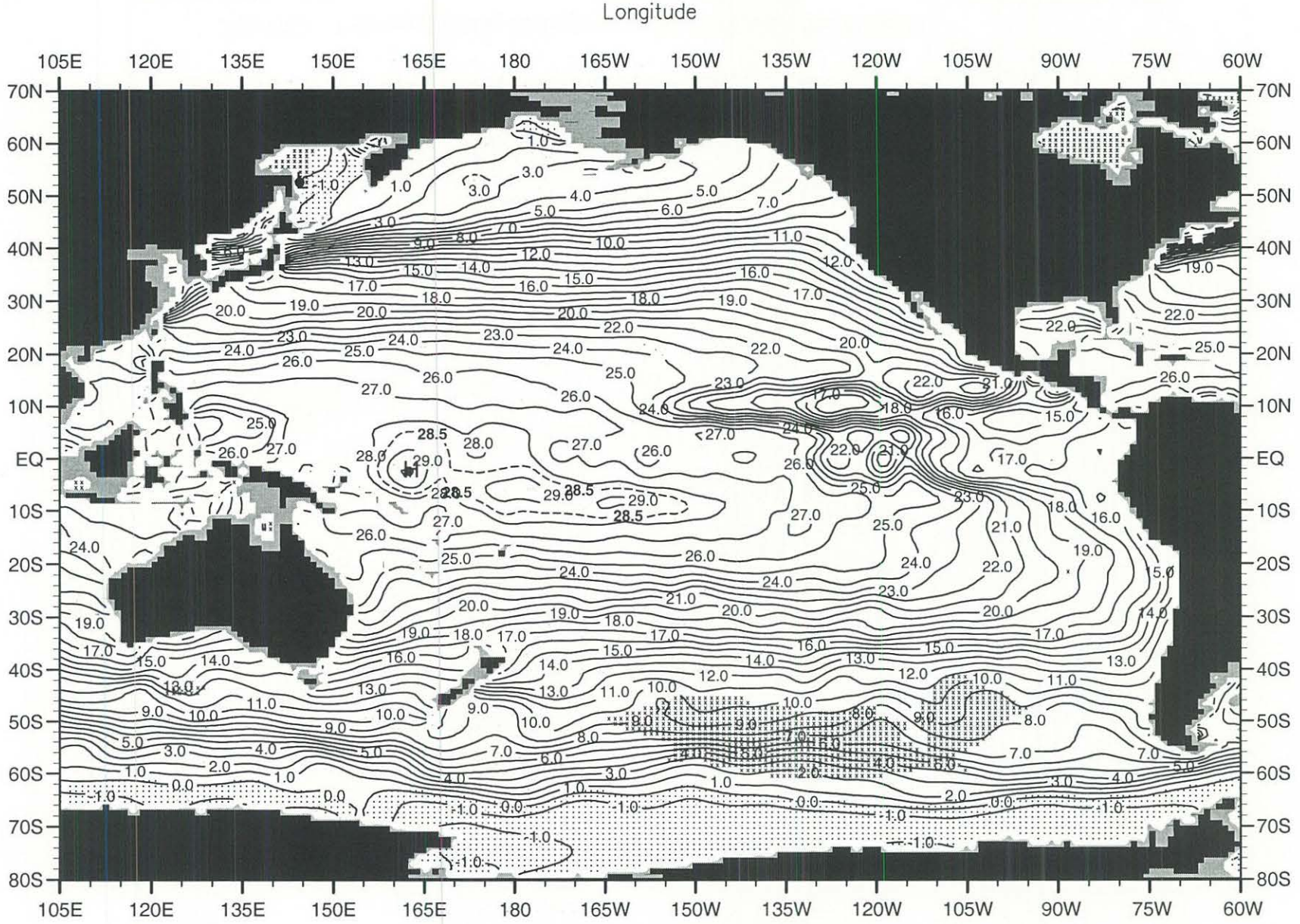


Fig. C31. February mean temperature (°C) at 75 m. depth .

Minimum Value= -2.10 Maximum Value= 29.54 Contour Interval: 1.00

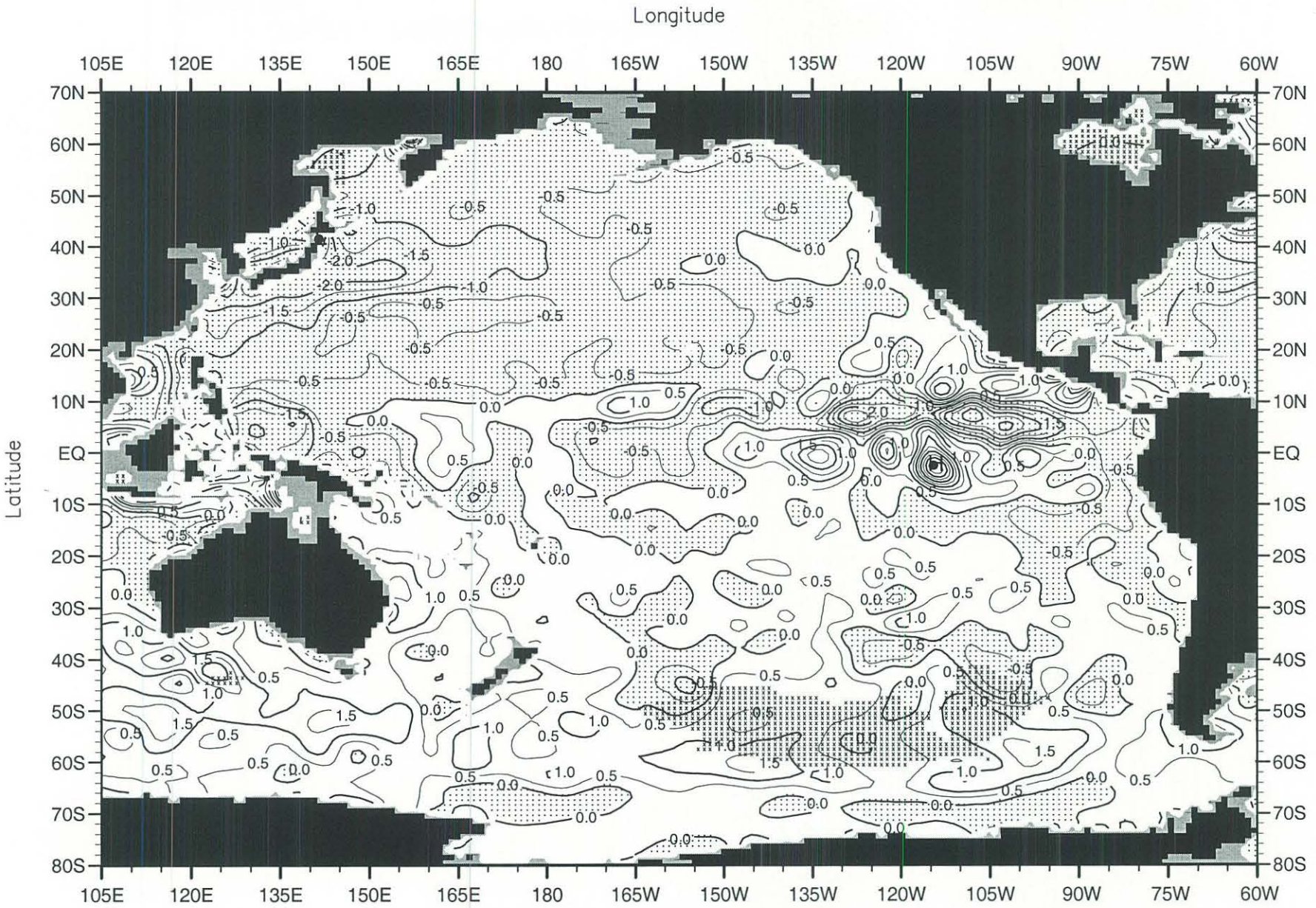


Fig. C32. February minus annual temperature (°C) at 75 m. depth .

Minimum Value= -4.15 Maximum Value= 4.94 Contour Interval: 0.50

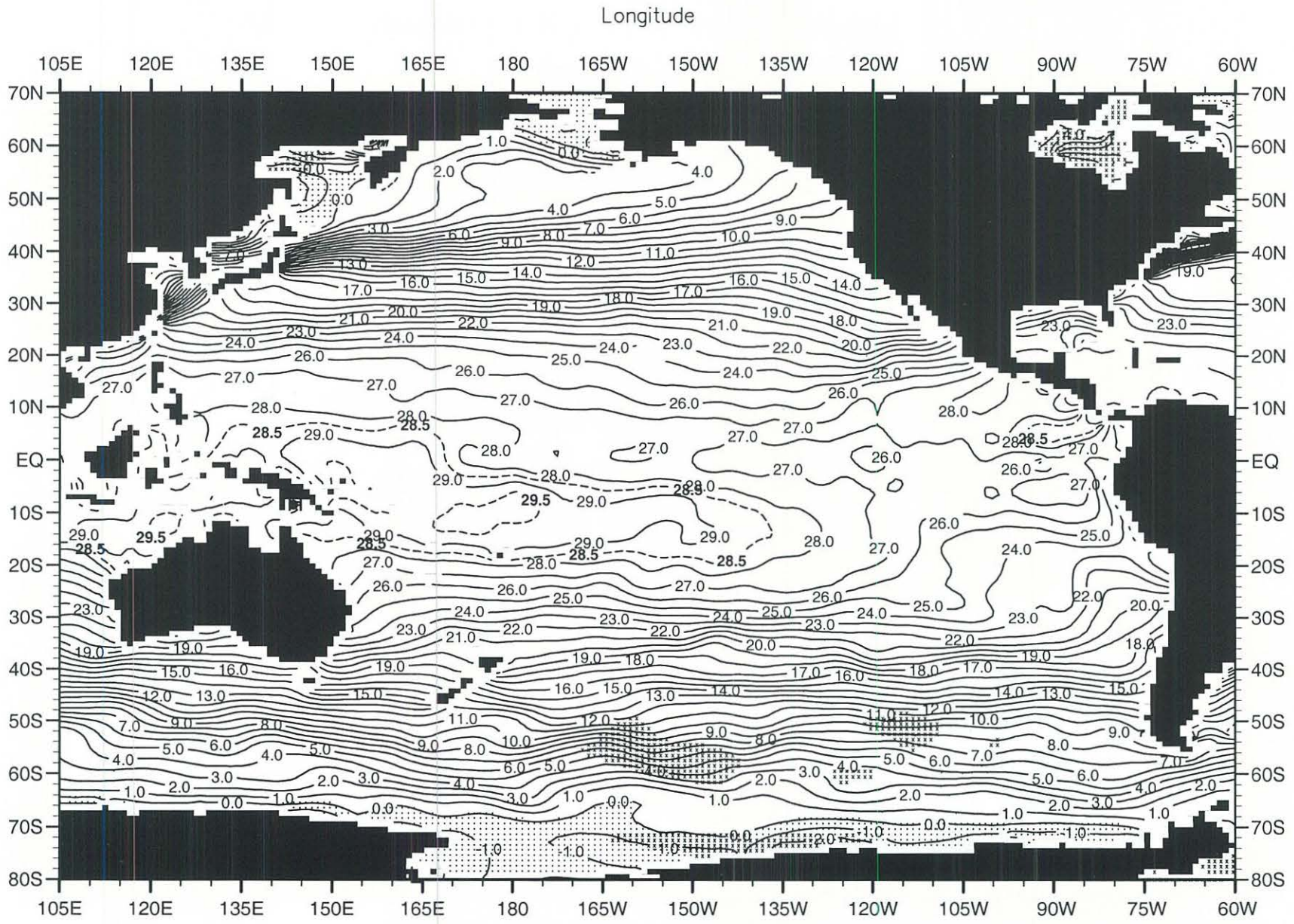


Fig. C33. March mean temperature (°C) at the surface .

Minimum Value= -2.10 Maximum Value= 29.81 Contour Interval: 1.00

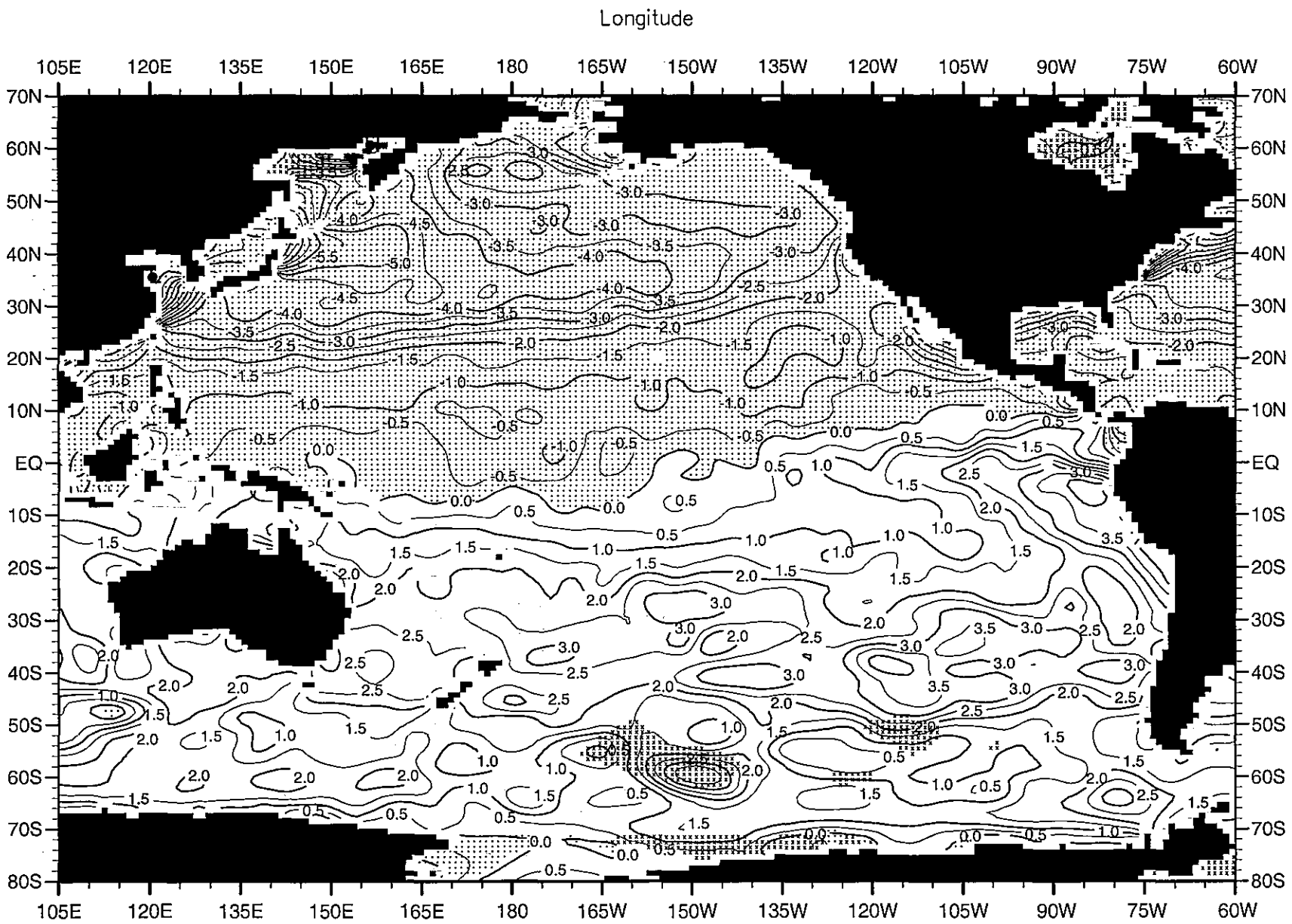


Fig. C34. March minus annual temperature (°C) at the surface .

Minimum Value= -9.88 Maximum Value= 5.96 Contour Interval: 0.50

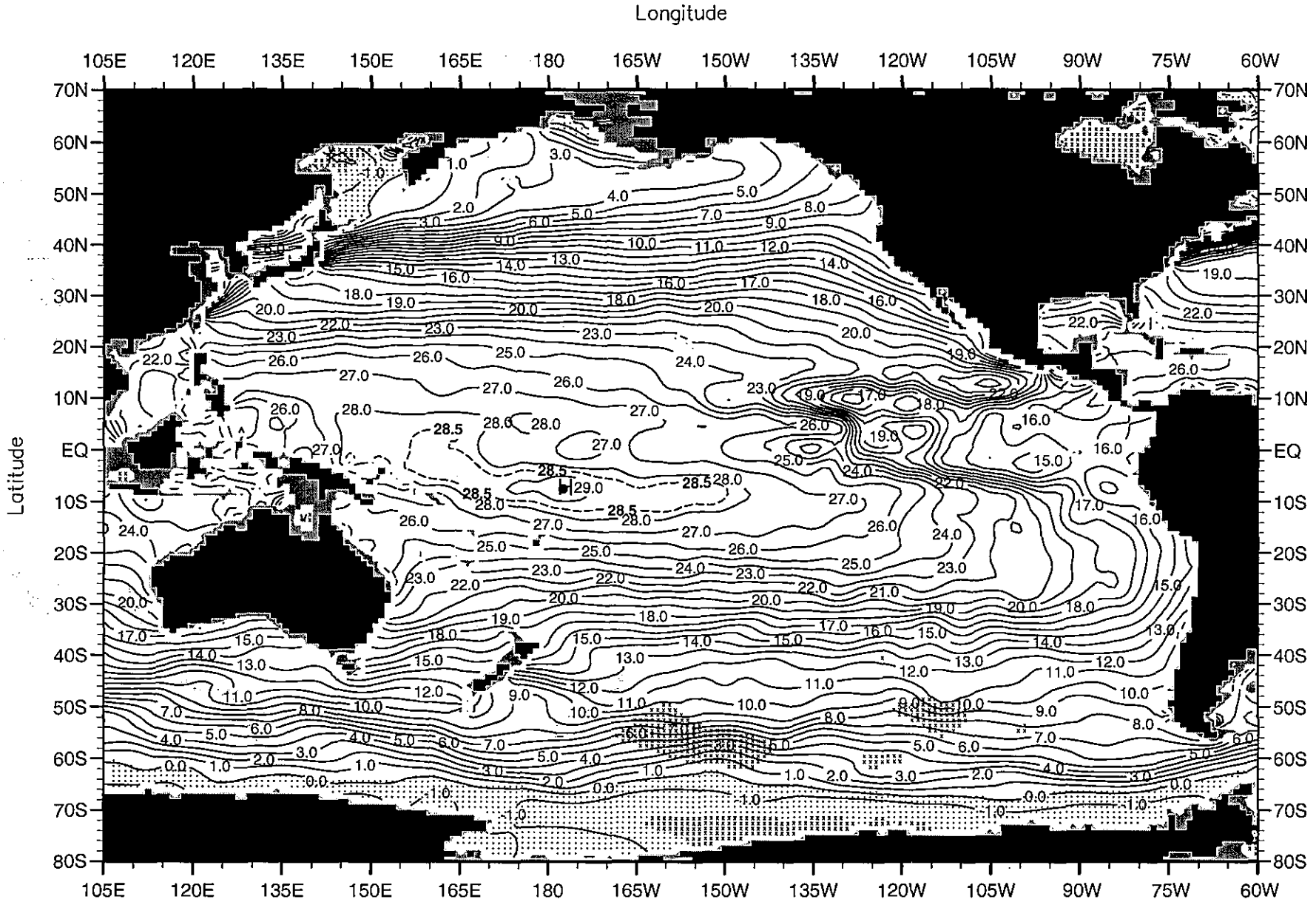


Fig. C35. March mean temperature (°C) at 75 m. depth .

Minimum Value= -2.10 Maximum Value= 29.43 Contour Interval: 1.00

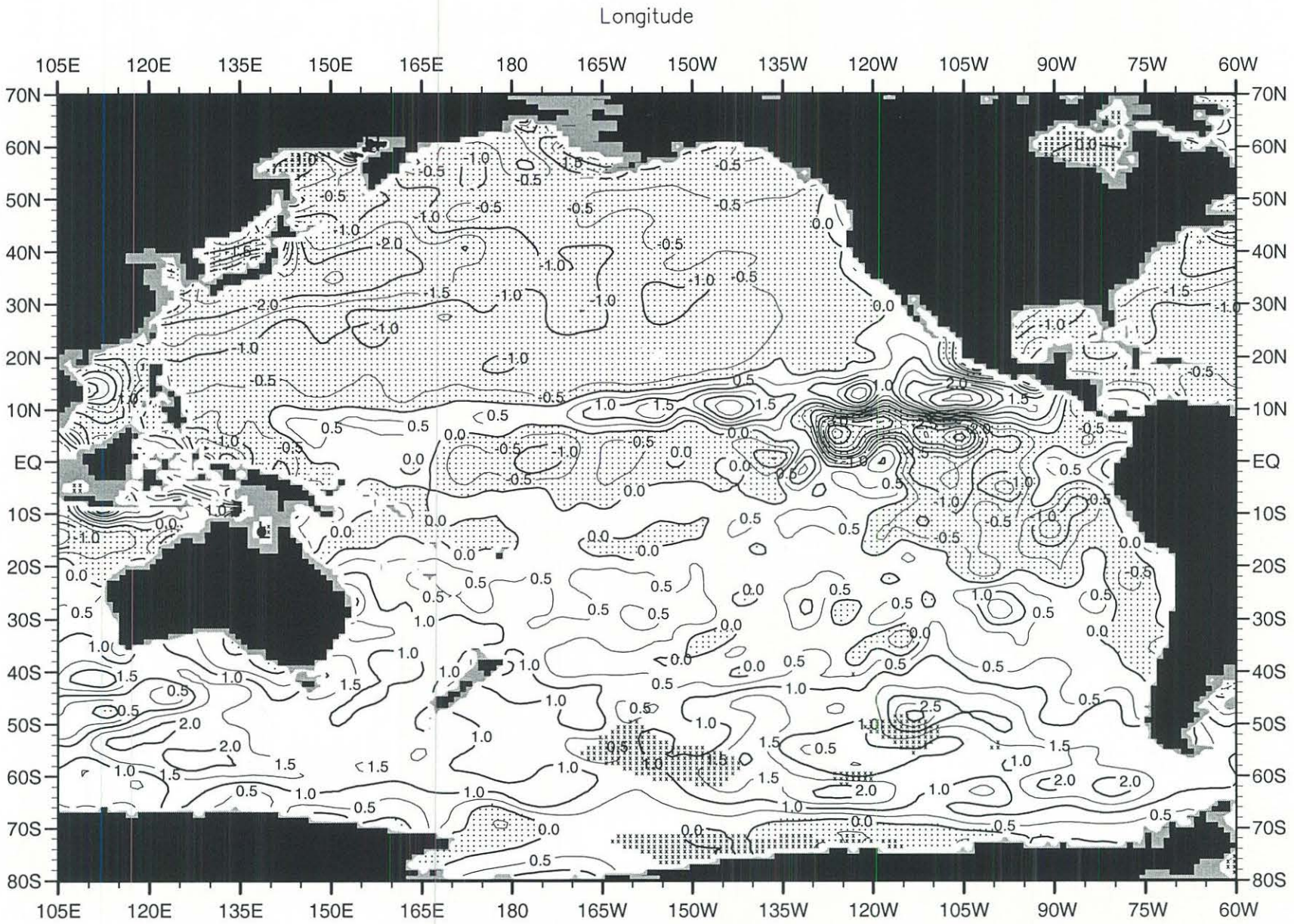


Fig. C36. March minus annual temperature (°C) at 75 m. depth .

Minimum Value= -6.27 Maximum Value= 7.99 Contour Interval: 0.50

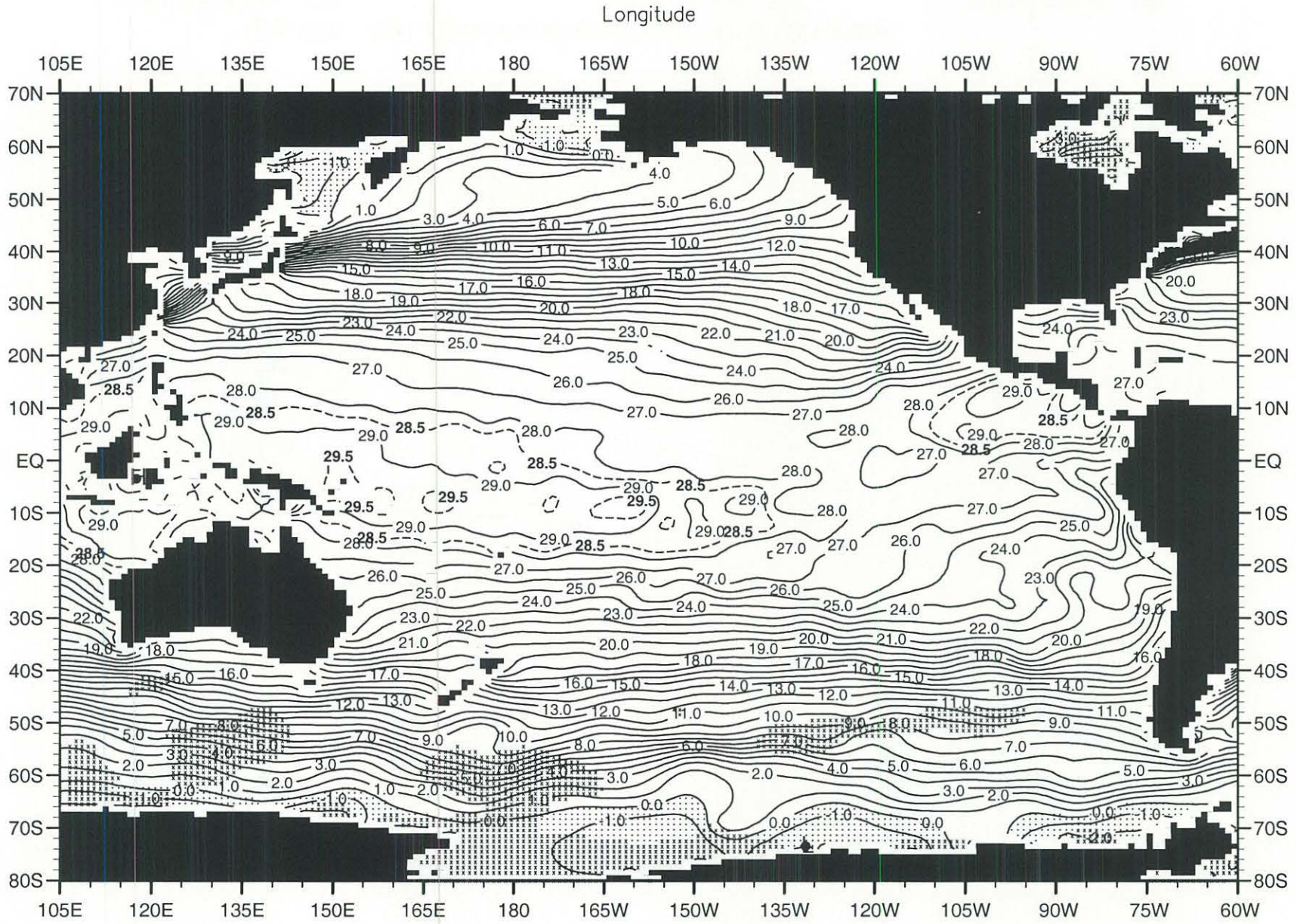


Fig. C37. April mean temperature (°C) at the surface .

Minimum Value= -2.10 Maximum Value= 30.73 Contour Interval: 1.00

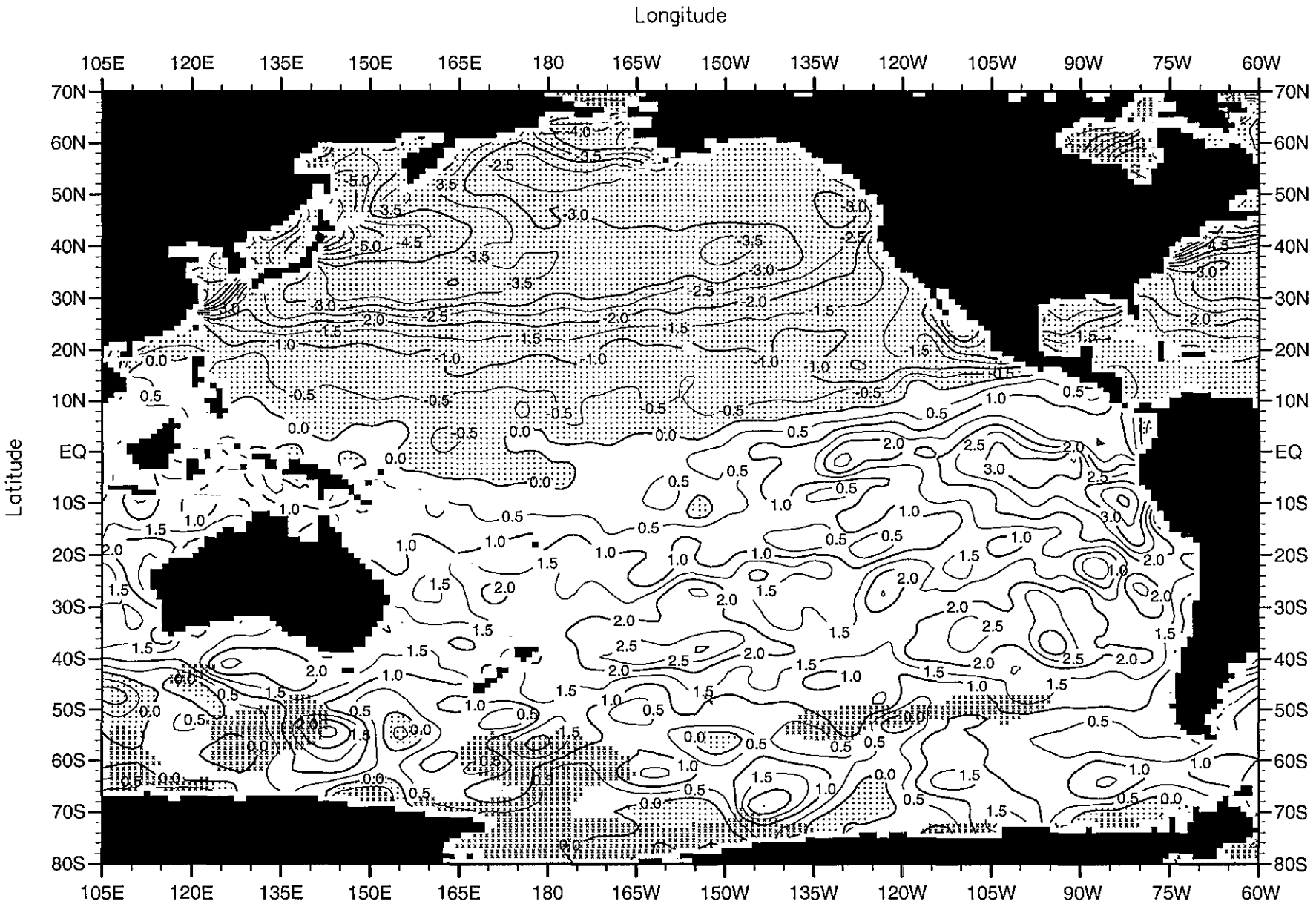


Fig. C38. April minus annual temperature (°C) at the surface .

Minimum Value= -7.36 Maximum Value= 5.26 Contour Interval: 0.50

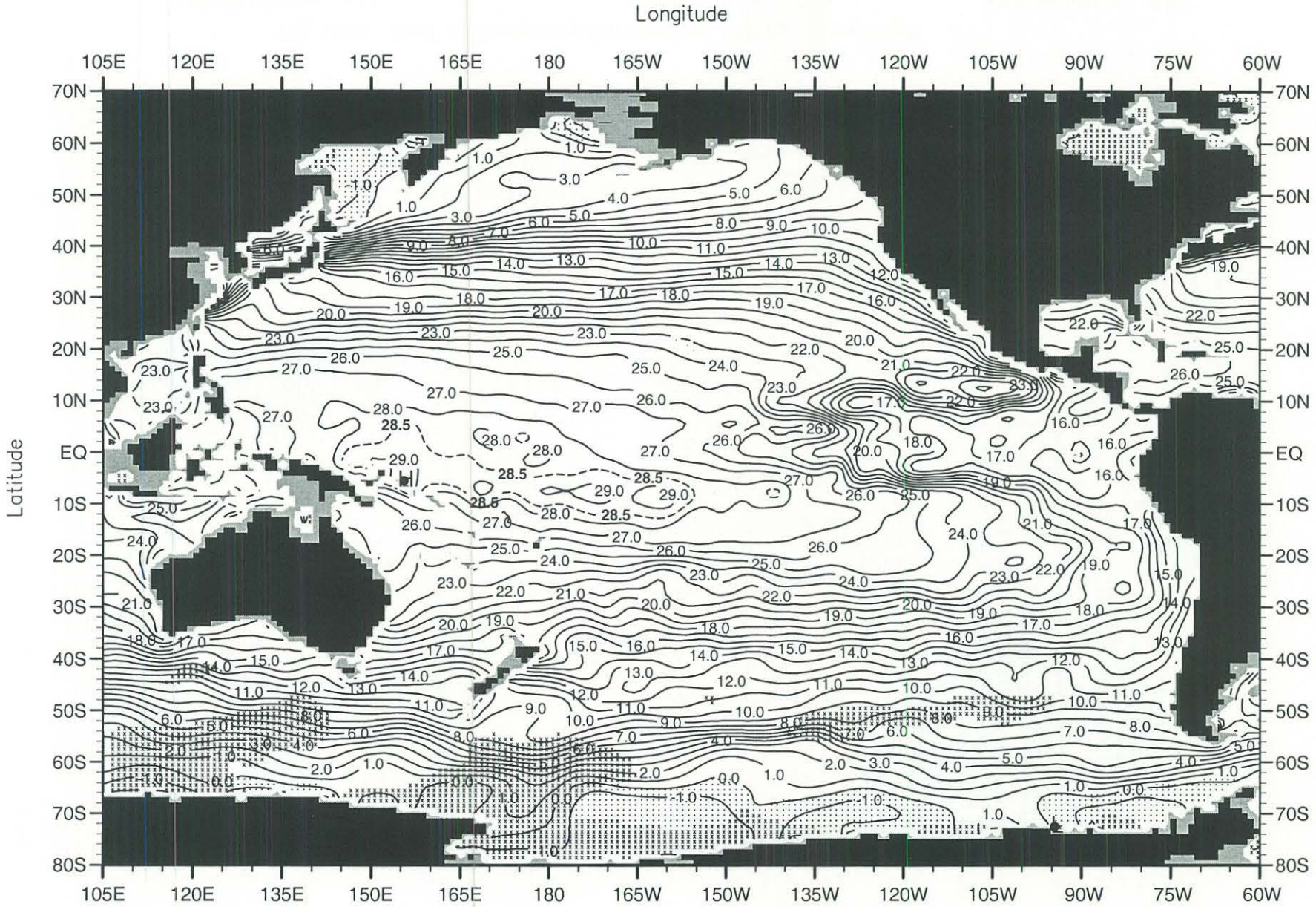


Fig. C39. April mean temperature (°C) at 75 m. depth .

Minimum Value= -2.10 Maximum Value= 29.53 Contour Interval: 1.00

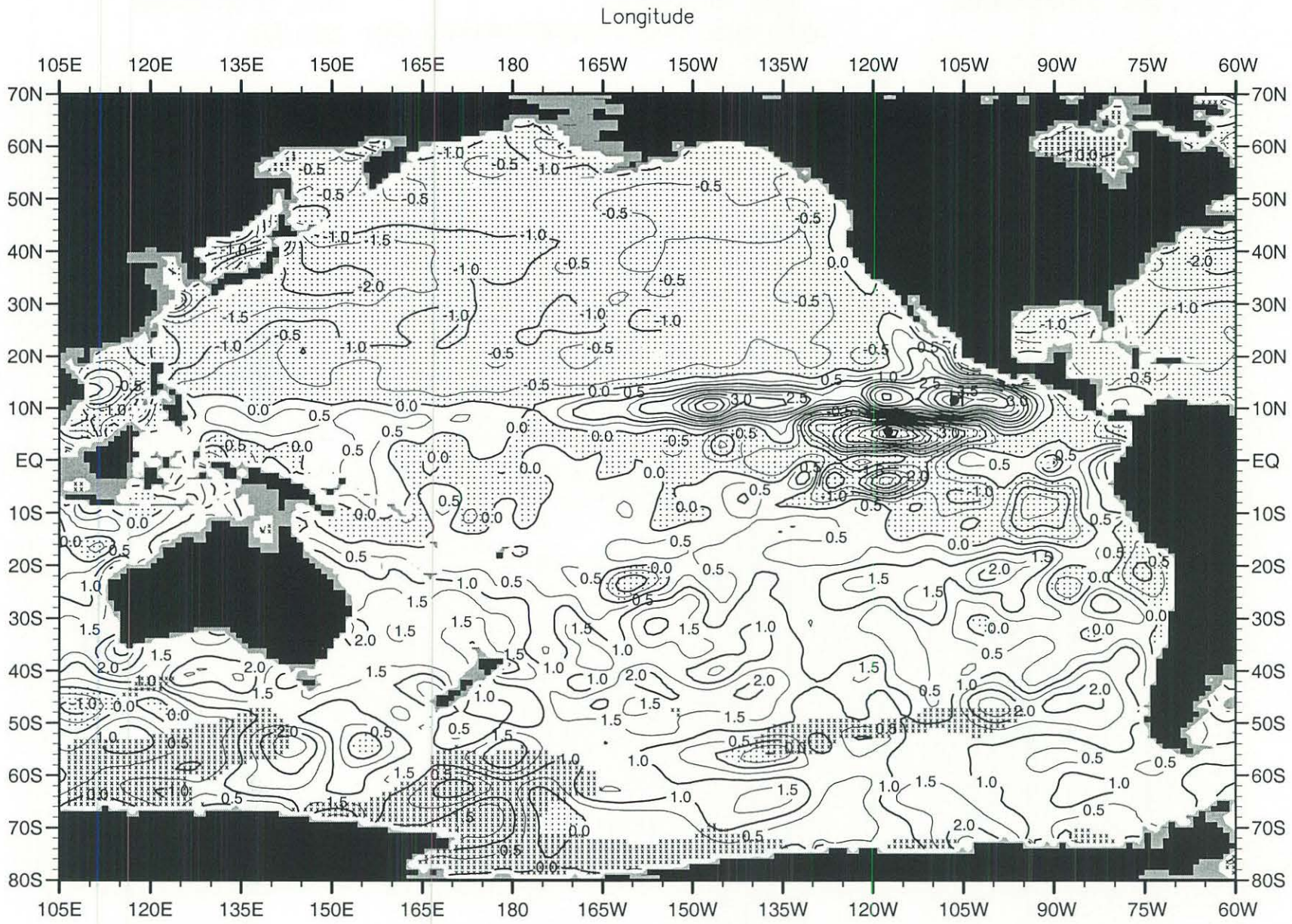


Fig. C40. April minus annual temperature (°C) at 75 m. depth .

Minimum Value= -6.17 Maximum Value= 4.89 Contour Interval: 0.50

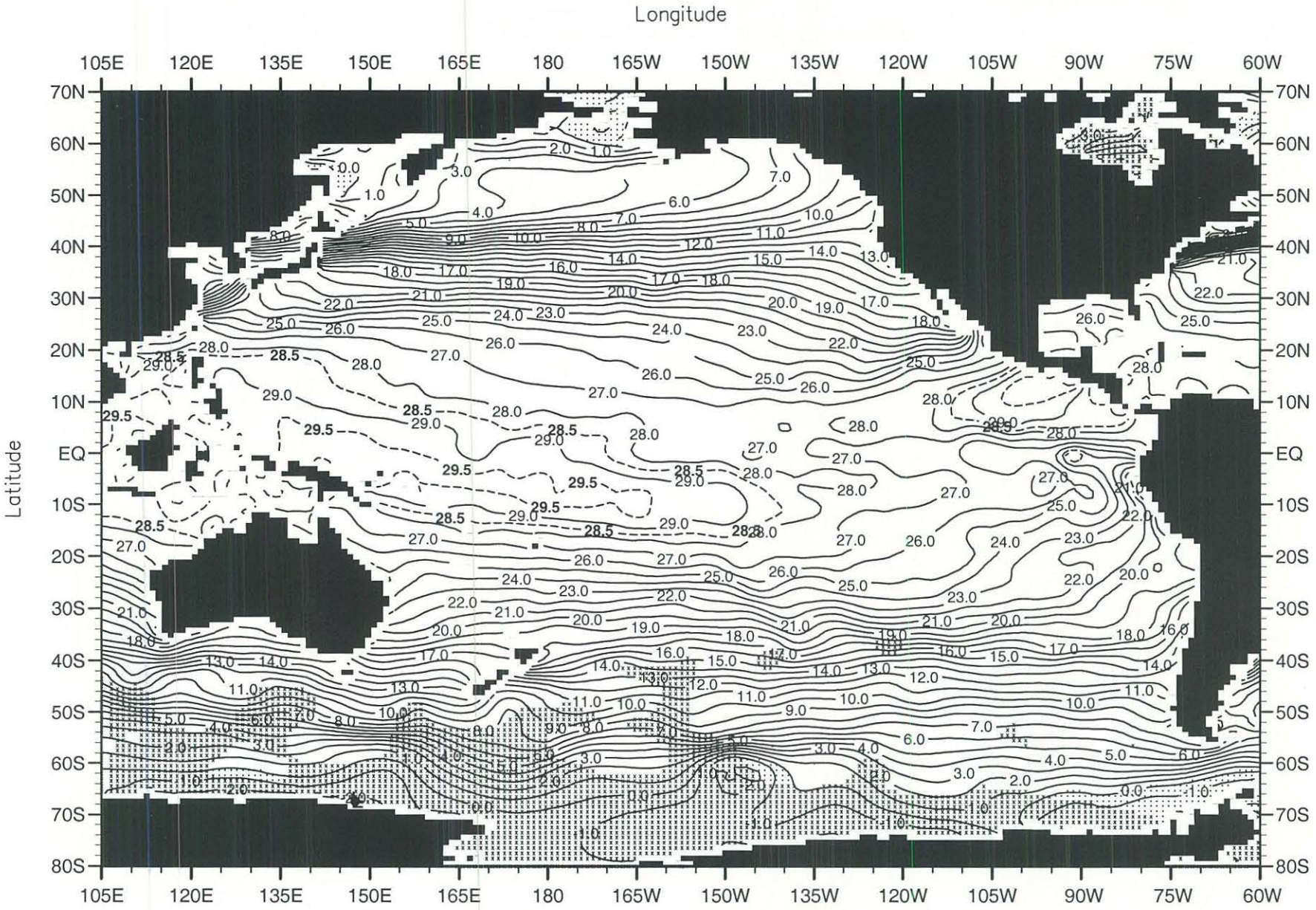


Fig. C41. May mean temperature (°C) at the surface .

Minimum Value= -2.10 Maximum Value= 30.44 Contour Interval: 1.00

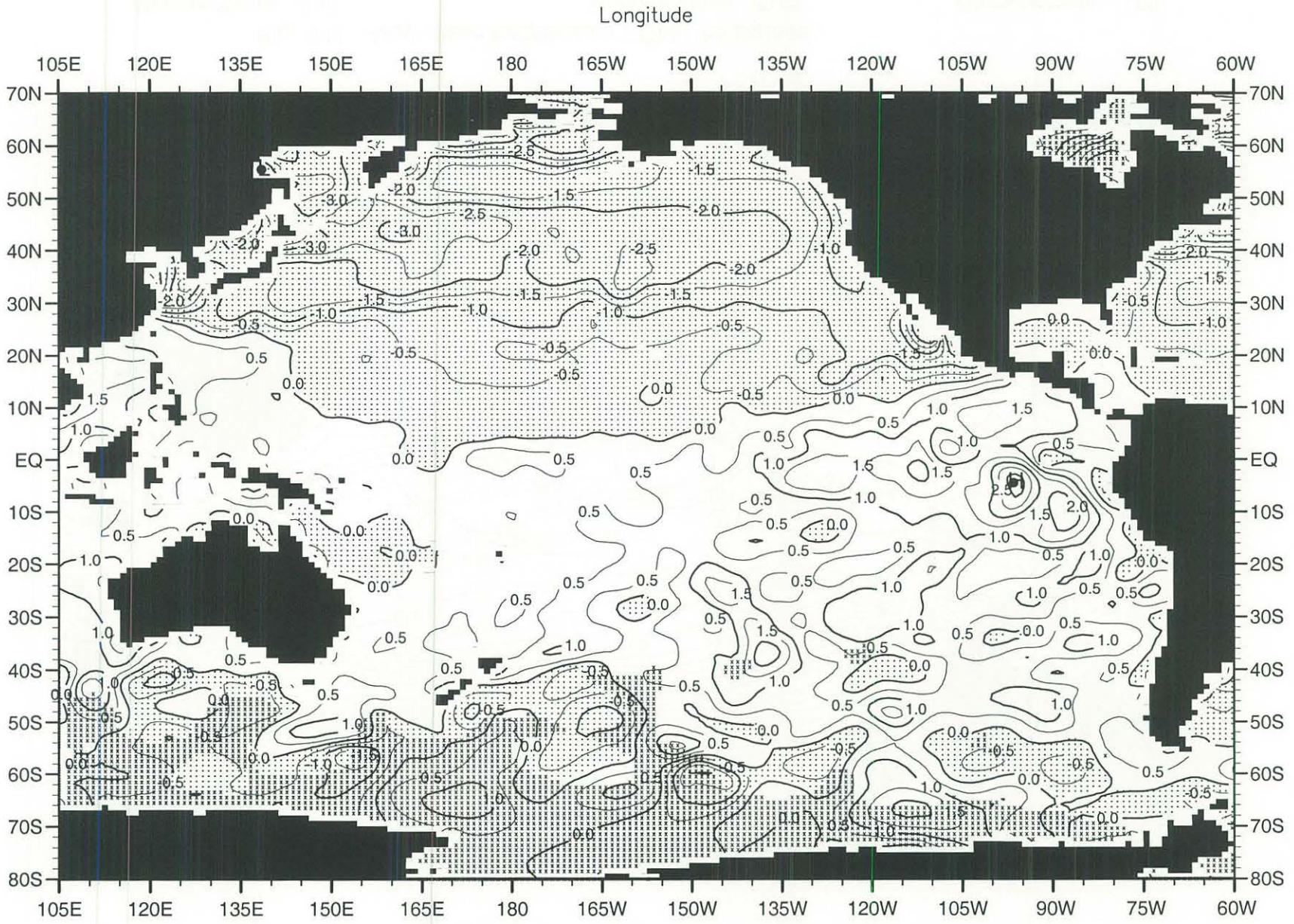


Fig. C42. May minus annual temperature (°C) at the surface .

Minimum Value= -4.82 Maximum Value= 3.27 Contour Interval: 0.50

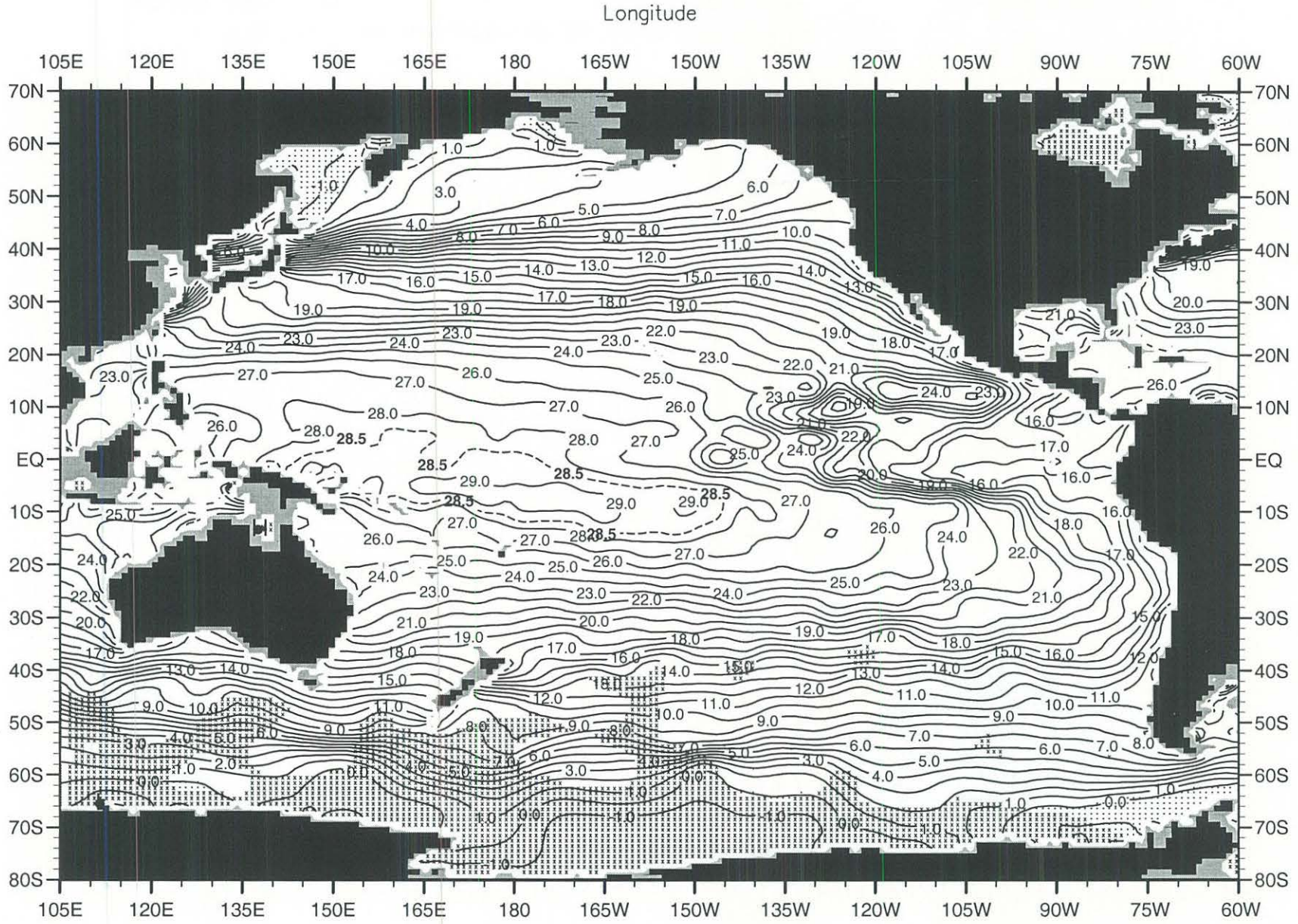


Fig. C43. May mean temperature (°C) at 75 m. depth .

Minimum Value= -2.10 Maximum Value= 30.27 Contour Interval: 1.00

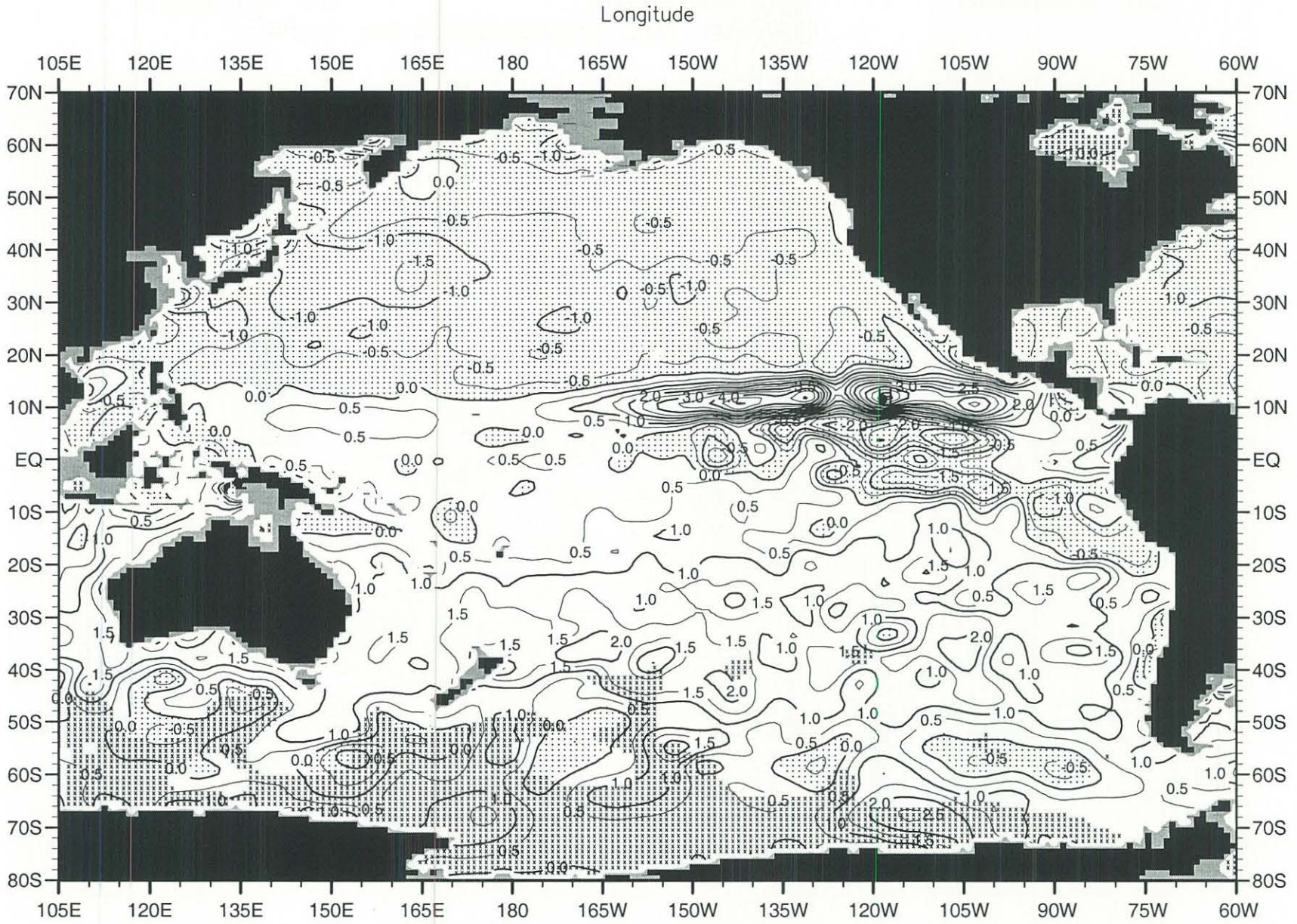


Fig. C44. May minus annual temperature (°C) at 75 m. depth .

Minimum Value= -4.26 Maximum Value= 5.24 Contour Interval: 0.50

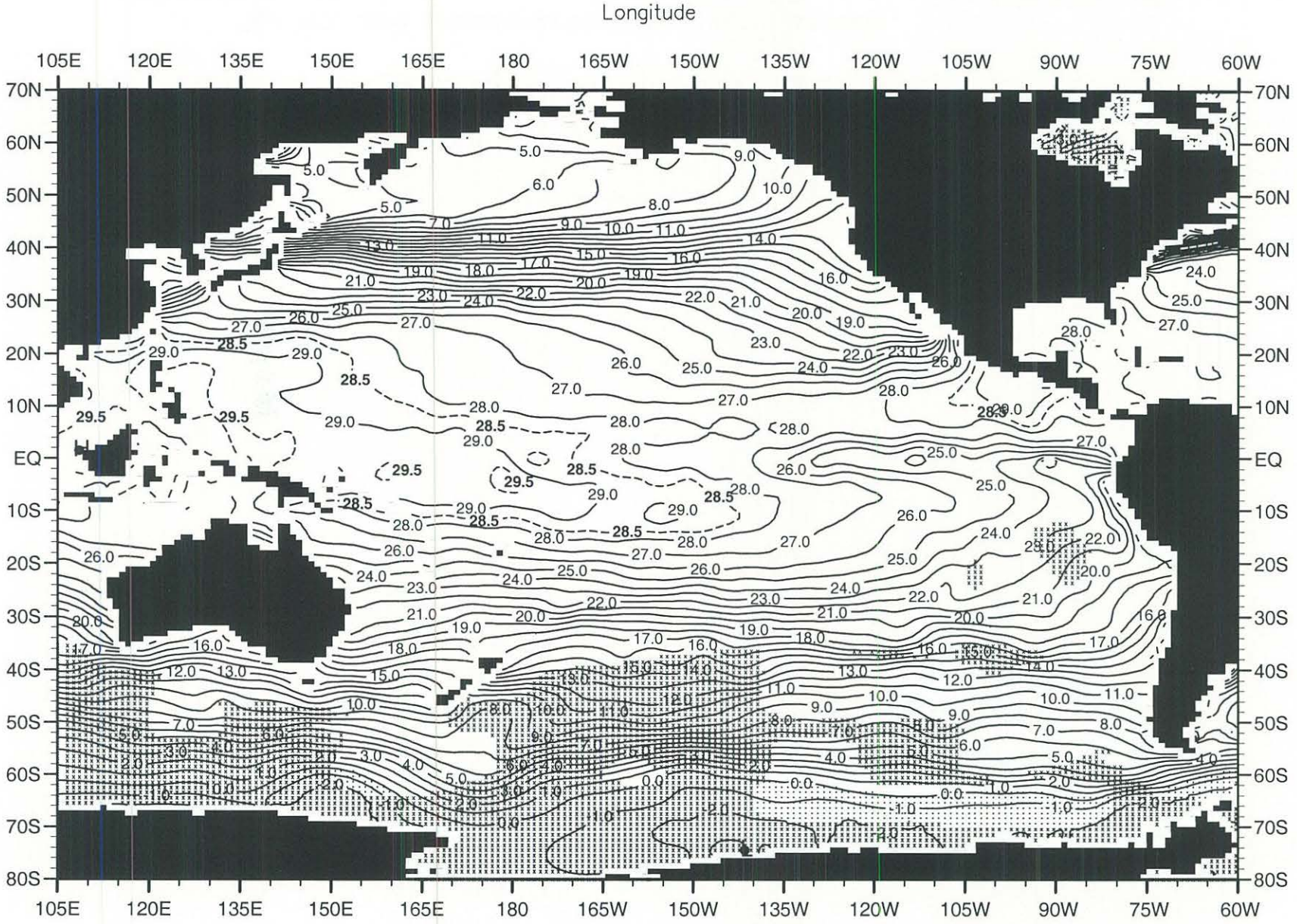


Fig. C45. June mean temperature (°C) at the surface .

Minimum Value= -2.10 Maximum Value= 29.98 Contour Interval: 1.00

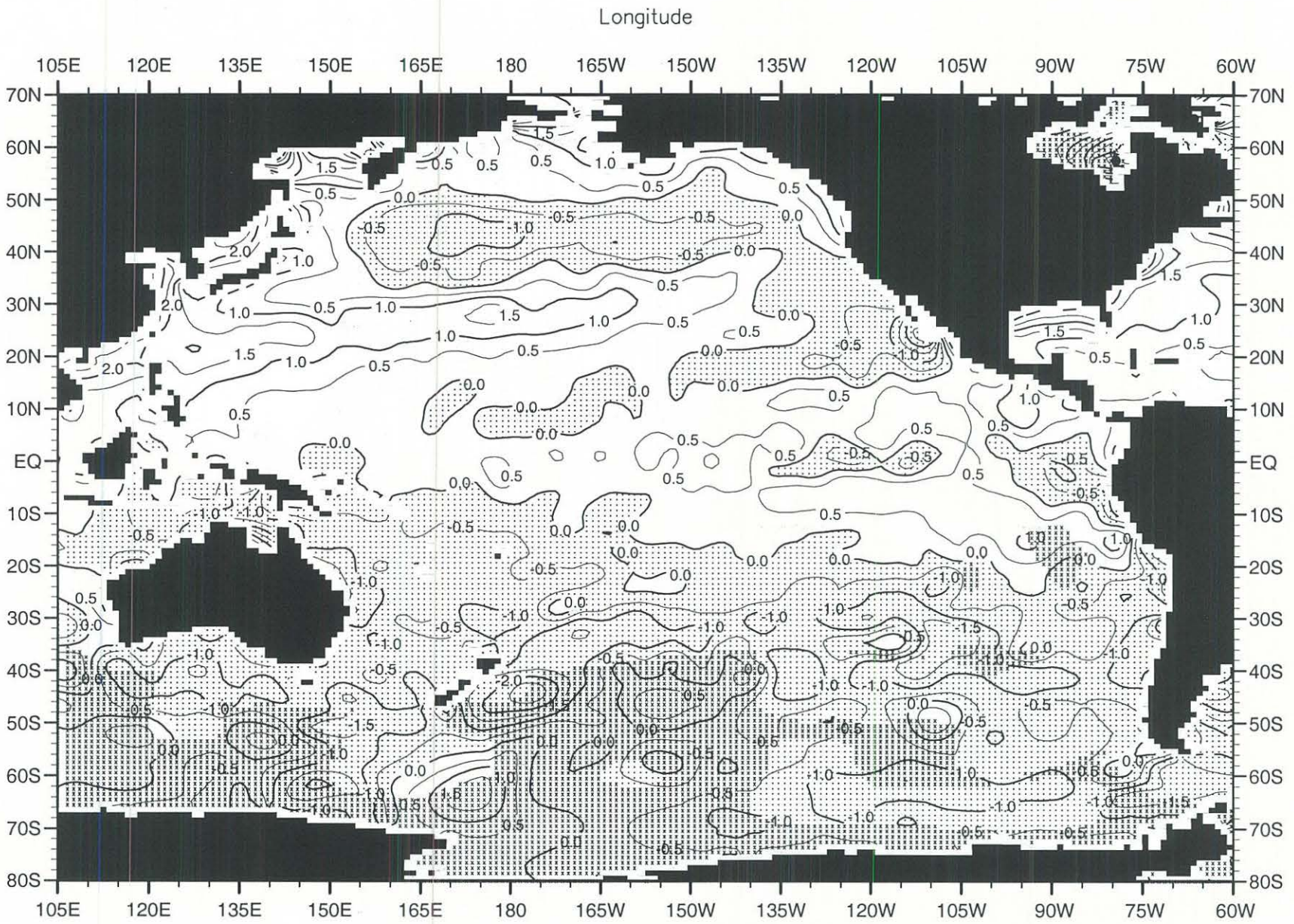


Fig. C46. June minus annual temperature (°C) at the surface .

Minimum Value= -4.22 Maximum Value= 10.49 Contour Interval: 0.50

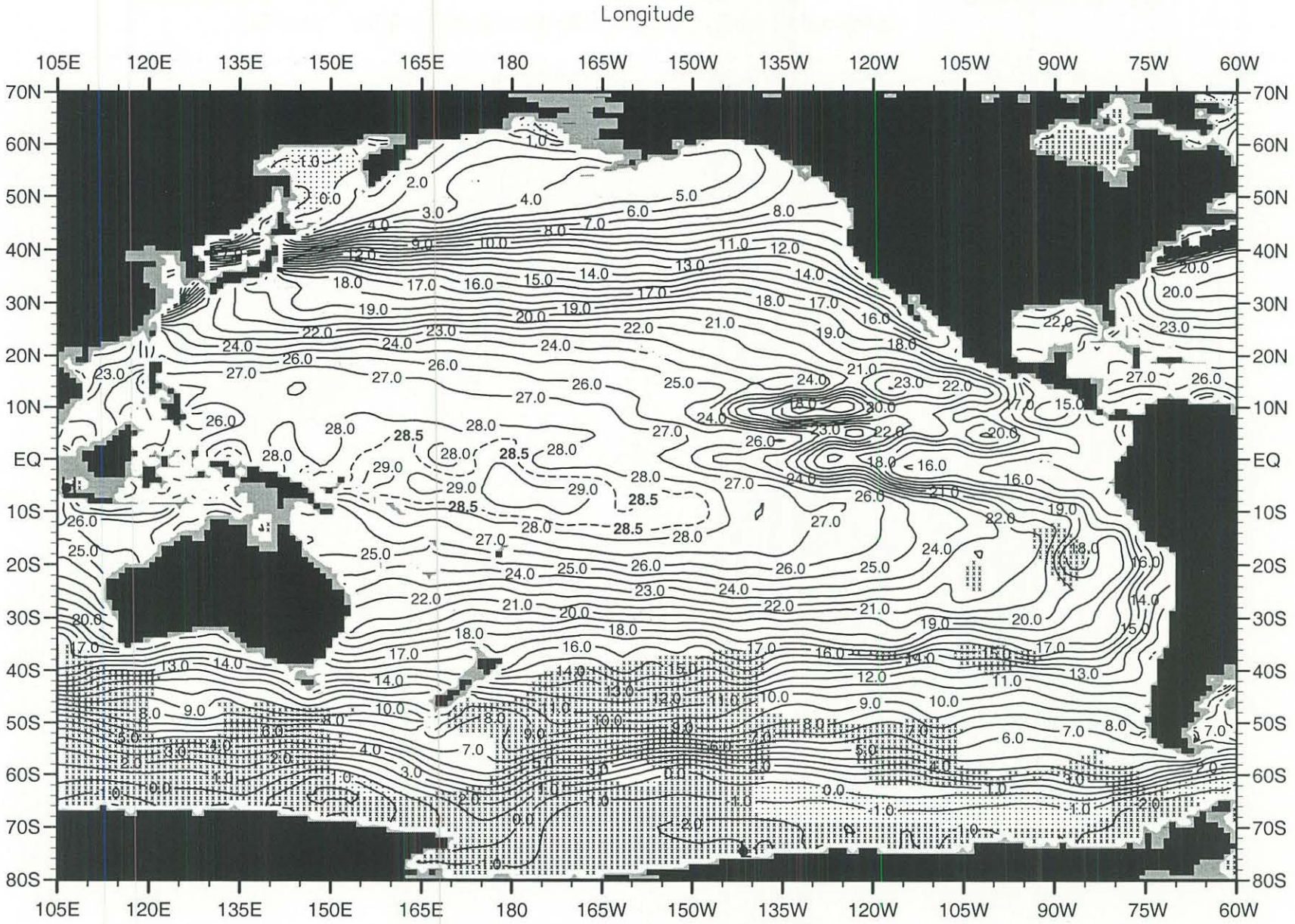


Fig. C47. June mean temperature (°C) at 75 m. depth .

Minimum Value= -2.10 Maximum Value= 29.52 Contour Interval: 1.00

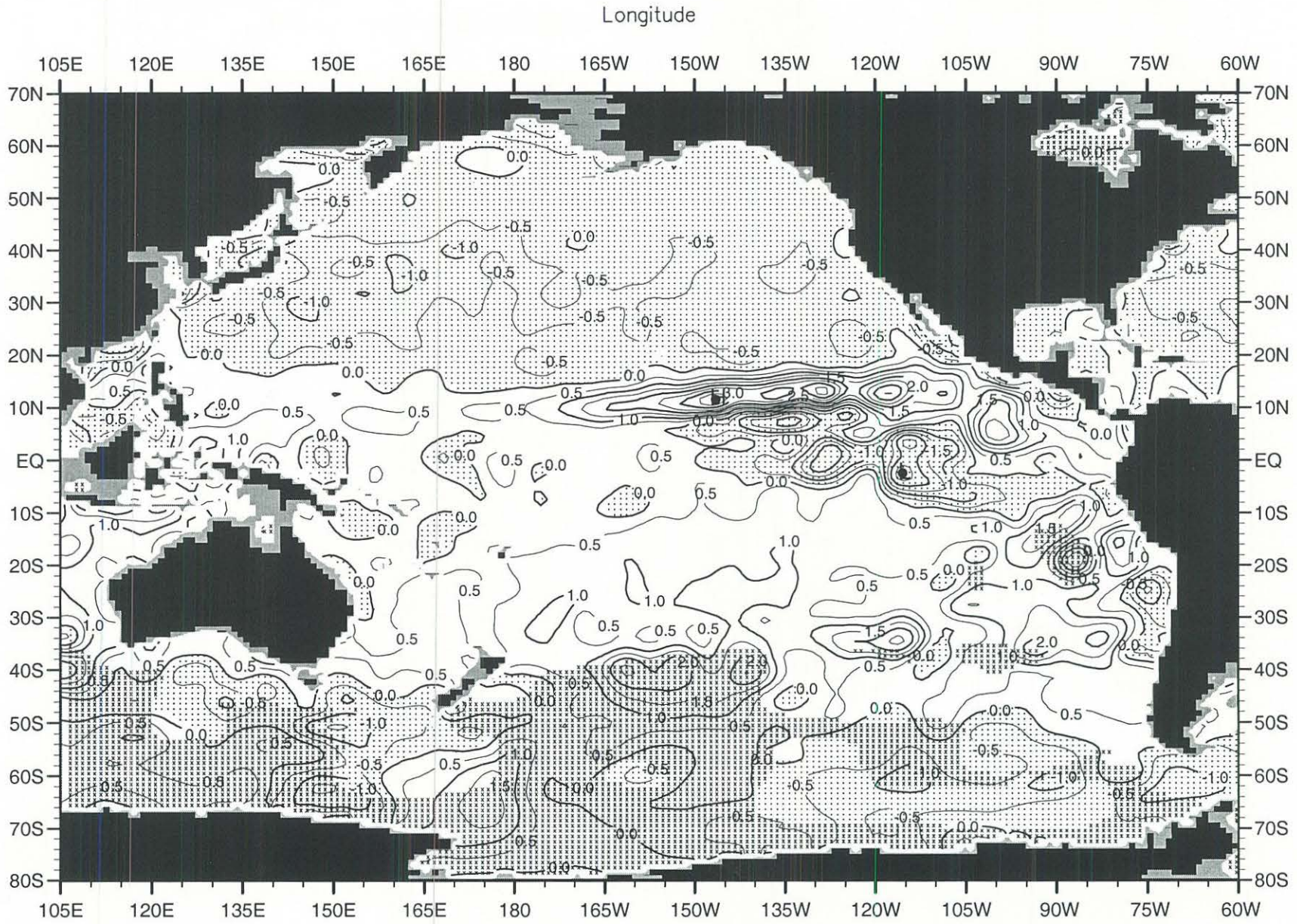


Fig. C48. June minus annual temperature (°C) at 75 m. depth .

Minimum Value= -2.82 Maximum Value= 3.99 Contour Interval: 0.50

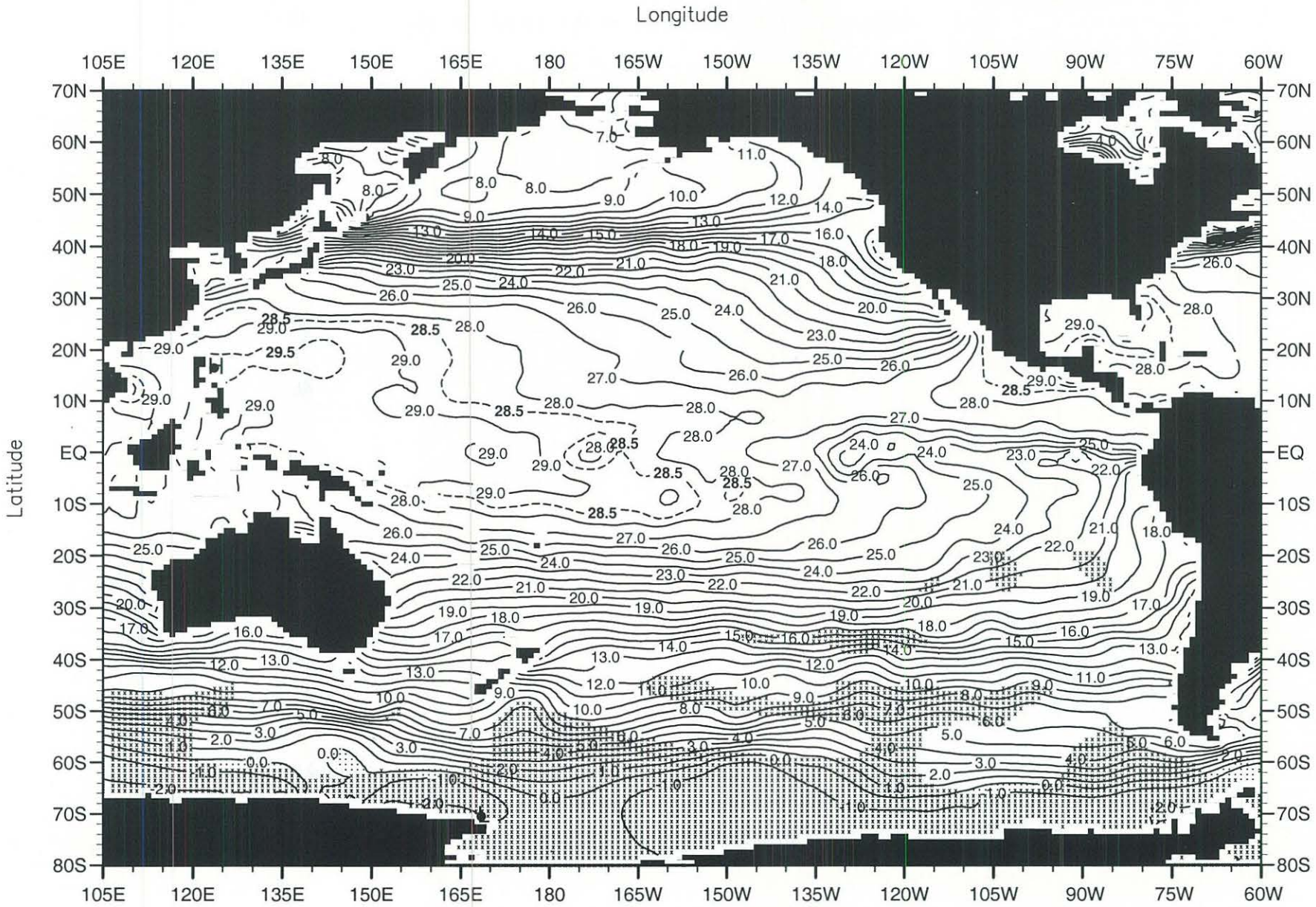


Fig. C49. July mean temperature (°C) at the surface .

Minimum Value= -2.10 Maximum Value= 29.96 Contour Interval: 1.00

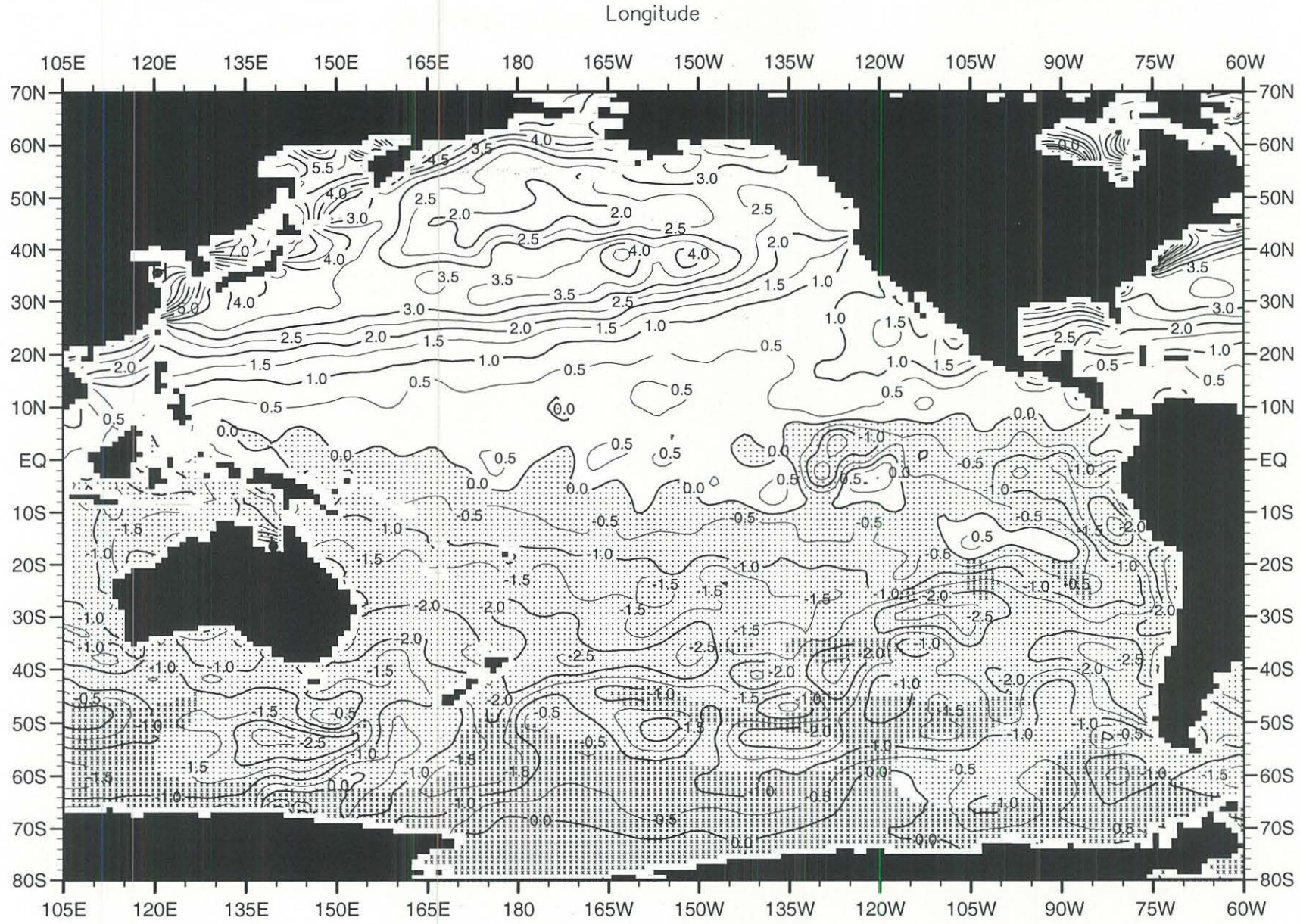


Fig. C50. July minus annual temperature (°C) at the surface .

Minimum Value= -4.64 Maximum Value= 9.13 Contour Interval: 0.50

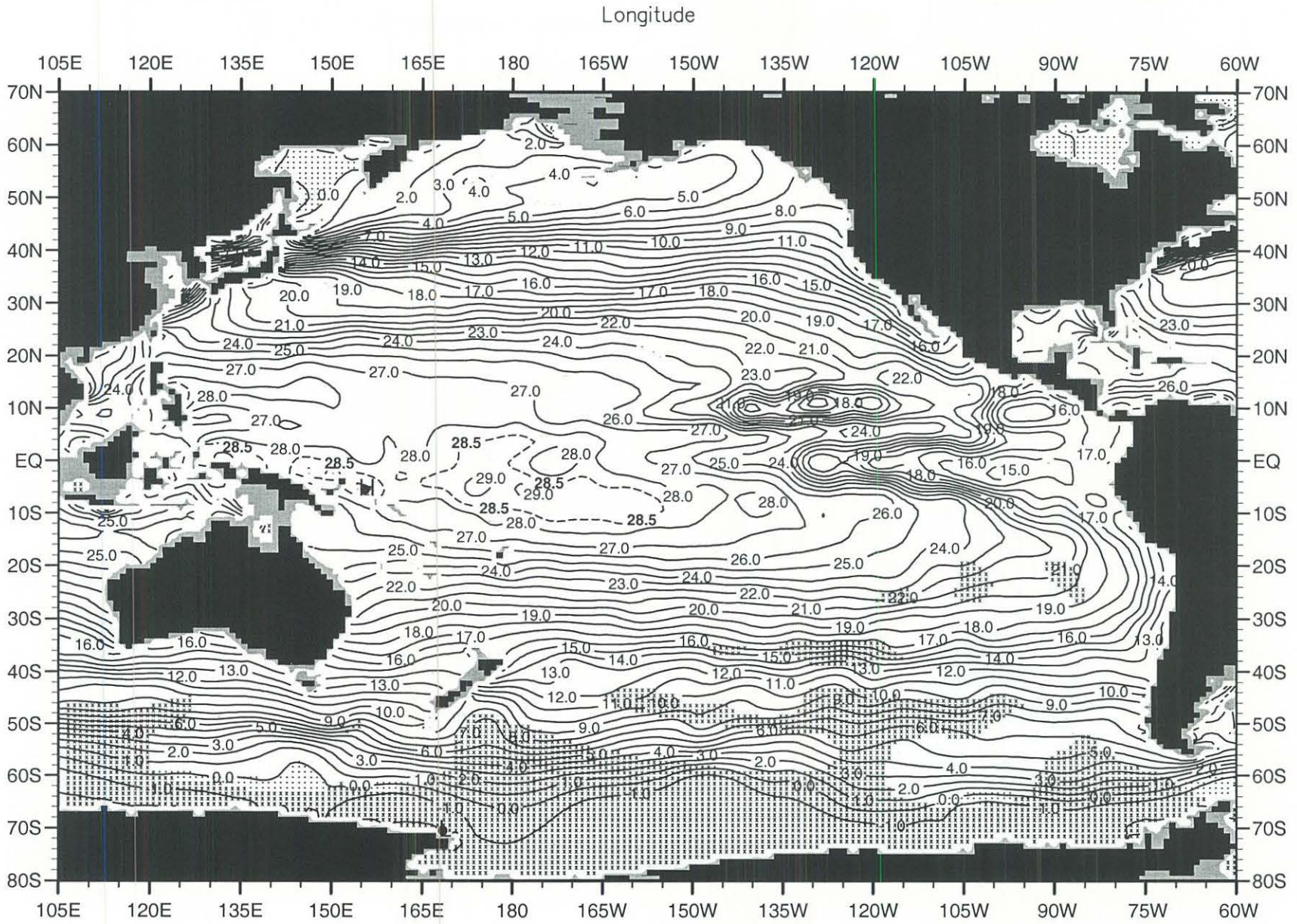


Fig. C51. July mean temperature (°C) at 75 m. depth .

Minimum Value= -2.10 Maximum Value= 29.25 Contour Interval: 1.00

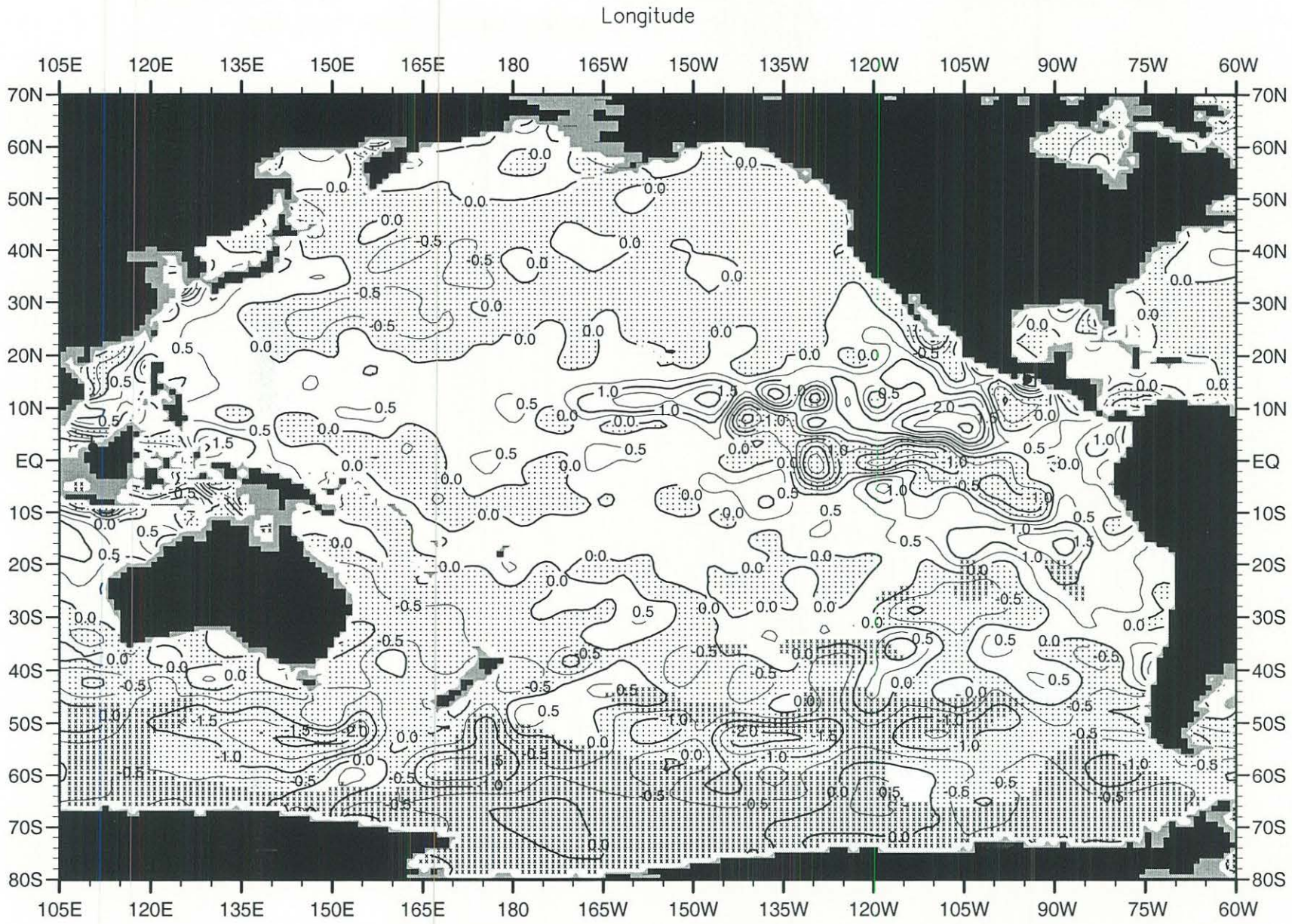


Fig. C52. July minus annual temperature (°C) at 75 m. depth .

Minimum Value= -3.20 Maximum Value= 3.40 Contour Interval: 0.50

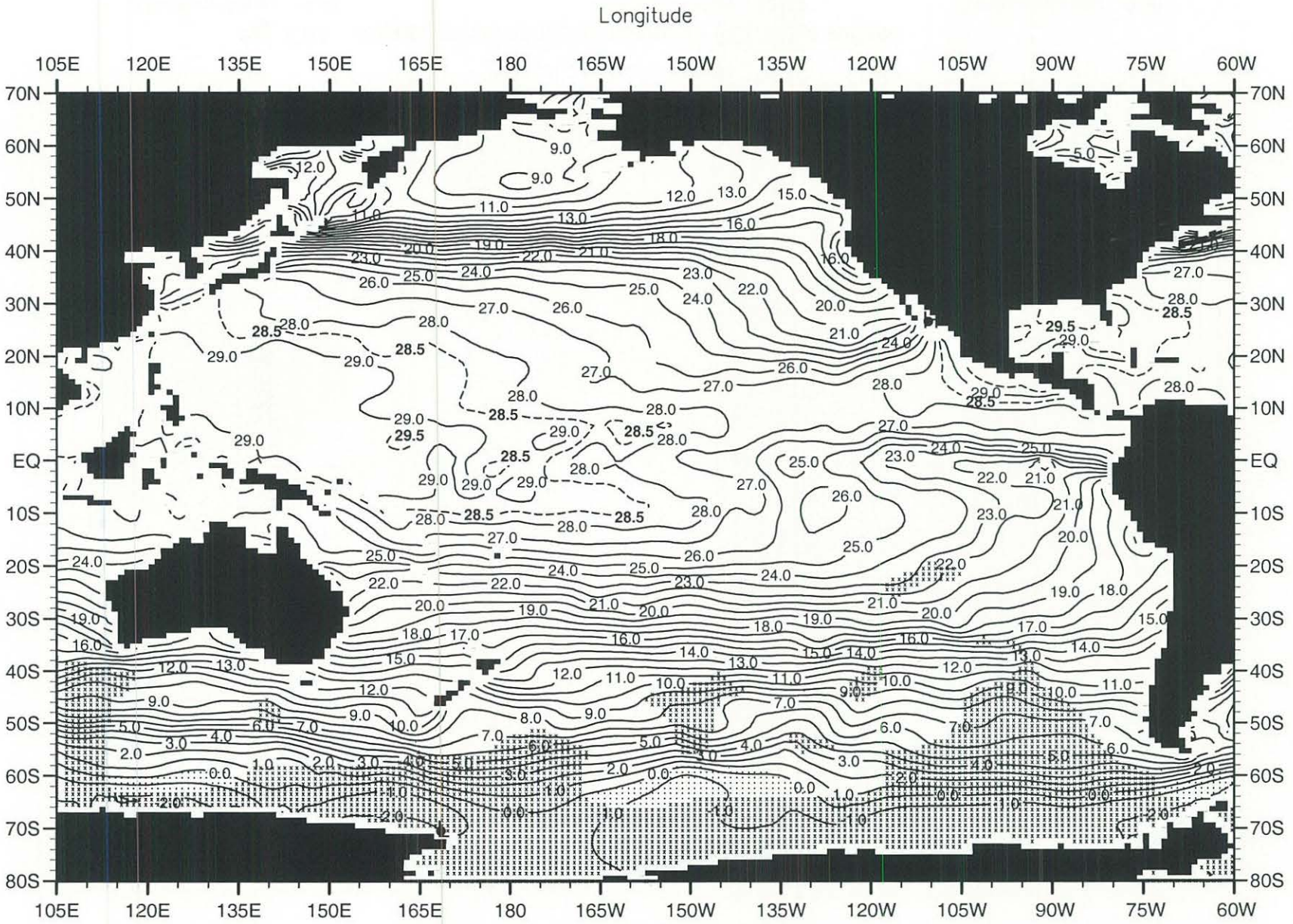


Fig. C53. August mean temperature (°C) at the surface .

Minimum Value= -2.10 Maximum Value= 30.71 Contour Interval: 1.00

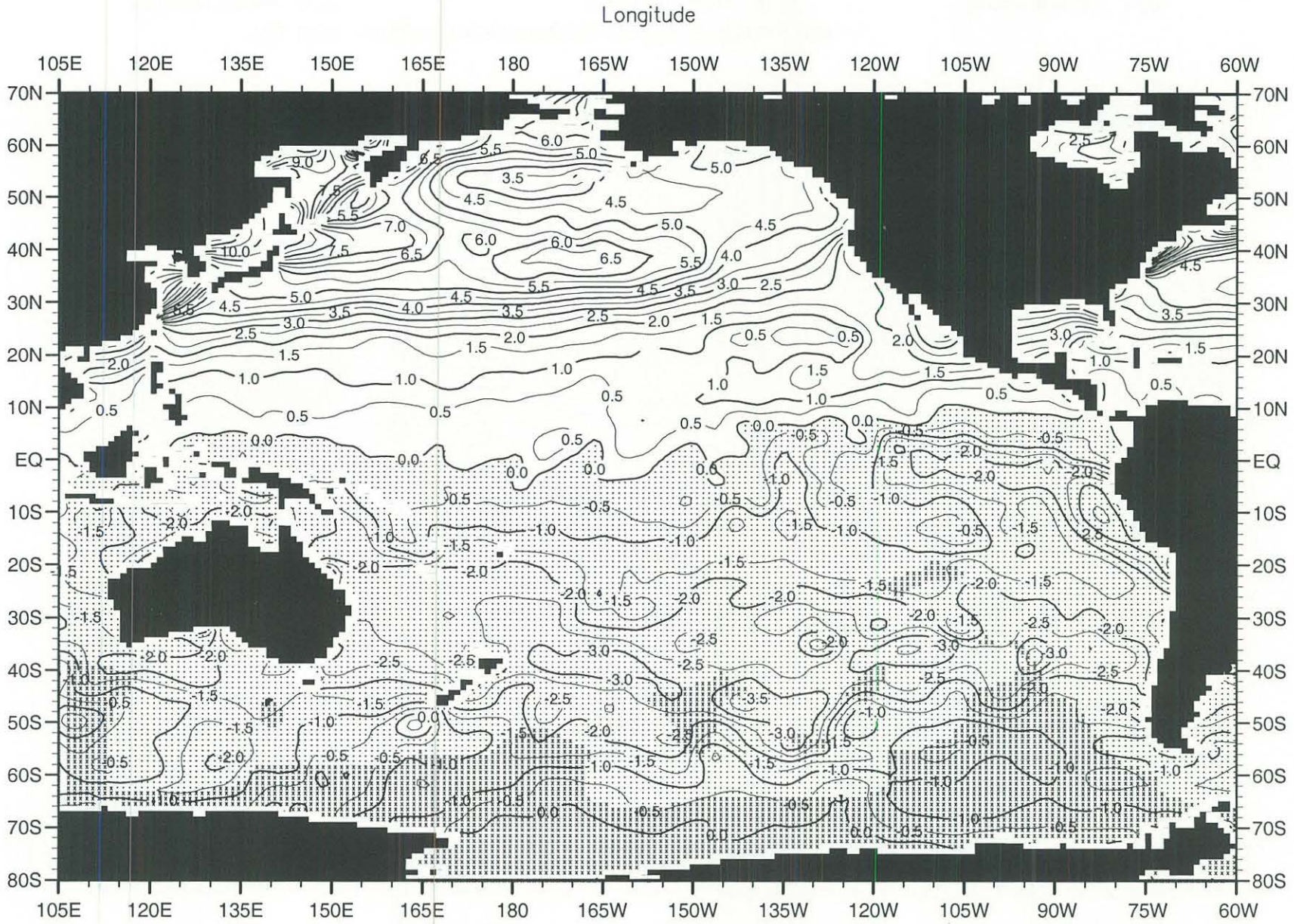


Fig. C54. August minus annual temperature (°C) at the surface .

Minimum Value= -4.45 Maximum Value= 12.19 Contour Interval: 0.50

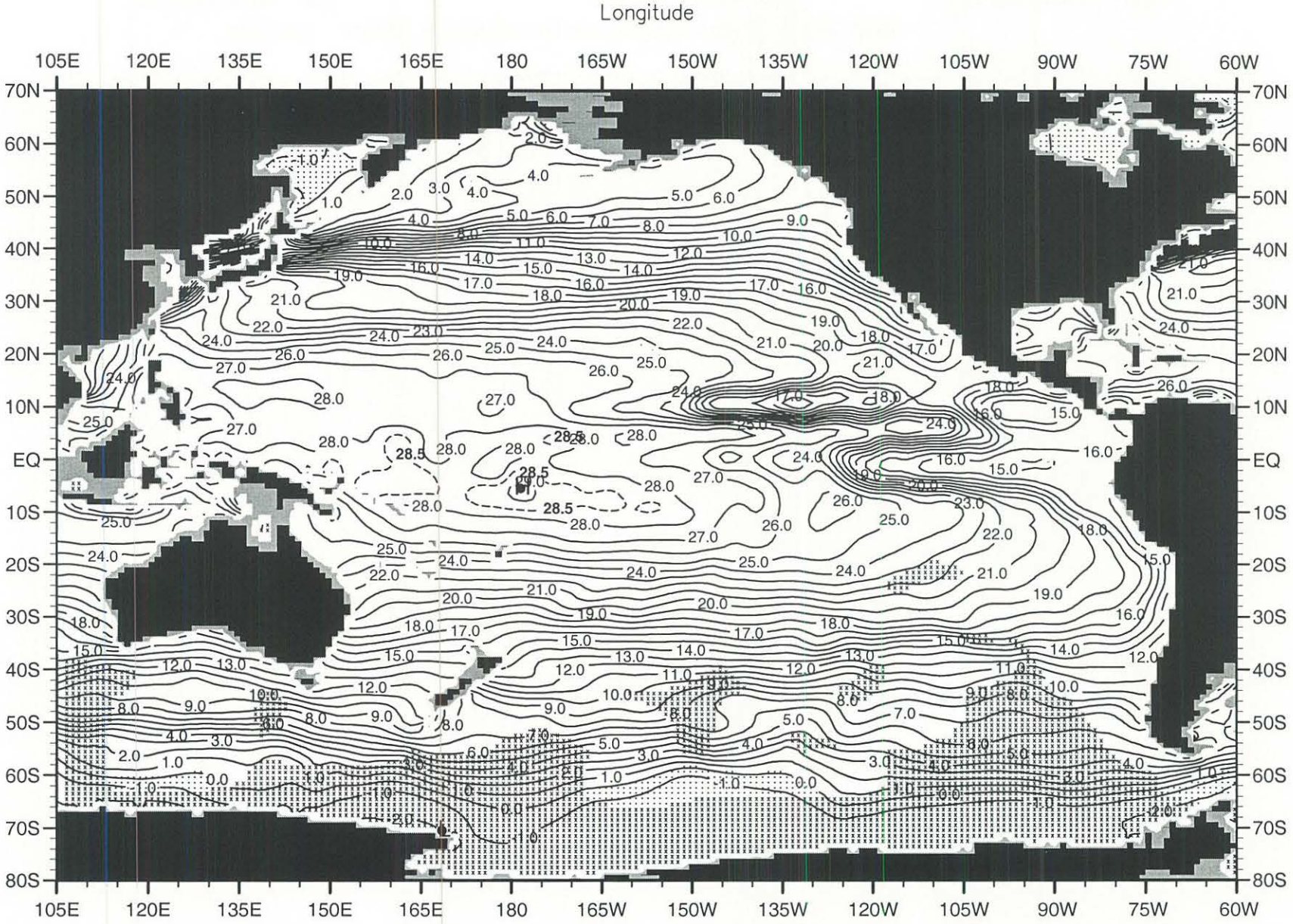


Fig. C55. August mean temperature (°C) at 75 m. depth .

Minimum Value= -2.10 Maximum Value= 29.27 Contour Interval: 1.00

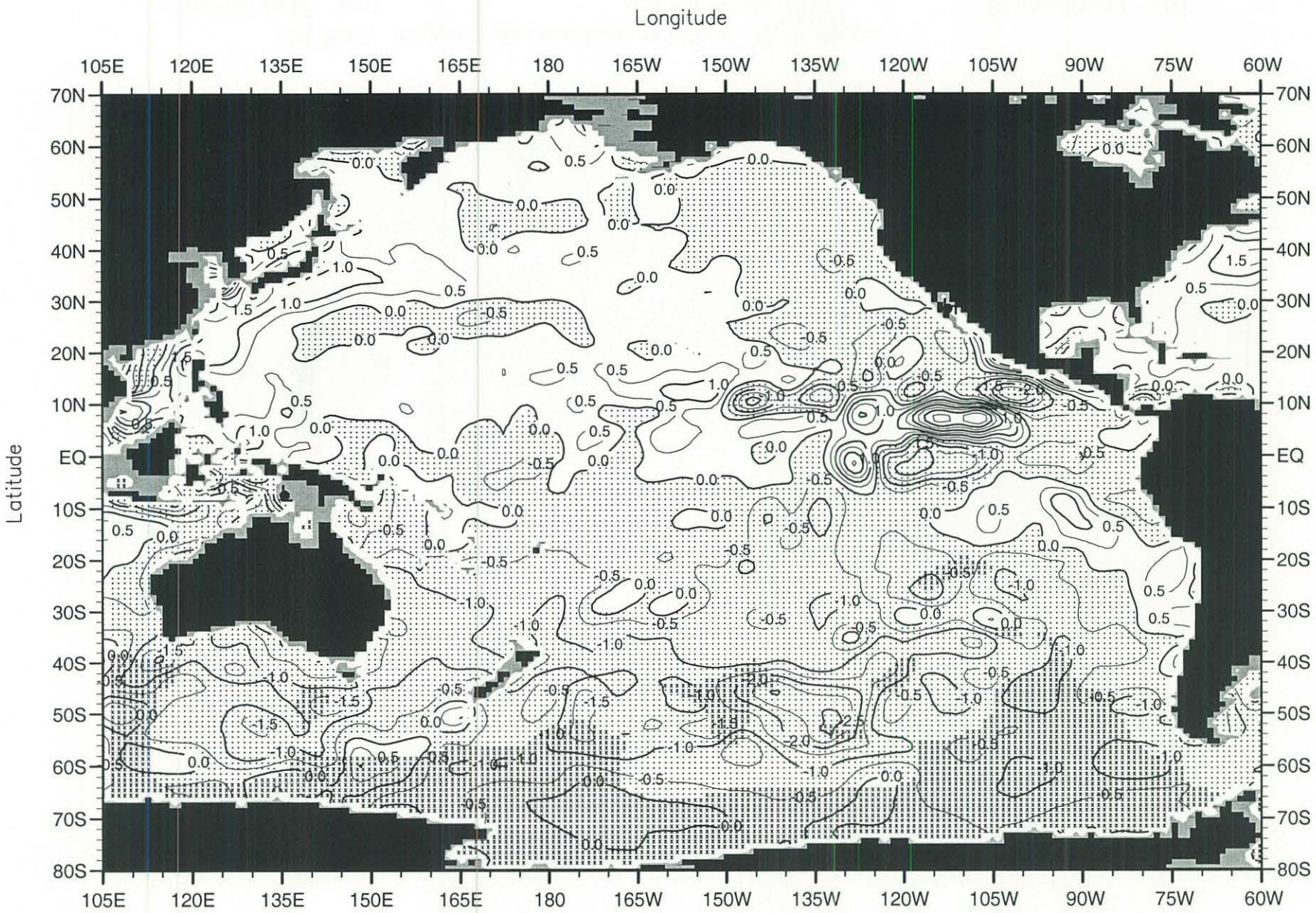


Fig. C56. August minus annual temperature (°C) at 75 m. depth .

Minimum Value= -3.38 Maximum Value= 3.93 Contour Interval: 0.50

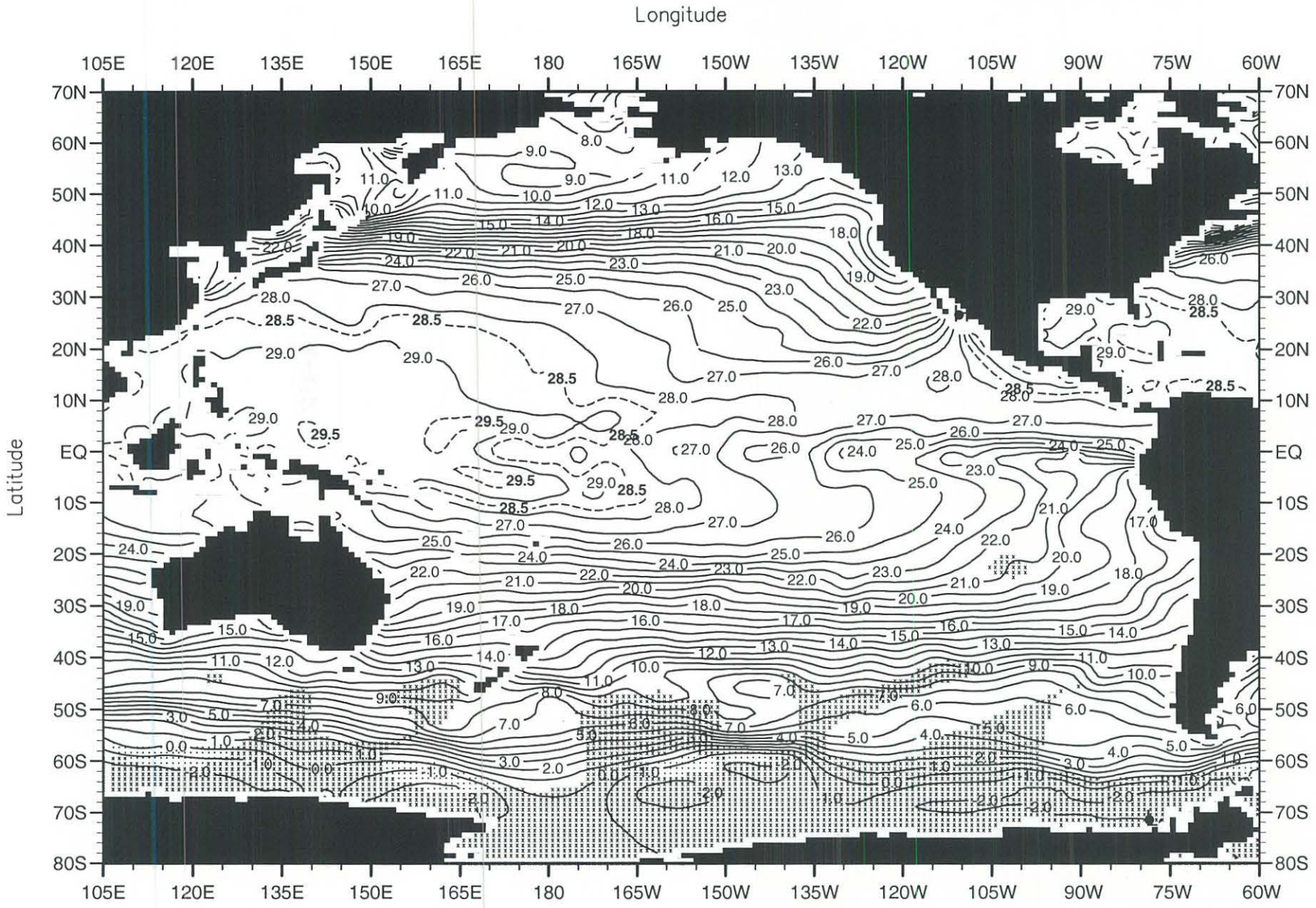


Fig. C57. September mean temperature (°C) at the surface .

Minimum Value= -2.10 Maximum Value= 31.86 Contour Interval: 1.00

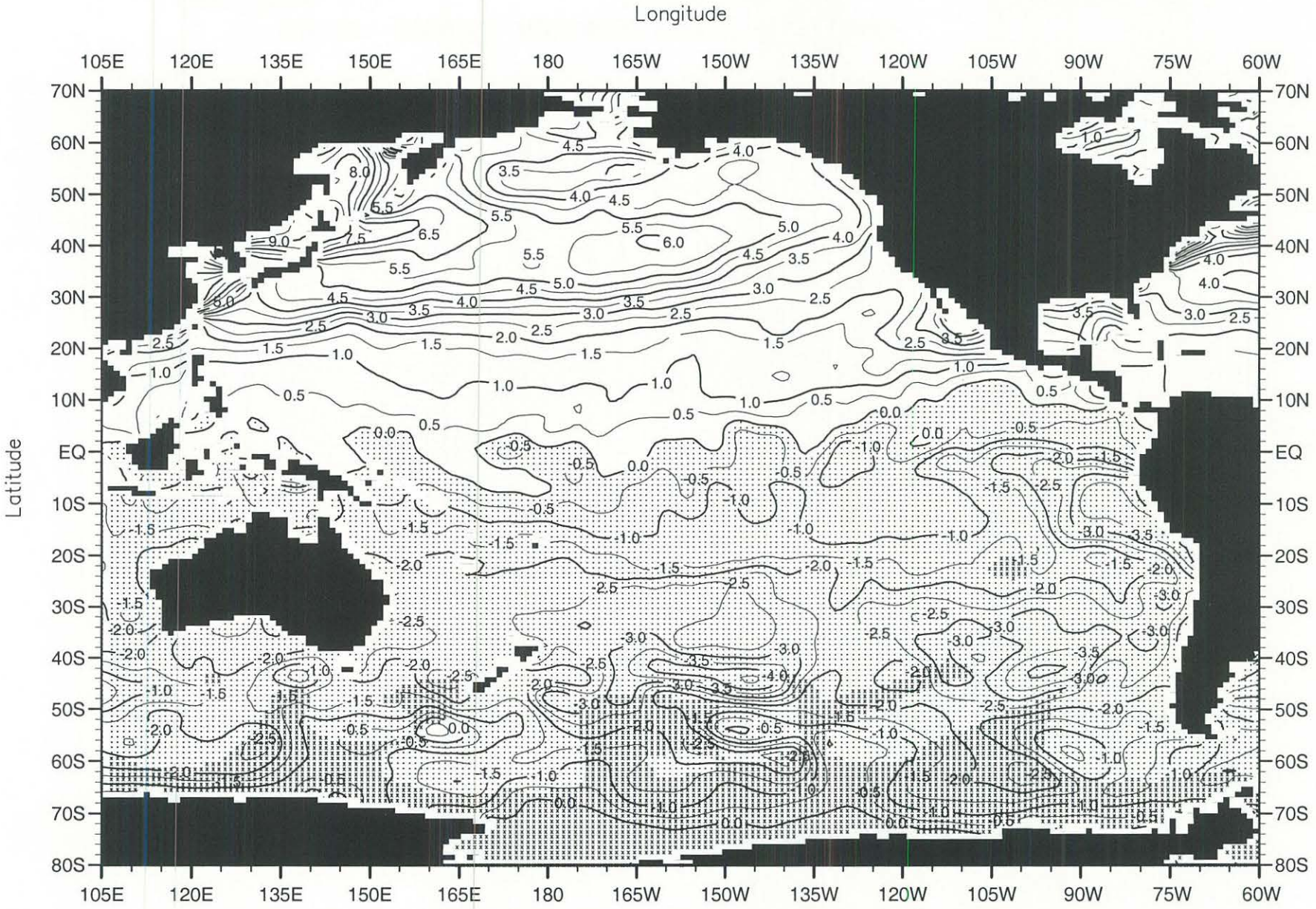


Fig. C58. September minus annual temperature (°C) at the surface .

Minimum Value= -5.17 Maximum Value= 10.46 Contour Interval: 0.50

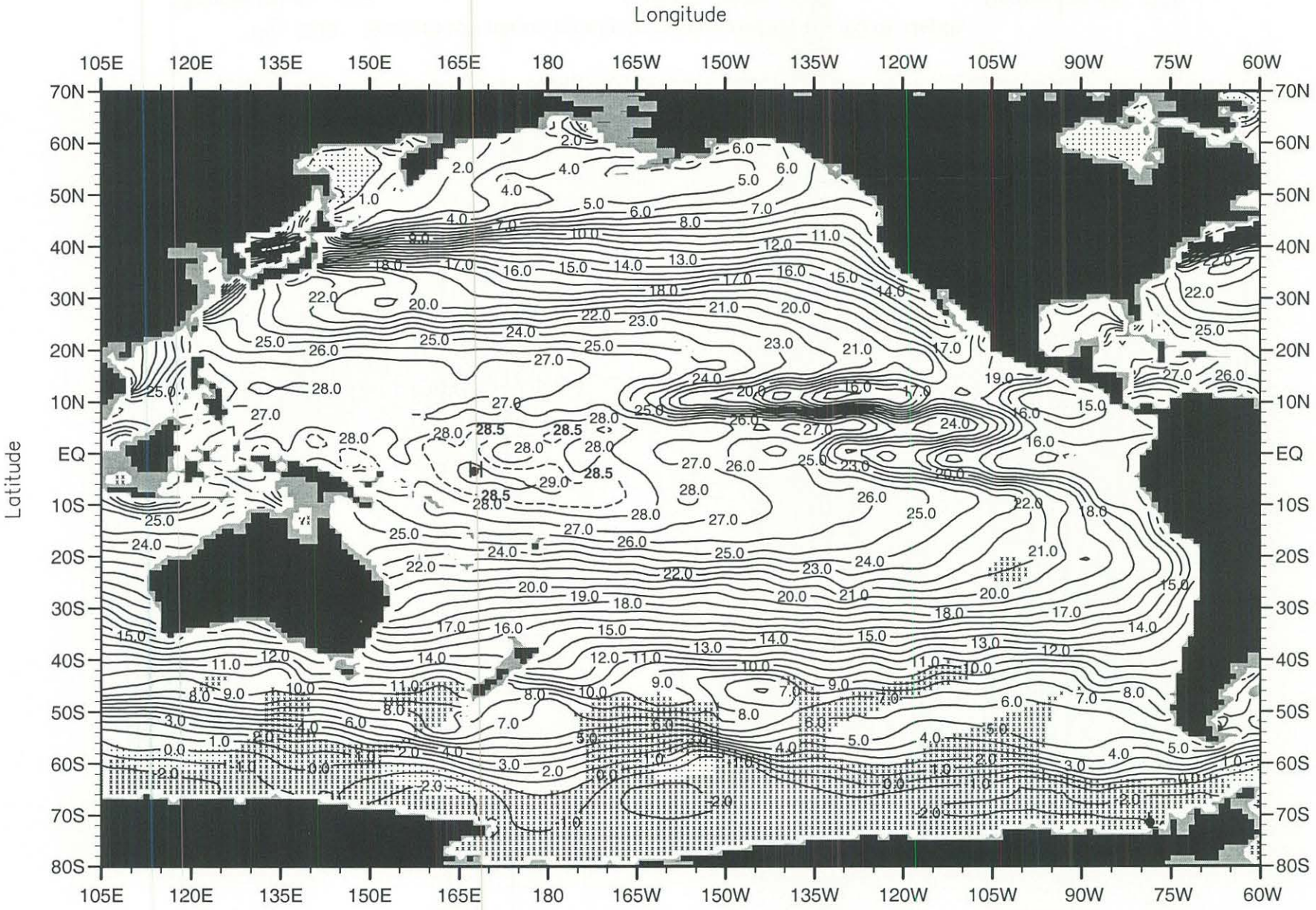


Fig. C59. September mean temperature (°C) at 75 m. depth .

Minimum Value= -2.10 Maximum Value= 29.20 Contour Interval: 1.00

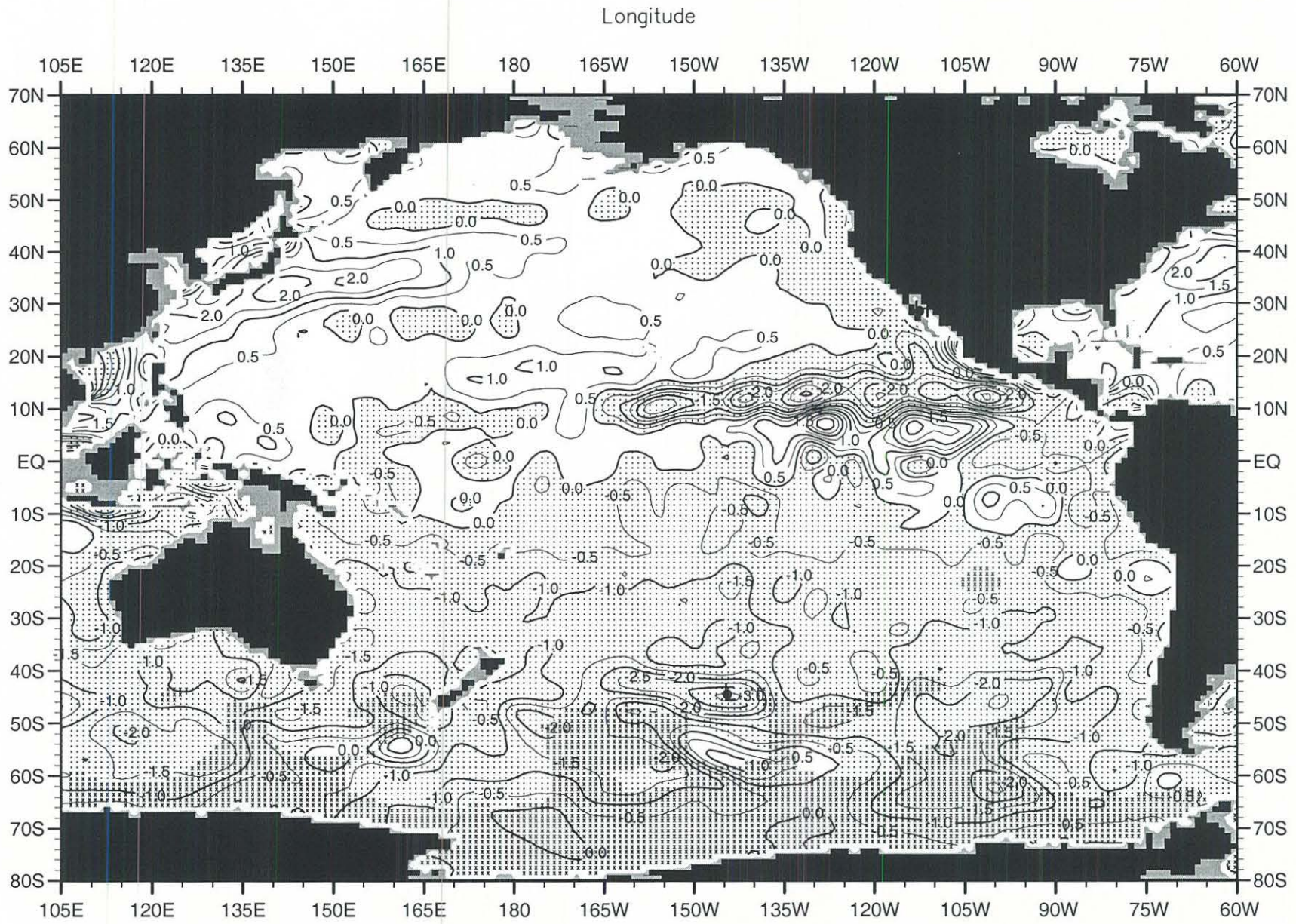


Fig. C60. September minus annual temperature (°C) at 75 m. depth .

Minimum Value= -3.62 Maximum Value= 4.45 Contour Interval: 0.50

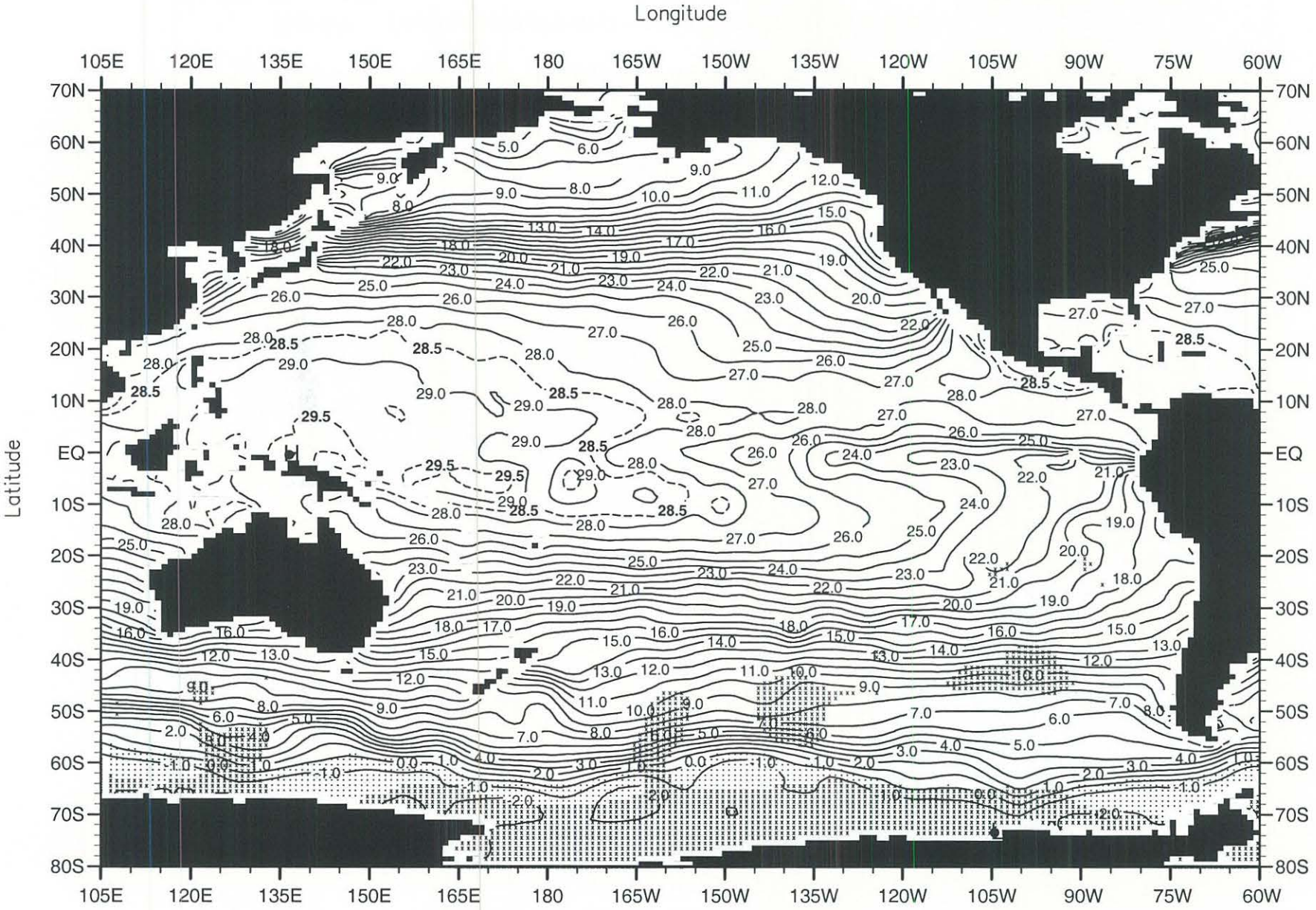


Fig. C61. October mean temperature (°C) at the surface .

Minimum Value= -2.10 Maximum Value= 30.22 Contour Interval: 1.00

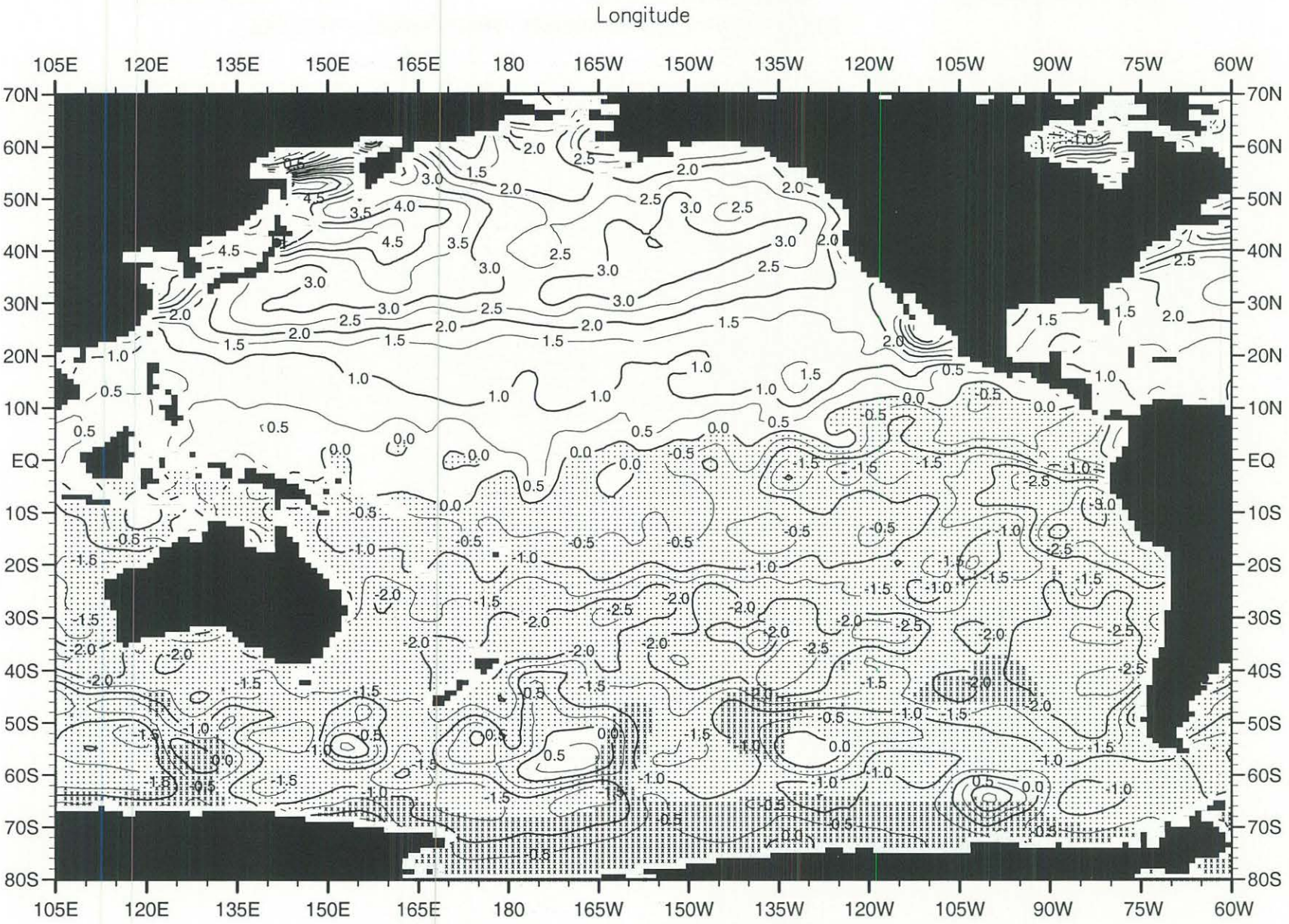


Fig. C62. October minus annual temperature (°C) at the surface .

Minimum Value= -3.75 Maximum Value= 6.18 Contour Interval: 0.50

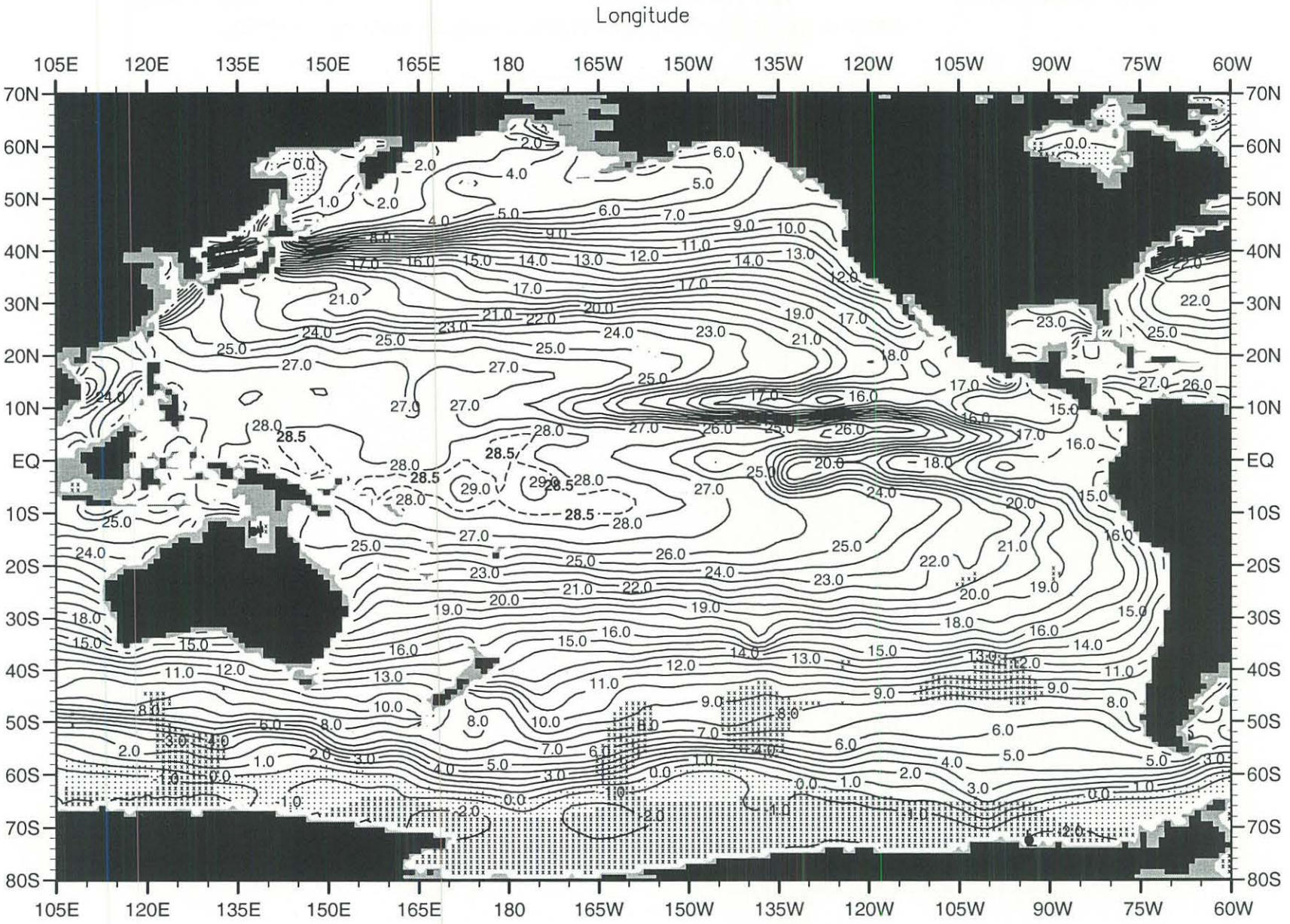


Fig. C63. October mean temperature (°C) at 75 m. depth .

Minimum Value= -2.10 Maximum Value= 32.60 Contour Interval: 1.00

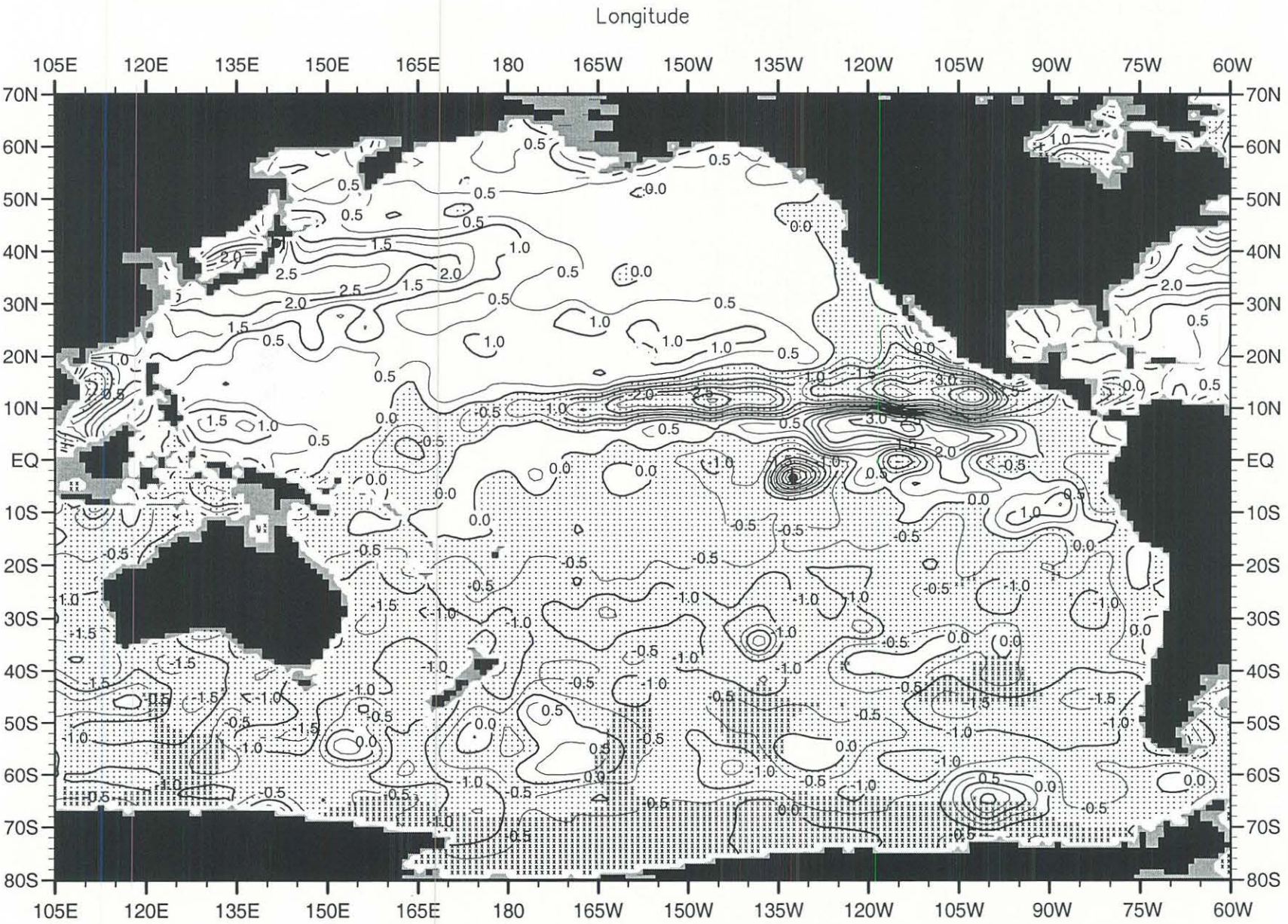


Fig. C64. October minus annual temperature (°C) at 75 m. depth .

Minimum Value= -4.98 Maximum Value= 4.64 Contour Interval: 0.50

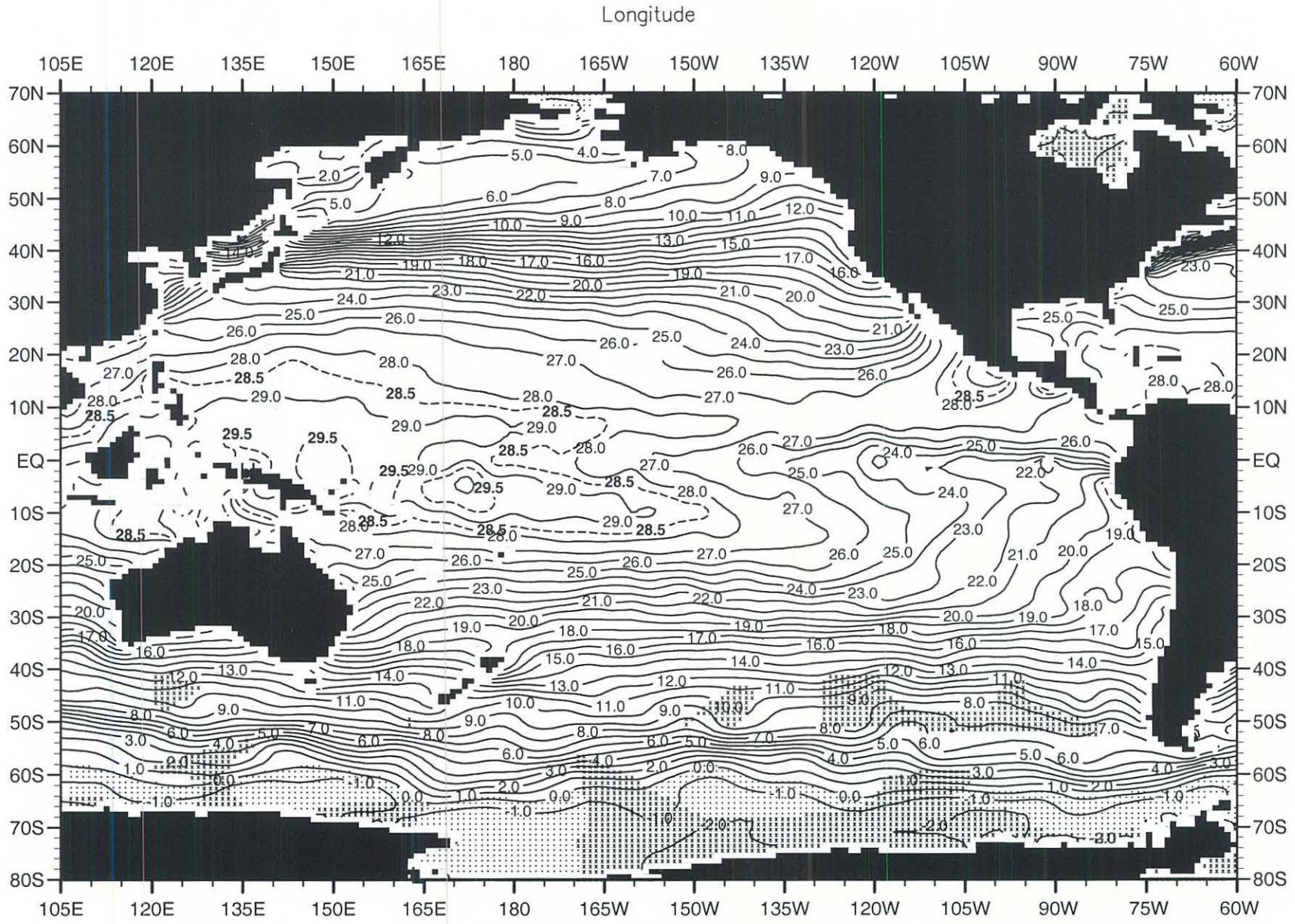


Fig. C65. November mean temperature (°C) at the surface .

Minimum Value= -2.10 Maximum Value= 31.05 Contour Interval: 1.00

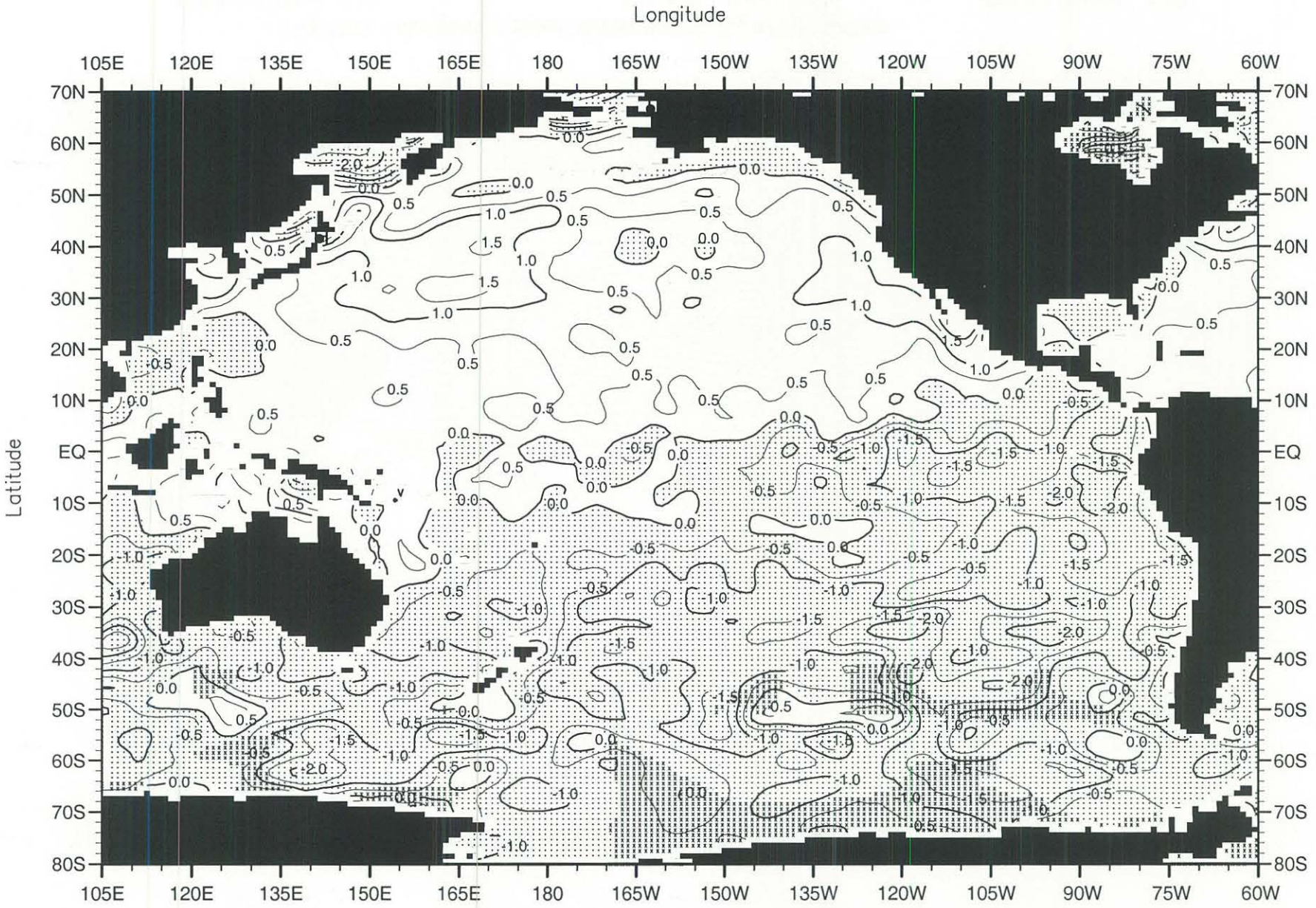


Fig. C66. November minus annual temperature (°C) at the surface .

Minimum Value= -3.52 Maximum Value= 3.29 Contour Interval: 0.50

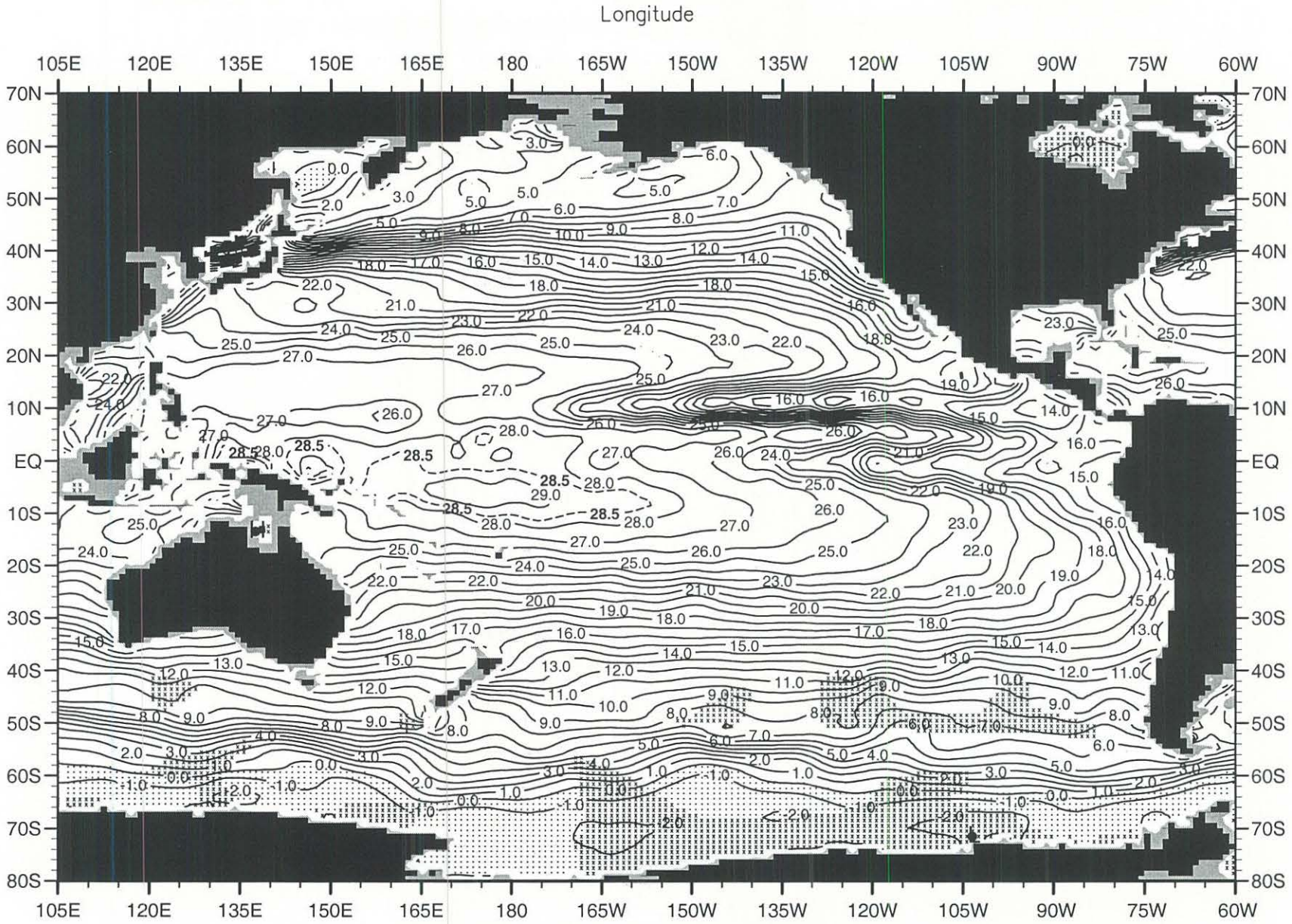


Fig. C67. November mean temperature (°C) at 75 m. depth .

Minimum Value= -2.10 Maximum Value= 33.73 Contour Interval: 1.00

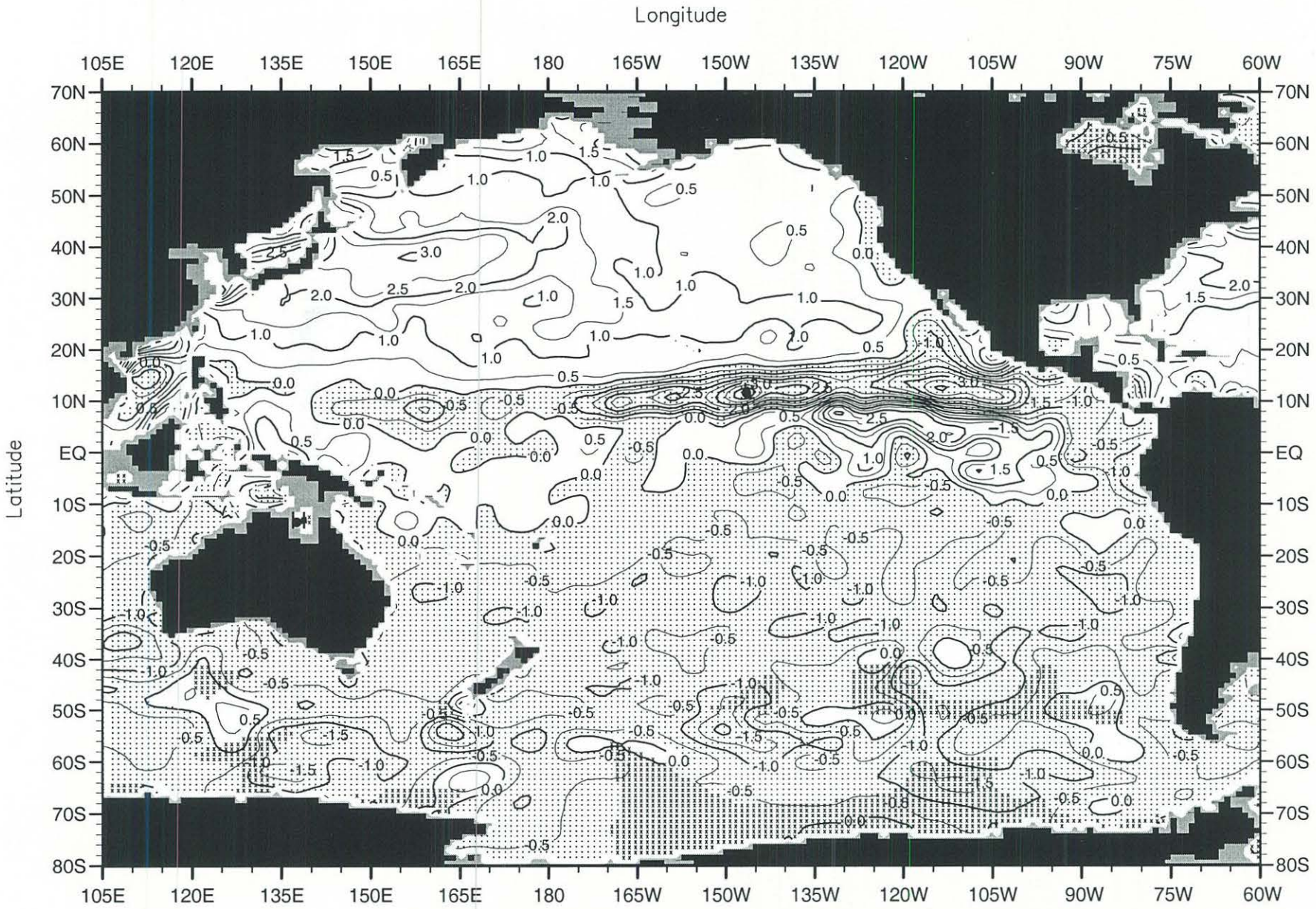


Fig. C68. November minus annual temperature (°C) at 75 m. depth .

Minimum Value= -4.49 Maximum Value= 5.37 Contour Interval: 0.50

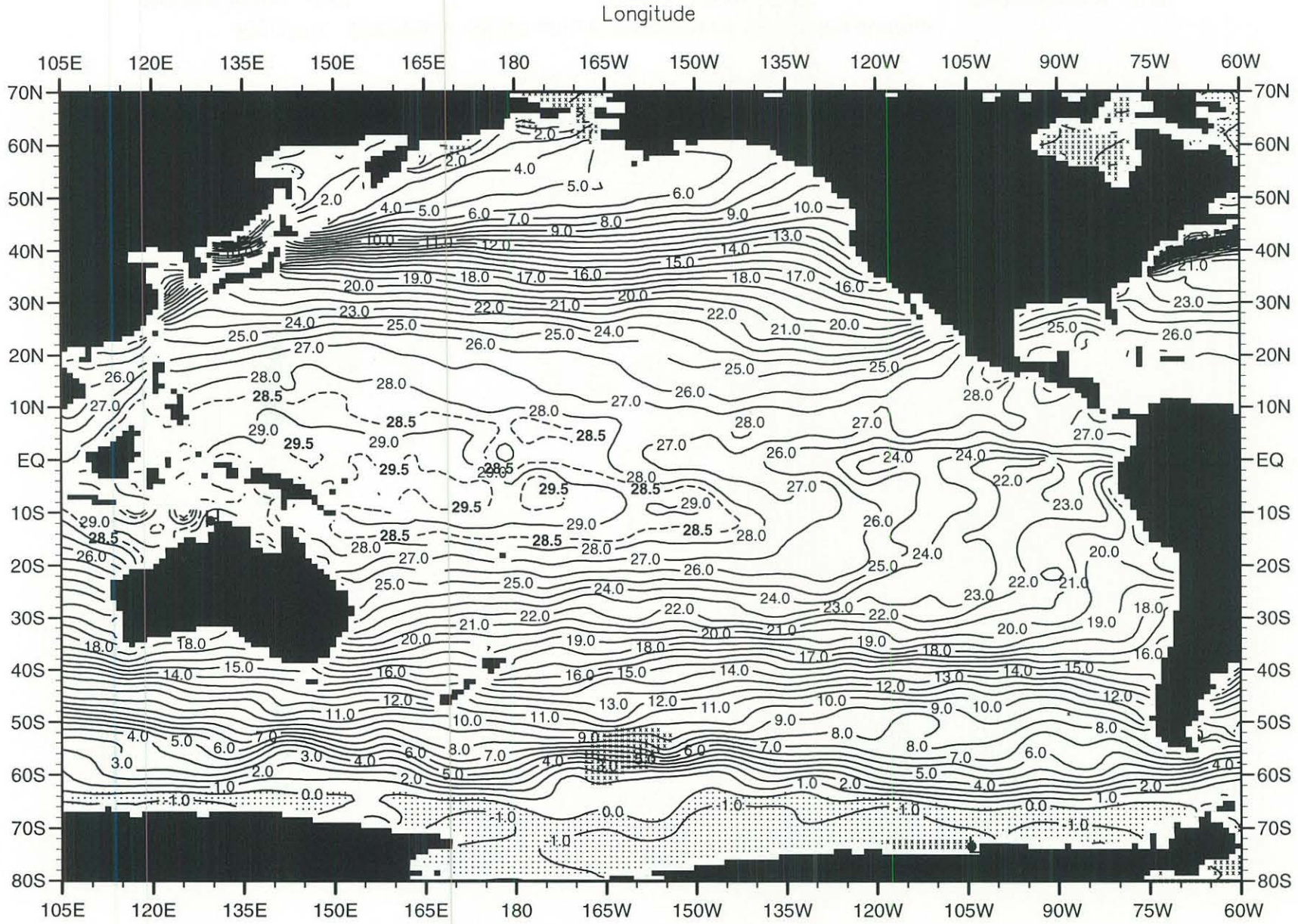


Fig. C69. December mean temperature (°C) at the surface .

Minimum Value= -2.10 Maximum Value= 30.79 Contour Interval: 1.00

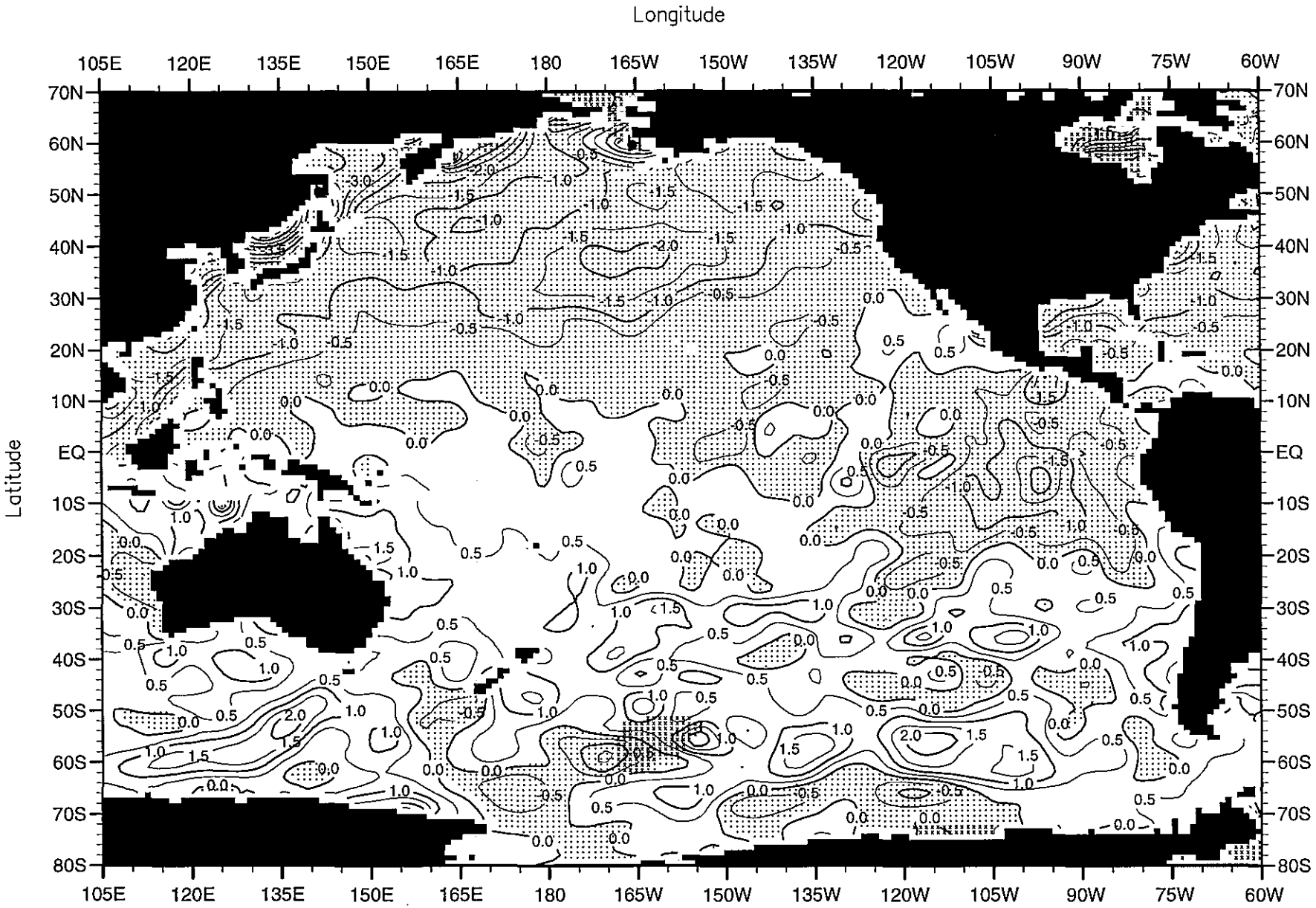


Fig. C70. December minus annual temperature (°C) at the surface .

Minimum Value= -6.23 Maximum Value= 2.69 Contour Interval: 0.50

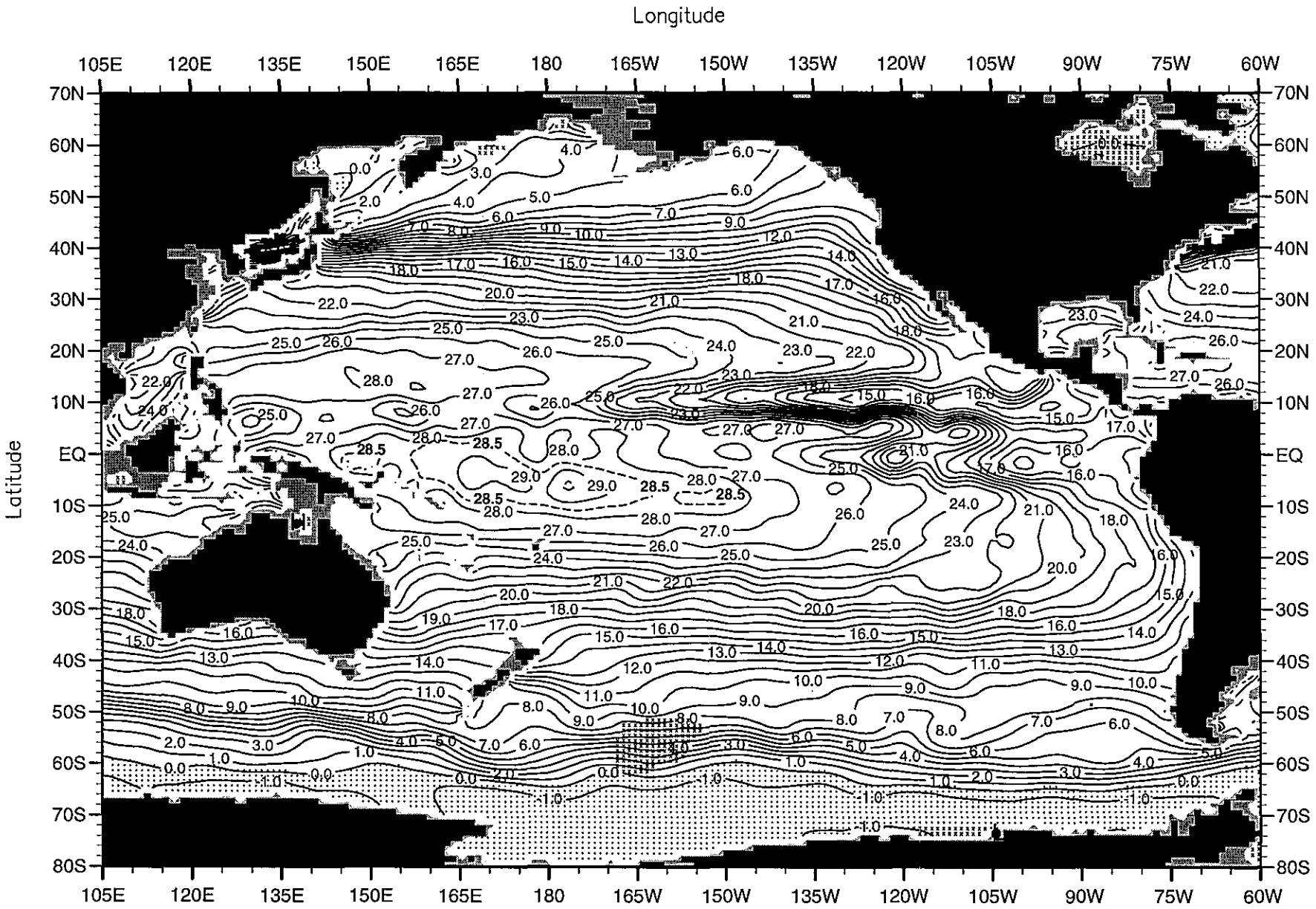


Fig. C71. December mean temperature (°C) at 75 m. depth .

Minimum Value= -2.10 Maximum Value= 31.50 Contour Interval: 1.00

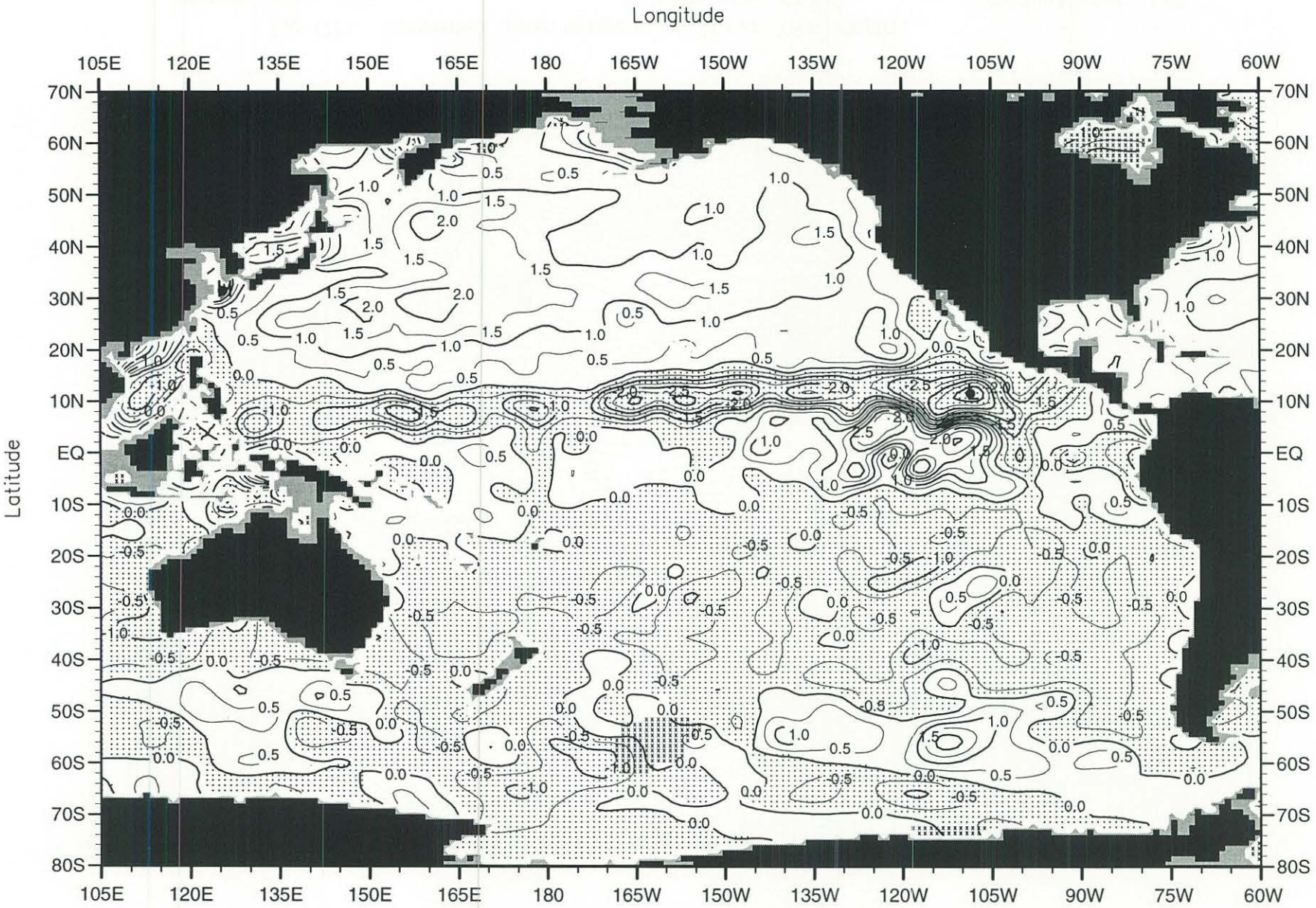


Fig. C72. December minus annual temperature (°C) at 75 m. depth .

Minimum Value= -4.44 Maximum Value= 3.89 Contour Interval: 0.50